REACTIONS OF GOLD(I) ELECTROPHILES WITH NUCLEOPHILES DERIVED FROM GROUP 6 FISCHER-TYPE CARBENE COMPLEXES

by
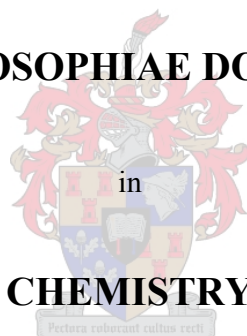
MATTHIAS WILHELM ESTERHUYSEN

DISSERTATION

submitted in fulfilment of the requirements
for the degree of

PHILOSOPHIAE DOCTOR

in

CHEMISTRY

in the

FACULTY OF SCIENCE

at the

UNIVERSITY OF STELLENBOSCH

SUPERVISOR: PROF. H.G. RAUBENHEIMER

JUNE 2002

Declaration

I, the undersigned, hereby declare that the work contained in this thesis is my own original work and that I have not previously in its entirety or in part submitted it at any university for a degree.

Signature:...

Date:..

SUMMARY

This study comprises the preparation and characterisation of various novel organometallic species of gold(I) by employing a range of anionic group 6 metal Fischer-type carbene complexes and group 6 metal-acyl complexes as synthons of the organic moieties introduced to the gold(I) electrophiles. The main objectives of this work are to develop the use of Fischer-type carbene complexes as synthons in the preparation of novel organometallic species along unusual reaction pathways and, in doing so, to expand the organometallic chemistry of gold(I), especially Au-C bond formation reactions.

By reacting various β-CH acidic Fischer-type alkoxy/dialkylamino/ alkthio(methyl)carbene complexes, first with a base, and then with a gold(I) electrophile (Ph_3PAu^+), easy access to vinyl ether/dialkylamine/thioether complexes of gold(I) coordinated to $M(CO)_5$ (M = Cr, Mo, W) fragments, is obtained. When methyl alkoxy- or dialkylaminocarbene complexes are employed, coordination of the novel alkoxyvinyl-gold(I)PPh$_3$ and dialkylaminovinyl-gold(I)PPh$_3$ species to the $M(CO)_5$ fragments occurs in an asymmetrical fashion through the vinyl functionalities of the novel gold(I) species. This usually unstable coordination mode for vinyl ethers is stabilised by delocalisation of partial positive charges from the α-gold vinyl carbon atoms to either the gold(I)PPh$_3$ fragment [for η^2-{alkoxyvinyl-gold(I)PPh$_3$}$M(CO)_5$ complexes] or the nitogen atoms of the vinyl amine group [for η^2-{dialkylaminovinyl-gold(I)PPh$_3$}$M(CO)_5$ complexes]. In the latter complexes this delocalisation occurs to such an extent that these complexes are best described as zwitterions. The corresponding negative charges in the bimetallic complexes reside on the $M(CO)_5$ fragments. As a representative example, uncoordinated ethoxyvinyl-gold(I)PPh$_3$ was isolated in high yield *via* a ligand replacement reaction with PPh$_3$. When Fischer-type alkthio(methyl)carbene complexes are employed in this conversion, novel sulphur coordinated {alkthiovinyl-gold(I)PPh$_3$}$Cr(CO)_5$ complexes are formed.

The reaction mechanism involved in these conversions is believed to be the gold(I) analogue of the hydrolysis of Fischer-type carbene complexes. In this mechanism the bimetallic η^2-vinyl ether coordinated {alkoxyvinyl-gold(I)PPh$_3$}M(CO)$_5$ complexes represent stabilised gold(I) analogues of postulated transition states in the hydrolytic decomposition of Fischer-type alkoxycarbene complexes. The term "aurolysis" is conceived to describe the conversion when Ph$_3$PAu$^+$ is employed as electrophile instead of H$^+$. The formation of the bimetallic η^2-vinyl ether coordinated complexes in the current conversion, furthermore, strongly supports the existence of similar transition states in the hydrolytic decomposition of Fischer-type alkoxycarbene complexes. This mechanism is also accepted for the formation of analogous η^2-{dialkylaminovinyl-gold(I)PPh$_3$}M(CO)$_5$ and {alkthiovinyl-gold(I)PPh$_3$}-S Cr(CO)$_5$ complexes when β-CH deprotonated Fischer-type dialkylamino- and alkthiocarbene complexes are employed in this reaction.

The reaction of anionic group 6 metal-acyl complexes and their nitrogen analogues, N-deprotonated Fischer-type aminocarbene complexes, leads to the formation of acylgold(I) and novel imidoylgold(I) complexes coordinated to M(CO)$_5$ (M = Cr, W) fragments. In the previous complexes poor stabilisation of the M(CO)$_5$ fragments allows halide anions to readily form ionic adducts with these groups. This characteristic of these products provides a useful reaction pathway to the first example of a free acylgold(I) complex, benzoyl-AuPPh$_3$. Coordination of the imine nitrogen atom to the M(CO)$_5$ fragments in the analogous bimetallic imidoylgold(I)-M(CO)$_5$ complexes is much stronger. These complexes are remarkably stable and could even be effectively isolated by means of low temperature silica gel chromatography.

As a preliminary reaction mechanism for this conversion we propose a mechanism that is closely related to the aurolysis mechanism described above. The only difference is that, instead of formal reductive elimination of vinyl ethers/amine/thioether complexes of gold(I) from the M(CO)$_5$ fragments, acyl and imidoyl complexes of gold(I) are produced in this step. Furthermore, the (Z)-stereoisomers of the bimetallic imidoylgold(I)-M(CO)$_5$ complexes generated in this conversion are exclusively obtained.

A second N-deprotonation-auration reaction sequence performed on suitable examples of the bimetallic imidoylgold(I)-M(CO)$_5$ complexes yields, as the only isolable product, a novel triangular Au$_2$Cr cluster complex, *cis*-{η^2-(Ph$_3$PAu)$_2$} PPh$_3$Cr(CO)$_4$. This complex is the isolobal equivalent for the unstable molecular hydrogen complex, (η^2-H$_2$)PPh$_3$Cr(CO)$_4$, and exhibits the shortest known Au-Au separation between two gold atoms in cluster complexes of the type Au$_2$M.

Finally, two novel and vastly different molecular structures of closely related anionic benzoylpentacarbonyl tungstates, one with Li$^+$ as counterion and another in which exactly half the Li$^+$-cations have been replaced by protons, highlight the importance of hydrogen bonding and ion-dipole interactions in determining the solid state structure of such complexes.
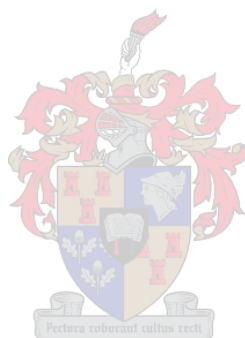
OPSOMMING

Hierdie studie behels die bereiding en karakterisering van verskeie nuwe organometaalkomplekse van goud(I). Hierdie komplekse is berei deur gebruik te maak van 'n wye reeks anioniese groep 6 metaal Fischer-tipe karbeenkomplekse asook anioniese groep 6 metaal asielkomplekse as sintetiese ekwivalente vir die organiese fragmente wat gedurende die sintese aan die goud atoom gebind word. Die hoofdoel van hierdie studie is om die gebruik van Fischer-tipe karbeenkomplekse as sintetiese voorgangers in die bereiding van nuwe organometaalverbindings te ontwikkel en om sodoende ook die organometaalchemie van goud verder uit te bou. Veral die ontwikkeling van nuwe sintetiese metodologieë vir die bereiding van Au-C bindings is hier van belang.

Verskeie Fischer-tipe alkoksie-/dialkielamino-/alktio-(metiel)karbeenkomplekse met suuragtige waterstofatome geleë op die β-metallo-koolstofatoom is eers onomkeerbaar gedeprotoneer. Byvoeging van die goud(I) elektrofiel, Ph_3PAu^+, lei - volgens 'n ongewone reaksiemeganisme - tot die vorming van onderskeie vinieleter-, dialkielvinielamien- en vinieltioeterkomplekse van goud(I). Hierdie komplekse is verder ook op verskillende wyses aan $M(CO)_5$ fragmente (M = Cr, Mo, W) gekoördineer.

Die vinieleter- en vinielamienkomplekse van goud(I), wat vorm wanneer alkoksie- en dialkielaminokarbeenkomplekse onderskeidelik in hierdie sintese aangewend word, koördineer onsimmetries deur hulle viniel dubbelbindings aan die vrygestelde $M(CO)_5$-groepe. Hierdie normaalweg onstabiele vorm van vinieleterkoördinasie, word gestabiliseer deur delokalisering van positiewe lading vanaf die α-goud viniel koolstofatoom na die $AuPPh_3$-fragment [vir die η^2-{alkoksieviniel-goud(I)PPh_3}$M(CO)_5$ komplekse] óf na die stikstofatoom van die dialkielvinielamien groep [vir die η^2-{dialkielaminoviniel-goud(I)PPh_3}$M(CO)_5$ komplekse]. Laasgenoemde komplekse kan as "zwitterione" beskryf word. Die onderskeie negatiewe ladings in hierdie komplekse bevind hulle hoofsaaklik op die $M(CO)_5$ groepe. Sterk koördinerende ligande (bv. PPh_3) verplaas die onsimmetriese viniel eter vanaf die $M(CO)_5$-fragment. Só kon, as 'n voorbeeld, die vrye etoksieviniel-goud(I)PPh_3-kompleks met 'n hoë opbrengs berei word. Wanneer β-gedeprotoneerde

Fischer-tipe tiokarbeenkomplekse met Ph_3PAu^+ reageer, vorm swawel gekoördineerde {tioviniel-goud(I)PPh$_3$}Cr(CO)$_5$ bimetalliese komplekse in stede van die π-komplekse.

Dit word voorgestel dat in die bogenoemde reaksies die goud(I)elektrofiel dieselfde rol vervul as die proton gedurende die hidrolise van Fischer-tipe alkoksiekarbeenkomplekse. Die bimetalliese, $η^2$-vinieleter-gekoördineerde {alkoksieviniel-goud(I)PPh$_3$}M(CO)$_5$-komplekse hier berei verteenwoordig dus stabiele goud(I) analoë van voorgestelde tusseprodukte in so 'n meganisme. Die term "aurolise" word voorgestel om die geval waar Ph_3PAu^+ in stede van H^+ as elektrofiel aangewend word te beskryf. Die vorming van bimetalliese, $η^2$-vinieleter-gekoördineerde komplekse in die huidige reaksie ondersteun die moontlike vorming van die voorgestelde tussenprodukte tydens die hidrolise van Fischer-tipe alkoksie(metiel)karbeenkomplekse. 'n Soortgelyke meganisme kan ook gebruik word om die vorming van die $η^2$-{dialkiellamienviniel-goud(I)PPh$_3$}M(CO)$_5$- en {alktioviniel-goud(I)PPh$_3$}-S Cr(CO)$_5$-komplekse vanuit β-CH gedeprotoneerde Fischer-tipe dialkielamino- en tiokarbeenkomplekse en Ph_3PAuCl te interpreteer.

Die reaksie van anioniese groep 6 oorgangsmetaal metaal-asielkomplekse en hulle stikstofanaloë, N-gedeprotoneerde Fischer-tipe aminokarbeenkomplekse, lewer onderskeidelik asiel- en imidoielkomplekse van goud(I) wat aan M(CO)$_5$ fragmente (M = Cr, W) koördineer. Die goud(I)asiel-M(CO)$_5$ koördinasie deur die asiel-suurstofatoom is baie swak en die M(CO)$_5$-eenheid in hierdie komplekse word maklik deur haliedanione en sekere oplosmiddel molekules verplaas. Die haliedanione vorm anioniese addukte met the M(CO)$_5$ fragmente. Hierdie eienskap van die bimetalliese komplekse verskaf sodoende 'n gerieflike sintetiese roete na die eerste voorbeeld van 'n vrye asielgoud(I)-kompleks, bensoiel-AuPPh$_3$. Koördinasie van die imienstikstofatoom aan M(CO)$_5$-groepe in die bg. imidoielkomplekse is egter veel sterker. Die bimetalliese {imidoielgoud(I)}M(CO)$_5$-komplekse is verbasend stabiel en kan selfs effektief deur middel van lae temperatuur SiO_2-kolomkromatografie geïsoleer word.

'n Soortgelyke reaksie meganisme as wat voorgestel word vir die aurolise van Fischer-tipe karbeenkomplekse word voorgestel vir hierdie reaksie. Die enigste verskil is dat die formele reduktiewe eliminasie van 'n viniel-eter, -amien of -tioeter vervang word met die vorming van asiel- of imidoielkomplekse van goud(I). Verder word die (Z)-isomere van die bimetalliese {imidoielgoud(I)}$M(CO)_5$-komplekse uitsluitlik in hierdie reaksie verkry.

Wanneer geskikte voorbeelde van bimetalliese {imidoielgoud(I)}$M(CO)_5$-komplekse 'n tweede keer gedeprotoneer word en gereageer word met Ph_3PAuCl, is die enigste isoleerbare produk van die reaksie 'n driehoekige Au_2Cr troskompleks, nl. *cis*-$\{\eta^2$-$(Ph_3PAu)_2\}PPh_3Cr(CO)_4$. Hierdie verbinding dien as 'n isolobale model vir die onstabiele molekulêre waterstof kompleks , $(\eta^2$-$H_2)PPh_3Cr(CO)_4$, en besit verder die kortste Au-Au afstand tussen twee goud atome in driehoekige troskomplekse wat nog tot dusvêr gerapporteer is.

Laastens is die kristalstrukture van twee nou verwante anioniese {bensoiel}$W(CO)_5$-komplekse bepaal. Die enigste verskil tussen die hierdie twee verbindings is dat die een slegs Li^+ as teenioon bevat terwyl presies die helfte van die Li^+-teenione in die tweede struktuur deur protone verplaas is. Hierdie klein verskil in samestelling veroorsaak egter drastiese verskille in die kristalstrukture van hierdie verbindings. Die belangrikheid van waterstof bindings en ioon-dipool interaksies in die bepaling van die vastetoestandstrukture van sulke verbindings word hierdeur beklemtoon.

Mutti
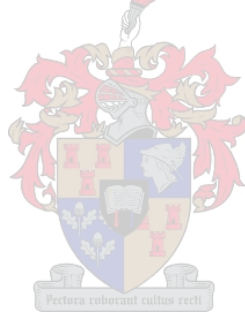
ACKNOWLEDGEMENTS

I would like to express my sincerest gratitude to all those who supported me in the work presented in this thesis. In particular I would like to thank the following people and institutions:

The Lord my God.

Catharine, for the unrivalled and unconditional love, support, understanding, advice, patience and friendship, which completes me.

Mutti, for believing in me all along.

Prof. H.G. Raubenheimer for excellent leadership, guidance and allowing me enough freedom to make this work my own.

The NRF, Stellenbosch University and Volkswagen Stiftung for financial support.

The members of the chemistry department at Stellenbosch University, especially Stephanie.
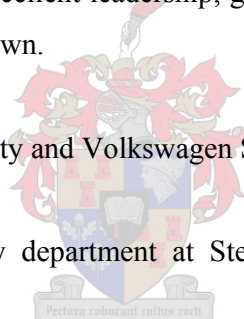
The late Mr. H.S.C. Spies, Elisna and Jean for outstanding NMR spectra.

Dr. J. Bacsa and Ms. Hong Su for the X-ray data collections.

Prof. G. Frenking, A. Timoshkin and Yu Chen for the collaboration on the quantum mechanical calculations.

Different aspects of the work in this study have been presented or published in the form of:

- An article: Raubenheimer H.G., Esterhuysen M.W., Timoshkin A., Chen Y., Frenking G. "Electrophilic addition of Ph_3PAu^+ to anionic alkoxy Fischer-type carbene complexes – a novel approach to metal stabilized bimetallic vinyl ether complexes", *Organometallics*, **2002**, *21*, 3173-3181.

- A lecture presented by Prof. H.G. Raubenheimer at the XIXth International Conference on Organometallic Chemistry (XIX ICOMC), 23rd-28th July 2000, Shanghai, China.

- A lecture presented by Prof. H.G. Raubenheimer at "Catalytic Gold – New industrial uses for Gold 2001" (CatGold I), 2nd-5th April 2001, Cape Town, South Africa.

- A lecture presented by Prof. H.G. Raubenheimer at the joint South African Chemical Society (SACI) & Catalysis Society of South Africa (CATSA) conference on Catalysis and Inorganic Chemistry, 4th-8th November 2001, Pilansberg, South Africa.

- A lecture presented by the author at the annual meeting of the South African Crystallographic Society (SACryst), 3rd-5th April 2002, Stellenbosch, South Africa.

- A lecture presented by the author at the South African Chemical Institute (SACI) - Young Chemists meeting (Western Cape section), 13th May 2002, Stellenbosch, South Africa.

- A lecture presented by the author at the Phillips Univrsität, Marburg, 14th December 2002, Marburg, Germany.
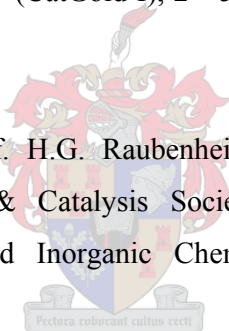
How much better to get wisdom than gold,

to choose understanding rather than silver!

Proverbs 16:16

CONTENTS

CHAPTER 1

INTRODUCTION AND AIMS

CHAPTER 2

NOVEL REACTIONS OF C-DEPROTONATED METHYL ALKOXY FISCHER-TYPE CARBENE ANIONS WITH TRIPHENYLPHOSPHINE GOLD(I) CHLORIDE

CHAPTER 3

NOVEL REACTIONS OF C-DEPROTONATED METHYL DIALKYLAMINO AND METHYL ALKYLTHIO FISCHER-TYPE CARBENE ANIONS WITH TRIPHENYLPHOSPHINE GOLD(I) CHLORIDE

CHAPTER 4

REACTIONS OF LITHIUM AND TETRABUTYLAMMONIUM ACYL- AND IMIDOYL-PENTACARBONYL CHROMATES AND TUNGSTATES WITH TRIPHENYLPHOSPHINE GOLD(I) CHLORIDE

Supplementary CD

The compact disk included in the back cover of this work contains:

- An electronic version (Word 2000) of the printed pages contained in this work, divided into the chapters presented here.

- Separate image files (Corel Draw) of the Figures, named according to the Figure captions presented in the hard copy.

- Separate files containing the Schemes (ISIS draw format), named according to the Scheme captions presented in the hard copy.

- All crystallographic information, including hkl data, cif files and structure factors, of the X-ray crystal structures presented in this work, numbered in separate directories according to the numbers assigned to these compounds in this work.

- Povray rendered 3D image files and animations (.avi format) of selected crystal structures presented in this work.

- Install files of the compression Codec (DivX4) required to view animations of the crystal structures.

ABBREVIATIONS

Å	Ångstrom (10^{-10} m)
Bu	Butyl
Cp	Cyclopentadienyl
CO	Carbon monoxide
Diglyme	Diethylene glycol dimethyl ether
Et	Ethyl
FAB-MS	Fast Atom Bombardment Mass Spectrometry
FT	Fourier Transform
^{i}Pr	Isopropyl
IR	Infrared
M^{+}	Molecular ion
M.p.	Melting point
M.W.	Molecular weight
Me	Methyl
MS	Mass Spectrometry
m/z	Mass/charge
NMR	Nuclear Magnetic Resonance
PPh$_3$	Triphenylphosphine
Ph	Phenyl
ppm	Parts per million
R	Alkyl, aryl or hydrogen group
^{t}Bu	Tertiary butyl
thf	Tetrahydrofuran
UV	Ultraviolet

NMR	br	Broad
	d	Doublet
	dd	Doublet of doublets
	δ	Chemical shift (ppm)
	J	Coupling constant (Hz)
	m	Multiplet
	ppm	Parts per million
	q	Quartet
	s	Singlet
	t	Triplet
Infrared	br	Broad
	m	Medium
	st	Strong
	sh	Shoulder
	v st	Very strong
	w	Weak
	v w	Very weak

CHAPTER 1

INTRODUCTION AND AIMS

1.1 General background

Interesting aspects of the versatile chemistry of Fischer-type carbene complexes combined with the unique reaction behaviour of gold(I) complexes are reported in this work. A short general discussion of important characteristics of both these fields of chemistry is therefore provided here.

1.1.1 Carbene chemistry

Carbenes, a neutral divalent form of carbon, are widely known and employed as building blocks in organic synthesis.[1] The main reason for this is that C-C bond formation reactions with carbenes often demonstrate remarkable stereoselectivity – a sought after reaction characteristic in organic syntheses (especially in the synthesis of natural products containing chiral centres). The simplest carbene is methylene ($:CH_2$), prepared by the thermolysis/photolysis of diazomethane. Other classical sources of carbenes include ketenes, trihalomethylmercury and α-haloalkyllithium compounds.[2] Carbenes are defined as divalent carbon atoms that are σ-bonded to only two other atoms (two hydrogen atoms in the case of methylene) and therefore possess two nonbonded electrons.[1] As a result of these electrons most carbenes are highly unstable and usually have a fleeting existence.

To facilitate their use, chemists have succeeded in devising two main methods of stabilising carbenes. These consist of preparing them as heterocyclic, sterically hindered molecules and/or as ligands coordinated to metal fragments. The latter method was first discovered by E.O. Fischer and A. Maasböl in 1964 and is currently still the most widely applied technique to stabilise the highly reactive unpaired electrons on carbenes.[3] Arduengo only reported the first preparation of stable free carbenes, as sterically hindered heterocyclic molecules, in 1991.[4] However, since N-heterocyclic carbenes are now, for the first time, available as "bottle-able" compounds (a phenyl substituted triazole-derived ylidene is the first commercially available

carbene),[5] their organic and organometallic chemistry has developed enormously in versatility and depth.[6] Despite this, the use of metal stabilised carbenes as building blocks in organic syntheses has, in the meantime, developed to such an extent - far beyond the original scope of organic carbene chemistry - that they have indeed become irreplaceable features in mainstream organic and organometallic chemistry.[7]

In transition metal carbene complexes the carbene carbon atom acts as a neutral $2e^-$-donor to the metal, and is consequently stabilised. Currently there are two main classes of carbene complexes, Fischer-type[3] and Schrock-type,[8] each bearing the names of their discoverers. The low valent, Fischer-type carbene complexes are characterised by an electrophilic carbene carbon atom, a transition metal that is usually in a low oxidation state, and a stabilising hetero-atom substituent (usually OR, NR_2 or SR) bonded to the carbene carbon atom. High valent, Schrock-type carbene complexes are characterised by a nucleophilic carbene carbon atom, a transition metal in a high oxidation state and the absence of a stabilising heteroatom on the carbene carbon atom.[7] It has, however, been pointed out that these definitions of carbene complexes are not applicable to all known examples.[9] For the purposes of this study only the particular characteristics of Fischer-type complexes will be discussed as only their reactions were investigated.

The metal carbene bond in Fischer-type carbene complexes is usually described by the Dewar-Chatt-Duncanson model as synergistic σ-electron donation from the lone pair on the carbene carbon atom to the empty metal d_{z^2} orbital, and metal back-donation of π-electrons from the metal d_{xz} or d_{yz} orbitals to the empty p(π) carbene carbon orbital (Scheme 1.1).[10]

Scheme 1.1

2
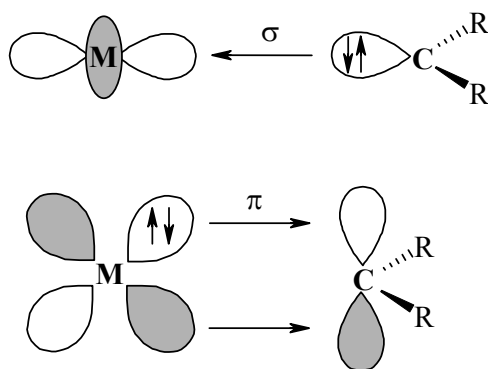
When Fischer and Maasböl prepared the first carbene complexes in 1964,[3] they found that low-valent metal carbonyls of Group 6 to 8 transition metals react with organolithium or Grignard reagents to produce metal-acyl anions that could be acidified and/or alkylated on the oxygen to give alkoxy(alkyl)transition metal carbene complexes in good yields (Scheme 1.2).
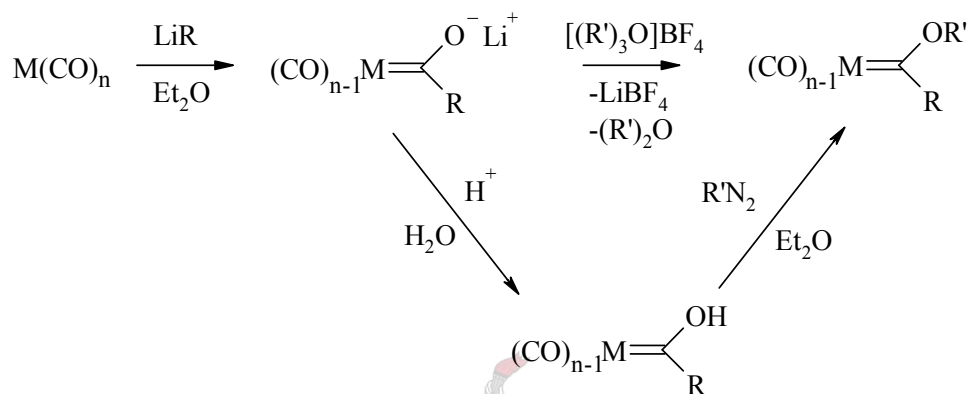
Scheme 1.2

Since the historic first synthesis of a carbene complex countless other examples have been prepared along a wide range of reaction paths. These preparative routes fall into two main categories: (1) The preparation of carbene complexes from non-carbene precursors, and (2) transformation reactions involving pre-existing carbene complexes. In the first category are: (1a) various transformation reactions of non-carbene ligands into carbene ligands - the carbene carbon atom is already attached to the metal centre in the complex precursor and (1b), addition reactions of carbene precursors to a metal fragment with concomitant transformation of the former into a carbene ligand.

The second category of preparative routes to Fischer-type carbene complexes is much more diverse, mainly as a result of the unique reaction characteristics that these complexes exhibit. In this category falls: (2a) transfer reactions of carbene ligands from one metal centre to another; (2b) several different modification reactions of the existing carbene ligand (further described below); (2c) insertion reactions of unsaturated organic molecules into the metal-carbene bond; (2d) changes of the

oxidation state of the central metal atom; and, (2e), modifications of the metal-ligand framework (described below). For a more detailed description of the various preparative routes to Fischer-type carbene complexes, see ref. 7 & 11.

Due to the unique electron-withdrawing properties of the metal carbonyl fragments in Fischer-type carbene complexes the carbene ligand can undergo a vast number of extremely useful modifications to yield countless variations on carbene complexes as well as many other useful organometallic species. This versatility of Fischer-type carbene complexes has led to their development as extremely useful synthons for a myriad of complex organic molecules. In this light, Fischer-type carbene complexes have been described as true "chemical multitalents".[12] By tailoring the electronic properties of the carbene complexes, through the introduction of various ligands to the metal fragment and different stabilising hetero-atoms to the carbene carbon atom, the reactive behaviour of Fischer-type carbene complexes (illustrated in Scheme 1.3 and the text description) can be "tuned" to meet the specific needs of a particular reaction.[12] As mentioned above, a characteristic of Fischer-type carbene complexes is the electrophilic nature of the carbene carbon atom which, therefore, is the preferred site of attack by nucleophiles, (**a**) in Scheme 1.3. This has become a very useful reaction for the preparation of Fischer-type carbene complexes stabilised by hetero-atoms other than oxygen (typically primary and sterically small secondary amines), thereby allowing modulation of the electrophilicity at the carbene carbon atom.[7]
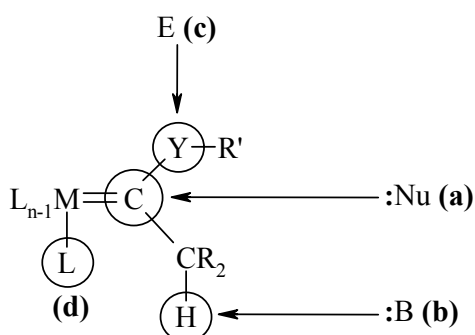
Scheme 1.3

Another extremely useful result of the electron-withdrawing nature of the metal fragment in Fischer-type carbene complexes is that the protons on carbon atoms in β-positions to the metal fragments are highly acidic (**b**). Countless electrophilic substitution reactions at the β-metallo carbon atom, yielding modified carbene

complexes, have been reported.[7] This characteristic, and the explanation for it, is discussed at length in the introduction to Chapter 2. Another result of the electron-withdrawing nature of the metal fragment in Fischer-type carbene complexes is that the hetero-atom (Y in Scheme 1.3) reacts with electrophiles (E – typically BX_3, X = Cl, Br, I), yielding a class of organometallic complex known as carbyne complexes (**c**).[13] Finally, similarly to the chemistry of metal carbonyl compounds, other ligands, typically phosphines, can be substituted for carbon monoxide at the metal atom [route **(d)** in Scheme 1.3].

Carbene complexes prepared and/or modified by the above-mentioned conversions to suit specific reaction conditions have proven their worth as reagents in various useful alkenylation,[14] cycloaddition (the so-called Dötz reaction),[14(a),15] insertion,[16] and cocyclization reactions,[17] to name but a few. These reactions of carbene complexes have been successfully applied to the preparation of many natural products, including peptides,[18] vitamins (K & E)[19] and several useful antibiotics.[20]

The intense research activity in the field of Fischer-type carbene complexes in the 1970's and 1980's has also led to their development as catalysts or catalyst precursors in several processes, including olefin metathesis reactions (and extension of the alkenylation reaction mentioned above),[21] polymerisation reactions of alkenes and alkynes,[22] and the catalytic preparation of various heterocyclic molecules.[23] Considering the scope of reactions of carbene complexes and the range of useful products obtained from these, it is clear that carbene complexes do their description as true "chemical multitalents" justice.

1.1.2 Gold chemistry

An examination of any organometallic textbook or encyclopaedia will show that the body of knowledge on organometallic gold compounds is remarkably underdeveloped compared to most of the remaining transition elements.[24] This is astonishing, since organogold derivatives have been known for almost 100 years.[25] Many fascinating and novel compounds and reactions involving organogold species have been discovered but, until recently, they have found little practical application. Since the 1970's the development of the organometallic chemistry of gold has, however, gained

considerable momentum. The stimulation of research in this field is partly the result of newfound applications for organogold compounds [e.g. in preparative organic chemistry,[26] as liquid crystals,[27] in thin film technology,[28] as pharmaceutical compounds (anti-tumourals and anti-arthritic),[29] in non-linear optics,[30] as luminescents[31] and as catalysts[32]] and partly the result of the development of routine structure determination by single crystal X-ray diffraction techniques. Structural determinations of organogold compounds by X-ray diffraction have provided chemists with a rapidly growing wealth of detailed structural information about these compounds. Not only were new oxidation states[33] and coordination numbers[24] discovered for gold, amongst a seemingly unlimited variety of compounds, but novel structural phenomena, mainly related to the repeated occurrence of unprecedented Au-Au contacts in the solid state, also came to light.[34] Indeed, the search for a satisfactory explanation for these short Au-Au contacts, also called "aurophilicity", has been a driving force behind many experimental and theoretical studies of organogold compounds.[35]

Structural chemists were the first to observe the effects of this strange interatomic attractive force between gold atoms, which, despite its weak nature, seemed to have a profound effect on molecular interactions and crystal lattices of gold compounds of all the known oxidation states.[36] Around this time, a revived interest in gold was developed by theoretical chemists and physicists who reconsidered the chemistry of the heaviest elements in the Periodic Table on the basis of relativistic effects.[37] These effects are especially important for those elements with extremely high nuclear charges, since they significantly modify the properties of the valence electrons in these elements. As a result the strange interatomic attractive force between gold atoms could be ascribed to relativistic effects. Since then the understanding of relativistic effects in gold chemistry has developed very well and it is currently consistent to the point where it is possible to not just analyse existing data, but to also predict new structures and properties.[38]

Relativistic effects for gold are currently understood, in simple terms, as follows: Electrons in atoms with high atomic numbers are under the influence of increased nuclear point charges and reach velocities that approach the velocity of light. These electrons, therefore, have to be treated according to Einstein's theories of relativity.

With the term v_e/v_l (v_e and v_l are the velocities of the electron and light respectively) close to 1, the 'relativistic mass' of the electron is significantly increased. This has a profound effect on the orbital radii (r) of these electrons. On the Periodic Table this effect, also called the 'relativistic contraction', reaches a pronounced maximum for gold with the ratio of the calculated relativistic to non-relativistic radii $[r_{(rel)}/r_{(non-rel)}]$ of the 6s orbital in gold being as low as ~0.81, compared to 0.94 for the 5s orbital in silver and 0.98 for the 4s orbital in copper.[24] In order to characterise the relativistic effect it is often divided into three interrelated 'symptoms'. 1) s-orbital, and to a smaller extent, p-orbital, contraction, 2) spin orbit coupling, and 3) d-orbital expansion. Combined, these 'symptoms' mean that the valence shell electrons in different subshells (s, p, d) are brought much closer in energy, especially with regards to the gap between the 6s and 5d states. Calculations have shown how these changes can partially 'mobilise' the $5d^{10}$ closed shell electrons for chemical bonding interactions, hence leading to weak Au-Au interactions.[39] The strength of these interactions (29-33 kJ/mol) is often described as being roughly the same range as hydrogen-bonding interactions. The interactions occur in the range 2.5-3.2Å and are thus shorter than the van der Waals contact (3.32Å) and in many cases the interatomic distance in gold metal (2.89Å).[36] There is, furthermore, evidence that Au-Au bonding may persist in solution[36] and even in the gas phase.[35] The availability of the Au(III) oxidation state, due to the relativistic destabilisation of the 5d orbital, and the marked tendency of the Au(I) oxidation state to form 14e⁻ linear two-coordinate complexes through particularly efficient 6s-6p-5d hybridisation, are just two further manifestations of this phenomenon.[39] Interestingly, the yellow colour of gold has also been attributed to these effects. The absorption is attributed to the 5d-to-Fermi level transitions, which set in at around 2.3 eV in gold. Elemental gold thus reflects red and yellow and strongly absorbs the blue and violet.[40] These characteristic properties of gold lead to the conclusion that it indeed occupies a unique position among the elements.

The preparation of organogold compounds is, like many other fields in gold chemistry, quite underdeveloped compared to the organometallic chemistry of most other transition metals. On the other hand, it is characterised by remarkably innovative approaches and an unexpected diversification in synthetic routes.[24] Organogold compounds are mostly prepared by transmetallation reactions of

organothallium, organozinc, organolithium or Grignard reagents with gold halides. Variations on these methods, to name but a few, include the use of tris[phosphinegold(I)]oxonium tetrafluoroborates instead of gold halides[41] and the use of stable gold(I)alkoxides or gold(I)acac, which yield organogold species upon reaction with CH-acidic ligands.[42] Using mainly the techniques mentioned above, chemists have prepared various organic derivatives of gold for both the common oxidation states of gold (+1 and +3). There is also an increasing number of organogold(II) compounds reported in the literature. However, these will be omitted from the following discussion as they are still very rare.[24] The predominant coordination numbers of gold are two (linear) for gold(I) and four (square planar) for gold(III) giving stable configurations with 14 and 16 electrons respectively. Homoleptic AuR and AuR_3 species are electron deficient and unstable. This is true even if they achieve a 'normal' coordination number through polymerisation *via* bridging halide, alkyl or aryl groups and 3-centre-2-electron bonds. Compounds of all possible stoichiometries are known, with one or two R-groups bonded to gold(I) and from one to four to gold(III), provided additional ligands are present to make up the required coordination number (Table 1.1).

Table 4.1: Possible stoichiometries in organogold compounds

Gold(I)		Gold(III)			
$AuR(L)$	AuR_2^-	$AuRX_2L$	$AuR_2(X)L$	AuR_3L	
$AuR(X)^-$		$AuRX_3^-$	$AuR_2X_2^-$	AuR_3X^-	AuR_4^-

L = neutral ligand; X = anionic ligand; R = organic group

1.2   Aims and objectives

The above brief introductory discussion of the chemistry of transition metal carbene complexes highlights their usefulness as synthons in organic transformations. However, whereas their chemistry as synthons in organic transformations has received an incredible amount of attention, their use as synthons in organometallic conversions is virtually unheard of. For unknown reasons the use of Fischer-type carbene complexes in preparative organometallic reactions did not develop alongside

the numerous studies investigating their usefulness in organic transformations. To our knowledge, the only exceptions are reports of carbene transfer reactions between transition metal ions[43] and the preparation of several metalloxy Fischer-type carbene complexes.[44] There are also isolated reports of reactions of a 'soft' electrophile (Ph_3PAuCl) with anionic Re-acyl complexes, $[Re_2(\mu\text{-}PPh_2)_2(CO)_7(ax\text{-}C(O)R)]$ (precursors of carbene complexes), and of SnR_3Cl with β-metallo carbon deprotonated Fischer-type carbene complexes.[45,46] Both the latter reactions are of great interest as they yield unusual and potentially useful organometallic species as products. Furthermore, metalloxy Fischer-type carbene complexes have recently proven their worth as efficient bimetallic catalysts in the copolymerisation of α-olefins (typically 1-pentene and 1-hexene)[44(b)] and have also been applied to the modulation of the reactivity of Fischer-type carbene complexes toward other organic transformations.[44(a)] Carbene transfer reactions between transition metals, although still poorly understood, have lead to the preparation of novel carbene complexes and could result in a better understanding of mechanistic aspects of catalytic processes in which such reactions are believed to play key roles.[43]

In the light of the usefulness of products obtained from the few reported reactions of Fischer-type carbene complexes with organometallic species, and the proven versatility of Fischer-type carbene complexes as synthons in organic transformations, we endeavoured to investigate reactions of group 6 Fischer-type carbene complexes, and more specifically nucleophiles derived from (or related to) these complexes (e.g. anionic "enolates", acyl-metal and imidoyl-metal complexes), with electrophilic gold(I) fragments. The chief objective of this study is to further the development of the utilisation of Fischer-type carbene complexes as useful synthons in organometallic conversions. In particular, conversions in which the Fischer-type carbene complexes are employed as synthetic equivalents of vinyl ether-, vinyl amine-, vinyl thioether-, acyl-, and imidoyl-anions in organometallic conversions with a gold(I) electrophile are investigated (Scheme 1.4). Also, with these conversions we aim to prepare and characterise novel organometallic complexes of gold(I) and thereby expand gold's relatively underdeveloped organometallic chemistry.

9

$$\left[L_{n-1}M = C \begin{array}{c} X \\ CH_2^- \end{array} \right] \equiv \left[{}^-C \begin{array}{c} X \\ CH_2 \end{array} \right]$$

X = OR, NR$_2$, SR

$$\left[L_{n-1}M = C \begin{array}{c} Y^- \\ R \end{array} \right] \equiv \left[{}^-C \begin{array}{c} Y \\ R \end{array} \right]$$
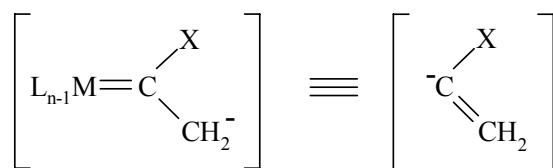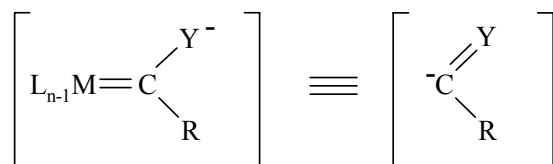
Y = OR, NR$_2$, SR

Scheme 1.4

The specific conversions studies were planned as follows:

As mentioned above, there is one isolated report in the literature of the reaction between β-metallo carbon deprotonated Fischer-type alkoxy carbene complexes and an organometallic fragment, SnR$_3$Cl. This reaction yields, instead of the expected β-metallo carbon SnR$_3$ substituted carbene complexes, useful α-stannyl vinyl ethers.[46] However, this report deals only with the products of the conversion and little attention is afforded to the reaction mechanism involved, or the possibility that other novel and potentially useful bimetallic complexes could be formed during this process. A related conversion, involving reactions between various group 6 metal β-metallo carbon deprotonated Fischer-type carbene complex derivatives and a gold(I) electrophile was envisaged. The principal objectives of this study were to: 1) determine what products are obtained in this conversion; 2) possibly further the use of Fischer-type carbene complexes as synthetic equivalents of anionic vinyl ether fragments; 3) propose a reaction mechanism for this conversion based on the products obtained and the well known, and successfully applied, isolobal relationship between Ph$_3$PAu$^+$ and H$^+$; 4) extend this reaction to Fischer-type carbene complexes with nitrogen and sulphur hetero-atoms and in the process prepare other novel gold(I) organometallic species; 5) determine whether this conversion can be employed to prepare novel bimetallic group

6 metal-gold(I) complexes. A large portion of the work reported here (chapters 2 & 3) deals with the study of this particular conversion and the novel products obtained from it. The intensive application of single crystal X-ray diffraction studies and, where necessary, quantum mechanical calculations in our investigations was, furthermore, also foreseen. Specific points addressed in this section of the study are listed in the introductions to the chapters.

Electrophilic addition reactions of metals to anionic metal-acyl complexes, yielding the metalloxy Fischer carbene complexes mentioned above, have mainly been described for anionic metal-acyl nucleophiles reacting with 'hard' electrophilic metal fragments (e.g. Cp_2TiCl_2, Cp_2ZrCl_2 and Cp_2HfCl_2). As noted above, the only exception to this is the recently reported addition of a gold(I) electrophile to an anionic Re-acyl complex, $[Re_2(\mu\text{-PPh}_2)_2(CO)_7(ax\text{-C(O)R})]^-$. This reaction yielded, instead of the expected metalloxy carbene complex, novel acylgold(I) complexes trapped by oxygen coordination to a $Re_2(\mu\text{-PPh}_2)_2(CO)_7$ fragment. An important objective of the work presented here is to determine if anionic group 6 metal acyl complexes react with a gold(I) electrophiles in the same manner as the Re-acyl complexes studied previously and, if so, to develop this synthetic route to prepare and characterise the first examples of free acylgold(I) complexes. Also, investigations into whether this reaction can be utilised as a novel method to prepare analogous imidoyl-gold(I) complexes, by employing N-deprotonated Fischer-type aminocarbene complexes as nucleophiles, instead of anionic metal-acyl complexes, were conducted. The specific points addressed in these investigations are listed in the introduction to chapter 4.

1.3   References

1.   Kirmse, W. *Carbene Chemistry*, 2nd ed., Academic Press, New York, **1971**.
2.   (a) Staudinger, H., Endle, R. *Ber. Dtsch. Chem. Ges.*, **1913**, *46*, 1437. (b) Staudinger, H., Goldstein, J. *Ber. Dtsch. Chem. Ges.*, **1916**, *49*, 1923. (c) Staudinger, H., Anthes, E., Pfenniger, F. *Ber. Dtsch. Chem. Ges.*, **1916**, *49*, 1928. (d) Seyferth, D., Burlitch, J.M., Minasz, R.J., Mui, Y.-P., Simmons,

H.D. Jr., Treiber, A.J.H., Dowd, S.R. *J. Am. Chem. Soc.*, **1965**, *87*, 4259. (e) Körbrich, G. *Angew. Chem., Int. Ed. Engl.*, **1967**, *6*, 41.

3. Maasböl, A., Fischer, E.O. *Angew. Chem., Int. Ed. Engl.*, **1964**, *3*, 580.

4. (a) Arduengo III, A.J., Harlow, R.L., Kline, M. *J. Am. Chem. Soc.*, **1991**, *113*, 361. (b) Arduengo III, A.J., Kline, M., Calabrese, J.C., Davidson, S. *J. Am. Chem. Soc.*, **1991**, *113*, 9704.

5. Arcos Organics, Dat. No. 30226-0010.

6. Herrmann, W.A. *Angew. Chem., Int. Ed. Engl.*, **2002**, *41*, 1290.

7. Dötz, K.H. *Angew. Chem., Int. Ed. Engl.*, **1984**, *23*, 5878.

8. Schrock, R.R. *Acc. Chem. Res.*, **1979**, *12*, 98.

9. Coalter III, J.N., Bollinger, J.C., Huffman, J.C., Werner-Zwanziger, U., Caulton, K.G., Davidson, E.R., Gérard, H., Clot, E., Eisenstein, O. *New. J. Chem.*, **2000**, *24*, 9.

10. (a) Dewar, M.J.S. *Bull. Soc. Chim. Fr.*, **1951**, *18*, C79. (b) Chatt, J., Duncanson, L.A. *J. Chem. Soc.*, **1953**, 2929.

11. Wulff, W.D. in "*Comprehensive Organometallic Chemistry II, Vol 12,*" Eds. Abel, E.W., Stone, F.G.A., Wilkinson, G., Hegedus, L.S., Pergamon, Oxford, **1995**, p 469.

12. de Meijere, A., Schirmer, H., Duetsch, M. *Angew. Chem., Int. Ed. Engl.*, **2000**, *39*, 3964.

13. Schubert, U., Hartley, F.R., Patai, S. "*The Chemistry of the Metal-Carbon Bond*", Wiley, Chichester, **1982**, p 233.

14. (a) Fischer, E.O., Dötz, K.H. *Chem. Ber.*, **1972**, *105*, 3966. (b) Casey, C.P., Burkhardt, T.J. *J. Am. Chem. Soc.*, **1972**, *94*, 6543. (c) Casey, C.P., Burkhardt, T.J., Bunnel, C.A., Calabrese, J.C. *J. Am. Chem. Soc.*, **1977**, *99*, 2127.

15. (a) Fischer, E.O., Dötz, K.H. *Chem. Ber.*, **1970**, *103*, 1273. (b) Dötz, K.H., Fischer, E.O. *Chem. Ber.*, **1972**, *105*, 1356.

16. (a) Connor, J.A., Rose, P.D. *J. Organomet. Chem.*, **1970**, *24*, C45. (b) Fischer, E.O., Dötz, K.H. *J. Organomet. Chem.*, **1972**, *36*, C4.

17. Dötz, K.H. *Angew. Chem., Int. Ed. Engl.*, **1975**, *14*, 644.

18. (a) Weiss, K., Fischer, E.O. *Chem. Ber.*, **1976**, *109*, 1868. (b) Weygand, F., Hoffmann, D., Wünsch, E. *Z. Naturforsch.*, **1966**, *B21*, 426.

19. (a) Dötz, K.H., I. Pruskil, *J. Organomet. Chem.*, **1981**, *209*, C4. (b) Dötz, K.H., I. Pruskil, Mühlemeier, J. *Chem. Ber.*, **1982**, *115*, 1278. (c) Dötz, K.H.,

Kuhn, W. *Angew. Chem., Int. Ed. Engl.*, **1983**, *22*, 732.; *Angew. Chem. Suppl.*, **1983**, 1045.

20. (a) Semmelhack, M.F., Bozell, J.J., Sato, T., Wulff, W.D., Spiess, E., Zask, A. *J. Am. Chem. Soc.*, **1982**, *104*, 5058. (b) Wulff, W.D., Tang, P.-C. *J. Am. Chem. Soc.*, **1984**, *106*, 434. (c) Kende, A.S., Tsay, Y.G., Mills, J.E. *J. Am. Chem. Soc.*, **1976**, *98*, 1967.

21. (a) Casey, C.P., Burkhardt, T.J. *J. Am. Chem. Soc.*, **1974**, *96*, 7808. (b) Schrock, R.R. *Science*, **1983**, *219*, 13.

22. (a) Katz, T.J., Lee, S.J. *J. Am. Chem. Soc.*, **1980**, *102*, 422. (b) Turner, H.W., Schrock, R.R., Fellmann, J.D., Holmes, S.J. *J. Am. Chem. Soc.*, **1983**, *105*, 4942.

23. (a) Ito, Y., Hirao, T., Saegusa, T. *J. Organomet. Chem.*, **1977**, *131*, 121. (b) Ito, Y., Hirao, T., Saegusa, T. *J. Org. Chem.*, **1975**, *40*, 2981.

24. (a) Puddephatt, R.J. in "*Comprehensive Organometallic Chemistry*", Eds. Abel, E.W., Stone, F.G.A., Wilkinson, G., Hegedus, L.S., Pergamon, Oxford, **1982**, p.765. (b) Grohmann, A., Schmidbaur, H. in "*Comprehensive Organometallic Chemistry II*", Eds. Abel, E.W., Stone, F.G.A., Wilkinson, G., Hegedus, L.S., Pergamon, Oxford, **1995**, p1. (c) Patai, S., Rappoport, Z. eds. "*The Chemistry of Organic Derivatives of Gold and Silver*", J. Wiley & Sons, Chichester, **1999**.

25. (a) Pope, W.J., Gibson, C.S. *J. Chem. Soc.*, **1907**, 2061. (b) Pope, W.J., Gibson, C.S. *Proc. Chem. Soc.*, **1908**, *23*, 245.

26. (a) Vicente, J., Bermúdez, M.D., Carrión, F-J., Jones, P.G. *Chem. Ber.*, **1996**, *129*, 1395. (b) Vicente, J., Bermúdez, M.D., Carrión, F-J. *Inorg. Chem. Acta*, **1994**, *220*, 1. (c) Sone, T., Ozaki, S., Kasuga, N.C., Fukuoka, A., Komiya, A. *Bull. Chem. Soc., Jpn.*, **1995**, *68*, 1523. (d) Murukami, M., Inouye, M., Suginome, M., Ito, Y. *Bull. Chem. Soc., Jpn.*, **1988**, *61*, 3649. (e) Cinellu, M.A., Zucca, A., Stoccoro, S., Mignhetti, G., Manassero, M., Sansoni, M. *J. Chem. Soc., Dalton Trans.*, **1995**, 2865.

27. (a) Coco, S., Espinet, P., Martin-Alvarez, J.M., Levelut, A.M. *J. Mat. Chem.*, **1997**, *7*, 19. (b) Bruce, D.W., Lalinde, E., Styring, P., Dunmur, D.A., Maitlis, P.M. *J. Chem. Soc., Chem. Commun.*, **1986**, 581.

28. (a) Messelhaüser, J., Flint, E.B., Suhr, H., *Appl. Surf. Sci.*, **1992**, *54*, 64. (b) Banasek Holl, M.M., Seider, P.F., Kowalczyk, S.P., McFreely, F.R. *Inorg. Chem.*, **1994**, *33*, 510. (c) Uchida, H., Saito, N., Sato, N., Yake, M., Ogi, K. *Jap. Patent,* 6-145985, **1994** & *Jap. Patent,* 5-331176, **1993**. (d) Banasek Holl, M.M., Kowalczyk, S.P., McFreely, F.R., Seider, P.F. *European Patent* 588 080 A1, **1994**. (e) Tamaki, A, Kochi, J.K. *J. Organomet. Chem.*, **1973**, *61*, 441.

29. (a) Buckly, R.G., Elsome, A.M., Frickler, S.P., Henderson, G.R., Theobald, B.R.C., Parish, R.V., Howe, B.P., Kelland, L.R. *J. Med. Chem.* **1996**, *39*, 5208. (b) Parish, R.V. *Gold Bull.*, **1987**, *20*, 3.

30. Olsen, A.W., Kafafi, Z.H. *J. Am. Chem. Soc.*, **1991**, *113*, 7758.

31. (a) Jones, W.B., Yuan, J., Narayanaswamy, R., Young, M.A., Elder, R.C., Bruce, A.E., Bruce, M.R.M. *Inorg. Chem.*, **1995**, *34*, 1996. (b) Li, D., Hong, X., Che, C-M., Lo, W-C., Peng, S-M. *J. Chem. Soc., Dalton Trans.*, **1993**, 2929. (c) Yam, V. W-W., Choi, S.W-K. *J. Chem. Soc., Dalton Trans.*, **1994**, 2057.

32. (a) Teles, J.H., Brode, S., Chabanas, M. *Angew. Chem., Int. Ed. Engl.*, **1998**, *37*, 1415. (b) Tamaki, A., Magennis, S.A., Kochi, J.K. *J. Am. Chem. Soc.*, **1974**, *96*, 6140. (c) Komiya, S., Sone, T., Usui, Y., Hirano, M., Fukoaka, A. *Gold Bull.*, **1996**, *29*, 131 and references therein. (d) Fukuda, Y., Utimoto, K. *Synthesis*, **1991**, 975. (e) Soloshonok, V.A., Hayashi, T. *Tetrahedron Asymm.*, **1994**, *6*, 1091, and references therein. (f) Saegusa, T., Ito, Y., Kobayashi, S., Hirota, K., Yoshioka, H. *Bull. Chem. Soc., Jpn.*, **1969**, *42*, 3310. (g) Parks, J.E., Balch, A.L. *J. Organomet. Chem.*, **1974,** *71*, 453.

33. Schmidbaur, H., Dash, K.C. *Adv. Inorg. Chem. Radiochem.*, **1982**, *25*, 239.

34. Puddephatt, R.J., *"The Chemistry of Gold"*, Elsevier, Amsterdam, **1978**.

35. Schmidbaur, H. *Gold. Bull.*, **1990**, *23*, 1 and references therein.

36. (a) Jones, P.G., *Gold Bull.*, **1981**, *14*, 102 and 159. (b) *ibid*., **1983**, *16*, 114. (c) *ibid*., **1986**, *19*, 46.

37. (a) Pyykkö, P., Desclaux, J.P. *Acc. Chem Res.*, **1979**, *12*, 276. (b) Pitzer, K.S., *ibid*., **1979**, *12*, 271 and references therein.

38. Pyykkö, P. *Chem. Rev.*, **1988**, *88*, 563 and references therein.

39. (a) Rösch, N., Görling, A., Ellis, D.E., Schmidbaur, H. *Angew. Chem., Int. Ed. Engl.*, **1989**, *28*, 1357. (b) Jiang, Y., Alvarez, S., Hoffmann, R. *Inorg. Chem.*, **1985**, *24*, 749. (c) Merz, K.M., Hoffmann, R. *Inorg. Chem.*, **1988**, *27*, 2120. (d) Mehrotra, P.K., Hoffmann, R. *Inorg. Chem.*, **1978**, *17*, 2187. (e) Dedieu, A., Hoffmann, R. *J. Am. Chem. Soc.*, **1978**, *100*, 2074.

40. Klapötke, T.M., Tornieporth-Oetting, "*Nichtmetallchemie*", VCH, Weinheim, **1994**, 71.

41. Perevalova, E.G., Reshetova, M.D., Kokhanyuk, G.M. *J. Gen. Chem. USSR*, **1984**, 2424.

42. Komiya, S., Iwata, M., Sone, T., Fukuoka, A. *J. Chem. Soc., Chem. Commun.*, **1992**, 1109.

43. (a) Liu, S.-T., Reddy, K.R. *Chem. Soc. Rev.*, **1999**, *28*, 315. (b) Barluenga, J., López, L.A., Löber, O., Tomás, M., Garcia-Granda, S., Alvarez-Rúa, C., Borge, J. *Angew. Chem., Int. Ed. Engl.*, **2001**, *40*, 18. (c) Sierra, M.A., del Amo, J.C., Mancheño, M.J., Gómez-Gallego, M. *J. Am. Chem. Soc.*, **2001**, *123*, 851.

44. (a) Barluenga, J., Fañanás, F.J. *Tetrahedron*, **2000**, *56*, 4597. (b) Brüll, R., Kgosane, D., Neveling, A., Pasch, H., Raubenheimer, H.G., Sanderson, R., Wahner, U.M. *Macromol. Symp.*, **2001**, *165*, 11.

45. Haupt, H.–J., Petters, D., Flörke, U. *J. Organomet. Chem.*, **1998**, *553*, 497.

46. McDonald, F. E.; Schultz, C. C.; Chatterjee, A. K. *Organometallics*, **1995**, *14*, 3628.

CHAPTER 2

NOVEL REACTIONS OF C-DEPROTONATED METHYL ALKOXY FISCHER-TYPE CARBENE ANIONS WITH TRIPHENYLPHOSPHINE GOLD(I) CHLORIDE

2.1   Introduction

As already mentioned in Section 1.1, one unique and extremely useful characteristic of Fischer-type carbene complexes, discovered by Kreiter in 1968, is the remarkable acidity of protons on their β-metallo carbon atoms.[1] In fact, alkoxy Fischer-type carbene complexes are some of the most acidic CH-acids known, with reported pK_a values ranging between ~8 (thf) and ~23 (acetonitrile) for $(CO)_5Cr=C(OCH_3)CH_3$.[2] By its very nature the β-metallo CH acidity is linked to the electrophilic character of the carbene carbon, which, in turn, is caused by the strongly electron-withdrawing properties of the metal carbonyl moiety. The acidity can best be explained on the basis of resonance forms of the carbene complexes and their conjugate bases. These describe delocalisation of electrons from the hetero-atom (for the neutral complexes) or the carbanionic centre (for the conjugate bases) to the metal atom from where electrons are delocalised to the ligands, L_n (Scheme 2.1).[3]

Scheme 2.1

16
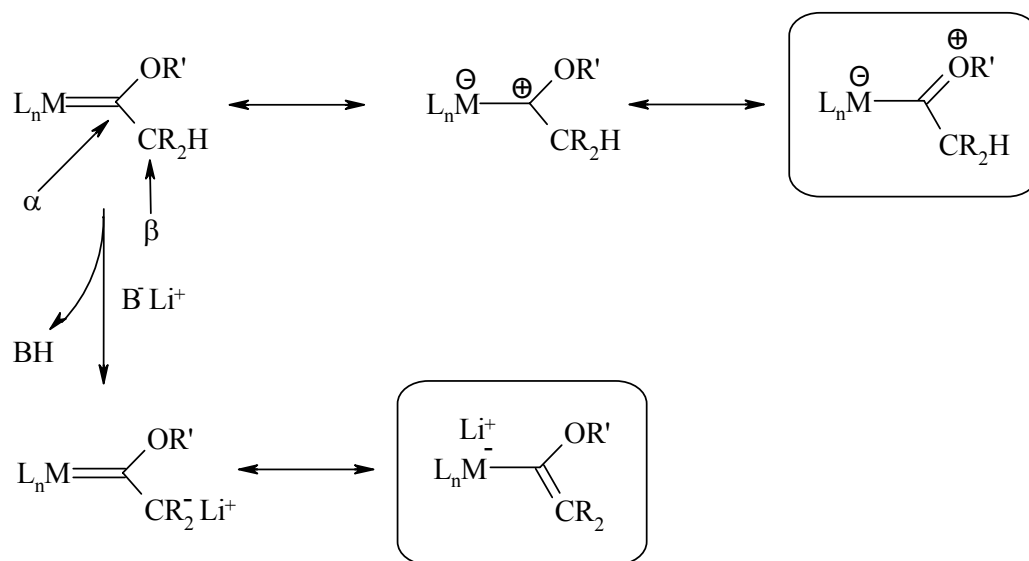
The conjugate bases of the carbene complexes are stabilised by the delocalisation of their negative charges to the metal atom, thus increasing the acidity of the neutral complexes. The extent of charge delocalisation from the carbanionic centre to the metal atom is, however, largely determined by the amount of charge already donated from the hetero-atom *via* the carbene carbon to the metal atom, thus linking the acidity of Fischer-type carbene complexes with the electron donating capabilities of their hetero-atoms.[2] The acidity of Fischer-type carbene complexes that are stabilised by other hetero-atoms than oxygen is discussed at length in Chapter 3. Furthermore, solid-state structures and spectroscopic studies of Fischer-type carbene complexes and their anions authenticate the highlighted resonance forms for Fischer alkoxycarbene complexes and their anions illustrated in Scheme 2.1.[4]

Since Kreiter's discovery, Casey has led the way in utilising the β-metallo CH acidity for the functionalisation of carbene ligands *via* deprotonation and alkylation reaction sequences.[3(b)] In this manner, countless useful β-substituted carbene complexes, which were often employed as synthons for the synthesis of more complex organic molecules, could be prepared [Scheme 2.2(a)].[5]

Conventional electrophilic addition products

**Alternative electrophilic addition products**

(a)

(b)
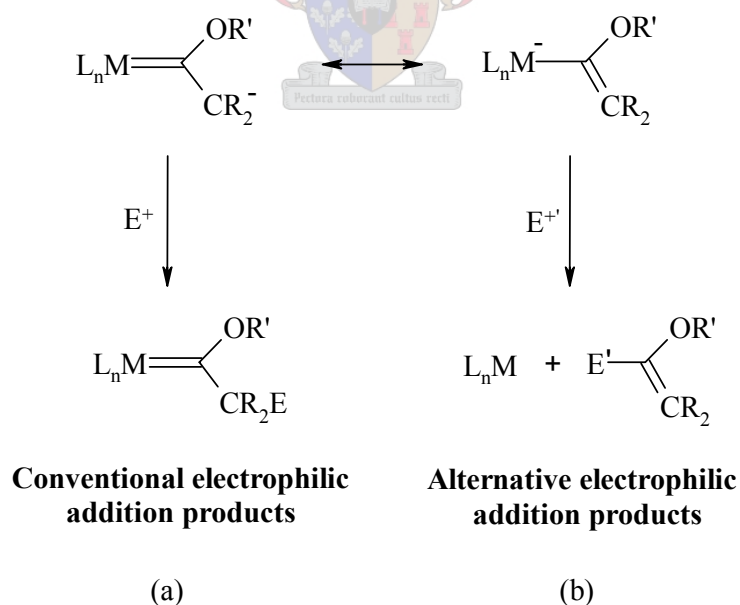
Scheme 2.2

Electrophilic addition at the β-C position is, however, not the only possible conversion in these reactions. In the presence of pyridine or tertiary amines, or during thermal decomposition in the presence of water or OH⁻-ions, it was found that

Fischer-type carbene complexes with acidic β-metallo hydrogen atoms readily yield vinyl ethers, aldehydes, alcohols and ketones, containing the functional groups from the original carbene ligand, as products of their decomposition.[2,6] At first Fischer ascribed these observations to cleavage of the metal-carbene bond by the pyridine ligand, followed by rearrangement of the free carbene to a vinyl ether, and suggested this as proof that these complexes could be employed as a source of free carbenes.[6]

Casey, however, postulated otherwise when he observed that pyridine does not catalyse the decomposition of Fischer-type carbene complexes when no acidic hydrogen on the β-metallo carbon atom is present. Taking this acidity of Fischer-type carbene complexes into account, he suggested a hydrolytic pathway for this conversion (Scheme 2.3).[3(b)]
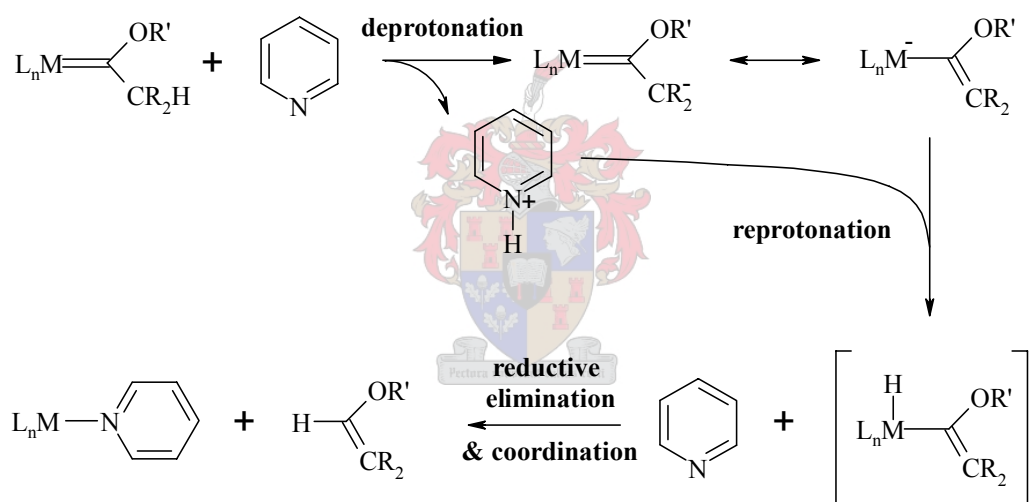
Scheme 2.3

In Casey's mechanism the basic pyridine deprotonates the acidic carbene complex [which is mainly represented by the α-metallo-vinyl ether resonance structure after deprotonation (Scheme 2.1)], reprotonates at the metal atom and finally coordinates to the metal pentacarbonyl fragment after a formal reductive elimination yields a free vinyl ether fragment as an alternative electrophilic addition product [Scheme 2.2 (b)].

Casey's suggested mechanism, as well as reactions of Fischer-type carbene complexes with other bases (e.g. OH⁻ ions), has been the subject of much attention by the group of Bernasconi.[2] By determining thermodynamic and kinetic parameters for several similar base hydrolysis reactions of Fischer-type carbene complexes, they

have concluded that Casey's mechanism is indeed by far the most likely.[7] Another possible mechanism for the hydrolysis reaction in the presence of a tertiary amine and water, suggested by Aumann (Scheme 2.4),[8] was ruled out by Bernasconi. This mechanism does not allow for the formation of vinyl ethers, as was observed by both Fischer and Casey, and also gives a poor fit to the kinetic and thermodynamic data measured by Bernasconi for these complexes. Aumann's proposal was an attempt to explain the occurrence of aldehydes and alcohols that were also found amongst the hydrolysis products of Fischer-type carbene complexes. He suggested that an OH^-, generated by the acid-base reaction of the amine with a water molecule, performs a nucleophilic attack at the carbene carbon atom, substituting the OR' group and forming the alcoholic product. Subsequent reprotonation from the conjugated acid of the amine then produces a hydroxycarbene complex that decomposes to an aldehyde and an amine-coordinated metal pentacarbonyl fragment.
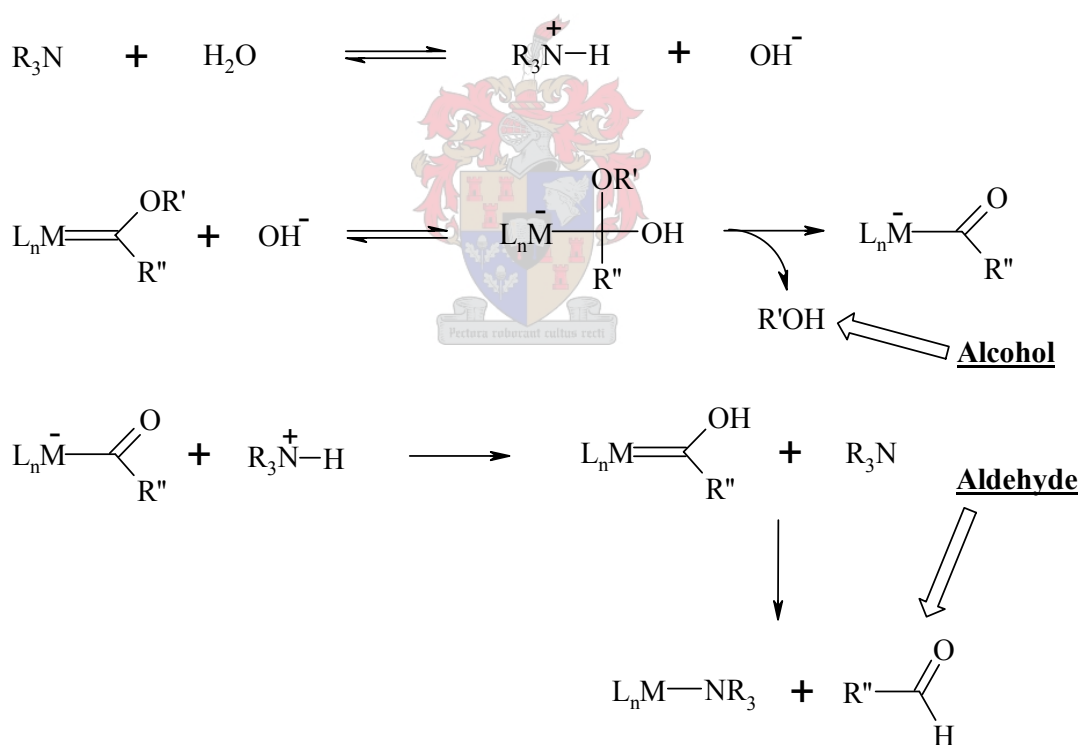
Scheme 2.4

Bernasconi explains the formation of aldehyde and alcoholic hydrolysis products after the initial hydrolysis of the carbene complexes, *via* Casey's mechanism, as follows: After the formation of the vinyl ether by reprotonation on the metal and formal reductive elimination, the vinyl ether coordinates to the $M(CO)_5$ fragment through the

vinyl moiety. This activates the vinyl ether towards further hydrolysis in a basic medium, thus converting it to the corresponding aldehyde and alcohol (Scheme 2.5).[7,9]
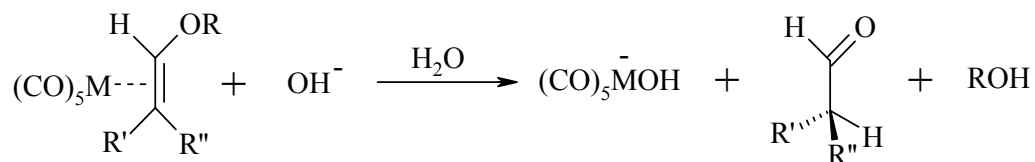
Scheme 2.5

Bernasconi's suggestion fits the experimental kinetic and thermodynamic data and is supported by the observation that bulkier vinyl ether fragments (e.g. PhCH=CHOMe) formed during the hydrolysis of the carbene complexes are not hydrolysed as they are sterically hindered from coordinating to the $M(CO)_5$ fragment. Also, when an excess of pyridine is present (as there was when Fischer first reported the formation of vinyl ethers in this reaction when he used pyridine as the solvent!),[4] the vinyl ether hydrolysis products are exclusively obtained, most likely because coordination of the vinyl ether to the $M(CO)_5$ fragment is hindered by a coordinating pyridine molecule. Furthermore, attempts to prepare neutral alkyl(vinyl)ether-$M(CO)_5$ complexes along other reaction pathways [e.g. displacement of CH_3CN by a vinyl ether in photochemically prepared $(CO)_5M(CH_3CN)$] have also resulted in the formation of the corresponding aldehyde and alcohol hydrolysis products described above, thus adding further weight to Bernasconi's proposed secondary hydrolysis mechanism.[10]

It is interesting to note that, according to Casey and Bernasconi's carbene hydrolysis mechanism, the base decomposition reaction of β-metallo CH acidic Fischer-type carbene complexes results in a shift of the electrophilic addition onto the α-metallo carbon atom from the β-metallo carbon, resulting in the formation of alternative electrophilic addition products [Scheme 2.2 (b)]. In other words: The delocalisation of the negative charge in the β-metallo carbon deprotonated Fischer carbene anion onto the metal carbonyl fragment effectively results in addition of an electrophile to a carbon atom which initially is electrophilic and known to be prone to nucleophilic attack. On these grounds this type of conversion can also be described as an "Umpolung".[11]

A literature search revealed that there are very few examples, other than the base hydrolysis of Fischer-type carbene complexes, where addition of electrophiles to the

α-metallo carbon atom has been achieved. The most notable example is one by the group of McDonald, where the addition of tributyltin chloride/triflate to β-C deprotonated Fischer-type carbene complexes to yield α-stannyl vinyl ethers is described.[12] This work has recently been applied to the synthesis of various useful α-stannyl vinyl ethers, to be used as synthons in the synthesis of complex heterocyclic organic compounds,[13] and serves as the sole example where this reaction mechanism has been employed to synthesise an alkoxyvinyl metal product. McDonald, however, generates the carbene complexes used in his reactions *in situ* by endocyclisation of 1-alkyn-5-ols with an $W(CO)_5L$ (L = labile ligand) moiety in the presence of a tertiary amine, and pays little attention to the reaction mechanism and the possible organometallic reaction intermediates suggested for this reaction.[12] In all known examples in which carbon electrophiles have been added to β-metallo carbon deprotonated Fischer-type carbene complexes, electrophilic addition occurs at the site of deprotonation.[5]

It is also worth mentioning that the addition of iodine to anionic Fischer-type carbene complexes in a basic medium and the 1,5 addition of halogens and pseudohalogens to cyclopropyl(thio)carbene-$Cr(CO)_5$ complexes yield alkoxyvinyl halides as one of the products. Although the latter reaction has recently been applied to the synthesis of organic compounds, the specific mechanisms are not straightforward and many competing conversions are involved.[14]

Interestingly, the reverse process of the alternative hydrolytic reaction pathway discussed above has recently been discovered. Its mechanism involves the formation of Fischer-type ruthenium carbene complexes from the insertion of π-coordinated vinyl ethers into Ru-H bonds followed by α-H migration back to the Ru atom. This facile isomerisation route to carbene complexes is believed to be enabled by the formation of a stable Ru-H bond and the presence of a 14e⁻ Ru-metal fragment.[15]

In light of the results described above, and more specifically, the lack of clear and definite examples of electrophilic addition reactions to Fischer-type alkoxy carbene anions that yield the alternative electrophilic addition products [Scheme 2.2(b)], we embarked on an investigation of the addition of the Ph_3PAu^+ electrophile to β-metallo carbon deprotonated Fischer-type alkoxy carbene anions. Ph_3PAu^+ [in the form of either Ph_3PAuCl or $Ph_3PAu(NO_3)$] was chosen as the model electrophile for several reasons: It is relatively stable;[16] it is non-toxic; it gives distinct and clear

21

spectroscopic data that can be directly interpreted; it is isolobal with H^+,[17] which is known to undergo the alternative electrophilic addition to Fischer carbene anions under certain conditions;[7] it is a large and 'soft' electrophile that is likely to interact with anionic transition metal ions; although it is sterically large, the linear geometry of gold(I) bonds allows for facile interaction with the metal centre of the carbene complex anion;[18] finally, the organometallic chemistry of gold(I), specifically Au-C bond formation reactions, is relatively underdeveloped.[16]

The contents of this chapter describes the results obtained in our endeavour and specifically addresses the following questions:

1) Would electrophilic addition of the Ph_3PAu fragment, as with R_3Sn fragment, occur at the metal centre, or at the site of deprotonation, as is usually the case?

2) If electrophilic addition occurs at the metal centre, would a formal reductive elimination of alkoxyvinyl-gold(I)PPh_3 occur or would a M-Au bond persist, like in many gold cluster complexes?

3) If a formal reductive elimination of a vinyl ether fragment does occur, would the formed alkoxyvinyl-gold(I)PPh_3 fragment, in the absence of other efficient ligands, coordinate to the newly formed metal pentacarbonyl fragment, and would this coordination, if it takes place, be through the vinyl double bond or through the oxygen atom in the vinyl ether?

4) If coordination of the alkoxyvinyl-gold(I)PPh_3 takes place through the vinyl group, would the vinyl ether, like other non-metallated $M(CO)_5$-coordinated alkyl(vinyl)ether fragments, be activated towards base hydrolysis or would stable bimetallic complexes be formed?

5) If stable bimetallic complexes are formed, could they be isolated and structurally characterised in order to determine the reason for their stability?

6) Finally, could such $M(CO)_5$ coordinated alkoxyvinyl-gold(I)PPh_3 fragments be liberated from the metal coordination by substitution with stronger binding ligands than olefins (e.g. PPh_3) to allow isolation and characterisation of the free alkoxyvinyl-gold(I)PPh_3 complexes?

2.2 Results and discussion

2.2.1 η^2-{Methoxyvinyl-gold(I)triphenylphosphine} M(CO)$_5$ and η^2-{Ethoxyvinyl-gold(I)triphenylphosphine} M(CO)$_5$ bimetallic complexes
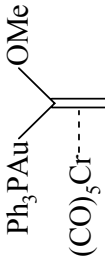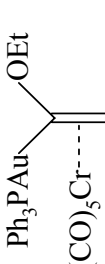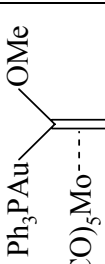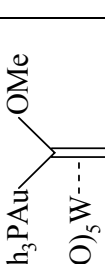
A. General preparation and discussion of the compounds η^2-{Ph$_3$PAu C(OR)=CH$_2$}M(CO)$_5$; M = Cr, R = Me (**1**) / R = Et (**2**); M = Mo, R = Me (**3**); M = W, R = Me (**4**) / R = Et (**5**)

The syntheses of complexes **1-5** (Scheme 2.6) were carried out by the deprotonation of the respective group 6 metal pentacarbonyl alkoxy(methyl)carbene complexes in thf at -78°C with 1 mole equiv. of *n*-butyllithium, followed by the addition of 1 mole equiv. Ph$_3$PAuCl or Ph$_3$PAu(NO$_3$). The reaction mixture was subsequently allowed to warm up to room temperature over a period of 3 hours. Product separation of dark-yellow to brown oily reaction mixtures (45-71% yields after separation) was carried out by low temperature (-15°C) silica gel column chromatography with pentane/diethyl ether (10:1) as eluant. Final purification was performed by crystallisation from diethyl ether solutions of **1-5** layered with pentane at -20°C. Physical data for the isolated new compounds are summarised in Table 2.1.

1: M = Cr, R = Me
2: M = Cr, R = Et
3: M = Mo, R = Me
4: M = W, R = Me
5: M = W, R = Et

Scheme 2.6

23
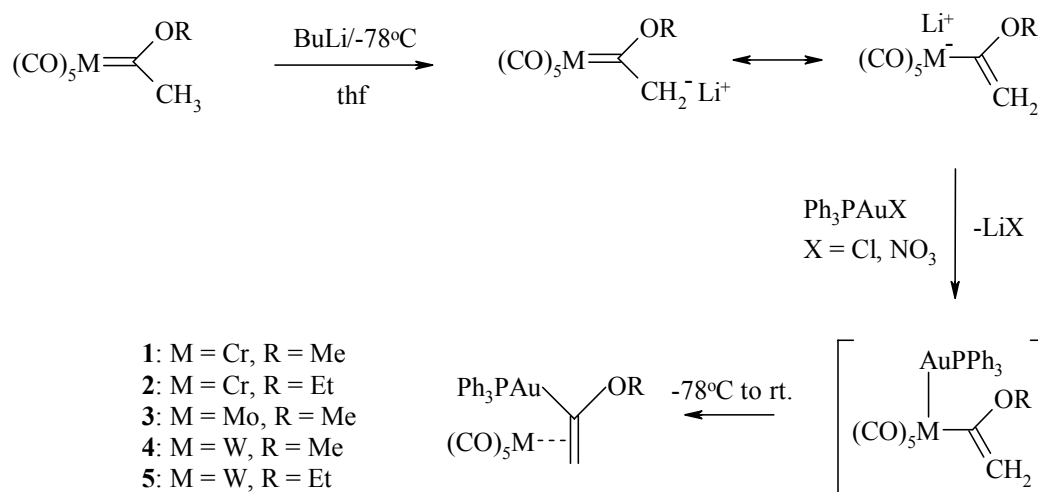
Table 2.1: Analytical Data for complexes **1-5**

Complex	Ph₃PAu $\diagup$ OMe, (CO)$_5$Cr	Ph₃PAu $\diagup$ OEt, (CO)$_5$Cr	Ph₃PAu $\diagup$ OMe, (CO)$_5$Mo	Ph₃PAu $\diagup$ OMe, (CO)$_5$W	Ph₃PAu $\diagup$ OEt, (CO)$_5$W
Complex	**1**	**2**	**3**	**4**	**5**
M.p. / °C	106 (decomp.)	96 (decomp.)	84 (decomp.)	112 (decomp.)	106 (decomp.)
Colour	yellow	yellow	dark yellow	yellow	yellow
Yield (%)	67	71	53	45	63
M.W. (g / mol)	708.37	722.40	752.32	840.23	854.25
Analyses (%)[a]					
C	44.25 (44.09)	45.12 (44.89)	41.45 (41.51)	37.35 (37.17)	37.81 (37.96)
H	2.98 (2.85)	3.02 (3.07)	2.64 (2.68)	2.62 (2.40)	2.45 (2.60)
O	13.26 (13.55)	13.38 (13.29)	12.90 (12.76)	11.53 (11.42)	11.38 (11.24)
P	4.30 (4.37)	4.21 (4.29)	4.15 (4.12)	3.85 (3.69)	3.60 (3.63)

[a] Required values given in parenthesis

We accept, as a working hypothesis, the hydrolysis reaction mechanism suggested by Casey and Bernasconi (Section 2.1) for the formation of the alkoxyvinyl-gold(I) complexes by sequential auration of the metal carbonyl, a formal reductive elimination of the gold vinyl ether and vinyl double bond coordination to the $M(CO)_5$ fragment.[7] The formation of these η^2-coordinated {alkoxyvinyl-gold(I)PPh$_3$}M(CO)$_5$ bimetallic complexes (**1-5**), *via* the hydrolysis-type reaction pathway can, on account of the well-documented and successfully applied isolobal relationship between Ph_3PAu^+ and H^+,[17] also be described as an "aurolysis" reaction.

Slippage of η^2-vinyl coordination modes towards η^1-coordination in general greatly activates olefin complexes towards nucleophilic addition reactions.[19] As discussed in section 2.1, such activation is observed in the complexation of non-metallated vinyl ethers to group 6 $M(CO)_5$ fragments and is also postulated by Bernasconi as a step in the formation of the final alcoholic and aldehyde hydrolysis products of Fischer-type carbene complexes (Scheme 2.5).[7] In contrast to the above-mentioned findings, activation of the alkoxyvinyl-gold(I)PPh$_3$ complexes, which are asymmetrically coordinated to $M(CO)_5$ fragments in complexes **1-5**, towards hydrolysis was not observed. In fact, **1-5** are stable in mildly basic or acidic environments and could be purified effectively by silica gel column chromatography. Control reactions to prepare the gold free ethyl(vinyl)ether-$M(CO)_5$ complexes in neutral media by irradiation of group 6 $M(CO)_6$ with UV light in thf followed by the addition of ethyl(vinyl)ether were attempted. Results, in accordance to those obtained by Bernasconi, indicated that a mixture of decomposition and hydrolysis products, mainly consisting of the expected acetaldehyde and ethanol hydrolysis products, had formed (*vide* NMR).[10]

The unique stability of the alkoxyvinyl-gold(I)PPh$_3$ asymmetric π-complexation, as determined by structural characterisation of complexes **1** and **4**, is mainly ascribed to zwitterionic resonance stabilisation of the partial positive charge on the α-gold vinyl carbon by its delocalisation to the Ph$_3$PAu fragment (structure **D** in Scheme 2.7). Evidence for such an assumption is presented in sections 2.2.1 (C) and (D).

Scheme 2.7
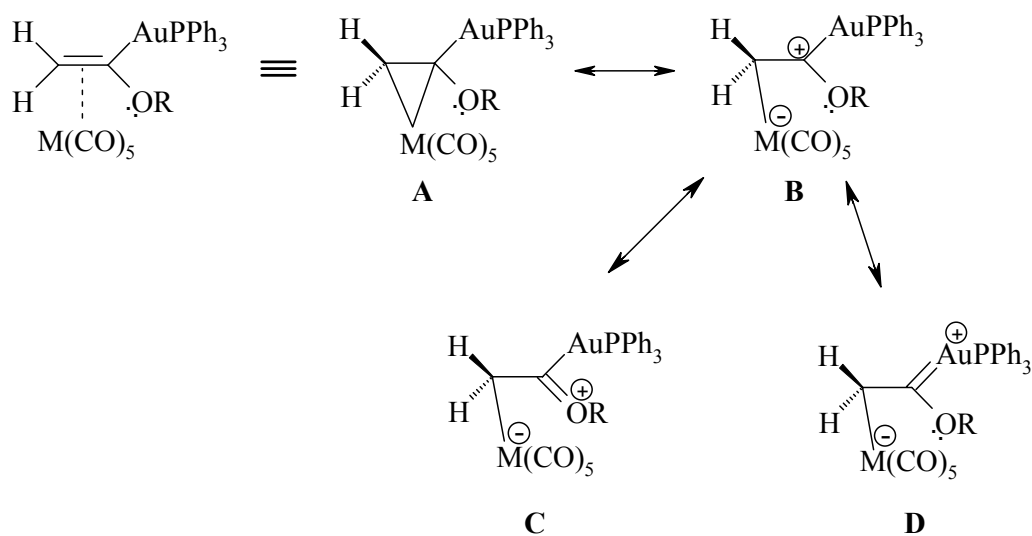
B. Preparation of alkoxyvinyl-gold(I)PPh₃ (**6**)
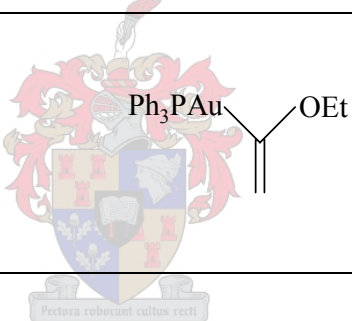
In order to investigate the effects that coordination of the vinyl moiety to the $M(CO)_5$ groups in **1-5** has on the vinyl ether, the uncoordinated alkoxyvinyl-gold(I)PPh₃ complex (**6**) was isolated and characterised. Complex **6** could be obtained in two ways: by freeing the η^2-coordinated alkoxyvinyl-gold(I)PPh₃ units in **2** and **5** with a stronger coordinating ligand (e.g. PPh₃) or by the transmetallation reaction of α-ethoxyvinyllithium with Ph₃PAuCl in thf (Scheme 2.8).

2: M = Cr
5: M = W
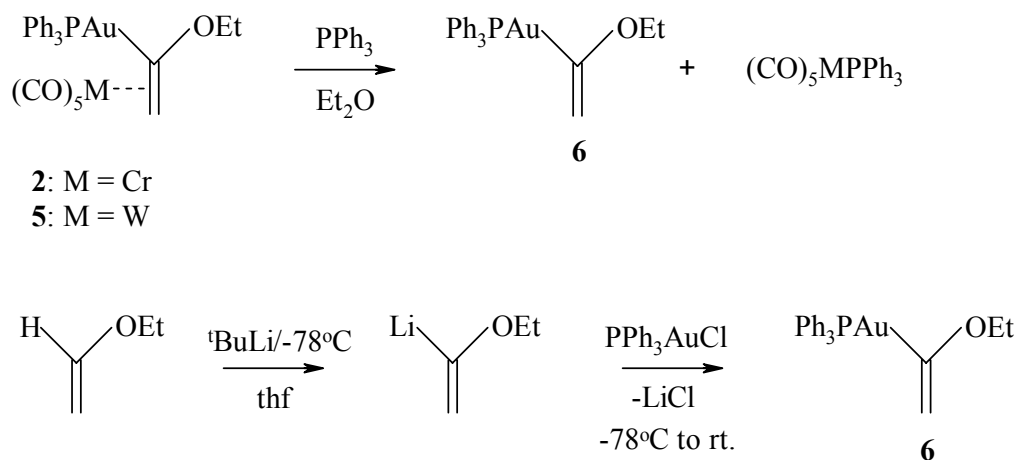
Scheme 2.8

The substitution reaction was carried out by the addition of PPh₃ to an ether solution of **2** or **5** at -15°C after which **6** was purified by flash column chromatography (SiO₂), followed by crystallisation from thf layered with pentane at -20°C (75% yield after separation). In the transmetallation reaction, α-ethoxyvinyllithium, prepared from ᵗBuLi and ethyl(vinyl)ether,[20] was reacted with 1 mole equiv. Ph₃PAuCl in thf at -78°C. Complex **6** was mechanically isolated in low yield as colourless crystalline needles after crystallisation of the reaction mixture from thf/pentane (-20°C). The balance of crystals consisted mainly of unreacted Ph₃PAuCl (NMR, TLC). Physical data for complex **6** are summarised in Table 2.2.

Table 2.2: Analytical data for complex **6**

Complex	
Complex	**6**
M.p. / °C	121 (decomp.)
Color	colourless
Yield (%)	75
M.W. (g / mol)	530.35
Analyses (%)[a]	
C	50.03 (49.82)
H	4.25 (4.18)
O	2.88 (3.02)
P	5.80 (5.84)

[a] Required values given in parenthesis

C.   Spectroscopic characterisation of complexes **1-6**

1.   NMR Spectroscopy

The ^{1}H, ^{13}C{^{1}H} and ^{31}P{^{1}H} NMR spectroscopic data for complexes **1-6** are summarised in Tables 2.3-2.8. The ^{1}H NMR spectra of **1-6** are characterised, in particular, by two distinctive signals, each integrating for a single proton and representing two chemically non-equivalent vinyl protons. For the methoxyvinyl-gold(I)PPh$_3$ π-complexes of Cr(CO)$_5$, Mo(CO)$_5$ and W(CO)$_5$ (**1**, **3** and **4**), these signals appear as broadened or doublet resonances at δ 2.23, 2.66 and 2.73 and doublet resonances at δ 3.80, 4.26 and 4.17 respectively. The signals at δ 3.80, 4.26 and 4.17 are assigned to the vinyl protons *trans* to the Ph$_3$PAu fragment coupling with the phosphorus atom across the vinyl group and the gold atom. Although all the signals for the vinyl proton *cis* to the Ph$_3$PAu fragment at δ 2.23, 2.66 and 2.73 show broadening, a 1.2 Hz $^4J_{P-H}$ coupling to the phosphorus atom is only observed for the tungsten complex (**4**). This is most likely due to the presence of trace amounts of paramagnetic group 6 metal decomposition products in the NMR samples of **1** and **3** that negatively affect the resolution of the proton NMR spectra and making it impossible to observe such fine couplings. No geminal $^2J_{H-H}$ coupling between the vinyl protons is present. The ^{1}H-resonances for the methoxy-CH$_3$ protons in **1**, **3** and **4** are found as singlets at δ 3.92, 3.83 and 3.85, roughly 1 ppm upfield from the signals for the same protons in the corresponding methoxy(methyl)carbene starting complexes.[21]

The ^{13}C{^{1}H} NMR signals for the η^2-coordinated β-gold vinyl carbons in **1**, **3** and **4** appear as doublets at δ 56.3, 61.7 and 57.1 while those for the α-gold vinyl carbon atoms, bonded directly to the Ph$_3$PAu fragments, emerge as doublets ($^2J_{C-P}$ =124.5 - 134.2 Hz) at δ 191.4, 186.0 and 185.2. The ^{13}C resonances for the OCH$_3$ groups in **1**, **3** and **4** occur at ~δ 61, nearly 10 ppm upfield from the signals for the same resonances in the corresponding metal pentacarbonyl methoxy(methyl)carbene complexes.[21]

The ^{1}H NMR spectra of the {ethoxyvinyl-gold(I)PPh$_3$}M(CO)$_5$ π-complexes [**2** (M = Cr) and **5** (M = W)] are similar to those of **1**, **3** and **4** with respect to the *cis* and *trans* vinyl proton resonances, which appear at δ 2.16 and 2.71 and δ 3.71 and 4.13 respectively. Again, 1.7 Hz $^4J_{P\text{-}H}$ coupling in the broadened doublet signal for the *cis* vinyl proton is only observed for the tungsten complex (**5**). The ^{1}H signals for the CH$_2$ protons in the ethoxy groups in **2** and **5**, however, display a complex doublet of doublets of quartets multiplicity, which is rationalised as follows: The CH$_2$ protons in the ethoxy groups are diastereotopic due to a chiral centre situated on the loosely coordinated α-gold vinyl carbon atom in these compounds. This thus gives rise to separate NMR signals for each proton (δ 4.26 and 4.42 in **2** and δ 4.06 and 4.42 in **5**). The quartet structure of these signals is ascribed to $^3J_{H\text{-}H}$ coupling with the terminal CH$_3$ protons in the ethoxy group. The signals are then further split into doublets by $^2J_{H\text{-}H}$ geminal coupling. The ^{13}C{^{1}H} NMR spectra of **2** and **5** compare well to those found for **1**, **3** and **4** with the doublet resonances for the η^2-coordinated α- and β- gold vinyl carbons appearing at δ 192.1 and 55.6 and δ 185.2 and 56.3 respectively.

The effect of the η^2-vinyl coordination to the electron withdrawing M(CO)$_5$ fragments in **1**-**5** on the electronic environment of the vinyl group can be observed clearly by comparing the NMR spectra of the free ethoxyvinyl-gold(I)PPh$_3$ complex (**6**) to those of **1**-**5**. In the ^{1}H NMR spectrum of **6** the signal for the *cis* vinyl proton appears as a broadened singlet at δ 3.76, roughly 1.0-1.5 ppm downfield from to the same resonances in complexes **1**-**5**. Similarly, the doublet signal for the *trans* vinyl proton in **6** at δ 4.64 is roughly 0.5-1.0 ppm downfield from its position in **1**-**5**. Also, ^{13}C NMR signals for the free vinyl carbon atoms in **6** lie downfield compared to the coordinated vinyl carbon atoms in complexes **1**-**5** (δ 94.4 for β-C$_{vinyl}$ and δ 202.5 for α-C$_{vinyl}$ compared to δ 55.6 – 61.7 and δ 185.2 – 192.1 in **1**-**5**). Such downfield shifts upon de-coordination of olefins from transition metals are common and can be ascribed to an increase in s-character of the vinyl carbon hybridisation (partial sp^3 character for these atoms in **1**-**5** compared to pure sp^2 character in **6**). Furthermore, it was found that this deshielding upon de-coordination of the vinyl ether moieties in complexes **1**-**5** is much more pronounced for the β-gold vinyl carbon atom than for the α-gold vinyl carbon atom. The ^{13}C chemical shifts for the β-gold vinyl carbon atoms, when comparing the ^{13}C NMR spectrum of the uncoordinated ethoxyvinyl-

29

gold(I)PPh$_3$ complex (**6**) to those of **1-5**, lie between 32.7 and 38.8 ppm downfield compared to downfield shifts of between 10.4 and 17.3 ppm observed for the α-gold vinyl carbon atom upon vinyl de-coordination. This result suggests a greater bonding contribution by the β-gold vinyl carbon atom to the M(CO)$_5$ fragment, with the α-gold vinyl carbon atom retaining more of its sp^2 character after coordination.
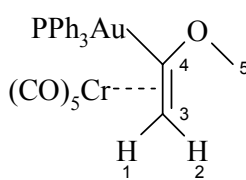
Such an interpretation of the NMR spectra is supported by the X-ray structures of **1** and **4**, which show the distinct presence of asymmetric η^2-vinyl ether coordination modes. In order for the α-gold vinyl carbon atom to retain more sp^2 character than the β-gold vinyl carbon, some π-bonding contribution from either the gold atom or the alkoxy group must occur (as proposed by resonance structures **C** and **D** in Scheme 2.7). Since the ^{1}H and ^{13}C resonances for the alkoxy-CH$_3$ and -CH$_2$ atoms appear appreciably upfield compared to their positions in the carbene starting material (in which some double bond character is ascribed to the C$_{carbene}$-OR bond)[21,22], it can be assumed that delocalisation of the partial positive charge on the α-gold vinyl carbon atom to the alkoxy fragment is not important and that a larger positive charge delocalisation takes place to the Ph$_3$PAu moiety (resonance structure **D**). This interpretation is strengthened by the ^{13}C chemical shifts measured for the α-vinyl carbon atom in **1-5** (δ 185.2 – 192.1), which also support partial carbene character for these atoms[23], as well as by DFT calculations carried out for the PH$_3$ analogue of **1**, **1M**, that report a partial positive charge (+0.28e) situated on the gold atom.

^{31}P{^{1}H} NMR spectra of **1-5** show singlet signals between 40.3 and 41.6 ppm and are consistent with resonances for PPh$_3$ on positive or partially positive Ph$_3$PAu fragments reported in the literature.[24] Resonance structure **D** is thus suggested as the most important contributing structure to the stabilisation of the asymmetric alkoxyvinyl-gold(I)PPh$_3$ coordination to the M(CO)$_5$ fragments in **1-5**.

Comparison of the ^{1}H and ^{13}C NMR spectra of **6** to the NMR spectra of non-metallated ethyl(vinyl)ether shows the effect of substituting the α-vinyl hydrogen atom in ethyl(vinyl)ether with the isolobal Ph$_3$PAu moiety. Curiously, the ^{1}H resonance for the β-vinyl hydrogen *cis* to the α-vinyl hydrogen atom appears slightly downfield (δ 3.94) compared to the corresponding signal in **6** (δ 3.76), while the signal for the β-vinyl hydrogen atom *trans* to the α-vinyl hydrogen appears 0.5 ppm
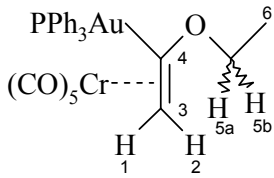
upfield at δ 4.14. Comparison of the ^{13}C NMR resonances is more fruitful. The α- and β-vinyl carbon atoms in ethyl(vinyl)ether resonate at δ 152.6 and δ 86.5, compared to δ 202.5 and δ 94.4 in **6**, indicating greater deshielding of these atoms in the latter complex. This can be ascribed to electron loss due to σ-donation from the α-gold vinyl carbon atom to the Ph$_3$PAu fragment.

Table 2.3

Complex	PPh$_3$Au, O, (CO)$_5$Cr, H^1, H^2 (structure with positions 3, 4, 5)
	1
Solvent	CDCl$_3$
Temperature (K)	298
^{1}H NMR H^1	2.23 (br s, 1H)
(600 MHz) H^2	3.80 (d, $^4J_{trans\ P\text{-}H}$ = 8.2 Hz, 1H)
H^5	3.92 (s, 3H)
Ph	7.4-7.6 (m, 15H)
^{31}P{H^1} NMR P	41.6 (s)
(243 MHz)	
^{13}C{H^1} NMR C^3	56.3 (d, $^3J_{P\text{-}C}$ = 8.7 Hz)
(150 MHz) C^4	191.4 (d, $^2J_{P\text{-}C}$ = 124.5 Hz)
C^5	61.3 (s)
Ph-C$_{ipso}$	130.1 (d, $^1J_{P\text{-}C}$ = 53.4 Hz)
Ph-C$_{ortho}$	129.7 (d, $^2J_{P\text{-}C}$ = 10.9 Hz)
Ph-C$_{meta}$	134.6 (d, $^3J_{P\text{-}C}$ = 13.6 Hz)
Ph-C$_{para}$	132.1 (s)
CO$_{cis}$	219.5 (s)
CO$_{trans}$	227.2 (s)
υ (CO) (cm^{-1})^a	1910 (st, A$_1^{(2)}$), 1924 (v st, 'E'), 1938 (v st, 'E'), 1978 (w, B$_1$), 2057 (w, A$_1^{(1)}$)
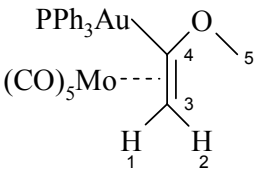
Table 2.4

Complex	
	2
Solvent	CD_2Cl_2
Temperature (K)	298
^{1}H NMR H^1	2.16 (br s, 1H)
(600 MHz) H^2	3.71 (d, $^4J_{trans\,P\text{-}H}$ = 8.4 Hz, 1H)
H^{5a}	4.26 (dq, $^2J_{H\text{-}H}$ = 10.0 Hz, $^3J_{H\text{-}H}$ = 7.1 Hz, 1H)
H^{5b}	4.42 (dq, $^2J_{H\text{-}H}$ = 10.0 Hz, $^3J_{H\text{-}H}$ = 7.1 Hz, 1H)
H^6	1.22 (t, $^3J_{H\text{-}H}$ = 7.1 Hz, 3H)
Ph	7.4-7.7 (m, 15H)
^{31}P{^{1}H} NMR P	41.4 (s)
(243 MHz)	
^{13}C{^{1}H} NMR C^3	55.6 (d, $^3J_{P\text{-}C}$ = 8.4 Hz)
(150 MHz) C^4	192.1 (d, $^2J_{P\text{-}C}$ = 120.9 Hz)
C^5	70.6 (s)
C^6	15.1 (s)
Ph-C$_{ipso}$	130.0 (d, $^1J_{P\text{-}C}$ = 53.7 Hz)
Ph-C$_{ortho}$	129.6 (d, $^2J_{P\text{-}C}$ = 11.7 Hz)
Ph-C$_{meta}$	134.5 (d, $^3J_{P\text{-}C}$ = 12.4 Hz)
Ph-C$_{para}$	131.9 (s)
CO$_{cis}$	219.3 (s)
CO$_{trans}$	227.0 (s)
υ (CO) (cm^{-1})^a	1910 (st, A$_1^{(2)}$), 1923 (v st, 'E'), 1938 (v st, 'E'), 1978 (w, B$_1$), 2056 (w, A$_1^{(1)}$)
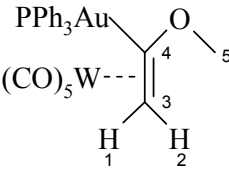
a Pentane solution in NaCl-cell

Table 2.5

Complex	

Structure label: PPh$_3$Au, O, (CO)$_5$Mo, positions 4, 5, 3, H^1, H^2

		3
Solvent		CD$_2$Cl$_2$
Temperature (K)		298
^{1}H NMR	H^1	2.66 (br s, 1H)
(600 MHz)	H^2	4.26 (d, $^4J_{trans\ \text{P-H}}$ = 8.6 Hz, 1H)
	H^5	3.83 (s, 3H)
	Ph	7.4-7.7 (m, 15H)
^{31}P{^{1}H} NMR	P	40.3 (s)
(121.4 MHz)		
^{13}C{^{1}H} NMR	C^3	61.7 (d, $^3J_{\text{P-C}}$ = 6.0 Hz)
(150 MHz)	C^4	186.0 (d, $^2J_{\text{P-C}}$ = 134.2 Hz)
	C^5	61.1 (s)
	Ph-C$_{ipso}$	130.1 (d, $^1J_{\text{P-C}}$ = 54.0 Hz)
	Ph-C$_{ortho}$	129.5 (d, $^2J_{\text{P-C}}$ = 12.0 Hz)
	Ph-C$_{meta}$	134.4 (d, $^3J_{\text{P-C}}$ = 14.5 Hz)
	Ph-C$_{para}$	131.9 (s)
	CO$_{cis}$	201.5 (s)
	CO$_{trans}$	206.1 (s)
υ (CO) (cm^{-1})^a		1910 (st, A$_1^{(2)}$), 1925 (v st, 'E'), 1934 (v st, 'E'), 1980 (w, B$_1$), 2060 (w, A$_1^{(1)}$)

^{a} Pentane solution in NaCl-cell

Table 2.6

Complex	PPh$_3$Au, O (CO)$_5$W--- (structure)
	4
Solvent	CD$_2$Cl$_2$
Temperature (K)	298
^{1}H NMR H^1	2.73 (d, $^4J_{cis\ P\text{-}H}$ = 1.2 Hz, 1H)
(600 MHz) H^2	4.17 (d, $^4J_{trans\ P\text{-}H}$ = 8.1 Hz, 1H)
H^5	3.85 (s, 3H)
Ph	7.4-7.7 (m, 15H)
^{31}P{H^1} NMR P	40.5 (s)
(121.4 MHz)	
^{13}C{H^1} NMR C^3	57.1 (d, $^3J_{P\text{-}C}$ = 9.8 Hz)
(150 MHz) C^4	185.3 (d, $^2J_{P\text{-}C}$ = 124.5 Hz)
C^5	61.6 (s)
Ph-C$_{ipso}$	130.0 (d, $^1J_{P\text{-}C}$ = 53.7 Hz)
Ph-C$_{ortho}$	129.6 (d, $^2J_{P\text{-}C}$ = 12.2 Hz)
Ph-C$_{meta}$	134.5 (d, $^3J_{P\text{-}C}$ = 14.6 Hz)
Ph-C$_{para}$	131.9 (s)
CO$_{cis}$	200.1 (s)
CO$_{trans}$	204.1 (s)
υ (CO) (cm^{-1})^a	1910 (st, A$_1^{(2)}$), 1924 (v st, 'E'), 1936 (v st, 'E'), 1976 (w, B$_1$), 2064 (w, A$_1^{(1)}$)

^{a} Pentane solution in NaCl-cell

Table 2.7

Complex	
	5
Solvent	CD_2Cl_2
Temperature (K)	298
^{1}H NMR — H^1	2.71 (d, $^4J_{cis\ P-H}$ = 1.7 Hz, 1H)
(600 MHz) — H^2	4.13 (d, $^4J_{trans\ P-H}$ = 8.0 Hz, 1H)
H^{5a}	4.06 (dq, $^2J_{H-H}$ = 9.5 Hz, $^3J_{H-H}$ = 7.1 Hz, 1H)
H^{5b}	4.42 (dq, $^2J_{H-H}$ = 9.5 Hz, $^3J_{H-H}$ = 7.1 Hz, 1H)
H^6	1.25 (t, $^3J_{H-H}$ = 7.1 Hz, 3H)
Ph	7.4-7.7 (m, 15H)
$^{31}P\{^1H\}$ NMR — P	40.8 (s)
(243 MHz)	
$^{13}C\{^1H\}$ NMR — C^3	56.3 (d, $^3J_{P-C}$ = 9.3 Hz)
(150 MHz) — C^4	185.2 (d, $^2J_{P-C}$ = 121.3 Hz)
C^5	70.3 (s)
C^6	15.0 (s)
Ph-C_{ipso}	130.7 (d, $^1J_{P-C}$ = 47.8 Hz)
Ph-C_{ortho}	129.5 (d, $^2J_{P-C}$ = 12.4 Hz)
Ph-C_{meta}	134.5 (d, $^3J_{P-C}$ = 12.9 Hz)
Ph-C_{para}	131.9 (s)
CO_{cis}	200.3 (s)
CO_{trans}	204.3 (s)
υ (CO) (cm^{-1})[a]	1910 (st, $A_1^{(2)}$), 1924 (v st, 'E'), 1935 (v st, 'E'), 1976 (w, B_1), 2064 (w, $A_1^{(1)}$)

[a] Pentane solution in NaCl-cell

Table 2.8

Complex	PPh_3Au — O — 6, 4, 5, 3, H$_1$ H$_2$ (structure)
	6
Solvent	CD_2Cl_2
Temperature (K)	298
^1H NMR H^1	3.76 (br s, 1H)
(600 MHz) H^2	4.64 (d, $^4J_{trans\ P-H}$ = 9.4 Hz, 1H)
H^5	3.92 (q, $^3J_{H-H}$ = 7.0 Hz, 2H)
H^6	1.25 (t, $^3J_{H-H}$ = 7.0 Hz, 3H)
Ph	7.4-7.6 (m, 15H)
$^{31}P\{H^1\}$ NMR P	42.9 (s)
(243 MHz)	
$^{13}C\{H^1\}$ NMR C^3	94.4 (d, $^3J_{P-C}$ = 6.7 Hz)
(150 MHz) C^4	202.5 (d, $^2J_{P-C}$ = 129.8 Hz)
C^5	66.2 (s)
C^6	15.7 (s)
Ph-C$_{ipso}$	131.1 (d, $^1J_{P-C}$ = 49.4 Hz)
Ph-C$_{ortho}$	129.5 (d, $^2J_{P-C}$ = 10.5 Hz)
Ph-C$_{meta}$	134.6 (d, $^3J_{P-C}$ = 14.2 Hz)
Ph-C$_{para}$	131.7 (s)

2.   Infrared spectroscopy

The infrared (IR) spectra of **1-5** were recorded as pentane solutions of the complexes in a NaCl cell and are summarised in Tables 2.3 – 2.7. The C_{4v}-local metal carbonyl symmetry in **1-5** allows for three IR active vibrational modes, two A_1 (one with weak intensity) and an intense E mode (a twofold degenerate mode). The IR spectra of **1-5**, however, all exhibit five clearly separated absorption bands in the carbonyl region which could be assigned as follows: One weak A_1 vibrational mode ($A_1^{(1)}$) between 2056 and 2064 cm^{-1}, assigned to the CO symmetric stretching in the M(CO)$_4$ plane; a strong A_1 vibrational mode ($A_1^{(2)}$) at ~1910 cm^{-1}, assigned to symmetric stretching of the single terminal CO ligand *trans* to the olefin coordination; a weak B_1 vibrational mode at ~1976 cm^{-1} [IR active due to distortion of the M(CO)$_4$ coordination plane by the large and asymmetric alkoxyvinyl-gold(I)PPh$_3$ 'ligands'], assigned to out-of-plane bending of the CO ligands in the M(CO)$_4$ plane. Finally, two very strong non-degenerate vibrational modes originating from the E vibrational mode at ~1935 cm^{-1} and ~1924 cm^{-1}, assigned to the asymmetric stretching of the CO ligands in the M(CO)$_4$ plane. Of all these vibrational modes, the $A_1^{(2)}$ mode has the greatest diagnostic value. Low frequency $A_1^{(2)}$ vibrations (compared to literature examples)[25] in metal carbonyl complexes of the type M(CO)$_5$L, as are observed for **1-5** (~1910 cm^{-1}), are indicative of good σ-donating, but poor π-accepting ligands (L). This is also reflected in the small reduction in the vinyl bond order and good retention of sp^2 geometry found for the coordinating vinyl carbon atoms in the crystal structures of **1** and **4** and suggest that back-donating from M(CO)$_5$ into the empty π^*-orbitals of the olefin is minimal. From this can be concluded that vinyl bonding to the M(CO)$_5$ fragment is mainly as a result of σ-donation from the olefin. Furthermore, the fact that two clearly separated and non-degenerate vibrational modes are observed instead of the E vibrational mode bears testimony to the size and asymmetry of the PPh$_3$-alkoxyvinyl-gold(I)PPh$_3$ 'ligands'.

3. Mass spectrometry

The positive-ion FAB-MS of complexes **1-6** were recorded in a *m*-nitrobenzylalcohol matrix. The spectra mainly exhibited the characteristic matrix peaks (*m/z* 154 and *m/z* 307) or the Ph_3PAu^+ (*m/z* 459) or $(Ph_3P)_2Au^+$ (*m/z* 721) decomposition and fragment peaks as the peaks of highest intensity. In all the mass spectra, however, strong molecular ion (M^+) peaks could be identified (intensity in parenthesis given in percentage relative to the peaks of highest intensity) [**1**: *m/z* 708(35); **2**: *m/z* 721 (90); **3**: *m/z* 752(50); **4**: *m/z* 841(60); **5**: *m/z* 855(70); **6**: *m/z* 531(70)]. Due to the 'soft' nature of the FAB-MS ionisation technique, fragmentation of **1-6**, other than for the formation of Ph_3PAu^+ and homoleptic $(Ph_3P)_2Au^+$, was very limited and there are thus no clear fragmentation patterns available for **1-6**. No sequential loss of CO ligands from the $M(CO)_5$ could be observed. Mass spectrometry techniques with 'harder' ionisation methods, like conventional electron ionisation (EI-MS), delivered only high intensity peaks for Ph_3PAu^+ (*m/z* 459) and a large number of unassignable weak intensity peaks for a myriad of other fragmentation and decomposition products of **1-6**.

D.   X-ray structure determination of complexes **1** and **4**

The low temperature crystal and molecular structures of **1** (173 K) and **4** (150 K) (Figures 2.1-2.3) were determined by X-ray diffraction techniques. Both structures show methoxyvinyl-gold(I)PPh₃ moieties coordinated in asymmetrical η^2-fashion to a square pyramidal $M(CO)_5$ [M = Cr (**1**), M = W (**4**)] fragment, thus filling the octahedral coordination sphere commonly encountered for Group 6 metals in the zero oxidation state. The structures of **1** and **4** represent the first crystal structures of neutral group 6 metal carbonyl compounds coordinated by vinyl ether ligands. The structures of **1** and **4** are, furthermore, isostructural as they belong to the same spacegroup and have very similar unit cell parameters. Selected bond lengths and angles for **1** and **4** are listed in Tables 2.9 and 2.10.

Analysis of the difference in the η^2 vinyl carbon-M bond lengths [0.252(11)Å in **1** and 0.307(5)Å in **4**] [Δ(M-C) = M-C(7) – M-C(1)] and M-C(1)-C(7) angles [85.0(5)° and

38

87.1(2)° in **1** and **4**], gives a clear indication of the asymmetric bonding of the vinyl ethers and shows that the asymmetry is greater for **4**, as illustrated in Figure 2.3. Also, the M-C(1) bond lengths in both structures are very similar [Cr-C(1) = 2.377(8)Å, W-C(1) = 2.393(3)Å], despite the substantial difference in atomic radius between Cr and W [Cr = 1.25 Å , W = 1.37 Å][26], illustrating that C(1) forms a stronger bond with the metal in **4** than in **1**. Slippage of the η^2-vinyl coordination mode towards a η^1-coordination is described by the displacement of the olefin centroid from the metal centre [as defined by extension of the M-C(6) bond]. The calculated slip shifts in **1** and **4** (0.00 Å and 0.04 Å) show that, although the olefin coordination is distinctly asymmetric, no meaningful lateral slippage of the metal towards either vinyl carbon atom has taken place. This is also reflected in the small M-C(1)-C(7) angles reported above, which are still more than 20° less than the tetrahedral ideal of 109.5° for pure sp^3 η^1-coordination. In all other known examples where similar asymmetric coordination of an olefin to a metal is observed the geometry of the terminal coordinating CH_2-carbon atom is much closer to that of an sp^3 carbon atom and much greater slip shifts are observed.[27] Whereas the olefin coordination shows a distinct tendency towards a η^1-mode, the bond geometry around the vinyl group suggests that there is still a significant bond contribution from the α-vinyl carbon [C(7)] to the $M(CO)_5$ fragment. C(4)-C(2)-C(7)-C(1) torsion angles of 9.4(5)° and 11.3(3)° in **1** and **4** show that the vinyl coordination is essentially parallel to the C(2)-M-C(4) coordination axis in the $M(CO)_5L$ octahedra.

Olefin bond lengths [C(1)-C(7)] in **1** and **4** of 1.345(11)Å and 1.378(5)Å compare well to such distances in known non-coordinated metallo vinyl ethers,[28] and indicate that, although formal π-complexation of the vinyl ether has taken place, there is not much reduction in the olefin bond order in the solid state (C=C in ethylene is 1.337 Å). The geometry of the vinyl moiety is slightly distorted from ideal sp^2 hybridisation with the greatest deviations from planarity in the mean squares plane defined by C(1), C(7), O(1) and Au in **1** and **4** being 0.071(6)Å and 0.073(3)Å for C(7). The positions of the vinyl hydrogen atoms could be determined from the difference Fourier map and support an sp^2 hybridisation slightly distorted toward sp^3 hybridisation for C(1) in both structures. These results are in agreement with spectroscopic data for **1** and **4**,

which suggest poor back-donation of electrons from the metal to the π^* orbitals of the olefin, thus largely conserving the sp^2 geometry of the coordinated vinyl ether moiety.

The slightly more reduced olefin bond order and the greater asymmetry observed in the olefin coordination in the structure of **4** suggest a greater degree of positive charge delocalisation to the Ph₃PAu fragment [and thus also negative charge delocalisation to the $W(CO)_5$ fragment], as suggested by resonance structure **D** (Scheme 2.7), in this compound. This observation agrees well with kinetic and thermodynamic results obtained by Bernasconi *et al.* for the $(CO)_5M=C(OCH_3)CH_3$ (M = Cr, W) carbene starting complexes in which a slightly greater β-metallo CH-acidity is reported for the tungsten complex.[2] These results suggest that, due to tungsten's greater polarisability or 'softness', the negative charges in the β-metallo CH deprotonated carbene complexes are more efficiently accommodated on a $W(CO)_5$ fragment than on a $Cr(CO)_5$ fragment, thus explaining the slightly greater asymmetry observed in the methoxyvinyl-gold(I)PPh₃ coordination in complex **4** compared to **1**.

Au-C(7) bond lengths in **1** and **4** [2.050(7)Å and 2.067(4)Å] compare well with literature values in which a gold(I) phosphine fragment is linked *via* carbon to electron withdrawing substituents[29] and, due to the poor correlation between Au-C bond length and bond order,[23] do not exclude the partial carbene character for these bonds suggested by the spectroscopic results and resonance structure **D**.

Reasons for the significant difference in the C(7)-O(1) bond lengths in **1** and **4** [1.368(9)Å and 1.432(4)Å] are not clear. Lengths for similar single bonds in non-coordinated metallo vinyl ethers in the literature,[28] however, correlate well with the C(7)-O(1) separation observed in **1**, suggesting that the C(7)-O(1) bond in **1** is not shortened, but rather that the C(7)-O(1) bond in **4** is lengthened.

Figure 2.1: Ortep view of complex **1**, showing numbering scheme

Table 2.9: Selected bond lengths (Å) and angles (°) with e.s.d.s in parenthesis for
complex **1**

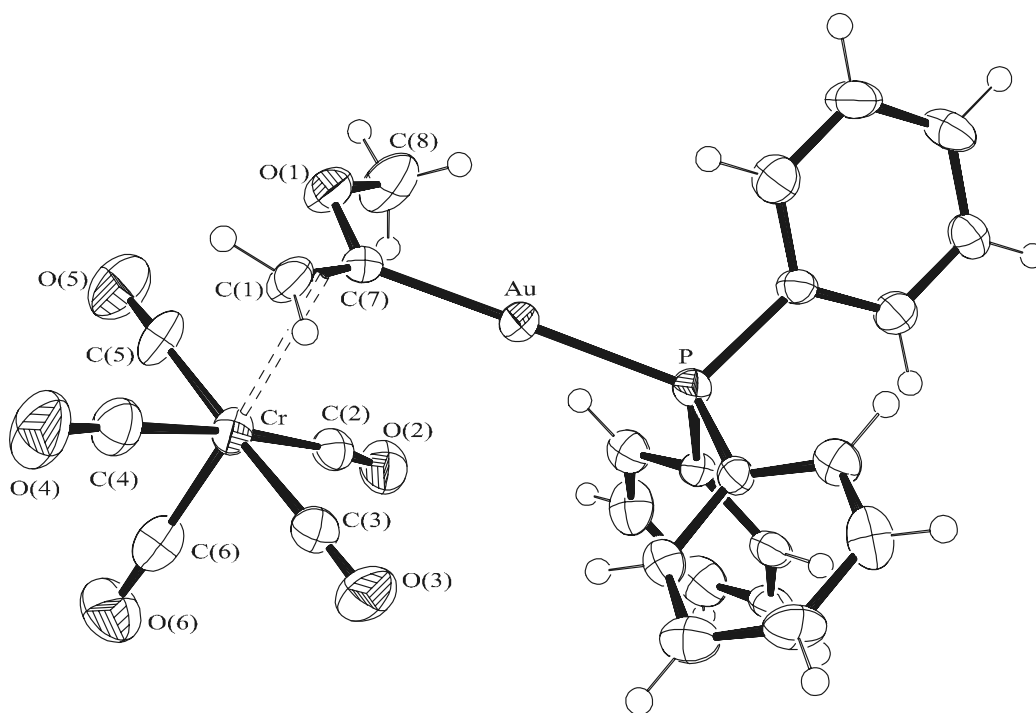| Bond lengths		Bond angles	
Au-C(7)	2.050(7)	Cr-C(1)-C(7)	85.0(5)
Cr-C(1)	2.377(8)	Cr-C(7)-C(1)	64.3(4)
Cr-C(7)	2.629(7)	C(7)-Au-P	179.2(2)
Au-P	2.291(2)	Au-C(7)-C(1)	124.4(6)
C(1)-C(7)	1.345(11)	Au-C(7)-O(1)	121.6(5)
C(7)-O(1)	1.368(9)	C(1)-C(7)-O(1)	112.9(7)
O(1)-C(8)	1.424(9)	C(7)-O(1)-C(8)	116.7(6)
Cr-C(2)	1.894(9)	Cr-C(2)-O(2)	173.2(6)
Cr-C(3)	1.904(9)	Cr-C(3)-O(3)	177.5(7)
Cr-C(4)	1.885(9)	Cr-C(4)-O(4)	176.4(8)
Cr-C(5)	1.894(10)	Cr-C(5)-O(5)	177.2(8)
Cr-C(6)	1.847(10)	Cr-C(6)-O(6)	178.2(8)
		C(1)-Cr-C(6)	163.6(3)
		C(7)-Cr-C(6)	165.1(3)
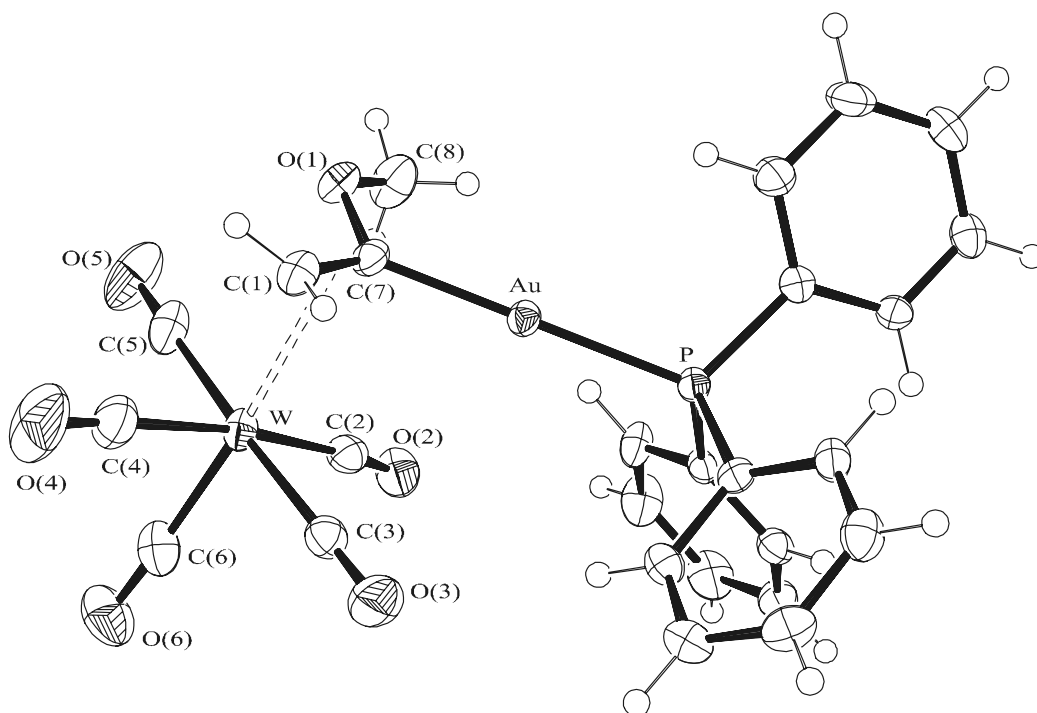
Figure 2.2: Ortep view of complex **4**, showing numbering scheme

Table 2.10: Selected bond lengths (Å) and angles (°) with e.s.d.s in parenthesis for complex **4**

Bond lengths		Bond angles	
Au-C(7)	2.067(4)	W-C(1)-C(7)	87.1(2)
W-C(1)	2.393(3)	W-C(7)-C(1)	62.3(2)
W-C(7)	2.700(4)	C(7)-Au-P	178.8(1)
Au-P	2.294(1)	Au-C(7)-C(1)	121.7(3)
C(1)-C(7)	1.378(5)	Au-C(7)-O(1)	121.2(3)
C(7)-O(1)	1.423(4)	C(1)-C(7)-O(1)	116.0(3)
O(1)-C(8)	1.436(4)	C(7)-O(1)-C(8)	118.7(3)
W-C(2)	2.030(4)	W-C(2)-O(2)	174.0(3)
W-C(3)	2.102(4)	W-C(3)-O(3)	179.1(3)
W-C(4)	2.048(5)	W-C(4)-O(4)	176.1(4)
W-C(5)	2.113(5)	W-C(5)-O(5)	176.2(3)
W-C(6)	1.935(4)	W-C(6)-O(6)	177.0(4)
		C(1)-W-C(6)	162.0(2)
		C(7)-W-C(6)	166.0(1)

Figure 2.3: Ortep views of complexes **1** and **4**, illustrating the slight difference in asymmetry observed in the η^2 {methoxyvinyl-gold(I)PPh$_3$}M(CO)$_5$ coordination (H atoms on phenyl rings omitted for clarity).

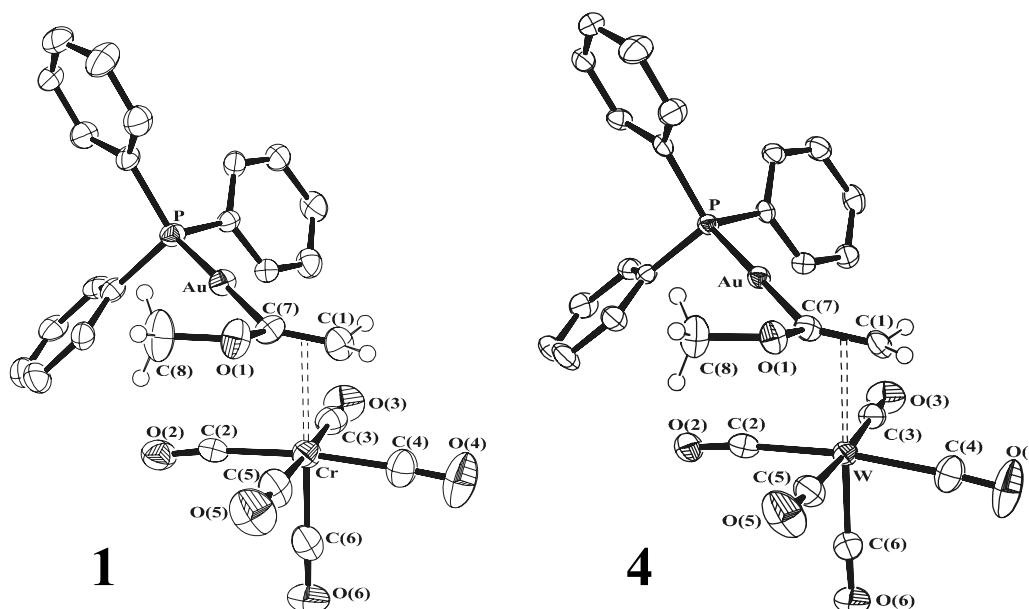Respective deviations from planarity from the least squares plane through M, C(2), C(3), C(4) and C(5) plane of –0.071(4)Å, 0.049(4)Å, -0.069(4)Å, 0.049(4)Å and 0.043(3)Å in **1** and -0.090(2)Å, 0.065(2)Å, -0.085(2)Å, 0.064(2)Å and 0.045(2)Å in **4** describe its distortion due to coordination of the large and asymmetric methoxyvinyl-gold(I)PPh$_3$ complex. These substantial distortions also support the clear observation of a weak IR-active B$_1$ and lifting of the degeneracy in the E vibrational mode in the IR spectra of these complexes.

Molecules of both complexes pack in the monoclinic, centrosymmetric spacegroup P2$_1$/c. Viewed along the b-axis of their unit cells (Figures 2.4 and 2.5), these molecules can be schematically represented as pyramids with bases roughly perpendicular to the C(7)-Au-P bond. Shown like this, the packing of molecules of **1** and **4** can be described as alternating, slightly offset, up-down rows of pyramids, as is also illustrated by the small pattern of triangles in each figure (signs in triangles indicate the direction of the apex of each pyramid $\oplus$ = along the b-axis into the page). No significant non-bonded intermolecular interactions are observed in either unit cell.
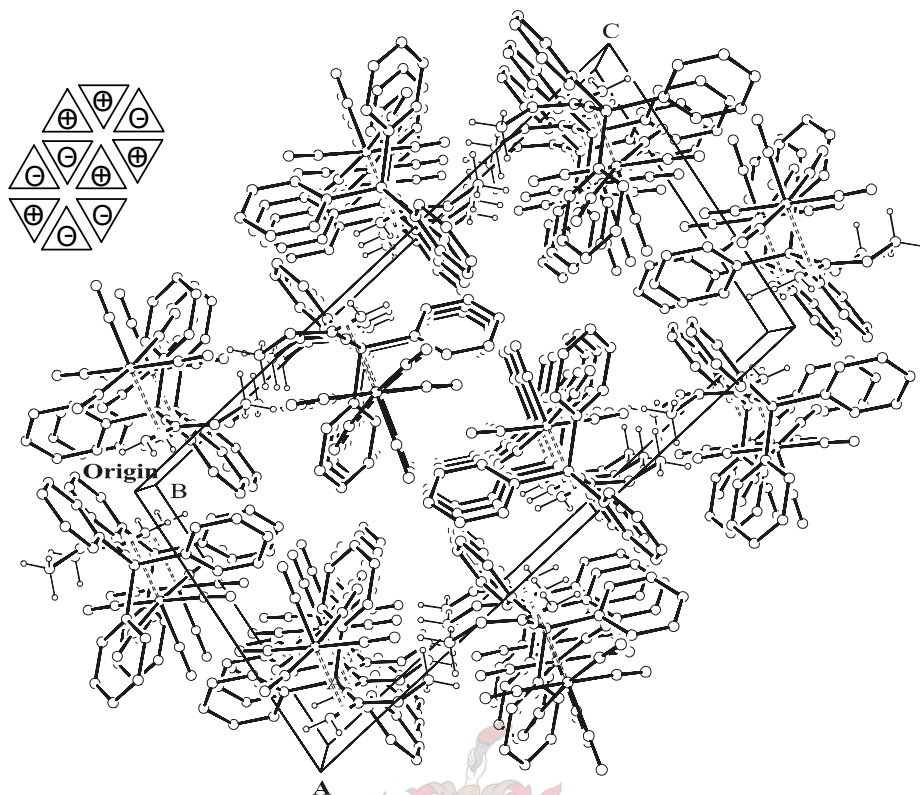
Figure 2.4: Unit cell and packing pattern of **1** viewed along the b-axis
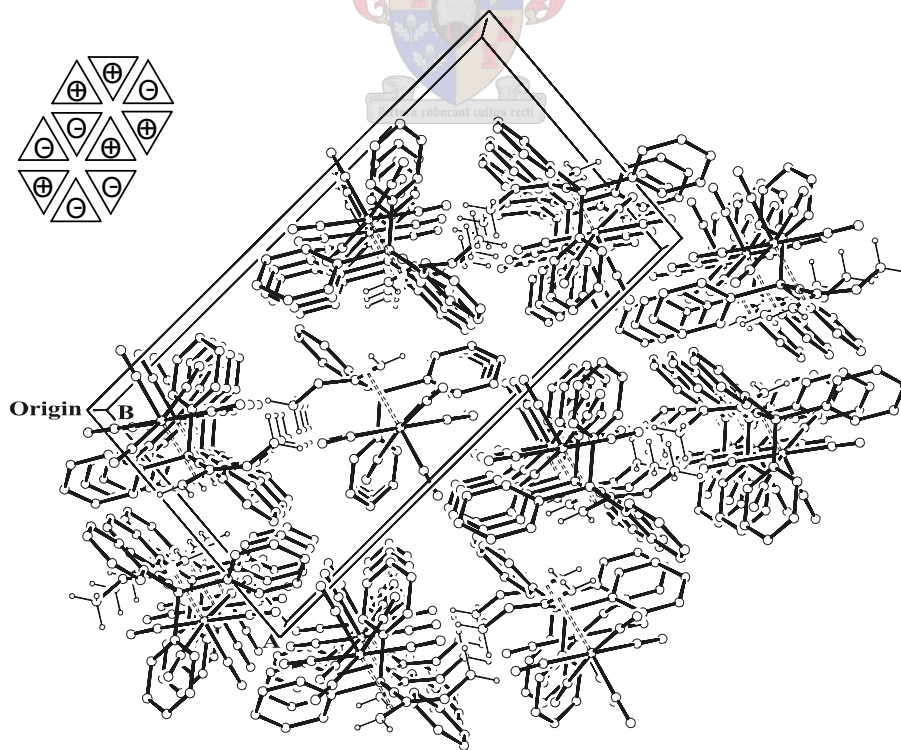
Figure 2.5: Unit cell and packing pattern of **4** viewed along the b-axis

E.   Quantum mechanical calculation of $\eta^2\text{-}\{H_3PAuC(OCH_3)=CH_2\}Cr(CO)_5$ (**1M**)

In order to analyse the bonding situation in **1**, DFT calculations of a model compound, **1M**, in which the PPh$_3$ ligand of complex **1** is substituted by PH$_3$, were carried out at the B3LYP[30] level of theory. Figure 2.6 shows the optimised geometry and the most important bond lengths and angles calculated for **1M**.
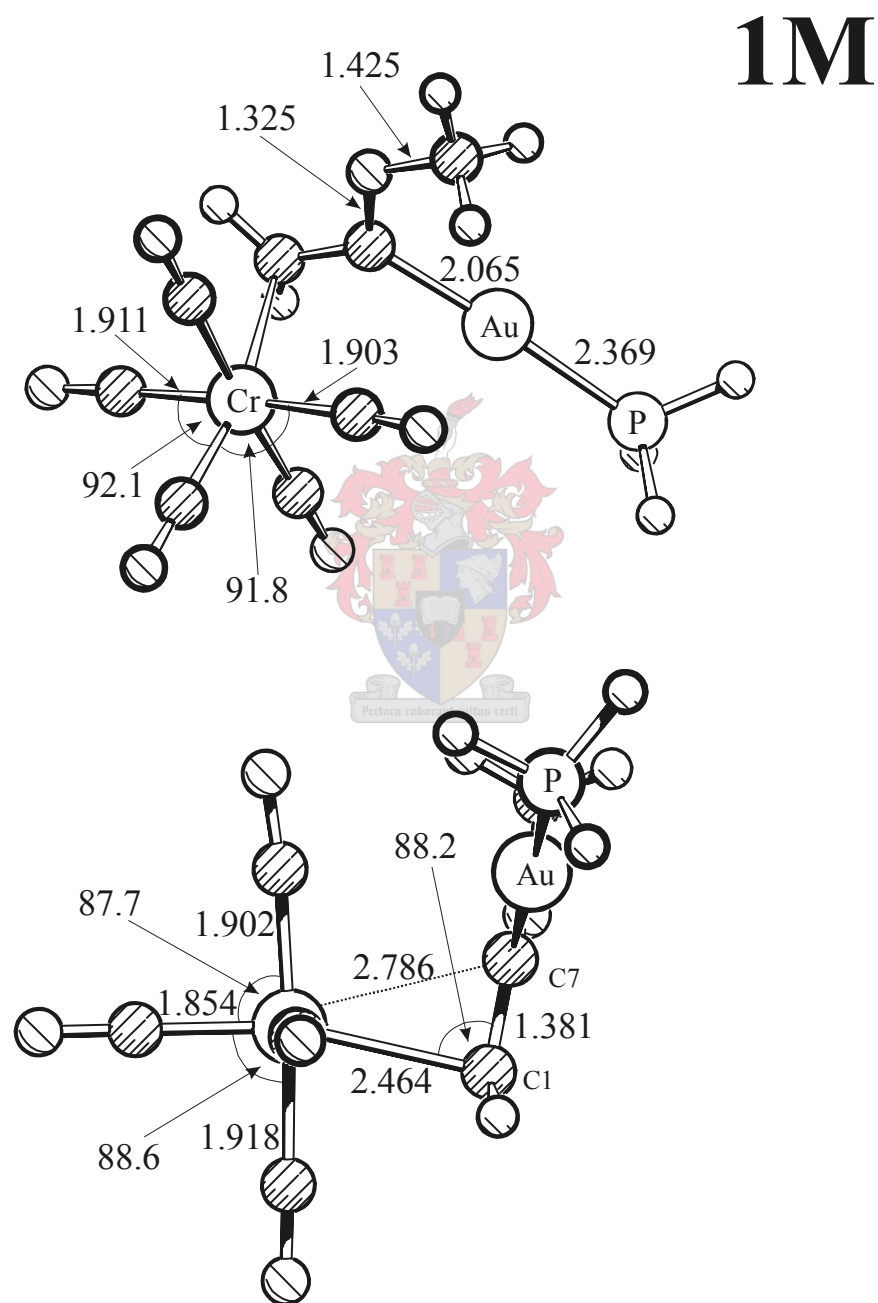
Figure 2.6: Optimised geometry and selected bond lengths and angles calculated for the model compound **1M**.

The calculated bond lengths and angles of **1M** are very similar to the X-ray structure obtained of **1**. The theoretical value for the C(1)-C(7) distance is 1.381Å, slightly longer than the experimental value of 1.345(11)Å. More important, however, are the Cr-C bond lengths of the coordinated vinyl group. Similarly to the experimental structure obtained by X-ray diffraction, the calculations also give rather different distances for each of the coordinating carbon atoms [C(1)-Cr = 2.464Å; C(7)-Cr = 2.786Å], indicating that the chromium is more strongly bonded to C(1) than to C(7). A topological analysis of the electron density distribution[31] suggests that the Cr-vinyl bonding takes place mainly *via* carbon atom C(1) of the ligand. The Laplacian distribution [$\nabla^2\rho(\mathbf{r})$] of **1M**, which is represented as a slice through the C(1)-C(2)-C(4)-C(6) plane (Figure 2.7)[32], shows that an area of π-charge concentration at the terminal C(1) atom of the vinyl ether ligand is distorted toward the chromium atom.

Figure 2.7: Representation of the Laplacian distribution [$\nabla^2\rho(r)$] calculated for **1M**

Dashed lines in Figure 2.7 show areas of electron depletion $[\nabla^2\rho(\mathbf{r}) > 0]$ while solid lines show areas of electron concentration $[\nabla^2\rho(\mathbf{r}) < 0]$. There is a droplet-like appendix of charge concentration pointing towards the chromium atom from C(1). Even more revealing regarding the bonding situation are the calculated bond pat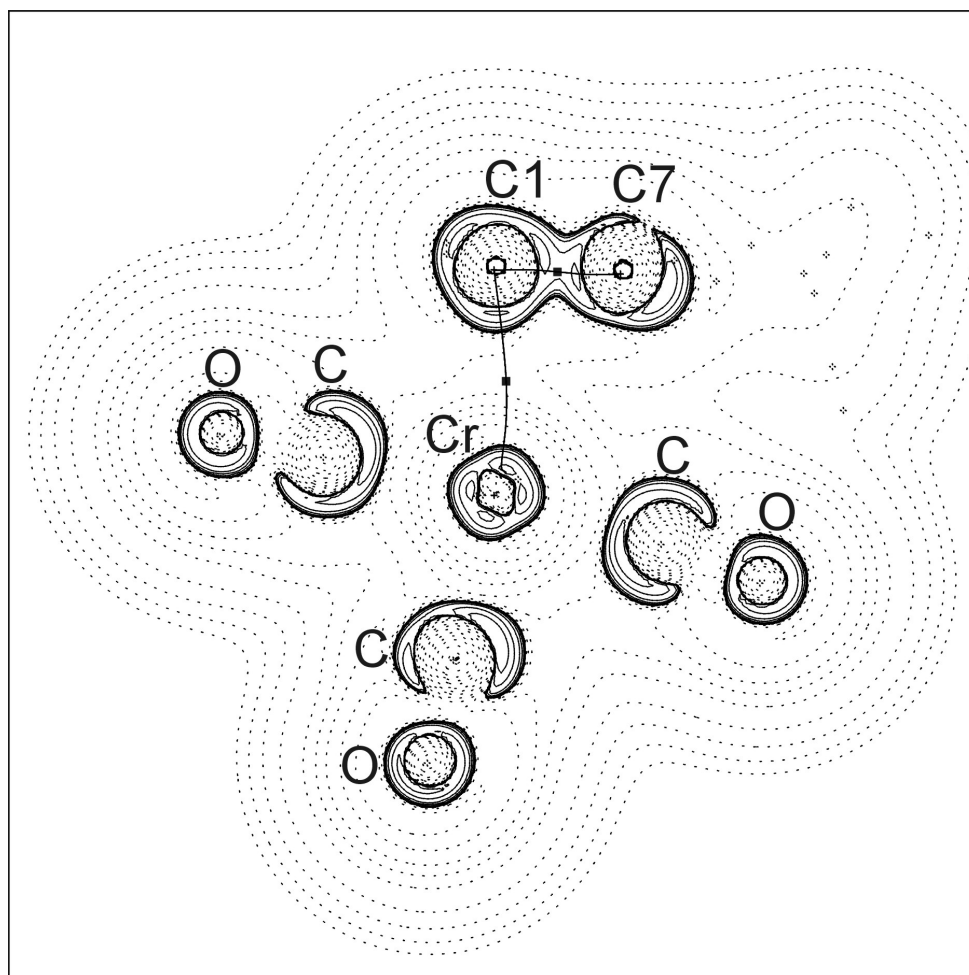hs, represented by the solid line between Cr and C(1) in Figure 2.7. These are defined by the presence of so-called 'saddle' points in the 2nd derivative of the calculated electron density distribution for **1M**. 'Saddle' points are points on the electron density map where a minimum in electron density in one direction is also a maximum in electron density in another, usually close to perpendicular, direction. As seen in Figure 2.7, there is indeed such a path between Cr and C(1), but not between Cr and C(7). The shape of the Laplacian distribution as well as the calculated bond path thus suggest that the Cr is primarily bonded to C(1) and that there is only a secondary interaction with C(7).

A selection of the calculated charges given by the NBO analysis[32] are listed in Table 2.11. A large partial negative charge resides at C(1) (-0.61e) and a small positive charge at C(7) (+0.03e). Positive partial charges are also calculated for Au (+0.28e) and the PH$_3$ ligand (+0.23e), while an overall negative charge (-0.19e) is calculated for the methoxy group. This means that the positive charge is delocalised over the C(7)-Au-PH$_3$ moiety, as proposed by resonance structure **D** (Scheme 2.7) and not towards the methoxy group, as suggested by resonance structure **C**. These results are in accordance with the interpretation of the spectroscopic data for **1-5**, nominating **D** (Scheme 2.7) as the main contributing structure in describing this class of complex. Despite the charge distribution, the calculations, in accordance with the crystal structure of **1**, also yield an almost planar (sp^2) arrangement for the alkene derivative. The bonding interaction between the alkene and the chromium atom in **1M**, is thus, according to the calculated charge distribution, best described as η^1-bonding of a terminal carbanion rather than η^2-bonding of an olefin. However, based on the asymmetric geometry of the calculated structure, which indicates that C(7) is most definitely still within bonding distance to the chromium atom and that the olefin coordination has not slipped to a pure η^1-bonding mode either, possible bonding interactions of the chromium atom to C(7) cannot be ignored.

Table 2.11: Charge distribution calculated for **1M**

Atom	Calculated natural charge
C(1)	-0.60814
C(7)	+0.03126
Au	+0.28073
PH$_3$	+0.22566
OCH$_3$	-0.18914

Coordination of the PH$_3$-methoxyvinyl-gold(I) complex to Cr(CO)$_5$ *via* the oxygen atom of the vinyl ether was also considered. DFT calculations for such an isomer (**1M'**), however, indicated that it would be 5.7 kcal/mol higher in energy than **1M**, showing that asymmetric vinyl coordination to Cr(CO)$_5$ in these compounds is preferred. The relative energies of the sulphur analogues of **1M** and **1M'** were also calculated. The DFT calculations predict that there is a reversal of stability in these complexes and that an isomer in which the PH$_3$-alkylthiovinyl-gold(I) 'ligand' coordinates through the Cr(CO)$_5$ moiety would have a 6.6 kcal/mol lower energy than the corresponding vinyl coordinated complex (see also Section 3.2.2 and 3.3).
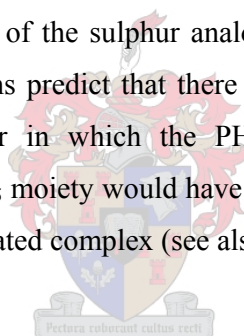
2.3   Conclusions and future work

The reaction of β-metallo carbon deprotonated Fischer-type group 6 metal pentacarbonyl alkoxycarbene complexes with Ph$_3$PAuCl leads to the exclusive formation of novel bimetallic η^2-{alkoxyvinyl-gold(I)PPh$_3$}M(CO)$_5$ (M = Cr, Mo, W) complexes, and not the expected β-metallo carbon substituted carbene complexes. Single crystal X-ray diffraction studies conducted on two examples of these complexes confirm their molecular structure and show that the alkoxyvinyl-gold(I)PPh$_3$ 'ligands' are coordinated to the M(CO)$_5$ fragments in an asymmetrical η^2-fashion through the vinyl moiety and not through the oxygen atom of the vinyl ether. Evidence presented in this chapter strongly suggests that this usually unstable coordination mode for vinyl ethers is stabilised by delocalisation of partial positive charges in the polarised vinyl coordination mode to the Ph$_3$PAu moiety. Quantum

mechanical calculations have shown that coordination of the alkoxyvinyl-gold(I)PPh$_3$ complexes to the M(CO)$_5$ fragments through the vinyl moiety instead of the vinyl ether oxygen atom is thermodynamically favoured. Quite surprisingly, isolation of the novel bimetallic η^2-{alkoxyvinyl-gold(I)PPh$_3$}M(CO)$_5$ complexes described in this chapter could be carried out very successfully by low temperature silica gel chromatographic procedures.

The reaction mechanism involved in this conversion is believed to be the isolobal gold(I) analogue of the postulated hydrolysis reaction of Fischer-type alkoxycarbene complexes. This mechanism involves electrophilic addition at the metal centre instead of at the site of deprotonation, leading to the formal reductive elimination of vinyl ether fragments form the metal carbonyl fragment. The term "aurolysis" is conceived to describe this conversion when gold is employed as electrophile. Hydrolysis of Fischer-type carbene complexes ultimately leads to the formation of alcohols and aldehydes as final products. These are currently believed to originate from the secondary hydrolysis of a proposed initial hydrolysis product - a metal coordinated vinyl ether complex. The bimetallic compounds prepared and characterised in this chapter represent stable gold(I) equivalents of this proposed initial product. This result illustrates how stabilisation of the asymmetric vinyl coordination in this intermediate by the Ph$_3$PAu moiety effectively enables its isolation, and creates new insights into the possibility of using transition metal fragments in stabilising usually unstable carbon-metal bonding modes. The isolation of these bimetallic compounds also supports the proposed reaction mechanism for the hydrolysis of Fischer-type carbene complexes with β-metallo carbon hydrogen atoms reported in the literature.

The novel alkoxyvinyl-gold(I)PPh$_3$ fragments in the bimetallic complexes can, furthermore, be conveniently liberated from the M(CO)$_5$ moiety and isolated in high yields. This serves to illustrate how Fischer-type carbene complexes can be employed as efficient synthons for the vinyl ether anion in organometallic conversions with gold(I) electrophiles. A preparation of ethoxyvinyl-gold(I)PPh$_3$ along a conventional transmetallation reaction pathway produces much poorer yields of the same species and does not provide the same possibilities of expansion of the gold vinyl ether products.

Potential future work sprouting from the results presented here, to name but a few interesting possibilities, include: The use of the free alkoxyvinyl-gold(I)PPh$_3$ complexes prepared here as monomers in polymerisation reactions to produce novel polymers that incorporate gold atoms. Alkylation/acidification reactions at the partially negatively charged β-gold vinyl carbon atom in the bimetallic η^2-{alkoxyvinyl-gold(I)PPh$_3$}M(CO)$_5$ complexes to prepare the first examples of cationic gold(I) Fischer-type alkoxycarbene complexes. Oxidative addition reactions of halides (X$_2$) to the isolated alkoxyvinyl-gold(I)PPh$_3$ complexes to prepare *trans*-dihalo-PPh$_3$-alkoxyvinyl-gold(III) complexes followed by alkylation/acidification reactions on these compounds to produce the first examples of cationic gold(III) Fischer-type alkoxycarbene complexes. Expansion of this conversion to include other 'soft' transition metal electrophiles (e.g. AgCl, HgCl etc.) with the aim of gaining new synthetic pathways to their vinyl ether complexes.

2.4 Experimental

2.4.1 Materials
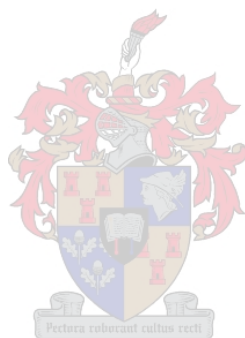
All solvents were dried and purified by conventional methods and freshly distilled under nitrogen shortly before use. Unless otherwise stated all common reagents were used as obtained from commercial suppliers without further purification. Ethyl(vinyl)ether was distilled under nitrogen gas before use. ^{n}BuLi was standardised before use according to the procedure reported by Winkle *et al*.[33] Ph$_3$PAuCl and the group 6 metal pentacarbonyl Fischer alkoxy carbene starting complexes were prepared according to procedures described in the literature.[34,21]

2.4.2 Physical methods

All reactions and manipulations involving organometallic reagents were carried out under a dry nitrogen atmosphere using standard Schlenk and vacuum-line techniques. NMR spectra were recorded on Varian INOVA 600 (600 MHz for ^{1}H, 151 MHz for ^{13}C{^{1}H} and 243 MHz for ^{31}P{^{1}H}) or Varian VXR 300 (300 MHz for ^{1}H, 75.4 MHz for ^{13}C{^{1}H} and 121.5 MHz for ^{31}P{^{1}H}) NMR spectrometers. ^{1}H and ^{13}C chemical shifts are reported in ppm relative to the ^{1}H and ^{13}C residue of the deuterated solvents. ^{31}P chemical shifts are reported in ppm relative to an 85% H_3PO_4 external standard solution. IR spectra (4000 to 400 cm^{-1}, resolution 4 cm^{-1}) were recorded on a Perkin-Elmer 1600 series FTIR spectrometer. A standardised Büchi 535 melting point apparatus was used to determine the melting/decomposition point reported here. FAB-MS were recorded on a Micromass DG 70/70E mass spectrometer at the University of Potchefstroom, South Africa, using xenon gas as bombardment atoms and *m*-nitrobenzylalcohol as matrix. Flash column chromatography was performed with "flash grade" silica (SDS 230-400 mesh).

Crystal structure data collection and correction procedures were carried out on a Nonius KappaCCD diffractometer by Dr. J. Bacsa of the University of Cape Town structural chemistry research group. All structure solution and refinement procedures were carried out by the author. Theoretical calculations were carried out by Prof. G. Frenking, Dr. A. Timoshkin and Dr. Y. Chen of the department of chemistry, Philipps-Universität Marburg, Marburg, Germany.

2.4.3 Preparations and procedures

2.4.3.1 Representative experimental procedures for the preparation of complexes **1-5**.

0.5 ml 1.6M ^{n}BuLi (1.2 mole equiv.) was added to a solution of the alkoxy(methyl) carbene complex (0.8 mmol) in 15 ml thf cooled to –78 ^{o}C. The mixture was stirred at that temperature for 30 min. after which 1 mole equiv. Ph$_3$PAuCl (395 mg) or Ph$_3$PAuNO$_3$ (417 mg) was added to the solution. The mixture was then allowed to

warm to room temperature over a period of 3 hours. Removal of the solvent *in vacuo* resulted in dark yellow to brown oily residues containing a mixture of products (TLC). The products were isolated in moderate yields [67% (**1**), 71% (**2**), 53% (**3**), 45% (**4**) and 63% (**5**)] as broad yellow bands by means of low temperature (-15 $^{\circ}$C) silica gel column chromatography (pentane/diethyl ether, 10:1). Yields were not optimized.

2.4.3.2   Experimental procedures for the preparation of complex **6**.

By substitution reaction with PPh$_3$:

PPh$_3$ (1 equiv., 0.05 mmol, 131 mg) was added to a cooled (–15 $^{\circ}$C) ether solution of **2** or **5** (0.05 mmol). The mixture was allowed to warm to room temperature over a period of 30 minutes. Removal of the solvent *in vacuo* resulted in a powdery, light-yellow mixture containing **6** and (CO)$_5$MPPh$_3$ (*vide*-NMR). **6** was purified by low temperature (-15 $^{\circ}$C) flash silica gel column chromatography (thf/pentane, 1:2), followed by crystallisation from thf layered with pentane at –20 $^{\circ}$C (75% yield after separation).

By transmetallation reaction with ^{t}BuLi:

A solution of α-ethoxyvinyllithium (0.8 mmol) in 15 ml thf was prepared analogously to the procedure for the preparation of α-methoxyvinyllithium with ^{t}BuLi described by Baldwin *et al*[20]. While stirring this solution at –78 $^{\circ}$C, 1 mole equiv. Ph$_3$PAuCl (0.8 mmol, 395 mg) was added, after which it was allowed to warm to room temperature over a period of 3 hours. Removal of the solvent *in vacuo* resulted in milky oily residues containing the product and unreacted Ph$_3$PAuCl. Complex **6** was isolated as needles in low yield (9%) by crystallisation from thf/pentane mixtures at –20 $^{\circ}$C. Yields were not optimized.

2.4.3.3 Crystal structure determination of complexes **1** and **4**.

The crystal data collection and refinement details for complexes **1** and **4** are summarised in Table 2.12 below. X-ray quality yellow platelet single crystals of **1** and **4** were obtained by crystallisation from concentrated diethyl ether solutions layered with pentane at –20°C. Low temperature (-100 °C for **1** and -123 °C for **4**) data were collected on an Enraf-Nonius KappaCCD diffractometer[35] using graphite monochromated Mo-K$_\alpha$ radiation (λ = 0.71073 Å) and scaled and reduced using DENZO-SMN[36]. The structures were solved by the heavy atom method (SHELXS)[37] and refined anisotropically for all the non-hydrogen atoms by full-matrix least squares calculations (SHELXL-97)[37] on F^2. All hydrogen atoms in **1** and **4** were placed in calculated positions, except those on the coordinating vinyl moiety, which were found on the difference Fourier map and refined isotropically. The isotropic displacement parameters of the calculated hydrogen atoms were fixed at 1.2 (aromatic hydrogens) and 1.5 (methyl hydrogens) times the equivalent isotropic displacement parameters of their parent atoms. ORTEP-III for windows[38] was used to generate the various figures of **1** and **4** at the 50% probability level.

All other crystallographic information, including the hkl data, cif files and structure factors, is included on the CD of supplementary material provided in the back cover of this work, or is available from the author upon request.

2.4.3.4 Quantum mechanical calculations.

The geometry of **1M** was optimized at the gradient corrected DFT level using the three-parameter fit of the exchange-correlation potential suggested by Becke[39] in conjunction with the LYP[40] exchange potential (B3LYP).[30] A quasi-relativistic small-core ECP with a (441/2111/N1) valence basis set for the metal atoms (N = 4 for Cr and N = 2 for Au)[41] and 6-31G(d) all electron basis sets[42] for the other atoms were employed in the geometry optimisations. This is the standard basis set II.[43] The nature of the stationary points was examined by calculating the Hessian matrix at B3LYP/II. All structures are energy minima on the potential energy surface. The calculations have been performed with the program package Gaussian 98.[44]

Table 2.12: Crystallographic Data for **1** and **4**

|	1	4
Chemical Formula	$C_{26}H_{20}O_6PAuCr$	$C_{26}H_{20}O_6PAuW$
MW (g/mol)	708.36	840.21
Crystal system	Monoclinic	Monoclinic
Space group	$P2_1/c$	$P2_1/c$
a (Å)	10.6147(4)	10.6980(10)
b (Å)	12.0314(4)	12.1060(10)
c (Å)	20.4580(9)	20.3520(10)
α (°)	90	90
β (°)	99.705(2)	94.423(1)
γ (°)	90	90
Volume (Å^3)	2575.3(2)	2627.9(4)
Z	4	4
d_{calcd} (g/cm^3)	1.827	2.124
Temp (K)	173(2)	150(2)
$\mu_{Mo\,K\alpha}$ (cm^{-1})	6.212	10.048
$2\theta_{max}$ (°)	25.49	27.00
Radiation	Mo Kα, graphite monochromated	Mo Kα, graphite monochromated
Crystal size (mm)	$0.012 \times 0.02 \times 0.15$	$0.13 \times 0.25 \times 0.25$
Index range	$-12 \leq h \leq 12$	$-13 \leq h \leq 10$
	$-14 \leq k \leq 12$	$-15 \leq k \leq 14$
	$-20 \leq l \leq 24$	$-26 \leq l \leq 22$
No. of reflections collected	12767	13102
No of independent reflections	4787 ($R_{int} = 0.0880$)	5627 ($R_{int} = 0.0272$)
No. of observed reflections	3158	4872
Refinement	Full matrix on F^2 (SHELXL)	Full matrix on F^2 (SHELXL)
Parameters	325	326
R_1 ($F_o > 2\sigma\,F_o$)	0.0454	0.0219
wR_2 (all data)	0.0867	0.0461

2.5 References

1. Kreiter, C. G. *Angew. Chem., Int. Ed. Engl.*, **1968**, *7*, 390.

2. Bernasconi, C. F. *Chem. Soc. Rev.*, **1997**, *26*, 299.

3. (a) Dötz, K.H. Angew. *Chem., Int. Ed. Engl.*, **1984**, 23, 5878. (b) Casey, C.P. in "*Transition Metal Organometallics in Organic Synthesis*", Alper, H., Ed. Academic Press, New York, **1979**.

4. Veya, P., Floriani, C., Chiesi-Villa, A., Rizzoli, C. *Organometallics*, **1994**, *13*, 214.

5. Brent Gunroe, T., White, P.S., Templeton, J.L. *Organometallics*, **1997**, *16*, 370 and references therein.

6. Fischer, E. O.; Plabst, D. *Chem. Ber.*, **1974**, *107*, 3326.

7. Bernasconi, C. F., Flores, F.X., Sun, W. *J. Am. Chem. Soc*, **1995**, *117*, 4875.

8. Aumann, R., Hinterding, P., Krüger, C., Goddard, R. J. *Organomet. Chem.*, **1993**, *459*, 145.

9. Crabtree, R.H. "*The Organometallic Chemistry of the Transition Metals*", Wiley-Interscience, New York, **1988**, p. 91.

10. Bernasconi, C. F., Sun, W. *Organometallics*, **1995**, *14*, 5615.

11. Seebach, D. *Angew. Chem., Int. Ed. Engl.*, **1979**, *18*, 239.

12. McDonald, F. E.; Schultz, C. C.; Chatterjee, A. K. *Organometallics*, **1995**, *14*, 3628.

13. (a) McDonald, F. E.; Reddy, K. S.; Díaz, Y. *J. Am. Chem. Soc*, **2000**, *122*, 4304. (b) Bowman, J. L.; McDonald, F. E. *J. Org. Chem.*, **1998**, *63*, 3680. (c) McDonald, F. E. Chatterjee, A. K. *Tetrahedron Lett.*, **1997**, *38*, 7687.

14. (a) Fuchibe, K.; Iwasawa, N. *Tetrahedron*, **2000**, *56*, 4907. (b) Herndon, J.W., Reid, M.D. *J. Am. Chem. Soc*, **1994**, *116*, 383.

15. Coalter III, J. N.; Bollinger, J. C.; Huffman, J. C.; Werner-Zwanziger, U.; Caulton, K. G.; Davidson, E. R; Gérard, H.; Clot, E.; Eisenstein, O. *New. J. Chem.* **2000**, *24*, 9.

16. (a) Abel, E.W., Stone, F.G.A., Wilkinson, G., Hegedus, L.S. *Comprehensive Organometallic Chemistry*, Pergamon, Oxford, **1982**. (b) Abel, E.W., Stone, F.G.A., Wilkinson, G., Hegedus, L.S. *Comprehensive Organometallic Chemistry II*, Pergamon, Oxford, **1995**. (c) Patai, S., Rappoport, Z. Eds. "*The Chemistry of Organic Derivatives of Gold and Silver*", J. Wiley & Sons, Chichester, **1999**.

17. (a) Hall, K.K.; Mingos, D.M.P. *Prog. Inorg. Chem.*, **1984**, *32*, 237. (b) Evans, D.G.; Mingos, D.M.P. *J. Organomet, Chem.*, **1982**, *232*, 171. (c) Hoffmann, R. *Angew. Chem., Int. Ed. Engl.,* **1982,** *21*, 711.

18. Green, M., Orpen, A.G., Salter, I.D., Stone, F.G.A. *J. Chem. Soc., Chem. Commun.*, **1982**, 813.

19. Eisenstein, O.; Hoffmann, R. *J. Am. Chem. Soc*, **1981**, *103*, 4308.

20. Baldwin, J.E., Hofle, G.A., Lever, Jr., O.W. *J. Am. Chem. Soc*, **1974**, *96*, 7125.

21. (a) Fischer, E.O., Kreiβl, F.R. in "*Synthetic Methods of Organometallic and Inorganic Chemistry (Herrmann/Brauer)*" Vol. 7 : Transition Metals Part 1, Herrmann, W.A., Ed. **1997**, p.129. (b) Fischer, E.O. *Adv. Organometallic Chem.*, **1976**, *14*, 1.

22. Mills, O.S.; Redhouse, A.D. *J. Chem. Soc. (A)*, **1968**, 642.

23. (a) Raubenheimer, H.G.; Desmet, M.; Kruger, G.J. *J. Chem. Soc., Dalton Trans.*, **1995**, 2067. (b) Desmet, M.; Raubenheimer, H.G.; Kruger, G.J. *Organometallics*, **1997**, *16*, 3324. (c) Raubenheimer, H.G.; Olivier, P.J.; Lindeque, L.; Desmet, M., Hrušak, J.; Kruger, G.J. *J. Organomet, Chem.*, **1997**, *544*, 91.

24. (a) Fernández, E.J.; López-de-Luzuriaga, J.M.; Monge, M.; Olmos, E.; Gimeno, M.C.; Laguna, A.; Jones, P.G. *Inorg. Chem.*, **1998**, *37*, 5532. (b) Bayler, A.; Schier, A.; Schmidbaur, H. *Inorg. Chem.*, **1998**, *37*, 4353. (c) Chan, W-H.; Mak, T.C.W.; Che, C-M. *J. Chem. Soc., Dalton Trans.*, **1998**, 2275.

25. (a) Cotton, F.A.; Kraihanzel, C.S. *J. Am. Chem. Soc*, **1962**, *84*, 4432. (b) Ainscough, E.W.; Brodie, A.M.; Furness, A.R. *J. Chem. Soc., Chem. Comm.*, **1971**, 1357. (c) Magee, T.A.; Matthews, C.N.; Wang, T.S.; Wotiz, J.H. *J. Am. Chem. Soc*, **1961**, *83*, 3200. (d) Brown, R.A., Dobson, G.R. *Inorg. Chim. Acta*, **1972**, *6*, 65.

26. Pauling, L. "*The Nature of the chemical bond*" 3rd ed., **1960** Cornell University Press: Ithaca, NewYork.

27. Kuhn, N.; Bohnen, H.; Blaser, D.; Boese, R. *Chem. Ber.*, **1994**, *127*, 1405 and references therein.

28. (a) Baird, G.J.; Davies, S.G., Jones, R.H.; Prout, K.; Warner, P. *Chem. Commun.*, **1984**, 745. (b) Veya, P.; Floriani, C.; Chiesi-Villa, A.; Rizzoli, C. *Organometallics*, **1994**, *13*, 214. (c) Xu, D.; Miki, K.; Tanaka, M.; Kasai, N.; Yasuoka, N.; Wada, M. *J. Organomet. Chem.*, **1989**, *371*, 267.

29. (a) Steinborn, D.; Becke, S.; Herzog, R.; Gunther, M.; Kircheisen, R.; Stoeckli-Evans, H.; Bruhn, C. *Z. Anorg. Allg. Chem.*, **1998**, *624*, 1303. (b) Raubenheimer, H.G.; Kruger, G.J.; Marais, C.F.; Hattingh, J.T.Z.; Linford, L.; van Rooyen, P.H. *J. Organomet. Chem.*, **1988**, *355*, 337. (c) Flörke, U.; Haupt, H.-J.; Jones, P.G. *Acta Crystallogr., Sect. C. (Cr. Str. Comm)*, **1996**, *52*, 609.

30. Stevens, P.J.; Devlin, F.J.; Chablowski, C.F.; Frisch, M.J. *J. Phys. Chem.* **1994**, *98*, 11623.

31. Reed, A.E.; Curtiss, L.A.; Weinhold F. *Chem. Rev.* **1988**, *88*, 899.

32. Bader, R.F.W. "*Atoms in Molecules: A Quantum Theory*", **1990**, Clarendon Press, Oxford.

33. Winkle, M.R., Lansinger, J.M., Roland, R.C. *J. Chem. Soc., Chem. Commun.*, **1980**, 87.

34. Fackler Jr., J.P. *Inorganic Syntheses*, **1982**, *21*, 325.

35. Nonius, B.V. "*COLLECT, Data collection software*", **1999**, Delft, The Netherlands.

36. Otwinowski, Z.; Minor, W. *Methods Enzymol.* **1997**, *276*, 307.

37. Sheldrick, G. M. *SHELX-97*. Program for crystal structure analysis, University of Göttingen, Germany, **1997**.

38. Farrugia, L.J. *J. Appl. Cryst.*, **1997**, *30*, 565.

39. Becke, A.D. *J. Chem. Phys.* **1993**, *98*, 5648.

40. Lee, C.; Yang, W.; Parr, R.G. *Phys. Rev. B*, **1988**, *37*, 785.

41. Hay, P.J.; Wadt, W.R. *J. Chem. Phys.* **1985**, *82*, 299.

42. (a) Ditchfield, R.; Hehre, W.J; Pople, J.A. *J. Chem. Phys.* **1971**, *54*, 724. (b) Hehre, W.J.; Ditchfield, R.; Pople, J.A. *J. Chem. Phys.* **1972**, *56*, 2257.

43. Frenking, G.; Antes, I.; Böhme, M.; Dapprich, S.; Ehlers, A.W.; Jonas, V.; Neuhaus, A.; Otto, M.; Stegmann, R.; Veldkamp, A.; Vyboishchikov, S.F. in *Reviews in Computational Chemistry*, Vol. 8, K.B. Lipkowitz and D.B. Boyd (Eds), VCH, New York, **1996**, 63.

44. Gaussian 98 (Revision A.8): Frisch, M.J.; Trucks, G.W.; Schlegel, H.B.; Scuseria, G.E.; Robb, M.A.; Cheeseman, J.R.; Zakrzewski, V.G.; Montgomery, J.A.; Stratmann, R.E.; Burant, J.C.; Dapprich. S.; Milliam, J.M.; Daniels, A.D.; Kudin, K.N.; Strain, M.C.; Farkas, O.; Tomasi, J.; Barone, V.; Cossi, M.; Cammi, R.; Mennucci, B.; Pomelli, C.; Adamo, C.; Clifford, S.; Ochterski, J.; Petersson, G.A.; Ayala, P.Y.; Cui, Q.; Morokuma, K.; Malick, D.K.; Rabuck, A.D.; Raghavachari, K.; Foresman, J.B.; Cioslowski, J.; Ortiz, J.V.; Stefanov, B.B.; Liu, G.; Liashenko, A.; Piskorz, P.; Komaromi, I.; Gomberts, R.; Martin, R.L.; Fox, D.J.; Keith, T.A.; Al-Laham, M.A.; Peng, C.Y.; Nanayakkara, A.; Gonzalez, C.; Challacombe, M.; Gill, P.M.W.; Johnson, B.G.; Chen, W.; Wong, M.W.; Andres, J.L.; Head-Gordon, M.; Replogle, E.S.; Pople, J.A. Gaussian Inc., Pittsburgh, PA, **1998**.
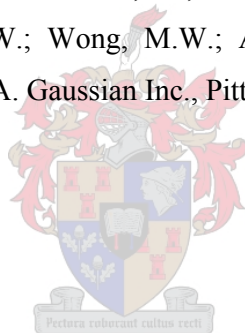
CHAPTER 3

NOVEL REACTIONS OF C-DEPROTONATED METHYL DIALKYLAMINO AND METHYL ALKYLTHIO FISCHER-TYPE CARBENE ANIONS WITH TRIPHENYLPHOSPHINE GOLD(I) CHLORIDE

3.1   Introduction

As mentioned in Chapter 1, the carbene carbon atoms in alkoxy Fischer-type carbene complexes are quite electrophilic due to their coordination to the strongly electron-withdrawing metal pentacarbonyl groups.[1] One consequence of this is that nucleophilic addition reactions of a wide range of sterically unhindered nucleophiles readily occur on these carbene carbon atoms (Scheme 3.1).

M = Cr, Mo, W
$Nu^1 = NH_3$, R"NH_2,
    small R"$_2$NH,
$Nu^2 = $ R"S^-, Ph$^-$
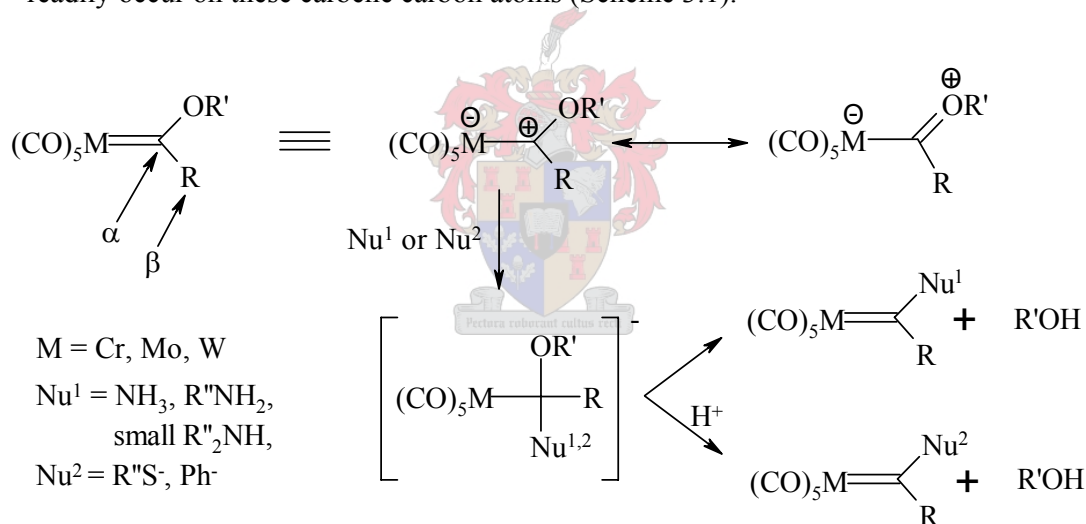
Scheme 3.1

Although the PPN$^+$ salts of resulting anionic tetrahedral intermediates are isolable, they are generally very unstable.[2] The better leaving group, usually the alkoxy group (R'O$^-$), is rapidly ejected to yield the substituted carbene complex. This reaction is widely regarded as an organometallic analogue of the transesterification reaction of organic esters and is one of the best methods for the preparation of Fischer-type carbene complexes stabilised by hetero-atoms other than oxygen.[1] In fact, this is also the procedure used to prepare the relatively unstable pentacarbonyl[bis(phenyl) carbene]chromium(0) carbene complex that contains no stabilising hetero-atoms.[3]

Although many nucleophiles react with Fischer-type carbene complexes in this manner, the nucleophilic addition of unhindered amines to carbene carbon atoms is the most efficient and widely applied conversion to follow this mechanism.[1] Fischer-type aminocarbene complexes, mostly prepared along this route, have frequently been applied in the synthesis of complex organic compounds containing N-heterocyclic rings and amino side-chains.[4] The aminocarbene complexes are also thermodynamically more stable than the corresponding alkoxycarbene complexes, certainly contributing to the efficiency of the conversion. The reason for this lies with increased π-electron donor capability of the nitrogen hetero-atom that is able to stabilise the electron deficiency on the $M(CO)_5$ fragment more efficiently than a more electronegative oxygen hetero-atom. Indeed, barriers to rotation around the $C_{carbene}$-N bond, affording isomers of aminocarbene complexes, are often found.[5] This indicates that π-electron donation from the nitrogen atom in such complexes is so strong that they are best represented by a zwitterionic resonance structure (structure **E** in Scheme 3.2).
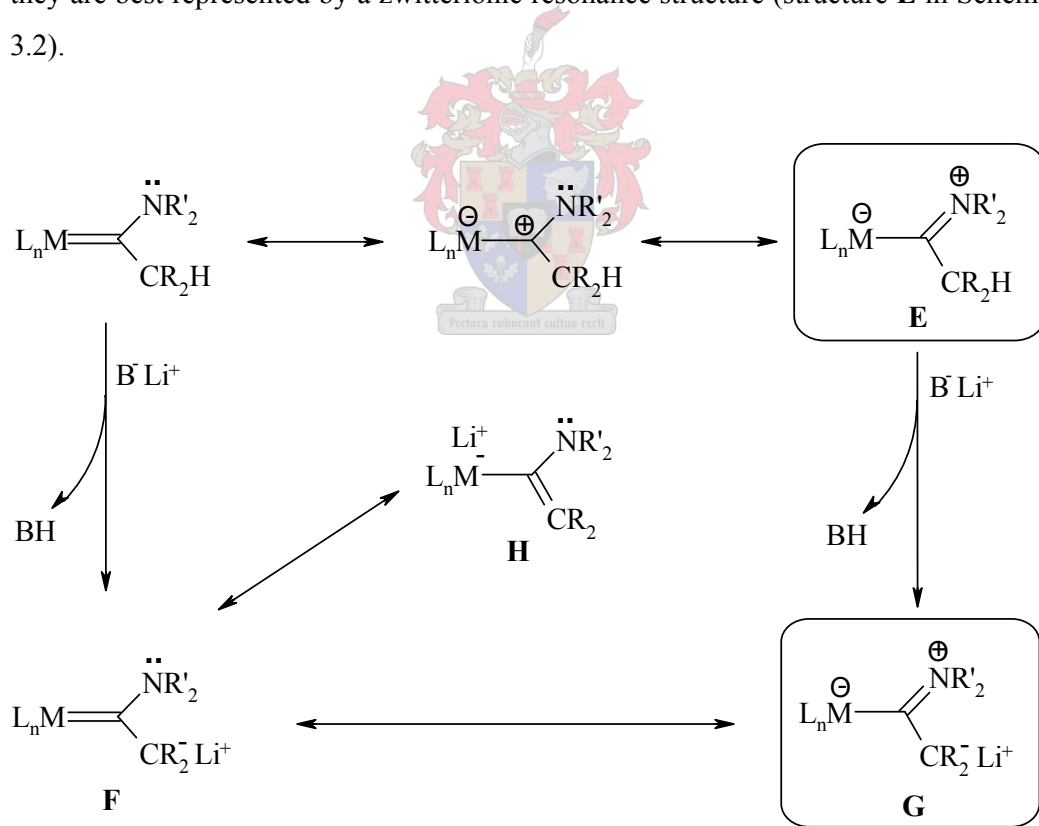
Scheme 3.2

Another consequence of the increased π-electron donation capability from the nitrogen hetero-atoms is that Fischer-type dialkylaminocarbene complexes with hydrogen atoms on the β-metallo carbon atom are much less acidic than their alkoxycarbene equivalents. Thermodynamic and kinetic studies conducted by the group of Bernasconi report pK_a values greater than 33.0 for $(CO)_5Cr=C[N(CH_3)_2]CH_3$ in acetonitrile compared to 22.7 reported for $(CO)_5Cr=C(OCH_3)CH_3$.[6] Bernasconi *et al* could also prove a direct link between the nitrogen π-electron donation and the β-metallo CH-acidity of aminocarbene complexes by considering the acidity of aminocarbene complexes with cyclic amino groups. The ring strain in the cyclic amino groups counteract the partial sp^2 hybridisation of the nitrogen hetero-atom when it is involved in π-electron donation to the carbene carbon atom, thus reducing its electron donating capability and increasing the acidity of these complexes.[6]

In aminocarbene complexes that contain tertiary amine hetero-atoms that can easily assume sp^2 geometry, the electron deficiency at the carbene carbon atom is already reduced to such an extent by π-electron donation from the nitrogen that the negative charge in the β-metallo CH-deprotonated bases of these complexes (resonance structures **F** & **G**, Scheme 3.2), largely remains at the site of deprotonation. This means that the contribution of resonance structure **H**, which is known to stabilise the conjugate bases of alkoxycarbene complexes, is significantly reduced.[7] The result is that irreversibly deprotonated aminocarbene anions, best represented by resonance structure **G** (Scheme 3.2), exhibit enhanced nucleophilicity and undergo efficient electrophilic addition reactions with a wide range of electrophiles exclusively at the β-metallo carbon atom, compared to the equivalent alkoxycarbene "enolates" which generally only react with the strongest electrophiles and mostly in low yields.[8]

Sulphur stabilised Fischer-type alkyl(thio)carbene complexes can also be prepared by the reaction outlined in Scheme 3.1. Their preparation is analogous to that of aminocarbene complexes except that instead of a nitrogen nucleophile, a sulphur nucleophile is employed.[9] The chemistry of Fischer-type thiocarbene complexes is, however, much less developed than that of alkoxy- and aminocarbene complexes. This is probably due to a number of reasons: Firstly, although the thiocarbene complexes themselves are reasonably stable, their synthesis is not always as

straightforward. This is probably due to the weaker nucleophilicity of the sulphur nucleophiles as a result of the much greater polarisability or 'softness' of sulphur.[10] Often the alkyl/arylthiol nucleophiles used in the preparation of thiocarbene complexes, especially the more sterically hindered ones, first have to be irreversibly deprotonated in order to increase their nucleophilicity to get any reaction at all, whereas neutral amines mostly react spontaneously as nucleophiles on the alkoxycarbene carbon atoms.[11(a),1] Secondly, thiocarbene complexes as well as the alkylthiols used in their synthesis are extremely pungent and often quite poisonous compounds – two characteristics which certainly make the synthesis of thiocarbene complexes less attractive. Lastly, thiocarbene complexes have, as of yet, not found much application in organic synthesis. The further use of thiocarbene complexes as building blocks for the synthesis of complex organic compounds has not developed nearly as far than that of alkoxy- and aminocarbene complexes.

Regarding the physical characteristics of thiocarbene complexes, much less is known about the reaction characteristics of these complexes compared to alkoxy- and aminocarbene complexes. Four recent studies by Bernasconi are the only works in which the physical chemistry of thiocarbene complexes have been described.[11] Bernasconi reports β-carbon CH-acid pK_a values for the thiocarbene complex $(CO)_5Cr=C(SCH_3)CH_3$ that are 3.5 to 4 units lower than the pK_a values reported for the oxygen analogue, $(CO)_5Cr=C(OCH_3)CH_3$. From this follows that the electrophilic carbene carbon atoms in thiocarbene complexes are poorly stabilised by π-electron donation from the sulphur hetero-atom to the metal carbonyl and that the structures of thiocarbene complexes are best represented by resonance structure **I** (Scheme 3.3). These characteristics of thiocarbene complexes have been confirmed by crystallographic studies which report short metal-carbene bonds and very little evidence of double bond character in the $C_{carbene}$-S bond.[12] After β-metallo deprotonation, the conjugate bases of the thiocarbene complexes are thus expected to be greatly stabilised by electron delocalisation from the β-metallo carbon atom to the $M(CO)_5$ fragment (resonance structure **M** in Scheme 3.3). This also means that electrophilic addition reactions at the β-metallo carbon atoms of thiocarbene complexes are expected to be less efficient than for alkoxy- and aminocarbene complexes and that electrophilic addition onto the metal atom, and subsequently onto

the α-metallo carbon atom, along the alternative electrophilic addition pathway described in Chapter 2 [Scheme 2.2(b)], would not be too surprising. Despite this there are no reports in the literature of such reactions. To our knowledge, there are also no reports of electrophilic addition reactions at the β-metallo carbon atoms of thiocarbene complexes, most likely due to the expected poor efficiency of this conversion as well as the poor development and application of the chemistry of thiocarbene complexes.
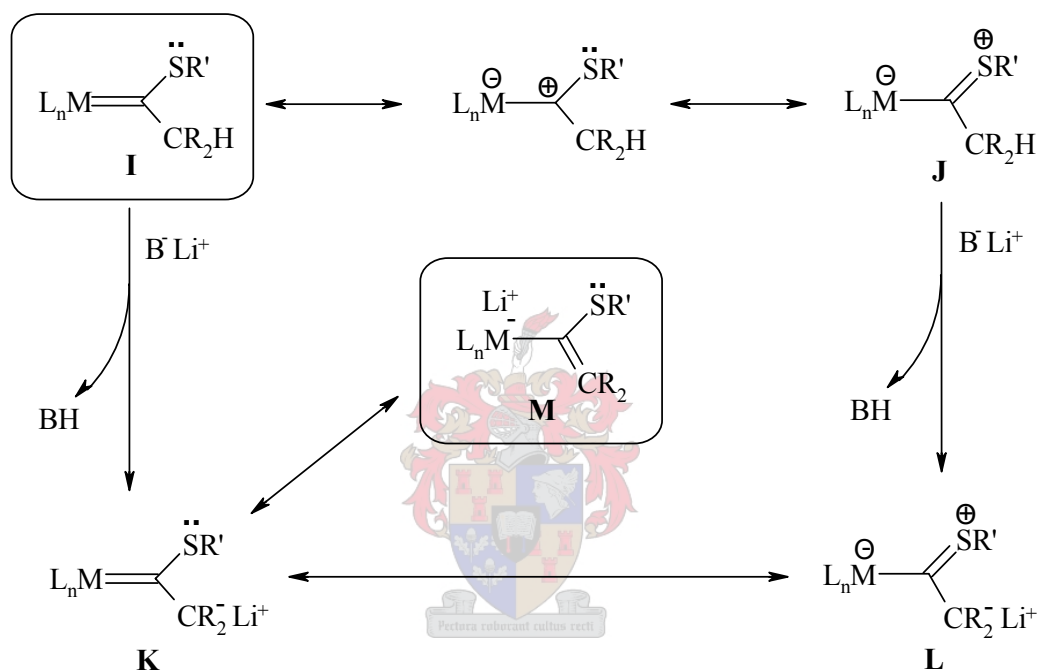
Scheme 3.3

In the light of the different physical properties of Fischer-type amino- and thiocarbene complexes compared to their alkoxycarbene counterparts, in particular their varying β-metallo CH-acidities and thus expected reaction characteristics, we endeavoured to extend the work described in Chapter 2, concerning the electrophilic addition of the Ph_3PAu^+ electrophile to β-metallo carbon deprotonated Fischer-type alkoxycarbene complexes, to include examples of similar reactions with amino- and thiocarbene complexes.

The contents of this chapter describes the results obtained in our study and specifically addresses the following questions:

1) Where does the electrophilic addition of Ph_3PAu^+ to β-metallo deprotonated Fischer-type amino- and thiocarbene complexes take place, at the site of deprotonation or effectively at the carbene carbon atom, as was observed for Fischer-type alkoxycarbene complexes (Chapter 2)?

2) If electrophilic addition takes place at the carbene carbon atom and dialkylaminovinyl-gold(I)PPh$_3$ and alkyl/arylthiovinyl-gold(I)PPh$_3$ fragments are formed along the same reaction path as the alkoxyvinyl-gold(I)PPh$_3$ moieties described in Chapter 2, would these also coordinate to the coordinatively unsaturated M(CO)$_5$ fragments to form η^2-{dialkylaminovinyl-gold(I)PPh$_3$}M(CO)$_5$ and η^2-{alkyl/arylthiovinyl-gold(I)PPh$_3$}M(CO)$_5$ complexes, or would coordination to the M(CO)$_5$ fragments, if any coordination occurs, involve the potential nitrogen or sulphur donor atoms in the respective amine/thioether groups?

3) If coordination of the dialkylaminovinyl-gold(I)PPh$_3$ and alkyl/arylthiovinyl-gold(I)PPh$_3$ fragments to the M(CO)$_5$ groups occurs through the olefin, would it be symmetric or asymmetric?

4) If olefin coordination occurs and is asymmetric, how is this, usually unstable coordination mode stabilised?

5) Would the products of the reactions be stable enough to be efficiently isolated and structurally characterised?

3.2 Results and Discussion

3.2.1 η^2-{Dimethylaminevinyl-gold(I)triphenylphosphine} M(CO)$_5$ and η^2-{Diethylaminevinyl-gold(I)triphenylphosphine} M(CO)$_5$ bimetallic complexes
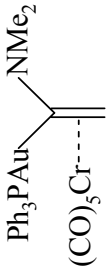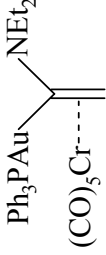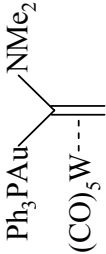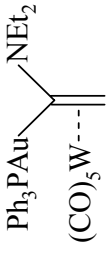
A.   General preparation and discussion of η^2-{Ph$_3$PAuC(N**R$_2$**)=CH$_2$}**M**(CO)$_5$
M = Cr, **R** = Me (**7**) / **R** = Et (**8**); **M** = W, **R** = Me (**9**) / **R** = Et (**10**)

The syntheses of complexes **7-10** (Scheme 3.4) were carried out in a similar fashion to complexes **1-5** discussed in Chapter 2. Product separation of oily, dark-yellow reaction mixtures (52-68% yields after separation) was carried out by low temperature (-15°C) silica gel column chromatography with pentane/diethyl ether (10:1) as eluant, followed by crystallisation from a diethyl ether solution layered with pentane at –20°C. Physical data for the isolated new compounds are summarised in Table 3.1.
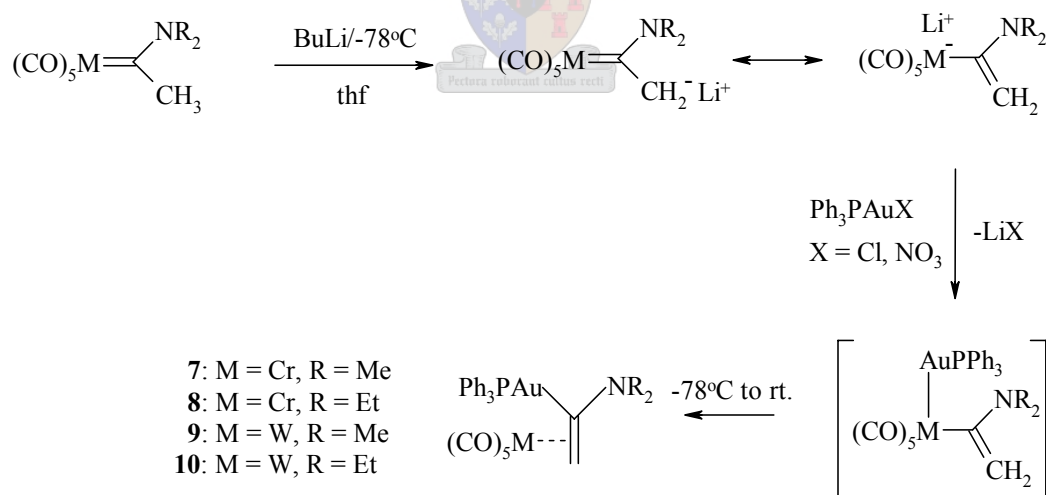
Scheme 3.4

Table 3.1: Analytical data for complexes **7-10**

Complex	$Ph_3PAu{-}C(NMe_2){=}[(CO)_5Cr]$	$Ph_3PAu{-}C(NEt_2){=}[(CO)_5Cr]$	$Ph_3PAu{-}C(NMe_2){=}[(CO)_5W]$	$Ph_3PAu{-}C(NEt_2){=}[(CO)_5W]$
	7	**8**	**9**	**10**
M.p. / °C	89 (decomp.)	82 (decomp.)	95 (decomp.)	85 (decomp.)
Color	yellow	yellow	yellow	yellow
Yield (%)	54	59	68	52
M.W. (g / mol)	721.41	749.47	853.27	881.32
Analyses (%)[a]				
C	45.03 (44.95)	46.61 (46.48)	38.24 (38.01)	39.65 (39.52)
H	3.28 (3.21)	3.76 (3.63)	2.93 (2.72)	3.28 (3.09)
N	2.10 (1.94)	2.02 (1.87)	1.70 (1.64)	1.75 (1.59)
O	11.49 (11.09)	10.85 (10.67)	9.40 (9.38)	9.20 (9.08)
P	4.01 (4.29)	4.05 (4.13)	3.32 (3.63)	3.50 (3.51)

[a] Required values given in parenthesis

66

Similarly to the formation of complexes **1-5**, described in Chapter 2, we accept the hydrolysis reaction mechanism suggested by Casey and Bernasconi (Section 2.1) for the aurolytic formation of the gold vinyl amine complexes **7-10**.[7] The formation of the bimetallic vinyl amine complexes **7-10** (Scheme 3.4) along the same reaction scheme as the formation of the bimetallic vinyl ether complexes **1-5** is quite unexpected. The increased nucleophilicity of the β-metallo carbon atom in the deprotonated aminocarbene complexes usually leads to efficient electrophilic addition exclusively at the β-carbon atom.[8] Also, unlike for alkoxycarbene complexes, no hydrolytic decomposition reaction mechanisms have thus far been suggested for Fischer-type aminocarbene complexes. To our knowledge the formation of the novel vinyl-coordinated {dialkylaminovinyl-gold(I)PPh$_3$}M(CO)$_5$ bimetallic complexes (**7-10**) by a reaction related to the hydrolysis of Fischer-type carbene complexes, which we call "aurolysis" (section 2.1), is the first example in which Fischer-type aminocarbene complexes have reacted in this manner.

Furthermore, despite the fact that the olefin coordination in complexes **7-10** is even more asymmetric than in **1-5** [as reported in the crystal structure of **7** in section 3.2.1 (C)], and is therefore expected to be highly unstable, these complexes also exhibit remarkable stability. In **7-10**, however, this stability is not ascribed to resonance stabilisation of a partial positive charge on the α-gold vinyl carbon atom to the Ph$_3$PAu fragment (structure **Q** in Scheme 3.5) as could be done for **1-5**, but rather to delocalisation of that charge to the nitrogen atom (resonance structure **P**). Evidence for such an assumption is reported in sections 3.2.1 (B) & (C).
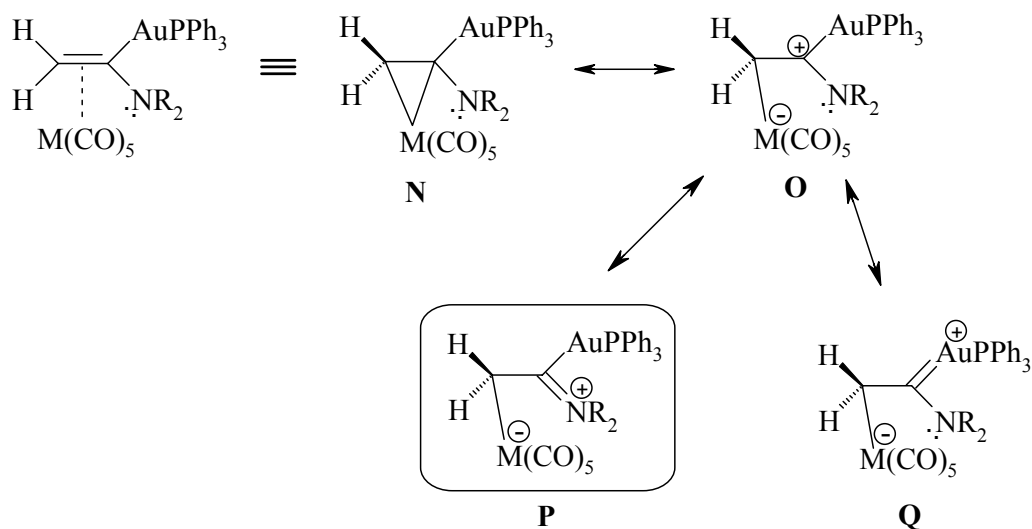
Scheme 3.5

B.   Spectroscopic characterisation of complexes **7-10**

1.   NMR Spectroscopy

The ^1H, $^{13}C\{^1H\}$ and $^{31}P\{^1H\}$ NMR spectroscopic data for complexes **7-10** are summarised in Tables 3.2-3.5. Similarly to the ^1H NMR spectra of **1-5** [Section 2.2.1 (C)] the ^1H NMR spectra of **7-10** are characterised, in particular, by two distinctive signals, each integrating for a single proton and representing two chemically non-equivalent terminal CH_2-vinyl protons. Resonances for the vinyl protons *cis* to the AuPPh$_3$ fragment in **7-10** appear, due to weak long range *cis*-$^4J_{P-H}$ coupling, as broadened singlet or narrow doublet resonances at δ 1.93, 1.97, 2.51 and 2.50, whereas those for the vinyl protons *trans* to the AuPPh$_3$ fragment appear as distinct doublets, due to more efficient *trans*-$^4J_{P-H}$ coupling, at δ 2.55, 2.52, 3.00 and 2.91. Compared to the equivalent chemical shifts of these protons in **1-5**, these signals are shifted ~0.2 ppm (*cis* vinyl protons) and ~1.2 ppm (*trans* vinyl protons) upfield. Similarly, the ^{13}C chemical shifts for the β-vinyl carbon atoms in **7-10** appear significantly upfield (15-20 ppm) from the corresponding signals in **1-5**, and are in fact quite close to the aliphatic region of the ^{13}C NMR spectrum (δ 36.5, 40.1, 36.0 and 42.1 for **7-10** respectively). These upfield shifts in the ^1H and ^{13}C NMR spectra suggest that the terminal vinyl CH_2-carbon atoms in **7-10** display less s-character than

68

those in **1-5**. These ^{1}H and ^{13}C NMR resonances are, however, still situated somewhat downfield compared to literature reported values for methylene groups directly bonded to negatively charged W(CO)$_5$ fragments.[13] The ^{13}C{^{1}H} resonances for the α-gold vinyl carbon atoms in **7-10** could be easily assigned due to their characteristically large $^{2}J_{C-P}$ coupling constants (117.6-134.2 Hz). They appear between δ 207.9 and 218.3, roughly 10-20 ppm downfield from the signals observed for such atoms in complexes **1-5**.

The combination of respective downfield and upfield shifted resonances for the α- and β-gold vinyl carbon atoms in **7-10**, compared to the position of the equivalent signals in the NMR spectra of **1-5**, suggest a greater degree of asymmetry in the vinyl coordination in **7-10**. The chemical shifts for the α-gold vinyl carbon atoms in **7-10**, furthermore, indicate that they are greatly deshielded and that they almost certainly are sp^{2}, or pseudo-sp^{2} hybridised. Whether these atoms are partially double bonded to the nitrogen atoms (resonance structure **P**, Scheme 3.5) or to the AuPPh$_3$ fragments (resonance structure **Q**) in **7-10** (or perhaps a bit to both), is unfortunately not clear from the NMR spectra of these compounds. At first it was thought that, should partial delocalisation of the positive charge occur to the nitrogen atom, this would impose a barrier to rotation around the C$_{α\text{-vinyl}}$-N bond, which in turn would be observable by the presence of separate ^{1}H and ^{13}C resonances for diastereotopic NCH$_3$ (**7** and **9**) and NCH$_2$ (**8** and **10**) groups. The possibility, however, exists that should hybridisation of the nitrogen atoms not be purely sp^{2} – which is very likely in such a delocalised system – and there is still a meaningful bonding contribution from the α-gold vinyl carbon atom to the M(CO)$_5$ fragments, the α-gold vinyl carbon atom may be a stereo centre. This would mean that **7-10**, like **1-5**, are chiral molecules, thus making the hydrogen and carbon atoms in the N(CH$_3$)$_2$ and N(CH$_2$CH$_3$)$_2$ groups diastereotopic, regardless of whether free rotation around the C-N bond is allowed or not.
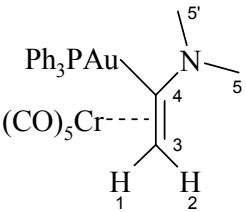
The proton resonances for diastereotopic NCH$_3$ groups in **7** and **9** appear as two clearly separated signals at δ 2.79 and 3.45, and 2.79 and 3.42, each integrating for 3 hydrogen atoms. In the ^{13}C NMR spectrum a single broadened resonance (δ 29.2 and 29.4 for **7** and **9**) represents both N(CH$_3$)$_2$ carbon atoms. Each diastereotopic methylene proton in **8** and **10** is separately represented as a doublet of quartets in the ^{1}H NMR spectrum. The quartet structure (J = 7.2-7.3 Hz) is assigned to $^{3}J_{H-H}$

coupling with the terminal methyl groups and the doublet structure (J = 10.0-10.2 Hz) is ascribed to $^2J_{H-H}$ geminal coupling. In the ^{13}C NMR spectrum of **8** and **10** the signal for the diastereotopic methylene carbon atoms, like those for the NCH$_3$ groups in **7** and **9**, appear as broad singlets [δ 25.2 (**8**) and δ 27.5 (**10**)] whereas two clearly separated peaks for the terminal CH$_3$ groups are observed [δ 12.5 and 13.6 in **8**; δ 12.9 and 14.0 in **10**].

Although the ^{1}H and ^{13}C NMR spectra do not give a clear picture of the positive charge delocalisation, it is clear from the chemical shifts of the terminal CH$_2$ vinyl protons and the α- and β-gold vinyl carbon atoms that the asymmetry in the vinyl coordination in **7-10** is greater than in **1-5**. This interpretation of the NMR spectra of **7-10** is supported by the X-ray structure of **7** [Section 3.2.1 (C)], indicating a zwitterionic structure for this molecule.

The ^{31}P{^{1}H} NMR spectra of **7-10** exhibit singlet peaks, with chemical shifts between 38.0 and 41.9 ppm, for the PPh$_3$ moiety coordinated to the gold atom. Curiously, these signals are situated meaningfully upfield (~3 ppm) compared to the ^{31}P resonances measured for the chromium methoxyvinyl- and ethoxyvinyl-gold(I)PPh$_3$ analogues (**1** and **2**) and slightly downfield (0.8-1.1 ppm) compared to the ^{31}P resonances observed for the corresponding tungsten methoxyvinyl- and ethoxyvinyl-gold(I)PPh$_3$ analogues (**4** and **5**). This result suggests a slightly more electropositive gold atom in the tungsten complexes (**9** and **10**), which may indicate that there might be a slight component of positive charge delocalisation to the gold atom in the tungsten complexes (as represented by resonance structure **S** in Scheme 3.5). Charge delocalisation of the positive charge in the chromium complexes (**7** and **8**), on the other hand, is only to the 'hard' nitrogen atom (resonance structure **P**), as is confirmed in the crystal structure of the chromium complex, **7** [Section 3.2.1 (C)].

Table 3.2

Complex		
		7
Solvent		CDCl$_3$
Temperature (K)		298
^{1}H NMR	H^1	1.93 (br s, 1H)
(600 MHz)	H^2	2.55 (d, $^4J_{trans\ \text{P-H}}$ = 8.5 Hz, 1H)
	H$^{5,\ 5'}$	2.79 (s, 3H), 3.45 (s, 3H)
	Ph	7.4-7.6 (m, 15H)
^{31}P{^{1}H} NMR	P	38.2 (s)
(243 MHz)		
^{13}C{^{1}H} NMR^a	C^3	36.5 (br s)
(150 MHz)	C^4	216.7 (d, $^2J_{\text{P-C}}$ = 134.2 Hz)
	C$^{5,\ 5'}$	29.2 (br s)
	Ph-C$_{ipso}$	130.2 (d, $^1J_{\text{P-C}}$ = 52.1 Hz)
	Ph-C$_{ortho}$	129.5 (d, $^2J_{\text{P-C}}$ = 10.9 Hz)
	Ph-C$_{meta}$	134.5 (d, $^3J_{\text{P-C}}$ = 13.2 Hz)
	Ph-C$_{para}$	131.8 (s)
	CO$_{cis}$	220.9 (s)
	CO$_{trans}$	226.5 (s)
υ (CO) (cm^{-1})^b		1896 (st, A$_1^{(2)}$), 1915 (v st, br, E), 1960 (v w, br B$_1$), 2044 (w, A$_1^{(1)}$)
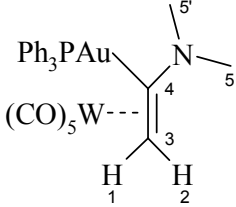
^{a}Measured in CD$_2$Cl$_2$

^{b} Pentane solution in NaCl-cell

Table 3.3

Complex	
	8
Solvent	CD_2Cl_2
Temperature (K)	298
^{1}H NMR (600 MHz) — H^1	1.97 (br s, 1H)
H^2	2.52 (br d, $^4J_{trans\ P\text{-}H}$ = 8.1 Hz, 1H)
H$^{5a,\ 5'a,\ 5b,\ 5'b}$	2.73 (dq, $^2J_{H\text{-}H}$ = 10.2 Hz, $^3J_{H\text{-}H}$ = 7.3 Hz, 1H)
	3.21 (dq, $^2J_{H\text{-}H}$ = 10.2 Hz, $^3J_{H\text{-}H}$ = 7.3 Hz, 1H)
	3.46 (dq, $^2J_{H\text{-}H}$ = 10.2 Hz, $^3J_{H\text{-}H}$ = 7.3 Hz, 1H)
	3.60 (dq, $^2J_{H\text{-}H}$ = 10.2 Hz, $^3J_{H\text{-}H}$ = 7.3 Hz, 1H)
H$^{6,\ 6'}$	1.12 (t, $^3J_{H\text{-}H}$ = 7.3 Hz, 3H),
	1.13 (t, $^3J_{H\text{-}H}$ = 7.3 Hz, 3H)
Ph	7.4-7.6 (m, 15H)
^{31}P{^{1}H} NMR (121.4 MHz) — P	38.0
^{13}C{^{1}H} NMR (150 MHz) — C^3	40.1 (br s)
C^4	218.3 (d, $^2J_{P\text{-}C}$ = 131.3 Hz)
C^5	25.2 (br, s)
C^6	12.5 (s), 13.6 (s)
Ph-C$_{ipso}$	130.2 (d, $^1J_{P\text{-}C}$ = 50.8 Hz)
Ph-C$_{ortho}$	129.3 (d, $^2J_{P\text{-}C}$ = 10.7 Hz)
Ph-C$_{meta}$	134.7 (d, $^3J_{P\text{-}C}$ = 13.1 Hz)
Ph-C$_{para}$	132.0 (s)
CO$_{cis}$	220.4 (s)
CO$_{trans}$	226.2 (s)
υ (CO) (cm^{-1})[a]	1893 (st, A$_1^{(2)}$), 1915 (v st, br, E), 1958 (v w, br B$_1$), 2043 (w, A$_1^{(1)}$)
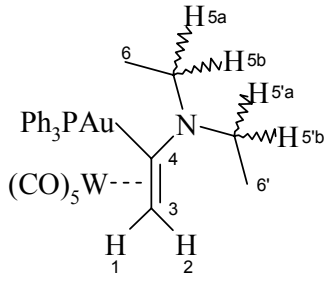
[a] Pentane solution in NaCl-cell

Table 3.4

Complex	
	9
Solvent	$CDCl_3$
Temperature (K)	298
^{1}H NMR H^1	2.51 (br s, 1H)
(600 MHz) H^2	3.00 (br s, 1H)
$H^{5,5'}$	2.79 (s, 3H), 3.42 (s, 3H)
Ph	7.4-7.6 (m, 15H)
^{31}P{^{1}H} NMR P	41.3 (s)
(243 MHz)	
^{13}C{^{1}H} NMR C^3	36.0 (d, $^3J_{P-C}$ = 3.6 Hz)
(150 MHz) C^4	207.9 (d, $^2J_{P-C}$ = 118.8 Hz)
$C^{5,5'}$	29.4 (br s)
Ph-C_{ipso}	129.8 (d, $^1J_{P-C}$ = 54.2 Hz)
Ph-C_{ortho}	129.2 (d, $^2J_{P-C}$ = 11.3 Hz)
Ph-C_{meta}	134.2 (d, $^3J_{P-C}$ = 13.5 Hz)
Ph-C_{para}	131.5 (s)
CO_{cis}	201.0 (s)
CO_{trans}	203.3 (s)
υ (CO) (cm^{-1})[a]	1900 (st, $A_1^{(2)}$), 1915 (v st, br, E), 1957 (v w, B_1), 2052 (w, $A_1^{(1)}$)

[a] Pentane solution in NaCl-cell

Table 3.5

Complex	
	10
Solvent	CD_2Cl_2
Temperature (K)	298
^{1}H NMR	H^1	2.50 (d, $^4J_{cis\ P-H}$ = 2.7 Hz, 1H)
(600 MHz)	H^2	2.91 (d, $^4J_{trans\ P-H}$ = 9.0 Hz, 1H)
	$H^{5a,\ 5'a,\ 5b,\ 5'b}$	2.96 (dq, $^2J_{H-H}$ = 10.0 Hz, $^3J_{H-H}$ = 7.2 Hz, 1H)
		3.45 (dq, $^2J_{H-H}$ = 10.0 Hz, $^3J_{H-H}$ = 7.2 Hz, 1H)
		3.64 (dq, $^2J_{H-H}$ = 10.0 Hz, $^3J_{H-H}$ = 7.2 Hz, 1H)
		3.83 (dq, $^2J_{H-H}$ = 10.0 Hz, $^3J_{H-H}$ = 7.2 Hz, 1H)
	$H^{6,\ 6'}$	1.20 (t, $^3J_{H-H}$ = 7.2 Hz, 3H),
		1.29 (t, $^3J_{H-H}$ = 7.2 Hz, 3H)
	Ph	7.4-7.6 (m, 15H)
^{31}P{H^1} NMR	P	41.9 (s)
(121.4 MHz)		
^{13}C{H^1} NMR	C^3	42.1 (d, $^3J_{P-C}$ = 2.4 Hz)
(150 MHz)	C^4	210.1 (d, $^2J_{P-C}$ = 117.6 Hz)
	$C^{5,\ 5'}$	27.5 (br, s)
	$C^{6,\ 6'}$	12.9 (s), 14.0 (s)
	Ph-C_{ipso}	130.2 (d, $^1J_{P-C}$ = 53.5 Hz)
	Ph-C_{ortho}	129.5 (d, $^2J_{P-C}$ = 12.6 Hz)
	Ph-C_{meta}	134.5 (d, $^3J_{P-C}$ = 12.7 Hz)
	Ph-C_{para}	131.8 (s)
	CO_{cis}	201.9 (s)
	CO_{trans}	203.8 (s)
υ(CO) (cm^{-1})[a]		1894 (st, $A_1^{(2)}$), 1912 (v st, br, E), 1958 (v w, B_1),
		2053 (w, $A_1^{(1)}$)

[a] Pentane solution in NaCl-cell

2. Infrared spectroscopy

The infrared (IR) spectra of **7-10** were recorded as pentane solutions of the complexes in a NaCl cell and are summarised in Tables 3.2 – 3.5. The IR spectra exhibit four absorption bands in the carbonyl region which could be assigned to $A_1^{(1)}$, $A_1^{(2)}$, B_1 and E vibrational modes [described in section 2.2.1(B)], and are consistent with molecules of the type $M(CO)_5L$. Compared to the corresponding IR absorptions in **1-5**, reported in Chapter 2, the IR absorption bands of **7-10** appear, in general, shifted roughly ~15 cm^{-1} to lower energy. Such a shift to lower frequency is symptomatic of greater back-donation from the metal atom to the π^*-orbitals of the CO ligands, thus decreasing the CO bond order and also the stretching frequency. This result is in agreement with the NMR data for **7-10**, which suggest greater polarisation of the vinyl coordination mode in these complexes and thus also a greater partial negative charge on the $M(CO)_5$ fragments. Such an interpretation of the IR spectra of **7-10** is confirmed by the crystal structure of **7**, reported below.

Apart from the ~15cm^{-1} "red shift" in the CO stretching frequencies of **7-10**, the IR spectra of **7-10** are in good agreement with those of **1-5**. The only other obvious difference is that the E-vibrational mode in complexes **7-10** remains broad and degenerate, indicating that, with greater asymmetry in the vinyl coordination mode comes less influence of the large and asymmetric dialkylaminovinyl-gold(I)PPh_3 π-complex donor on the $\upsilon(CO)$ frequencies. This is most likely as a result of the decreased steric influence that the dialkylaminovinyl-gold(I)PPh_3 moiety when it is further removed from the $M(CO)_5$ fragment.

3. Mass spectrometry

The positive-ion FAB-MS of complexes **7-10** were recorded in a *m*-nitrobenzylalcohol matrix. Similarly to the mass spectra reported for **1-6** in Chapter 2, the mass spectra of **7-10** are characterised by high intensity peaks for Ph_3PAu^+ (*m/z* 459), the homoleptic rearrangement product $(Ph_3P)_2Au^+$ (*m/z* 721) and clear molecular ion peaks (intensity in parenthesis given in percentage relative to the peaks of highest intensity) [**7**: *m/z* 721(20); **8**: *m/z* 750(35); **9**: *m/z* 852(50); **10**: *m/z* 881(65)].

Due to the 'soft' nature of the FAB ionisation technique, very poor fragmentation patterns for the complexes were observed. Strong peaks for the uncoordinated dialkylaminovinyl-gold(I)PPh$_3$ moieties [*m/z* 529 for **7** and **9** and *m/z* 558 for **8** and **10**] could, however, be clearly identified for each complex. In the mass spectra of **7** and **10** these signals were in fact the peaks of highest intensity. The strongest peaks in the mass spectra of **8** and **9** correspond to *m/z* 459 (Ph$_3$PAu$^+$).

C.   X-ray structure determination of complex **7**

The low temperature (173 K) crystal and molecular structure of complex **7** (Figure 3.1) was determined by X-ray diffraction techniques. The structure clearly shows, similar to the oxygen analogue of **7**, complex **1** [Section 2.1.1 (D)], a dimethylaminevinyl-gold(I)PPh$_3$ moiety coordinated in highly asymmetrical fashion to a square pyramidal Cr(CO)$_5$ fragment. Selected bond lengths and angles are listed in Table 3.6.

Of greatest interest in the structure of **7** is the highly asymmetric geometry of the η^2-{dimethylaminevinyl-gold(I)PPh$_3$}Cr(CO)$_5$ π-coordination. When analysing the difference in the Cr-vinyl carbon bond lengths [Δ(M-C) = M-C(7) – M-C(1), 0.610(5)Å] and the Cr-C(1)-C(7) angle [100.9(4)°] it becomes clear that the coordination of the dimethylaminevinyl-gold(I)PPh$_3$ fragment to the Cr(CO)$_5$ moiety is actually mainly in a covalent η^1-fashion through the terminal vinyl CH$_2$-group and that there is very little evidence of bonding between the chromium atom and the α-gold vinyl carbon atom [Cr-C(7) = 2.947(5) Å]. Slippage of the η^2-vinyl coordination to the asymmetrical η^1-mode is also described by a 0.39Å displacement of the olefin centroid from the metal centre [as defined by extension of the C(6)-Cr bond] in the Cr(CO)$_5$ coordination sphere. This, together with the large Cr-C(1)-C(7) angle and difference in Cr-C bond lengths mentioned above, indicates that the hybridisation of the β-gold vinyl carbon atom is close to sp^3. The positions of the vinyl hydrogen atoms could be determined from the difference Fourier map and also support a pseudo sp^3 hybridisation for the terminal vinyl carbon atom. A long olefin bond [C(1)-C(7) = 1.406(8)Å], compared to the structures of uncoordinated metallo vinyl amines[14] and **1**,

points to substantial reduction of the vinyl double bond order whereas the short N-C(7) bond [N-C(7) = 1.348(7)Å] suggests some double bond character for this bond.[15] Small deviations from planarity of 0.034(5), -0.013(2), -0.011(1) and -0.011(1)Å for N, C(7), C(8) and C(9) from the least squares plane through them describe a near planar sp^2 geometry for the nitrogen atom. The Au-C(7) bond length in **7** [Au-C(7) = 2.067(5)Å] seems only slightly longer that in the oxygen analogue [complex **1**: Au-C(7) = 2.050(7)Å], although not significantly.

From the structure of **7**, can be concluded that the highly polarised, and usually unstable, bonding mode of the dimethylaminevinyl-gold(I)PPh$_3$ fragment in this complex is mainly stabilised by the efficient delocalisation of a positive charge from the α-gold vinyl carbon atom to the nitrogen atom, as illustrated by resonance structure **P** (Scheme 3.5). Evidence for delocalisation of the positive charge to the Ph$_3$PAu fragment, as was concluded for **1**-**5** (Chapter 2), was not found in the structure of **7**. It must, however, be stressed that Au-C separations are very insensitive to bond order [see Section 2.2.1(D)]. The structure, furthermore, shows that the extent of positive charge delocalisation to the nitrogen atom in **7** is so much that this complex is best represented as a zwitterionic η^1-bonded {dimethylaminevinyl-gold(I)PPh$_3$}Cr(CO)$_5$ complex (Figure 3.1). A literature search revealed one other structure, a Mo(CO)$_5$ complex of 1,3,4,5-tetra-methyl-2-methylene imidazoline, in which similar terminal asymmetrical coordination of a vinyl moiety to an M(CO)$_5$ group is observed. This complex is also described as a zwitterion, with a negative charge located on the Mo atom and the corresponding positive charge delocalised to the nitrogen atoms in the 1,3,4,5-tetra-methyl-2-methylene imidazoline ring.[13]
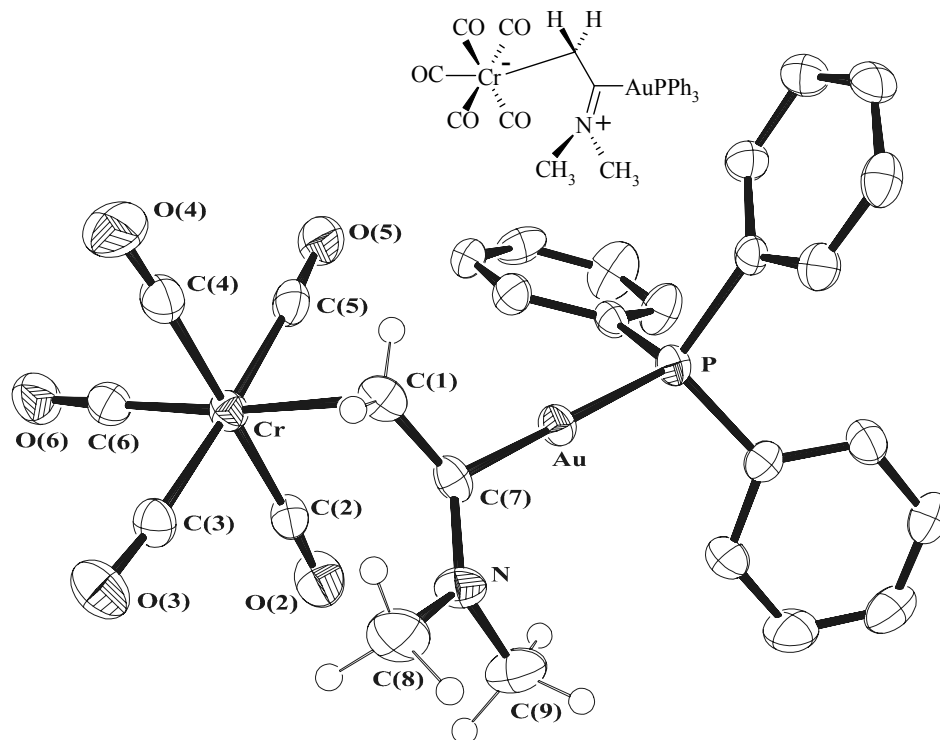
Figure 3.1: Ortep view of **7** (hydrogen atoms on phenyl rings omitted for clarity), showing the numbering scheme

Table 3.6: Selected bond lengths (Å) and angles (°) with e.s.d.s. in parenthesis for complex **7**

Bond lengths		Bond angles	
Au-C(7)	2.067(5)	Cr-C(1)-C(7)	100.9(4)
Cr-C(1)	2.337(6)	Cr-C(7)-C(1)	51.1(3)
Cr-C(7)	2.947(5)	C(7)-Au-P	174.9(1)
Au-P	2.295(1)	Au-C(7)-C(1)	118.3(4)
C(1)-C(7)	1.406(8)	Au-C(7)-N	118.7(4)
C(7)-N	1.348(7)	C(1)-C(7)-N	122.6(5)
N-C(8)	1.463(7)	C(7)-N-C(8)	122.3(5)
N-C(9)	1.446(8)	Cr-C(2)-O(2)	176.7(5)
Cr-C(2)	1.911(6)	Cr-C(3)-O(3)	174.6(5)
Cr-C(3)	1.905(6)	Cr-C(4)-O(4)	176.9(5)
Cr-C(4)	1.901(6)	Cr-C(5)-O(5)	175.7(5)
Cr-C(5)	1.895(6)	Cr-C(6)-O(6)	179.3(6)
Cr-C(6)	1.836(6)	C(1)-Cr-C(6)	172.8(2)
		C(7)-Cr-C(6)	159.0(2)

Distortion of the $Cr(CO)_4$ coordination plane through Cr, C(2), C(3), C(4) and C(5), due to the asymmetric bonding of the large dimethylaminevinyl-gold(I)PPh$_3$ fragment, is described by respective deviations of 0.017(2), 0.009(3), -0.018(3), 0.010(3) and -0.018(3)Å from the least squares plane through these atoms. These values show that the distortion of this plane is considerably less than in the structures of **1** and **4** (Chapter 2) and support the observation that the degeneracy in the E vibrational mode in the IR spectra of **7**-**10** is not lifted. A C(4)-C(2)-C(7)-C(1) torsion angle of 0.7(3)° shows that the vinyl amine coordination in **7** is essentially parallel to the C(2)-Cr-C(4) coordination.

In the unit cell molecules of **7** pack in the centrosymmetric spacegroup P2$_1$/c in regular rows along the a-axis. Each row is related to the next by the two-fold screw axis parallel to the a-axis in the centre and edges of the unit cell (Figure 3.2). Furthermore, along each of the packed rows of molecules along the a-axis, clear non-bonded face-edge phenyl-interactions are found. In these interactions, illustrated in Figure 3.3, one PPh$_3$ phenyl ring (C11-C16) interacts with an adjacent PPh$_3$ phenyl ring in a neighbouring molecule (C31-C36), as well as with the one vinyl hydrogen atom (H1a) in that molecule. These intermolecular interactions also account for the small C(32)-C(31)-P-Au torsion angle [18.4(5)°] observed in the molecular structure of **7**. No further significant intermolecular interactions are observed in the unit cell of **7**.
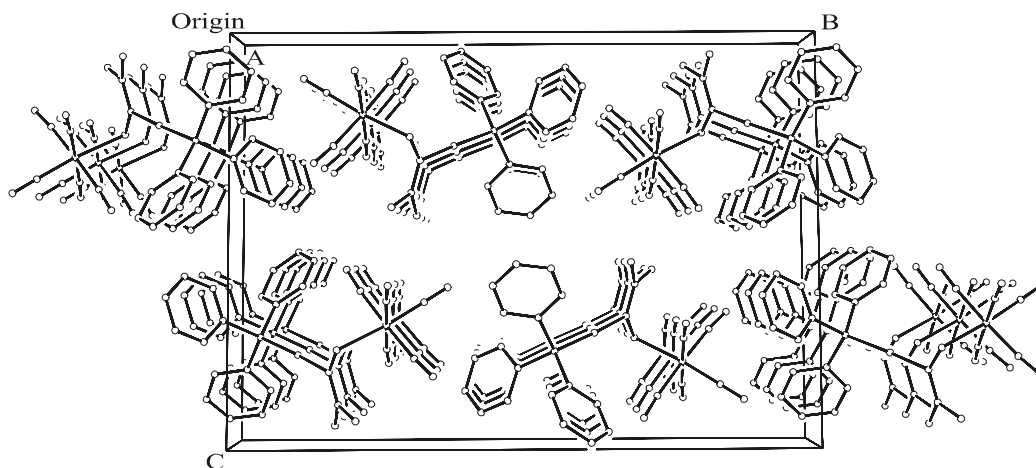
Figure 3.2: Unit cell and packing pattern of **7** viewed along the a-axis
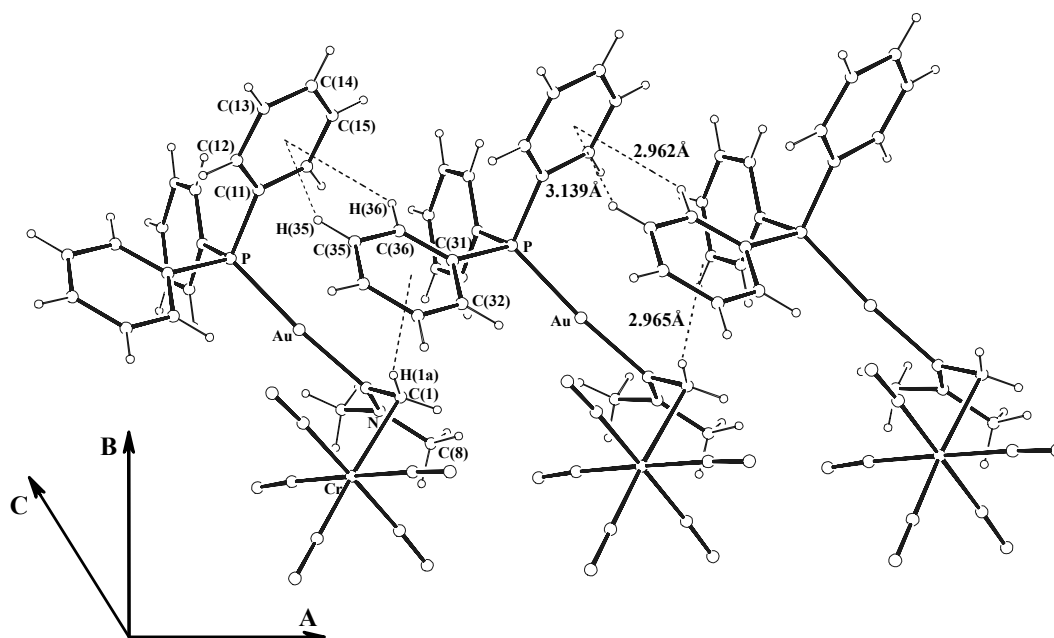
Figure 3.3: Intermolecular face-edge phenyl-interactions found along the a-axis of **7**

3.2.2 S-coordinated {alkyl/arylthiovinyl-gold(I)triphenylphosphine} Cr(CO)$_5$ bimetallic complexes

A.   General preparation and discussion of {Ph$_3$PAuC(S**R**)=CH$_2$}$-S$ Cr(CO)$_5$
R = Me (**11**); **R** = ^{n}Pr (**12**); **R** = Ph (**13**)

The synthesis of complexes **11**-**13** (Scheme 3.6) was carried out in a similar fashion to complexes **7**-**10** discussed section 3.2.1(A). Product separation of oily, dark-yellow reaction mixtures (21-36% yields after separation) was carried out by low temperature (-15°C) silica gel column chromatography with pentane/diethyl ether (10:1) as initial eluant, followed by crystallisation (only for **13**) from a concentrated pentane solution of the complex cooled to –20°C. Physical data for the new compounds, where available, are summarised in Table 3.7.
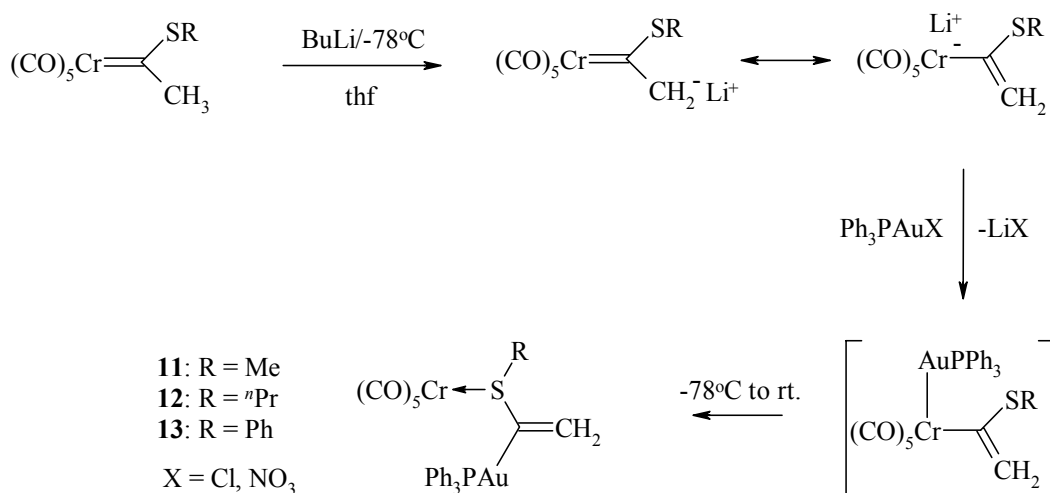
Scheme 3.6

Table 3.7: Analytical Data for complexes **11-13**

Complex			
Complex	**11**	**12**	**13**
M.p. / °C	- [a]	- [a]	86 (decomp.)[b]
Colour	yellow	yellow	yellow-brown
Yield (%)	21	36	23
M.W. (g / mol)	724.43	752.49	786.50
Analyses (%)[c]			
C	45.56 (43.11)	47.03 (44.69)	46.95 (47.34)
H	3.20 (2.78)	3.90 (3.21)	2.73 (2.82)
O	11.86 (11.04)	11.49 (10.63)	10.24 (10.17)
P	4.05 (4.28)	3.87 (4.12)	3.87 (3.94)
S	4.21 (4.43)	4.05 (4.26)	4.03 (4.08)

[a] Products isolated as oils

[b] Melting point of crystals containing **13** and **13'** [See Section 3.2.2 (D)]

[c] Required values given in parenthesis

Likewise to the formation of complexes **1-5** and complexes **7-10**, described in Chapter 2 and section 3.2.1 respectively, we propose the hydrolysis reaction mechanism suggested by Casey and Bernasconi (Section 2.1),[7] which we call "aurolysis" when gold(I) electrophiles are involved instead of protons, for the formation of the {alkyl/arylthiovinyl-gold(I)PPh$_3$}-*S* Cr(CO)$_5$ bimetallic complexes, **11-13**. The formation of these novel complexes was not unexpected. As discussed in the introduction to this chapter, Fischer-type thiocarbene complexes with β-hydrogens are known to be even more acidic than their oxygen counterparts.[11] The conjugated bases of such thiocarbene complexes are greatly stabilised by negative charge delocalisation to the M(CO)$_5$ group, as illustrated by resonance structure **M** in Scheme 3.3, thus permitting electrophilic addition reactions to occur at the Cr(CO)$_5$ fragments after which the electrophile binds to the coordinated carbon atom. Despite this, there are, to our knowledge, no reports of electrophilic addition reactions to β-metallo carbon atom deprotonated thiocarbene complexes that occur on these atoms. Also, hydrolytic decomposition reactions of Fischer-type thiocarbene complexes have not yet been reported. This is most likely due to the fact mentioned before that the chemistry of thiocarbene complexes, in stark contrast to those of alkoxy- and aminocarbene complexes, remains largely unstudied.

In spite of the fact that complexes **11-13** are formed along the same reaction path as the analogous vinyl ether (**1-5**) and vinyl amine (**7-10**) complexes and contain analogous functional groups, they have a different molecular structure. In **11-13**, the alkyl/arylthiovinyl-gold(I)PPh$_3$ moieties do not, like the analogous alkoxyvinyl-gold(I)PPh$_3$ and dialkylaminovinyl-gold(I)PPh$_3$ groups in **1-5** and **7-10**, coordinate to the M(CO)$_5$ fragment through their vinyl functionality, but rather through their sulphur atoms. This coordination mode for **11-13** was predicted by DFT calculations, which determined that it is 6.6 kcal/mol lower in energy than the isomeric structure in which olefin coordination occurs. The oxygen analogues of **11-13**, complexes **1-5**, on the other hand have a 5.7 kcal/mol higher energy when coordination to Cr(CO)$_5$ occurs through the ether oxygen atom instead of the vinyl group [Section 2.2.1 (E)]. This illustrates that, although sulphur is a relatively poor π-electron donor, as observed in (CO)$_5$Cr=C(SCH$_3$)CH$_3$ where its poor π-electron donating capabilities accounts for strong β-CH acidity, it bonds stronger to Cr(CO)$_5$ groups than the thiovinyl ether group. Further evidence for this is presented in sections 3.2.2 (C & D).

Interestingly, this result also predicts that the hydrolysis of Fischer-type thiocarbene complexes containing β-hydrogen atoms should result in the formation of stable S-coordinated alkyl/aryl(vinyl)thioether-M(CO)$_5$ complexes instead of the mixture of aldehyde and alcoholic products found after the hydrolysis of Fischer-type alkoxycarbene complexes. No secondary vinylthioether hydrolysis step is expected since it is unlikely that vinyl coordination, which is seemingly responsible for activating the vinyl moiety toward the second hydrolysis (usually base hydrolysis with OH$^-$), would take place.

B.   Isolation of Ph$_3$PAu^{n}Bu (**14**)

In the synthesis of complexes **1**-**13**, the main by-product of the reactions was identified as Ph$_3$PAu^{n}Bu (**14**). Although **14** was also occasionally present in very small amounts in the reaction mixtures of **1-10**, it was only chromatographically isolated as a fast moving, colourless band from the reaction mixtures of **11-13**. Its formation in significant amounts in these reactions (5-15% yield based on Ph$_3$PAuCl) is probably related to the fact that the thiocarbene starting materials used here are the most unstable carbene complexes employed in this study. Some measure of decomposition of the thiocarbene starting complexes before use in the synthesis of **11-13** was frequently observed. The thiocarbene starting complexes are, furthermore, also the most difficult type to isolate in analytically pure form and are often included in oily mixtures with solvents and/or the excess of the thiols used in their synthesis, especially the less volatile ones like thiophenol.

During the first step of the preparation of **11-13**, a slight excess of ^{n}BuLi, remaining after the deprotonation of the thiocarbene complexes, is thus easily foreseeable. This reacts with the equivalent of Ph$_3$PAuCl, added in the second step of the synthesis, to form **14** through a simple transmetallation reaction (Scheme 3.7). Although **14** must almost certainly have been accidentally prepared previously in other sequential deprotonation-auration reactions with ^{n}BuLi and Ph$_3$PAuCl, it's characterisation, to our knowledge, has thus far not been reported. For this reason the spectroscopic and physical data of **14** (Table 3.8 and 3.12) are included in this chapter.

$$\text{Ph}_3\text{PAuCl} \quad + \quad {}^n\text{BuLi} \quad \xrightarrow[\text{thf}]{-78^{\circ}\text{C}} \quad \text{Ph}_3\text{PAu}^n\text{Bu} \quad + \quad \text{LiCl}$$

14
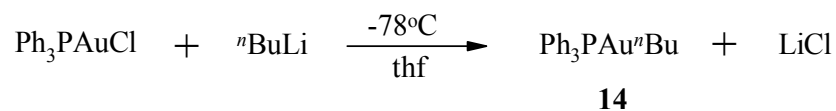
Scheme 3.7

Table 3.8: Analytical Data for complex **14**

Complex	$\text{Ph}_3\text{PAu}^n\text{Bu}$
Complex	**14**
M.p. / $^{\circ}$C	106 (decomp.)
Colour	colourless
Yield (%)[a]	5-15
M.W. (g / mol)	516.38
Analyses (%)[b]	
C	51.24 (51.17)
H	4.73 (4.68)
P	5.91 (6.00)

[a] Yield is dependant on the efficiency of the synthesis of **11-13**

[b] Required values given in parenthesis

C.   Spectroscopic characterisation of complexes **11-14**

1.   NMR Spectroscopy

The ^{1}H, ^{13}C\{^{1}H\} and ^{31}P\{^{1}H\} NMR spectroscopic data for the new complexes **11-13** are summarised in Tables 3.9-3.11. The ^{1}H NMR spectra of **11-13** exhibit two distinctive signals, each integrating for a single proton, representing two chemically non-equivalent vinyl protons. Unlike the ^{1}H NMR spectra of **1-5** and **7-10**, where these signals are shifted upfield as a result of metal coordination to the vinyl group [δ 1.93-2.73 (*cis*-H$_{\text{vinyl}}$) and 2.50-4.26 (*trans*-H$_{\text{vinyl}}$) in **1-5** and **7-10**], the *cis* and *trans*-vinyl proton resonances in **11-13** appear in the usual region for protons in uncoordinated vinyl groups, at δ 5.38-5.64 (*cis*-H$_{\text{vinyl}}$) and 5.76-6.07 (*trans*-H$_{\text{vinyl}}$).

Similarly, the $^{13}C\{^1H\}$ resonances for the terminal CH_2-vinyl carbon atoms in **11-13** appear ~70-85 ppm downfield from their position in the ^{13}C NMR spectra of **1-5** and **7-10**, at δ 121.7, 125.4 and 125.7, in the aromatic region of the ^{13}C NMR spectrum. Resonances representing the β-vinyl carbon atoms in **11-13** could be easily identified on account of their characteristically large $^2J_{C-P}$ coupling constants (125.2-129.4 Hz) and appear at δ 181.9, 182.5 and 180.8 respectively. The ^{13}C NMR spectra of **11-13** also clearly show the presence of $Cr(CO)_5$ groups in complexes **11-13** as two characteristic resonances, representing the *cis* and *trans* CO groups in $Cr(CO)_5$, are found at ~216 and ~223 ppm.

The chemical shifts reported here for the vinyl groups in **11-13** are consistent with chemical shifts reported for other uncoordinated vinyl thioethers and therefore strongly suggest that the vinyl thioether moieties in **11-13** are not coordinated to $Cr(CO)_5$ fragments though their vinyl functionality, but rather through their vinyl thioether sulphur atoms. Further evidence for this assumption is presented in the discussion of the infrared spectra of **11-13** and the X-ray crystallographic investigation of **13**, reported below.
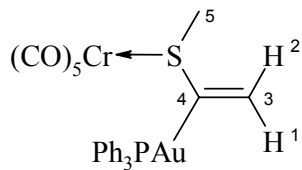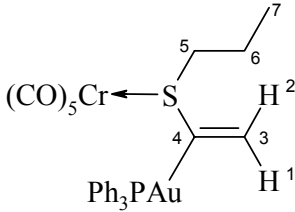
Table 3.9

Complex		(CO)$_5$Cr←S (with labels 5, 4, 3, 2, 1, Ph$_3$PAu, H^1, H^2)
		11
Solvent		CDCl$_3$
Temperature (K)		298
^{1}H NMR	H^1	5.43 (br, 1H)
(600 MHz)	H^2	5.76 (br, 1H)
	H^5	2.47 (br s, 3H)
	Ph	7.2 – 7.7 (m, 15H)
^{31}P{H^1} NMR	P	41.5 (s)
(243 MHz)		
^{13}C{H^1} NMR	C^3	121.7 (br, s)
(150 MHz)	C^4	181.9 (d, $^2J_{P-C}$ = 129.4 Hz)
	C^5	39.7 (s)
	Ph-C$_{ipso}$	129.5 (d, $^1J_{P-C}$ = 59.6 Hz)
	Ph-C$_{ortho}$	129.8 (d, $^2J_{P-C}$ = 9.9 Hz)
	Ph-C$_{meta}$	134.9 (d, $^3J_{P-C}$ = 13.9 Hz)
	Ph-C$_{para}$	132.1 (s)
	CO$_{cis}$	216.4 (s)
	CO$_{trans}$	223.2 (s)
υ (CO) (cm^{-1})^a		1918 (st, A$_1^{(2)}$), 1943 (st, br, sh, E), 1987 (w, br B$_1$), 2063 (m, A$_1^{(1)}$)
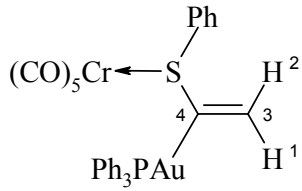
^{a}Pentane solution in NaCl-cell

Table 3.10

Complex	₅Cr←S with propyl chain (5,6,7), vinyl carbons 3,4, H¹, H², Ph₃PAu

		12
Solvent		CDCl₃
Temperature (K)		298
^{1}H NMR	H^1	5.38 (d, $^4J_{cis\,\text{P-H}}$ = 2.7 Hz, 1H)
(600 MHz)	H^2	5.88 (d, $^4J_{trans\,\text{P-H}}$ = 12.5 Hz, 1H)
	H^5	2.80 (t, $^3J_{\text{H-H}}$ = 7.1 Hz, 2H)
	H^6	1.73 (m, 2H)
	H^7	0.92 (t, $^3J_{\text{H-H}}$ = 6.4 Hz, 3H)
	Ph	7.3–7.7 (m, 15H)
^{31}P{H^1} NMR	P	42.5 (s)
(243 MHz)		
^{13}C{H^1} NMR	C^3	125.4 (br, s)
(150 MHz)	C^4	182.4 (d, $^2J_{\text{P-C}}$ = 125.2 Hz)
	C^5	46.3 (s)
	C^6	23.0 (s)
	C^7	13.2 (s)
	Ph-C$_{ipso}$	129.8 (d, $^1J_{\text{P-C}}$ = 50.2 Hz)
	Ph-C$_{ortho}$	129.2 (d, $^2J_{\text{P-C}}$ = 9.3 Hz)
	Ph-C$_{meta}$	134.2 (d, $^3J_{\text{P-C}}$ = 14.2 Hz)
	Ph-C$_{para}$	131.5 (s)
	CO$_{cis}$	215.9 (s)
	CO$_{trans}$	222.7 (s)
υ (CO) (cm^{-1})^a		1917 (st, br, A$_1^{(2)}$), 1932 (st, br, 'E'), 1937 (st, br, 'E') 1980 (w, br B$_1$), 2063 (m, A$_1^{(1)}$)

^{a} Pentane solution in NaCl-cell
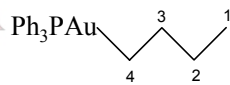
Table 3.11

Complex		
		13
Solvent		CDCl$_3$
Temperature (K)		298
^{1}H NMR	H^1	5.64 (d, $^4J_{cis\text{ P-H}}$ = 5.1 Hz, 1H)
(600 MHz)	H^2	6.07 (d, $^4J_{trans\text{ P-H}}$ = 12.0 Hz, 1H)
	Ph, S-Ph	7.1-7.6 (m. 20H)
^{31}P{H^1} NMR	P	41.9 (s)
(243 MHz)		
^{13}C{H^1} NMR	C^3	125.7 (s)
(150 MHz)	C^4	180.8 (d, $^2J_{\text{P-C}}$ = 126.9 Hz)
	PPh$_3$-C$_{ipso}$	129.9 (d, $^1J_{\text{P-C}}$ = 51.5 Hz)
	PPh$_3$-C$_{ortho}$	129.1 (d, $^2J_{\text{P-C}}$ = 11.8 Hz)
	PPh$_3$-C$_{meta}$	134.1 (d, $^3J_{\text{P-C}}$ = 13.5 Hz)
	PPh$_3$-C$_{para}$	131.3 (s)
	SPh-C$_{ipso}$	140.4 (s)
	SPh-C$_{o/m/p}$	128.2 (s), 128.8 (s), 131.8 (s)
	CO$_{cis}$	215.4 (s)
	CO$_{trans}$	223.1 (s)
υ (CO) (cm^{-1})^a		1921 (st, A$_1^{(2)}$), 1944 (st, br, sh, E), 1987 (w, br B$_1$), 2065 (m, A$_1^{(1)}$)

^{a} Pentane solution in NaCl-cell

The ^{1}H, ^{13}C{^{1}H} and ^{31}P{^{1}H} NMR spectroscopic data for complex **14** are summarised in Table 3.12. ^{1}H and ^{13}C resonances for atoms in the ^{n}Bu chain appear between δ 0.94–1.86 and δ 14.7–34.7 respectively. These signals could be assigned to the individual methyl and methylene groups in the ^{n}Bu chain as indicated in Table 3.12 on account of the clear combinations of $^3J_{H\text{-}H}$, $^3J_{P\text{-}H}$, $^3J_{P\text{-}C}$ and $^2J_{P\text{-}C}$ couplings they exhibit. Of particular interest in the ^{13}C NMR spectrum of **14** is the extremely efficient two bond $J_{P\text{-}C}$ coupling (95.4Hz) of the α-gold CH$_2$ group (C$_4$) with the ^{31}P atom across the gold atom. This coupling constant is more than double the size of the one bond $J_{P\text{-}C}$ coupling (44.7 Hz) observed for the ^{13}C$_{ipso}$ atoms in the PPh$_3$ residue. This observation serves to illustrate that there is very effective transfer of nuclear spin information between the ^{31}P and ^{13}C nuclei across the bonding electrons of the gold atom in **14**. A similar situation is also observed in the ^{13}C NMR spectra of **1-13** where very large coupling constants (117.6 – 134.2 Hz) are observed for $^2J_{P\text{-}C}$ coupling across a gold atom, whereas ^{31}P-^{13}C$_{ipso}$ $^1J_{P\text{-}C}$ coupling in the PPh$_3$ groups in **1-13** is never larger than 59.6 Hz.

Table 3.12

Complex	**14**	Ph$_3$PAu (with positions 1, 2, 3, 4)
Solvent		CDCl$_3$
Temperature (K)		298
^{1}H NMR:	H^1	0.94 (t, $^3J_{H\text{-}H}$ = 7.4 Hz, 3H)
(300 MHz)	H^{2,3}	1.4-1.6 (m, 4H)
	H^4	1.86 (dt, $^3J_{P\text{-}H}$ = 4.3 Hz, $^3J_{H\text{-}H}$ = 7.2 Hz, 2H)
	Ph	7.4-7.6 (m, 15H)
^{31}P{^{1}H} NMR:	P	46.4 (s)
^{13}C{^{1}H} NMR:	C^1	14.7 (s)
(75.41 MHz)	C^2	34.7 (s)
	C^3	30.0 (d, $^3J_{P\text{-}C}$ = 4.3 Hz)
	C^4	31.3 (d, $^2J_{P\text{-}C}$ = 95.4 Hz)
	Ph-C$_{ipso}$	132.7 (d, $^1J_{P\text{-}C}$ = 44.7 Hz)
	Ph-C$_{ortho}$	129.7 (d, $^2J_{P\text{-}C}$ = 10.5 Hz)
	Ph-C$_{meta}$	134.6 (d, $^3J_{P\text{-}C}$ = 13.3 Hz)
	Ph-C$_{para}$	131.6 (d, $^4J_{P\text{-}C}$ = 2.4 Hz)

2. *Infrared spectroscopy*

The infrared (IR) spectra of **11-13** were recorded as pentane solutions of the complexes in a NaCl cell and are summarised in Tables 3.9 – 3.11. The spectra display clear patterns of four (**11** and **13**) and five (**12**) absorption bands in the carbonyl region that are consistent with the presence of $Cr(CO)_5L$ moieties in these complexes. The five absorption bands in the IR spectrum of **12** are similar to those observed for **1-5** [Section 2.2.1(C)] and are assigned as noted in Table 3.10. The IR spectra of **11** and **13** display only the four usual absorption bands in the carbonyl region associated with complexes of the type $M(CO)_5L$, in which the degeneracy of the E vibrational mode has not been lifted, and were assigned as noted in Tables 3.9 and 3.11 [Section 3.2.1 (B)]
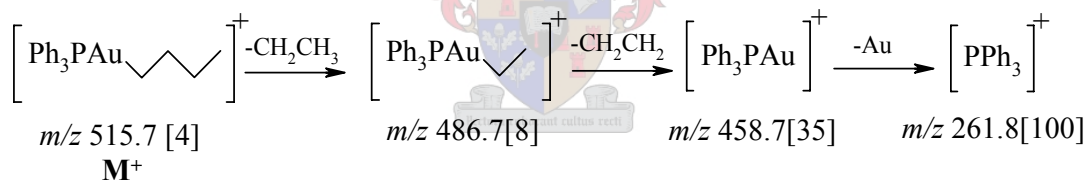
As discussed for the IR spectra of **1-5** and **7-10**, the most informative IR absorption mode for complexes of the type $Cr(CO)_5L$ is the $A_1^{(2)}$ peak assigned to the symmetric stretching of the single terminal CO ligand *trans* to the ligand (L) coordination. In the IR spectra of **11-13** these peaks appear blue shifted (7-27 cm^{-1}) between 1917 and 1921 cm^{-1}, compared to complexes **1-5** and **7-10**. Such a blue shift indicates that the ligand (L) in **11-13** has a smaller $\sigma_{donor}/\pi_{acceptor}$ ratio than the asymmetrically coordinating vinyl ether and vinyl amine groups in **1-5** and **7-10**, since it competes more effectively with the CO ligand *trans* to it for π-electron back-donation from the chromium atom.

Of note is that the remaining $\upsilon(CO)$ absorption bands, in particular the sharp and well defined $A_1^{(1)}$ and B_1 bands measured for **11-13**, are also significantly shifted to higher energy compared to their position in the IR spectra of the oxygen (**1** and **2**: ~12 cm^{-1} average shift) and nitrogen (**7** and **8**: ~24 cm^{-1} average shift) analogues. From this is concluded that of all the chromium pentacarbonyl compounds in this study (**1**,**2**,**7**,**8** and **11-13**), complexes **11-13** have the least amount of electron density located on their chromium atoms. This interpretation of the IR data is consistent with sulphur coordination to $Cr(CO)_5$ as opposed to vinyl coordination. Stable asymmetric vinyl coordination to $Cr(CO)_5$, as observed in complexes **1**,**2**,**7** and **8**, results in delocalisation of a partial negative charge to the chromium atom, effectively increasing the electron density there and lowering the CO stretching frequencies.

The fact that clearly resolved, non-degenerate vibrational modes, originating form the E vibrational mode, are only observed in the υ(CO) absorption bands of **12** is a testimony to the greater asymmetry of the ^{n}PrS group in this molecule compared to **11** and **13**, which contain more symmetrical MeS and PhS groups and hence only display a single two-fold degenerate E vibrational mode.

3.   *Mass spectrometry*

The positive-ion FAB mass spectra of complexes **11-13** were recorded in a *m*-nitrobenzylalcohol matrix. The spectra mainly exhibited the characteristic matrix peaks (*m/z* 154 and *m/z* 307) or the Ph_3PAu^+ (*m/z* 459) or $(Ph_3P)_2Au^+$ (*m/z* 721) decomposition and fragment peaks as the peaks of highest intensity. No molecular ion, or other sensible fragmentation peaks were observed for **11-13**. This can possibly be ascribed to the fact that pure samples of **11-13** were only obtained as relatively unstable viscous oils. The conventional EI-mass spectrum of **14** is illustrated in Scheme 3.8 (relative intensities in parentheses).

$$\left[Ph_3PAu \diagdown \diagup \diagdown \right]^+ \xrightarrow{-CH_2CH_3} \left[Ph_3PAu \diagup \diagdown \right]^+ \xrightarrow{-CH_2CH_2} \left[Ph_3PAu \right]^+ \xrightarrow{-Au} \left[PPh_3 \right]^+$$

$\qquad$ *m/z* 515.7 [4] $\qquad\qquad$ *m/z* 486.7[8] $\qquad\qquad$ *m/z* 458.7[35] $\qquad$ *m/z* 261.8[100]

$\qquad\qquad$ **M$^+$**

Scheme 3.8

D.   X-ray structure determination of complex 13

The low temperature (177 K) molecular structure of complex **13** (Figure 3.4) was determined by X-ray diffraction techniques. The structure clearly shows, as proposed by the NMR and IR spectroscopic data, coordination of a PPh$_3$-phenylthiovinyl-gold(I) moiety to a Cr(CO)$_5$ fragment through the sulphur atom of the thioether group. In the crystal **13** co-crystallised together with **13'** (Figures 3.5 and 3.6), a bimetallic gold(I)thiol-Cr(CO)$_5$ bimetallic complex consisting of a Ph$_3$PAuSPh fragment coordinated to Cr(CO)$_5$ through the sulphur atom of the thiophenol group. The final crystallographically refined ratio of **13**:**13'** is 1:2.866, indicating that there is in actual

fact nearly three times more of **13'** present in the crystal structure than of **13**. The asymmetric unit of the total structure consists of one molecule of **13'** linked by a weak relativistic (or 'aurophilic') Au-Au interaction [Au(1)-Au(2) = 3.197(1)Å] to a molecule of **13** (at 51.7% site occupancy, Figure 3.5) which shares that site with a second molecule of **13'**, present at 48.3% site occupancy (Figure 3.7). The molecules of **13** and **13'**, occupying the same site furthermore share the atom positions in the AuPPh$_3$ moiety and only differ in the positions of their respective thiophenol, vinyl (only for **13**) and Cr(CO)$_5$ fragments. Within the structure of **13**, disorder is observed for the oxygen atom of the CO ligand *trans* to the sulphur coordination [O(7)]. Two positions could be identified and refined for this atom on the difference Fourier map with a final refined site occupancy ratio of 0.552 : 0.448 [O(7'1) : O(7'2)]. Selected bond lengths and angles in each of the crystallographically unique fragments in the crystal structure are listed in Tables 3.13-3.15 according to the numbering schemes shown in the preceding figures (3.4-3.7).

Despite the rather inaccurate bond lengths and angles obtained for **13**, as a result of the partial site occupancy found for this part of the structure, the actual connectivity in **13** could be established beyond any doubt. The poor accuracy of the bond lengths and angles in the vinyl group of **13** do, however, not allow comparison of these to those of **1** and **7** or literature examples of uncoordinated vinyl ethers/amines/thioethers. The accurate bond lengths determined for the Au(2)-P(2) bond [2.275(2)Å] as well as the bond lengths and angles in the PPh$_3$ moiety of **13** (and **13'**) are normal.[17] A C(11)-Au(2)-P(2) angle of 168.7(7)° [bent towards Au(1)], although poorly determined, describes the distortion of the usually linear gold(I) coordination mode as a result of the relativistic Au-Au interaction between Au(1) and Au(2) [Figure 3.5]. A similar, and more certain, description of the distortion of Au(1) toward Au(2) is given by the S(1)-Au(1)-P(1) angle [171.12(7)°] in **13'** (Figure 3.6).
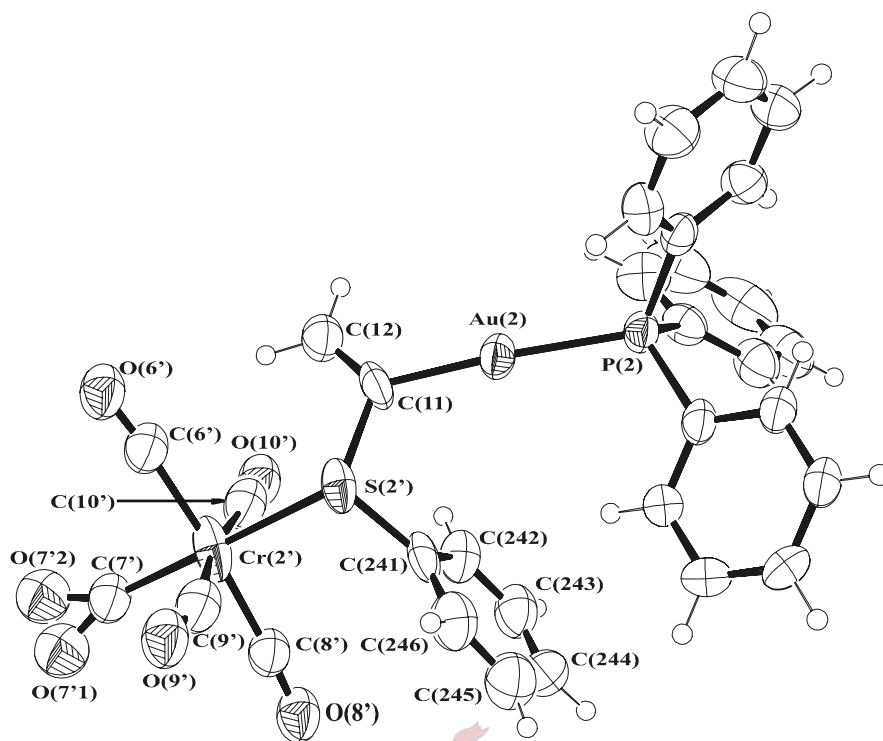
Figure 3.4: Ortep view of **13** (~51.7% site occupancy), showing numbering scheme

Table 3.13: Selected bond lengths (Å) and angles (°) with e.s.d.s in parenthesis for **13**

Bond lengths		Bond angles	
Au(2)-C(11)	2.03(2)	C(11)-Au(2)-P(2)	168.7(7)
C(11)-C(12)	1.32(3)	Au(2)-C(11)-C(12)	128.0(18)
C(11)-S(2')	1.81(2)	Au(2)-C(11)-S(2')	112.7(13)
Au(2)-P(2)	2.275(2)	Cr(2')-S(2')-C(11)	118.0(8)
S(2')-Cr(2')	2.457(5)	C(11)-S(2')-C(241)	102.1(9)
S(2')-C(241)	1.79(2)	C(7')-Cr(2')-S(2')	177.9(8)
Cr(2')-C(6')	1.93(3)	C(6')-Cr(2')-C(8')	175.5(10)
Cr(2')-C(7')	2.01(2)	C(9')-Cr(2')-C(10')	170(2)
Cr(2')-C(8')	1.93(3)	Cr(2')-C(6')-O(6')	175(2)
Cr(2')-C(9')	1.95(7)	Cr(2')-C(8')-O(8')	174(2)
Cr(2')-C(10')	1.90(4)	Cr(2')-C(9')-O(9')	159(5)
Au(1)-Au(2) [*]	3.197(1)	Cr(2')-C(10')-O(10')	175(3)

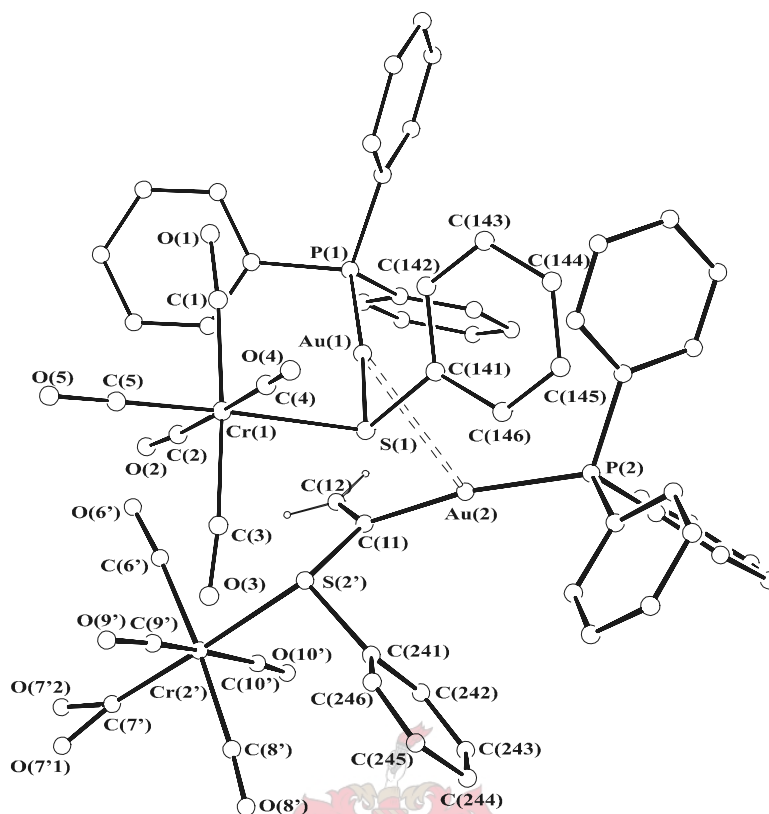[*] Aurophilic interaction between Au(1)-Au(2) shown in Figure 3.5

93

Figure 3.5: Ortep view of **13** and **13'** (~51.7% site occupancy for **13**), showing
numbering scheme and aurophilic Au-Au interaction (hydrogen
atoms on phenyl rings omitted for clarity)

The structure of the uncoordinated gold(I)thiophenol fragment of **13'**, Ph$_3$PAuSPh,
has been reported in the literature no less than three times (!).[18] All three reported
structures are isostructural and consist of dimers of the compound that are linked, in a
similar fashion to the structure reported above, by weak aurophilic interactions [Au-
Au = 3.135 Å]. The bond lengths and angles observed in these structures compare
very well to those found for **13'** and even the S(2'')-Au(2)-Au(1)-S(1) torsion angles
[88.5(2)°] between the molecules in **13'** differ by surprisingly little (~7.5°) compared
to this angle in Ph$_3$PAuSPh considering that there are sterically bulky Cr(CO)$_5$
fragments coordinated to the sulphur atoms in the current structure. The greatest
difference between the structure of Au-Au linked dimers of **13'** and those of
Ph$_3$PAuSPh is the length of the Au-S bond. Despite the fact that the diffraction data
for the current structure was collected at 177 K, whereas the literature examples are
all room temperature structures, the Au-S bond is 0.053(5)Å longer in **13'**. A possible
explanation for this is that electron loss to the strongly electron withdrawing Cr(CO)$_5$

fragment in **13'** weakens this bond slightly. A slightly lengthened S-Ph bond in **13'** [S(1)-C(141) = 1.787(8)Å], compared to this bond in Ph$_3$PAuSPh [1.755(5)Å], supports this interpretation. Slight distortions from planarity of the Cr(CO)$_4$ coordination plane in **13'**, as defined by C(1), C(2), C(3), C(4) and Cr, due to coordination of the Ph$_3$PAuSPh moiety to this fragment are described by respective deviations of 0.010(4), 0.000(4), 0.010(4) and 0.001(4)Å from the least squares plane through these atoms.

The exact reason for the formation of **13'** is not clear. There are several possible ways in which it could have formed from the reaction mixture of **13**, or during the crystallisation process. The most likely mechanism is one in which some thiophenol (HSPh), stubbornly remaining after the synthesis of the thiocarbene starting complex (even after several cycles of re-crystallisation) or formed during the decomposition of the thiocarbene starting complex, is deprotonated by ^{n}BuLi during the synthesis of **13** (Scheme 3.6). The LiSPh could then react with Ph$_3$PAuCl to form the stable and known gold(I)thiol compound, Ph$_3$PAuSPh. With the sulphur atom in Ph$_3$PAuSPh situated next to a gold atom, it is not unreasonable to assume that it could be a better σ-donor ligand than the sulphur atom in phenylthiovinyl-gold(I)PPh$_3$. A substitution reaction in which the phenylthiovinyl-gold(I)PPh$_3$ 'ligands' in **13** are substituted by Ph$_3$PAuSPh to form **13'** is thus envisaged. Other less likely possibilities for the formation of **13'** include, elimination of acetylene from **13**, promoted by the preference of gold to form bonds with sulphur, and the hydrolysis of the phenylthiovinyl-gold(I)PPh$_3$ moiety by thiophenol, forming **13'** and free phenyl(vinyl)thioether.
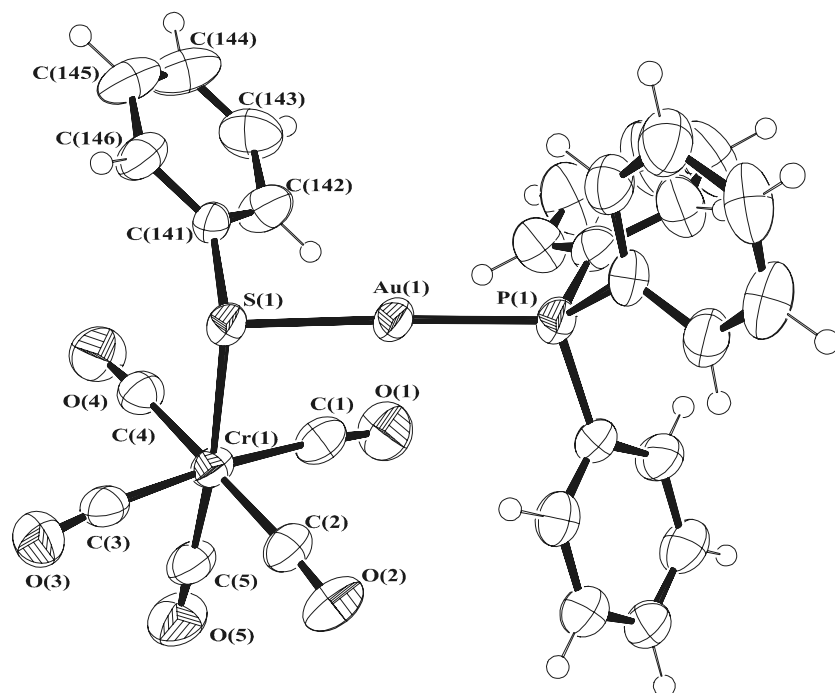
Figure 3.6: Ortep view of **13'**, showing numbering scheme

Table 3.14: Selected bond lengths (Å) and angles (°) with e.s.d.s in parenthesis for **13'**

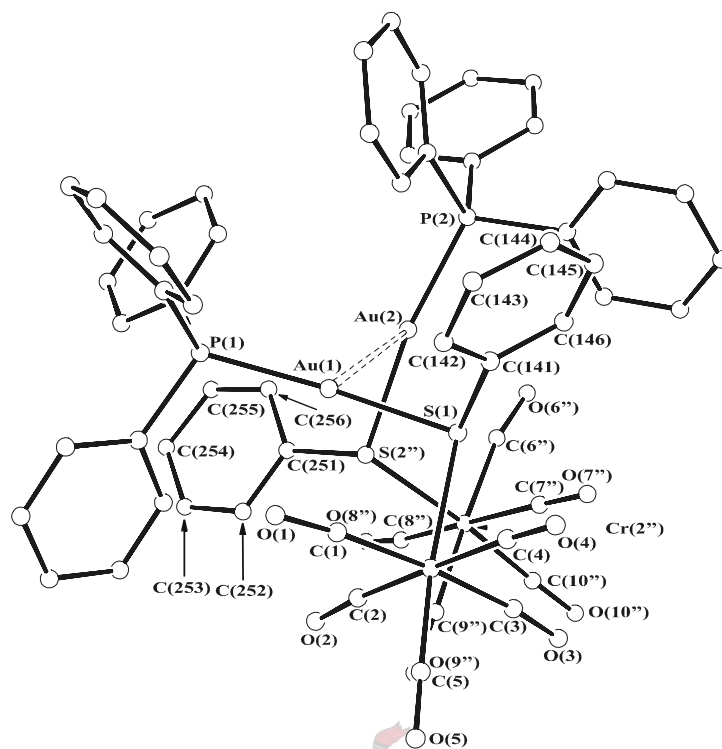| Bond lengths		Bond angles	
Au(1)-S(1)	2.326(2)	S(1)-Au(1)-P(1)	171.12(7)
S(1)-C(141)	1.787(8)	Au(1)-S(1)-C(141)	100.2(2)
S(1)-Cr(1)	2.502(2)	Au(1)-S(1)-Cr(1)	100.86(7)
Au(1)-P(1)	2.258(2)	Cr(1)-S(1)-C(141)	109.4(3)
Cr(1)-C(1)	1.898(10)	C(1)-Cr(1)-C(3)	174.3(4)
Cr(1)-C(2)	1.901(9)	C(2)-Cr(1)-C(4)	178.6(4)
Cr(1)-C(3)	1.887(9)	S(1)-Cr(1)-C(5)	174.7(3)
Cr(1)-C(4)	1.903(9)	Cr(1)-C(1)-O(1)	175.1(8)
Cr(1)-C(5)	1.832(9)	Cr(1)-C(2)-O(2)	173.7(8)
		Cr(1)-C(3)-O(3)	174.1(7)
		Cr(1)-C(4)-O(4)	176.6(8)
		Cr(1)-C(5)-O(5)	178.9(8)

Figure 3.7: Ortep view of dimeric structure of **13'** (~48.3% site occupancy for second molecule of **13'**) found in the crystal (hydrogen atoms omitted for clarity)

Table 3.15: Selected bond lengths (Å) and angles (°) with e.s.d.s in parenthesis for the second molecule of **13'** (~48.3% site occupancy) found in the crystal

Bond lengths		Bond angles	
Au(2)-S(2'')	2.373(6)	S(2'')-Au(2)-P(2)	170.3(2)
S(2'')-Cr(2'')	2.490(8)	Au(2)-S(2'')-C(251)	107.6(10)
S(2'')-C(251)	1.77(4)	Au(2)-S(2'')-Cr(2'')	108.3(2)
Au(2)-P(2)	2.275(2)	Cr(2'')-S(2'')-C(251)	109.1(10)
Cr(2'')-C(6'')	1.90(5)	C(6'')-Cr(2'')-C(9'')	177.8(14)
Cr(2'')-C(7'')	1.91(2)	C(7'')-Cr(2'')-C(8'')	174.0(10)
Cr(2'')-C(8'')	1.91(2)	S(2'')-Cr(2'')-C(10'')	174.6(7)
Cr(2'')-C(9'')	1.88(3)	Cr(2'')-C(6'')-O(6'')	168(3)
Cr(2'')-C(10'')	1.85(3)	Cr(2'')-C(7'')-O(7'')	177(2)
		Cr(2'')-C(8'')-O(8'')	172(3)
		Cr(2'')-C(9'')-O(9'')	171(3)
		Cr(2'')-C(10'')-O(10'')	177(3)

A view along the a-axis of the crystal structure (Figure 3.8) shows how molecules of **13** and **13'**, linked by the weak Au-Au relativistic interactions (indicated by the dashed lines in the figure) pack in regular rows along the a-axis in the centrosymmetric spacegroup $P2_1/c$. The conformation in which two molecules of **13'** are present in the asymmetric unit (~48.3% site occupancy) is omitted for clarity in Figure 3.8. Other than the Au(1)-Au(2) relativistic interaction, no significant intermolecular, are observed in the crystal structure.
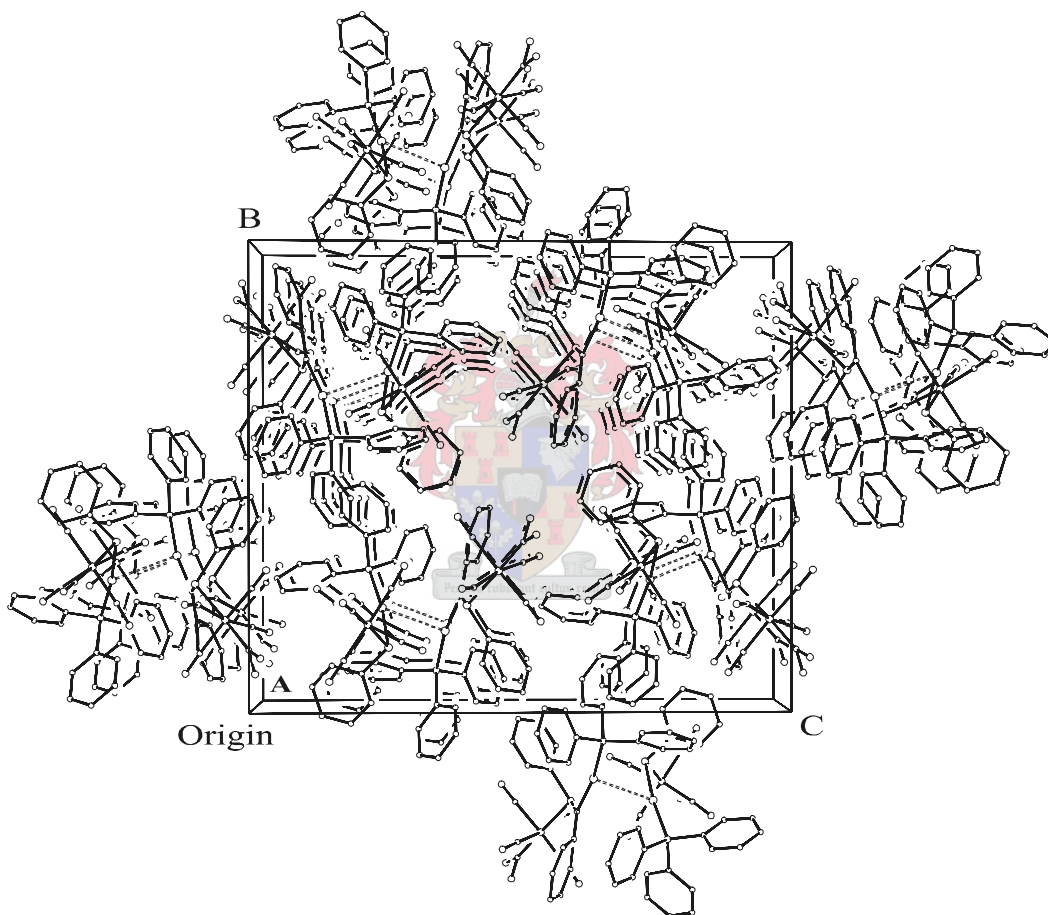

Figure 3.8: Packing diagram of molecules of **13** (at 51.7% site occupancy) and **13'** found in the crystal (Au-Au interactions indicated by dashed lines) viewed along the a-axis of the unit cell

3.3 Conclusions and future work

The reaction of β-metallo carbon deprotonated Fischer-type group 6 metal pentacarbonyl dialkylamino- and alkyl/arylthiocarbene complexes with Ph_3PAuCl leads to the formation of novel bimetallic η^2-{dialkylaminovinyl-gold(I)PPh$_3$}M(CO)$_5$ (M = Cr, W) and {alkyl/arylthiovinyl-gold(I)PPh$_3$}-S Cr(CO)$_5$ complexes, and not the expected respective β-substituted carbene complexes. The reactions described in this chapter are the first of their kind involving either dialkylamino- or alkyl/arylthiocarbene Fischer-type complexes and illustrate how these complexes can be employed as efficient anionic dialkylvinyl amine and alkyl/arylvinyl thioether synthons in preparative organometallic reactions. An aurolytic [Section 2.2.1(a) & 2.3] reaction mechanism, involving addition of the electrophile at the metal centre followed by a formal reductive elimination of the respective dialkylvinyl amine and alkylvinyl thioether products, is suggested for both conversions.

Single crystal X-ray diffraction studies conducted of examples of both types of complexes prepared here confirm their molecular structures. The crystal structure of η^2-{dimethylaminevinyl-gold(I)PPh$_3$}Cr(CO)$_5$ shows that the dialkylaminovinyl-gold(I)PPh$_3$ π-complex donors in these compounds are coordinated to the M(CO)$_5$ fragments in a highly asymmetrical η^2-fashion through the vinyl moiety. Evidence presented here strongly suggests that this usually unstable coordination mode for vinyl groups is stabilised by delocalisation of partial positive charges from the polarised vinyl group to the nitrogen atom of the dialkylaminovinyl-gold(I)PPh$_3$ fragments. The extent of this delocalisation is so much that these complexes are best described as zwitterions. In contrast to this result, the alkyl/arylthiovinyl-gold(I)PPh$_3$ fragments in the {alkyl/arylthiovinyl-gold(I)PPh$_3$}-S Cr(CO)$_5$ complexes described in this chapter are coordinated to the Cr(CO)$_5$ fragments through their thioether functionality while their vinyl moiety remains uncoordinated. This finding is in agreement with DFT calculations, which determined that the sulphur-coordinated isomers of these compounds have a lower energy than the vinyl-coordinated isomers. There is thus a reversal of stability, ascribed to sulphur's superior σ-donation and π-acceptor capabilities in comparison to the vinyl group, between the possible

conformational isomers when exchanging the hetero-atom in the vinyl coordinated oxygen analogues of the complexes described in Chapter 2 with sulphur. Furthermore, in the crystal {phenylthiovinyl-gold(I)PPh$_3$}-S Cr(CO)$_5$ co-crystallised with a by-product of the reaction, {phenylthio-gold(I)PPh$_3$}-S Cr(CO)$_5$.

Similarly to the compounds described in Chapter 2, the complexes prepared and characterised here could, quite surprisingly, be isolated by means of low temperature silica gel chromatography. Lastly, a by-product of the reactions investigated here, Ph$_3$PAu^{n}Bu, was isolated and characterised.

Potential future work sprouting from the results presented here, to name but a few interesting possibilities, include: Isolation of the free dialkylaminovinyl-gold(I)PPh$_3$ and alkyl/arylthiovinyl-gold(I)PPh$_3$ complexes by ligand substitution reactions. Alkylation/acidification reactions at the β-gold vinyl carbon atom in the dialkylaminovinyl-gold(I)PPh$_3$ and alkyl/arylthiovinyl-gold(I)PPh$_3$ complexes to prepare the first examples of cationic gold(I) Fischer-type amino- and thiocarbene complexes. Oxidative addition reactions of halides (X$_2$) to the isolated dialkylaminovinyl-gold(I)PPh$_3$ and alkyl/arylthiovinyl-gold(I)PPh$_3$ complexes to prepare *trans*-dihalo-PPh$_3$-dialkylaminovinyl-gold(III) and *trans*-dihalo-PPh$_3$-alkyl/arylthiovinyl-gold(III) complexes. Alkylation/acidification reactions on these compounds could then also produce the first examples of cationic gold(III) Fischer-type amino- and thiocarbene complexes. Expansion of this conversion to include other 'soft' transition metal electrophiles (e.g. AgCl, HgCl etc.) with the aim of gaining new synthetic pathways to their vinyl amine and vinyl thioether complexes.

3.4   Experimental

3.4.1   Materials

All solvents were dried and purified by conventional methods and freshly distilled under nitrogen shortly before use. Unless otherwise stated, all common reagents were used as obtained from commercial suppliers without further purification. ^{n}BuLi was standardised before use according to the procedure reported by Winkle *et al.*[19] Ph$_3$PAuCl and the group 6 metal pentacarbonyl Fischer-type dialkylamino(methyl)- and organothio(methyl)carbene starting complexes were prepared according to procedures described in the literature.[20-22]

3.4.2   Physical methods

All reactions and manipulations involving organometallic reagents were carried out under a dry nitrogen atmosphere using standard Schlenk and vacuum-line techniques. NMR spectra were recorded on Varian INOVA 600 (600 MHz for ^{1}H, 151 MHz for ^{13}C{^{1}H} and 243 MHz for ^{31}P{^{1}H}) or Varian VXR 300 (300 MHz for ^{1}H, 75.4 MHz for ^{13}C{^{1}H} and 121.5 MHz for ^{31}P{^{1}H}) NMR spectrometers. ^{1}H and ^{13}C chemical shifts are reported in ppm relative to the ^{1}H and ^{13}C residue of the deuterated solvents. ^{31}P chemical shifts are reported in ppm relative to an 85% H$_3$PO$_4$ external standard solution. IR spectra (4000 to 400 cm^{-1}, resolution 4 cm^{-1}) were recorded on a Perkin-Elmer 1600 series FTIR spectrometer. FAB-MS were recorded on a Micromass DG 70/70E mass spectrometer at the University of Potchefstroom, South Africa, using xenon gas as bombardment atoms and *m*-nitrobenzylalcohol as matrix. Flash column chromatography was performed with "flash grade" silica (SDS 230-400 mesh). Melting/decomposition point were determined on a standardised Büchi 535 melting point apparatus. Crystal structure data collection and correction procedures were carried out on a Nonius KappaCCD diffractometer by Dr. J. Bacsa and Ms. Hong Su of the University of Cape Town structural chemistry research group. All structure solutions and refinements were carried out by the author. Theoretical calculations were carried out by Prof. G. Frenking, Dr. A. Timoshkin and Dr. Y. Chen of the department of chemistry, Philipps-Universität Marburg, Marburg, Germany.

3.4.3 Preparations and procedures

3.4.3.1 Complexes **7-13** were prepared along the same experimental procedure as described for **1-5** in section 2.4.3.1 with the respective dialkylamino- and alkyl/arylthiocarbene complexes instead of the alkoxycarbene complexes employed previously. The products were isolated in moderate to low yields [54% (**7**), 59% (**8**), 68% (**9**), 52% (**10**), 21% (**11**), 36% (**12**) and 23% (**13**)] as broad yellow bands by means of low temperature (-15 ^{o}C) silica gel column chromatography using pentane/diethyl ether, 10:1, as initial eluant and increasing the polarity to a pentane/diethyl ether ratio of ~2:1 once the non-polar impurities and unreacted starting material have been eluted from the column. Yields were not optimized.

3.4.3.3 Crystal structure determination of complexes **7** and **13**.

The crystal data collection and refinement details for complexes **7** and **13** are summarised in Table 3.16. X-ray quality yellow platelet single crystals of **7** were obtained by crystallisation from a concentrated diethyl ether solution layered with pentane at –20°C, whereas crystals containing **13** were obtained by crystallisation from a concentrated pentane solution at –20°C. Low temperature (-95 ^{o}C for **7** and -96 ^{o}C for **13**) data were collected on an Enraf-Nonius KappaCCD diffractometer[23] using graphite monochromated Mo-K$_{\alpha}$ radiation (λ = 0.71073 Å) and scaled and reduced using DENZO-SMN[24]. The structure of **7** was solved by the heavy atom method (SHELXS)[25] and refined anisotropically for all the non-hydrogen atoms by full-matrix least squares calculations (SHELXL-97)[25] on F^2. All hydrogen atoms in **7** were placed in calculated positions, except those on the asymmetrically coordinating vinyl moiety, which were found on the difference Fourier map and refined isotropically.

The structure of **13** was solved by direct methods (SHELXS)[25] after which several successive cycles of refinement on F^2 yielded all the positions of the disordered atoms. The sum of the site occupancies of the partial molecular fragments of **13** and **13'** that share the same site in the crystal lattice was restrained to 1 after which all the non-hydrogen atoms, except O(7)', which exhibits disorder, were allowed anisotropic thermal motion. Bond lengths in the C(24x) and C(25x) phenyl rings were restrained to sensible values and the carbon atoms in both rings were subjected to rigid body (DELU), flat geometry (FLAT) and similar U_{ij} (SIMU) restraints to improve their geometry. Two O(7)' atomic positions [O(7)'1 and O(7)'2] could be found for the disorder observed in this CO ligand. The sum of the site occupancies of both O(7)' atomic sites was restrained to the refined site occupancy of the disordered fragment they belong to. All hydrogen atoms in **13** were placed in calculated positions. The isotropic displacement parameters of the calculated hydrogen atoms in both structures were fixed at 1.2 (aromatic hydrogens) and 1.5 (methyl hydrogens) times the equivalent isotropic displacement parameters of their parent atoms. ORTEP-III for windows[26] was used to generate the various figures of **7** and **13** at the 50% probability level.

All other crystallographic information, including the hkl data and structure factors, is included on the CD of supplementary material provided in the back cover of this work, or is available from the author upon request.

Table 3.16: Crystallographic Data for **7** and **13**

	7	13
Chemical Formula	$C_{27}H_{23}O_5NPAuCr$	$1.4827\ (C_{29}H_{20}O_5SPCrAu)$. $0.5173\ (C_{31}H_{22}O_5SPCrAu)$
MW (g/mol)	721.4	1534.43
Crystal system	Monoclinic	Monoclinic
Space group	$P2_1/c$	$P2_1/c$
a (Å)	6.6251(2)	12.4049(2)
b (Å)	23.8365(8)	20.7908(3)
c (Å)	17.0238(5)	23.8896(3)
α (°)	90	90
β (°)	97.573(1)	91.437(1)
γ (°)	90	90
Volume ($Å^3$)	2664.9(1)	6159.38(15)
Z	4	4
d_{calcd} (g/cm^3)	1.798	1.655
Temp (K)	178(2)	177(2)
$\mu_{Mo\ K\alpha}$ (cm^{-1})	6.003	5.265
$2\theta_{max}$ (°)	25.00	26.00
Radiation	Mo Kα, graphite monochromated	Mo Kα, graphite monochromated
Crystal size (mm)	$0.10 \times 0.22 \times 0.33$	$0.25 \times 0.30 \times 0.35$
Index range	$-7 \leq h \leq 4$	$-15 \leq h \leq 14$
	$-28 \leq k \leq 28$	$-24 \leq k \leq 25$
	$-20 \leq l \leq 20$	$-25 \leq l \leq 29$
No. of reflections collected	8192	33837
No of independent reflections	4422 ($R_{int} = 0.0494$)	12099 ($R_{int} = 0.0328$)
No. of observed reflections	3729	10327
Refinement	Full matrix on F^2 (SHELXL)	Full matrix on F^2 (SHELXL)
Parameters	335	868
$R_1\ (F_o > 2\sigma F_o)$	0.0333	0.0476
wR_2 (all data)	0.0890	0.1087

3.5   References

1.   (a) Dötz, K.H. Angew. *Chem., Int. Ed. Engl.*, **1984**, 23, 5878. (b) Casey, C.P. in "*Transition Metal Organometallics in Organic Synthesis*", Alper, H., Ed. Academic Press, New York, **1979**. (c) Barluenga, J., Flórez, J., Fañanás, F.J. *J. Organomet. Chem.*, **2001**, *624*, 5.

2.   Fischer, E.O., Held., W., Kreissl, F.R. *Chem. Ber.*, **1977**, *110*, 3842.

3.   Casey, C.P., Burkhardt, T.J., Bunnel, C.A., Calabrese, J.C. *J. Am. Chem. Soc.*, **1977**, *99*, 2127.

4.   For examples see: (a) Connor, J.A., Rose, P.D. *J. Organomet. Chem.*, **1972**, *46*, 329. (b) Weiss, K., Fischer, E.O., *Chem. Ber.*, **1973**, *106*, 1277. (c) Wulff, W.D. *Organometallics*, **1998**, *17*, 3116.

5.   (a) Fischer, H., Kreissl, F.R. in "*Transition Metal Carbene Complexes*", Dötz, K.H., Fischer, H., Hofmann, P., Kreissl, F.R., Schubert, U., Weiss, K. eds., Verlag Chemie, Weinheim **1983**. (b) Anderson, B.A., Wulff, W.D., Powers, T.S., Tribbitt, S., *J. Am. Chem. Soc.*, **1992**, *114*, 10784.

6.   Bernasconi, C.F., Leyes, A.E., Ragains, M.L., Shi, Y., Wang, H., Wulff, W.D. *J. Am. Chem. Soc.*, **1998**, *120*, 8632.

7.   Bernasconi, C. F. *Chem. Soc. Rev.*, **1997**, *26*, 299.

8.   Wulff W.D., Anderson, B.A., Isaacs, L.D. *Tetrahedron Lett.*, **1989**, *30*, 4061 and references therein.

9.   Fischer, E.O., Leupold, M., Kreiter, C.G., Müller, J. *Chem. Ber.*, **1972**, *105*, 150.

10.   (a) Sander, E.G., Jencks, W.P. *J. Am. Chem. Soc.*, **1968**, *90*, 6154. (b) Hine, J., Weimar, Jr, R.D., *J. Am. Chem. Soc.*, **1965**, *87*, 3387. (c) Pearson, R.G., Songstad, J., *J. Am. Chem. Soc.*, **1967**, *89*, 1827.

11.   (a) Bernasconi, C.F., Flores, F.X., Kittredge, K.W. *J. Am. Chem. Soc.*, **1998**, *120*, 7983. (b) Bernasconi, C.F., Ali, M. *J. Am. Chem. Soc.*, **1999**, *121*, 3039. (c) Bernasconi, C.F., Kittredge, K.W., Flores, F.X. *J. Am. Chem. Soc.*, **1999**, *121*, 6630. (d) Bernasconi, C.F., Ali, M. *J. Am. Chem. Soc.*, **1999**, *121*, 11384.

12.   (a) Hoare, R.J., Mills, O.S. *J. Chem. Soc., Dalton Trans.*, **1972**, 653. (b) Qui, Z., Sun, J., Chen, J., *Organometallics*, **1998**, *17*, 600.

13.   Kuhn, N., Bohnen, H., Bläser, D., Boese, R. *Chem. Ber.*, **1994**, *127*, 1405.

14. (a) Delis, J.G.P., Aubel, P.G., Vrieze, K., van Leeuwen, P.W.N.M., Veldman, N., Spek, A.L. *Organometallics*, **1997**, *16*, 4150. (b) Campora, J., Husdon, S.A., Messiot, P., Maya, C.M., Palma, P., Camona, E., Martinez-Cruz, L.A., Vegas, A. *Organometallics*, **1999**, *18*, 5225.

15. Fehlhammer, W.P., Dahl, L.F. *J. Am. Chem. Soc.*, **1974**, *94*, 3370.

16. (a) Rösch, N., Görling, A., Ellis, D.E., Schmidbaur, H. *Angew. Chem., Int. Ed. Engl.*, **1989**, *28*, 1357. (b) Jiang, Y., Alvarez, S., Hoffmann, R. *Inorg. Chem.*, **1985**, *24*, 749. (c) Merz, K.M., Hoffmann, R. *Inorg. Chem.*, **1988**, *27*, 2120. (d) Mehrotra, P.K., Hoffmann, R. *Inorg. Chem.*, **1978**, *17*, 2187. (e) Dedieu, A., Hoffmann, R. *J. Am. Chem. Soc.*, **1978**, *100*, 2074.

17. Abel, E.W., Stone, F.G.A., Wilkinson, G., Hegedus, L.S. *Comprehensive Organometallic Chemistry*, Pergamon, Oxford, **1982**.

18. (a) Nakamoto, M., Hiller, W., Schmidbaur, H. *Chem. Ber.*, **1993**, *126*, 605. (b) Fackler, Jnr., J.P., Staples, R.J., Elduque, A., Grant, T. *Acta. Crystallogr., Sect. C (Cr. Str. Comm.)*, **1994**, *50*, 520. (c) Kuz'mina, L.G., Baukova, T.V., Churakov, A.V., Kuz'min, V.S., Dvortsova, N.V. *Koord. Khim.*, **1997**, *23*, 301.

19. Winkle, M.R., Lansinger, J.M., Roland, R.C. *J. Chem. Soc., Chem. Commun.*, **1980**, 87.

20. "*Synthetic Methods of Organometallic and Inorganic Chemistry (Herrmann/Brauer)*" Vol. 7 : Transition Metals Part 1, Herrmann, W.A., Ed. **1997**.

21. Fischer, E.O., Leupold, M. *Chem. Ber.*, **1972**, *105*, 599.

22. Lam, C.T., Senoff, C.V., Ward, J.E.H. *J. Organomet. Chem.*, **1974**, *70*, 273.

23. Nonius, B.V. "*COLLECT, Data collection software*", **1999**, Delft, The Netherlands.

24. Otwinowski, Z.; Minor, W. *Methods Enzymol.* **1997**, *276*, 307.

25. Sheldrick, G. M. *SHELX-97*. Program for crystal structure analysis, University of Göttingen, Germany, **1997**.

26. Farrugia, L.J. *J. Appl. Cryst.*, **1997**, *30*, 565.

CHAPTER 4

REACTIONS OF LITHIUM AND TETRABUTYLAMMONUIM ACYL- AND IMIDOYL-PENTACARBONYL CHROMATES AND TUNGSTATES WITH TRIPHENYLPHOSPHINE GOLD(I) CHLORIDE

4.1   Introduction

Transition metal-acyl complexes comprise an extremely important class of organometallic compounds. It has long been known that metal-acyl complexes are a ubiquitous feature in many homogenous catalytic processes, especially ones in which carbon monoxide is involved,[1] and have hence been the subject of many reactivity and theoretical studies.[2] Transition metal-acyl complexes are also useful models for key catalytic intermediates in heterogeneous catalytic processes,[3] such as the Fischer-Tropsch process operated by SASOL, where Fe-surface alkyl and acyl species are believed to play an important role in the formation of oxygenates (mainly formates, alcohols and ketones).[4] Furthermore, anionic transition metal-acyl complexes are also important intermediates in many synthetic routes to useful organometallic compounds, including Fischer's classical, and Semmelhack's more recent, routes to carbene complexes. Both these routes involve the formation of anionic metal-acyl species that, upon oxygen alkylation, yield a wide variety of carbene complexes.[5,6] Because of the electronic properties of low-valent metal centres in neutral metal-acyl complexes, the acyl moiety is viewed as a close relative of ketones or esters. This analogy has been utilised successfully in developing much of the chemistry of metal-acyl complexes, especially reduction and alkylation reactions.[7]

Three different coordination modes are known for mononuclear transition metal-acyl complexes (**I-III** in Scheme 4.1). All three have been authenticated by X-ray crystallography, but while there are many examples of η^1 and η^2 acyl coordination (types **I** and **II**),[8] there are only a handful of examples of these complexes that exhibit agostic interactions (type **III**).[9] The occurrence of agostic type **III** metal-acyl complexes can be linked to the ester-like property of these compounds that activates

β-metallo hydrogen atoms. This effect has also been observed in reactions of neutral metal-acyl complexes containing β-metallo hydrogen atoms with basic reagents, which leads to the formation of useful alkali metal salts of enolate anions (Scheme 4.2).[10] The enolate anions have subsequently been extensively studied as asymmetric induction reagents in many areas of organometallic and organic chemistry.[11]
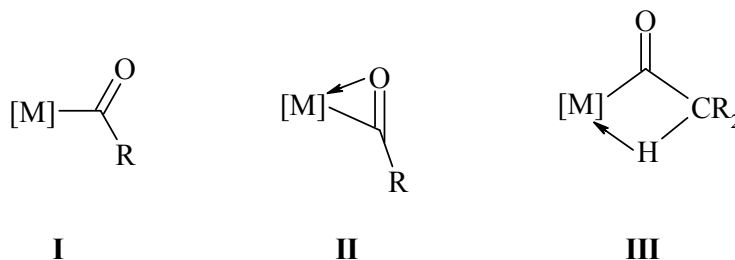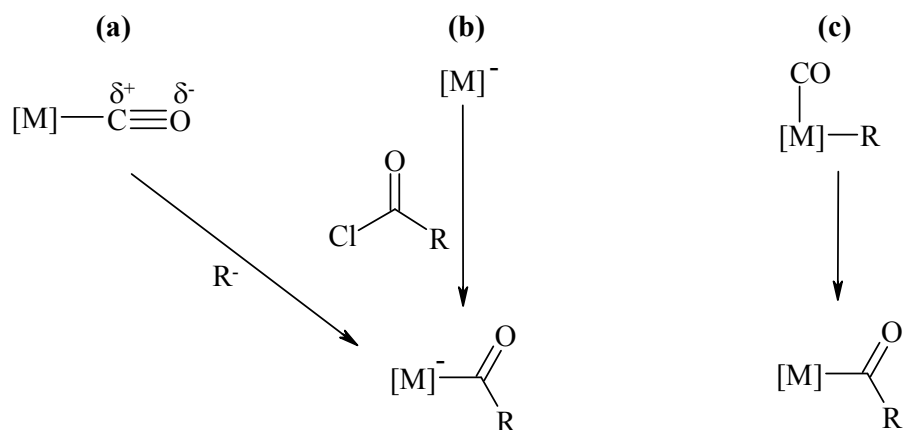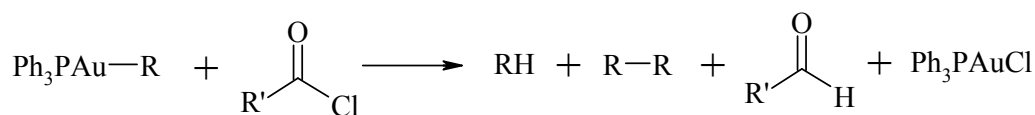

Scheme 4.1
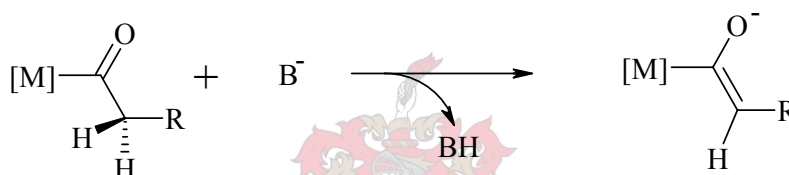
Scheme 4.2

Transition metal-acyl complexes are mostly prepared *via* three main reaction pathways: the attack by nucleophilic carbon reagents at metal-bound CO; acylation at a nucleophilic metal centre; and the migratory insertion reaction of a CO ligand into a M-C bond [Scheme 4.3 (a-c)].[1,12] From a catalysis point of view the latter, also frequently referred to as catalytic carbonylation, is the more interesting route. This route provides a mechanism for the incorporation of CO feedstock into organic compounds and polymers (mostly co-polymers with ethylene) and is indeed unequalled in importance in catalytic conversions involving CO. This transformation has many practical applications and a great number of catalytic carbonylations are employed in both laboratory and industrial syntheses.[1] Routes (a) and (b) (Scheme 4.3) to metal-acyl complexes have mainly found application in the laboratory preparation of metal-acyl and other important organometallic species, including carbene complexes, as briefly described above.
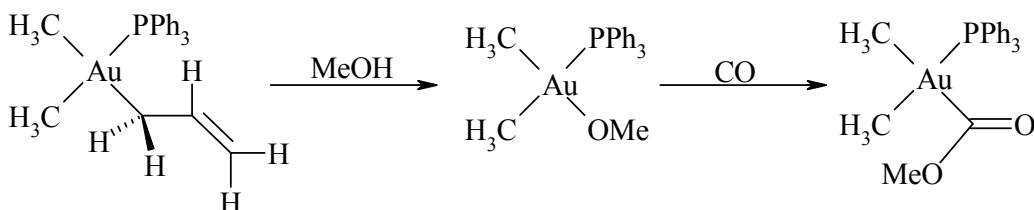
Scheme 4.3

Transition metal-acyl compounds, mostly prepared by one of the reaction paths outlined in Scheme 4.3, are known for most transition metal elements.[1] Until recently a notable exception to these was gold.[13] The reason for this partly resides with the unusual and unstable manner in which low-valent gold binds CO. The near absence of gold to carbon π-back donation in gold carbonyl complexes is manifested in strong carbon-oxygen bonds and, consequently, rather weak gold-carbon bonds in these compounds. This is reflected in the fact that $[Au(CO)_2^+(solv)]$ has the highest CO-stretching frequencies observed so far for a metal carbonyl derivative (2254 cm^{-1}),[14] 111 cm^{-1} higher than the stretching frequency of free CO.[15] All six known gold carbonyl compounds exhibit similar tendencies in their CO stretching frequencies.[16] Despite the fact that this predicts a highly electropositive CO carbon atom, reaction of carbon nucleophiles (e.g. RMgX) with gold carbonyls, for unknown reasons, yields only coupled R groups, liberated CO and precipitated gold metal.[17]

Reactions of nucleophilic gold compounds, RAuPPh$_3$, with acyl halides also do not yield the expected gold-acyl products. More complicated reactions are observed that have been suggested to follow an electron transfer mechanism.[18] The proposed mechanism initially involves electron transfer to the acyl halide to give $[Ph_3PAuR]^+$• and $[R'COCl]^-$•, after which breakdown occurs to produce Ph$_3$PAuCl and the radicals R• and R'C(O)•. These radicals either abstract hydrogen or dimerise to give the final organic products observed in this reaction (Scheme 4.4).

Scheme 4.4

Also, there are no reports in the literature of simple insertion reactions of CO into Au-C bonds in gold chemistry. It has, however, been observed that Au-C(O)OR derivatives can be obtained from reactions of gold(III) complexes under conditions where alkoxy (OR) complexes may be expected as intermediates (e.g. Scheme 4.5).[19]

Scheme 4.5

From the above-mentioned reactions it becomes clear that the synthesis of gold-acyl complexes along conventional reaction pathways is not possible. A recent paper by Haupt, however, describes a novel conversion for the first (and only) preparation of this species.[13] Haupt reacts anionic rhenium acyl complexes, prepared by the nucleophilic addition of an alkyl/aryl fragment to a bridged Re-carbonyl complex $[Re_2(\mu\text{-}PPh_2)_2(CO)_8]$, with an electrophilic gold compound (Ph_3PAuCl). From this conversion he was able to isolate and structurally characterise the first acylgold(I) complexes trapped as O-coordinated axial ligands to $Re_2(\mu\text{-}PPh_2)_2(CO)_7$ fragments. Although this conversion is an effective route to coordinated acylgold(I) complexes, the free acylgold(I) complexes remained elusive.

These attempts at preparing free acylgold(I) complexes, the potential importance of this species for the organometallic chemistry of gold (particularly regarding catalytic conversions), and the unique reaction characteristics of gold electrophiles (see chapters 2 and 3) piqued our interest in this research topic. We embarked on an investigation to develop an effective preparation for novel free acylgold(I) complexes along a related reaction path as is described by Haupt. Instead of employing Re-carbonyl complexes, our investigation centred around the use of the well-studied anionic group 6 metallo-acyl complexes as source of the acyl moiety. Previous work

in our laboratory involved the use of these metallo-acyl species in the preparation of bimetallic titanoxy- and zirconoxy-carbene complexes. These were found to be extremely effective α-olefin copolymerisation catalysts after treatment with MAO.[20] The reaction of a 'soft' gold electrophile (Ph₃PAuCl) with these species rather than the 'hard' electrophiles employed previously (Cp₂TiCl₂, Cp₂ZrCl₂ and Cp₂HfCl₂), therefore, extends the aforementioned work to include other possible reactions of such anionic metal-acyl species. The development of efficient isolation procedures of the desired products, once attained, also needed attention. Furthermore, we planned to extend such a reaction pathway to the preparation and characterisation of analogous imidoyl-gold(I) complexes. Although many interesting imidoyl complexes of gold have been reported all of these involve imine groups that are either situated in heterocyclic ring systems[21] or contain hetero-atoms (O or N) bonded to the α-carbon atom.[22] Lastly, to further the body of knowledge regarding the useful group 6 lithium acyl metallates generally employed in this study, unusual, yet anticipated, solid state interactions of these compounds were investigated.

The contents of this chapter describe the results obtained from our investigation based on the following questions:

1)   Do anionic group 6 metal-acyl complexes react with Ph₃PAuCl to yield the acylgold(I) species?

2)   Would these species, if they were indeed found, be stabilised by coordination to M(CO)₅ fragments through their acyl oxygen atoms?

3)   Could a procedure be developed to gain easy access to the free acylgold(I) complexes from this conversion and, if so, could these novel compounds be isolated and characterised?

4)   Could this type of conversion be extended to the analogous preparation of novel bimetallic metal carbonyl coordinated imidoyl-gold(I) complexes, by employing N-deprotonated aminocarbene compounds instead of anionic metal-acyl species?

5)   Finally, what insights into a possible reaction mechanism for these conversions could be gained from the results of this study?

4.2 Results and Discussion

4.2.1 Acyl complexes of gold(I): {acetyl/benzoyl-AuPPh₃}M(CO)₅ bimetallic complexes and their LiBr and [NBu₄]Cl adducts

A. General preparation and discussion of {Ph₃PAuC(O)R}-*O* M(CO)₅,
M = Cr, R = Me (**15**) / R = Ph (**16**); M = W, R = Me (**17**) / R = Ph (**18**),
[{BrW(CO)₅}-*O* {Et₂O}{Ph₃PAuC(O)Ph}₂-*O* Li] (**18'**), Ph₃PAuC(O)Ph (**19**)
and [ClW(CO)₅][Bu₄N] (**20**)

The synthesis of complexes **15-18** (Scheme 4.6) was carried out by the addition of 1 mole equiv. Ph₃PAuCl to a cooled (-78 °C) diethyl ether solution of the lithium acetyl/benzoylpentacarbonyl chromates and tungstates, freshly prepared by the addition of 1.1 mole equiv. MeLi or PhLi to the respective M(CO)₆ complexes. The reaction was complete after the reaction mixture was allowed to warm up to room temperature over a period of 3 hours.
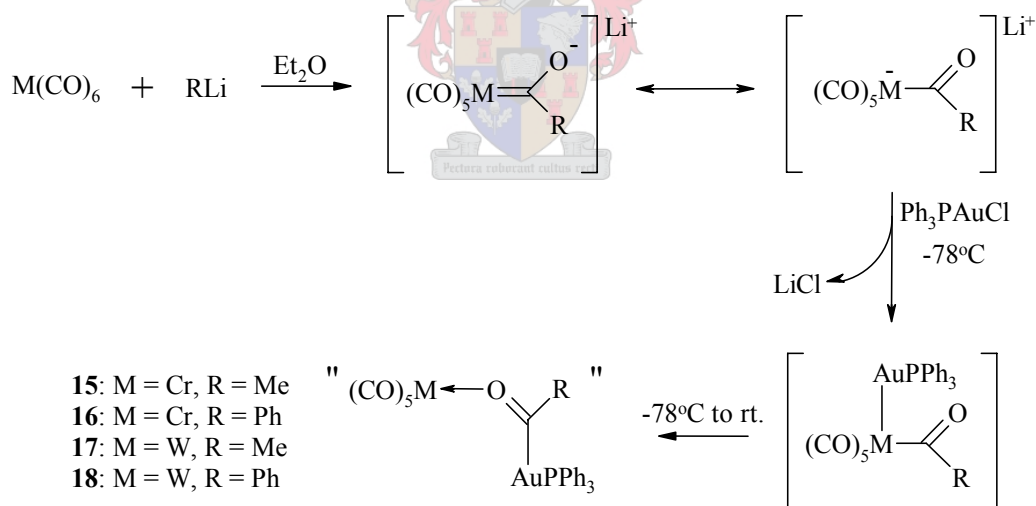
Scheme 4.6

Although there is evidence pointing to acylgold(I) oxygen-coordination to the M(CO)₅ fragments in complex mixtures **15-18** under certain conditions, this coordination mode could not be proven beyond all reasonable doubt. Nevertheless, based on our evidence, reported below, and the characterisation of a similar coordination mode for acylgold(I) complexes by Haupt,[13] such a coordinated structure for these complexes is assumed here.

Isolation of the assumed products **15**-**18**, after removal of precipitated LiCl from the reaction mixture, by filtration through Celite™ or silica gel, proved to be challenging as decomposition of the complexes - indicated by rapid darkening of the reaction mixture - was frequently observed during this process. Complete removal of solvent (*in vacuo*) from the unfiltered reaction mixture also generally resulted in the decomposition of these compounds, as did any attempted chromatographic separation procedure. Some clues to the reasons for this instability, as well as to the nature of the acylgold(I)-M(CO)$_5$ coordination, were found in the discovery that the benzoyl-AuPPh$_3$ components in **18** were isolable in moderate yields (65% based on Au) when coordinated to Li-cations in LiBr adducts of the W(CO)$_5$ fragments formed in the conversion (Scheme 4.9).
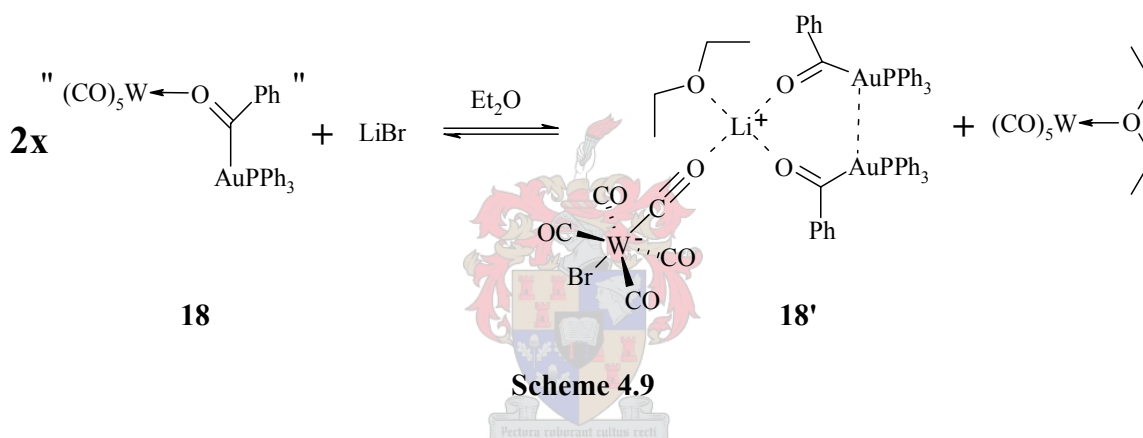
Scheme 4.9

The formation of the electrostatically associated ionic complex, **18'**, is proposed to proceed as follows: LiBr, originally present in the freshly prepared PhLi solution (Scheme 4.10) employed to synthesise the lithium benzoylpentacarbonyl tungstate in the first step of the synthesis (Scheme 4.6), reacts with W(CO)$_5$ in the reaction mixture of **18**. The ionic species, [BrW(CO)$_5$][Li], is formed, which precipitates, or rapidly crystallises, from the cooled (-20°C) reaction mixture with two benzoyl-AuPPh$_3$ fragments and an Et$_2$O solvent molecule coordinated to the Li$^+$-cation.
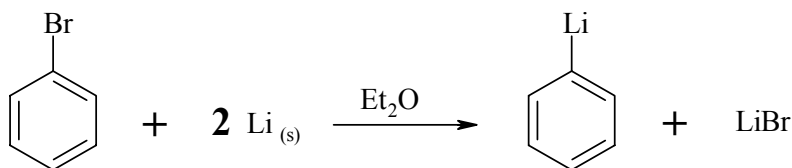
Scheme 4.10

A single crystal X-ray structure determination revealed this unexpected molecular structure for **18'** and also confirmed that the electrophilic addition of Ph₃PAu⁺ to lithium acylpentacarbonyl tungstates indeed results in the formation of the acylgold(I) organyls.

The formation and precipitation/crystallisation of **18'** is driven by its poor solubility in Et₂O. Equilibria of halide salts and coordinatively unsaturated M(CO)₅ fragments are well known.[23] The fact that this reaction occurs in the reaction mixture of **18** is a testimony to the poor stabilisation that the W(CO)₅ fragments in this reaction mixture receive. The instability of the products in the reaction mixtures of **15-18** is thus most likely as a result of weak acylgold(I) organyl, or possibly weak solvent (Et₂O), oxygen-coordination to the M(CO)₅ fragments. No precipitation or crystallisation of **18'**, could be achieved in the presence of thf. This confirms that the availability of a coordinatively unsaturated W(CO)₅ fragment and the insolubility of the ionic product are vital to the formation of the LiBr adduct [thf molecules are known to coordinate much better to M(CO)₅ fragments than Et₂O molecules, allowing the (thf)Cr(CO)₅ complex to be structurally characterised].[24] The reason why the W(CO)₅ fragments in mixture **18** prefer to react with residual LiBr, originating from the PhLi solution, rather than with LiCl, which is a by-product of the reaction (Scheme 4.6), probably lies with the 'softer' nature of the Br-atoms.

Reactions to prepare the assumed {acetyl-AuPPh₃}M(CO)₅ bimetallic species, **15** and **17**, were conducted using commercially supplied MeLi. The products of these reactions are much less stable than those of **16** and **18**. This is reflected in their NMR spectra, especially their ¹³C{¹H} NMR spectra, which remain largely unresolved. The addition of thf to the reaction mixture of **15** enabled the isolation and characterisation of Cr(CO)₅(thf) and the acetyl-AuPPh₃ complex in an orange oil, with only solvent impurities still present. The reason for the reduced stability of the acetyl-AuPPh₃ complexes is unknown.

Some evidence for benzoyl-AuPPh₃ oxygen-coordination to M(CO)₅ fragments (M = Cr, W), forming the bimetallic complexes **16** and **18**, could be found in the NMR spectra of these reaction mixtures as well as the FAB mass spectrum of the reaction mixture of **16**. When dissolved in CD₂Cl₂, crystals of **18'**, give a ¹³C{¹H} NMR

spectrum that is consistent with the presence of W(CO)$_5$ and two chemically unique benzoyl-AuPPh$_3$ complexes, one presumably coordinated to the W(CO)$_5$ group. This result suggests that the reaction to form [BrW(CO)$_5$][Li] is at least partly reversed in CD$_2$Cl$_2$ and that coordination of the benzoyl-AuPPh$_3$ complexes to W(CO)$_5$ may indeed occur if no excess of solvent competing with the benzoyl-AuPPh$_3$ complex for coordination to W(CO)$_5$ is present. Further indirect evidence for the occurrence of the bimetallic complexes **16** and **18** in the NMR samples (CD$_2$Cl$_2$) of their reaction mixtures is presented in the NMR discussion below. The FAB mass spectrum of complex **16**, exhibiting a clear M$^+$ peak for the assumed bimetallic species, could be obtained.

Based on the above-mentioned observations, and the solid-state structure of **18'**, an equilibrium system, in which the acylgold(I) complexes, solvent molecules and halide anions compete to coordinate/bond to the M(CO)$_5$ fragments in the reaction mixtures of **15-18** is proposed (Scheme 4.11 – cations are omitted for clarity). The population of the different species in this system is determined by the types and amounts of solvent molecules present, the solubility of each species in the solvent, and the concentration of halide anions (Cl$^-$/Br$^-$) present.
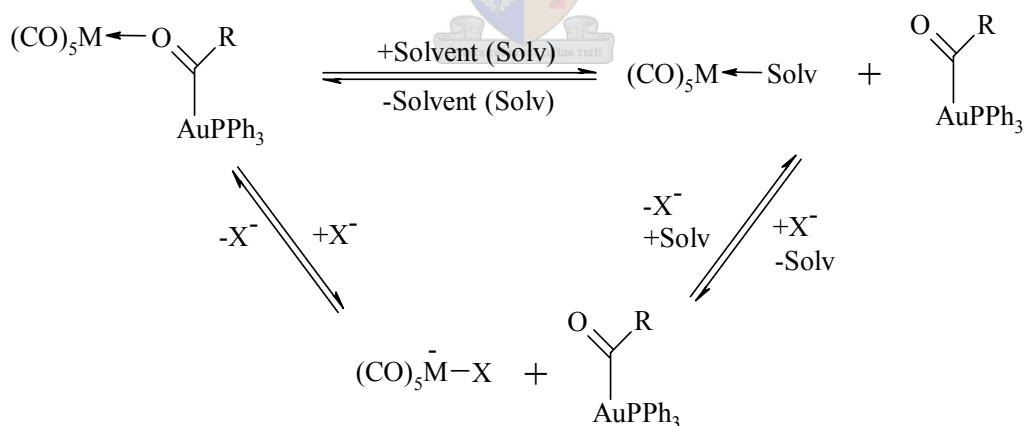
Scheme 4.11

The unexpected formation of LiBr adducts of W(CO)$_5$, observed in the crystal structure of **18'**, prompted further investigation into the reactions of such weakly stabilised fragments with halide anions, with the main objective of preparing the first

free acylgold(I) complex, benzoyl-AuPPh$_3$ (**19**) (Scheme 4.12). If, instead of lithium benzoylpentacarbonyl tungstate, tetrabutylammonium benzoylpentacarbonyl tungstate was employed as starting material, the reaction with Ph$_3$PAuCl led to the formation of benzoyl-AuPPh$_3$, [^{n}Bu$_4$N][Cl] and a poorly stabilised W(CO)$_5$ fragment. The W(CO)$_5$ fragment rapidly reacts with the [^{n}Bu$_4$N][Cl] to yield the ionic species, [ClW(CO)$_5$][^{n}Bu$_4$N] (**20**), which is sparingly soluble in Et$_2$O and rapidly precipitates from the cooled (0°C) reaction mixture. Since the ^{n}Bu$_4$N$^+$-cation in **20** cannot accommodate acyl coordination, as is observed for the Li-cation in the crystal structure of **18'**, the free benzoyl-AuPPh$_3$ complex (**19**) remains in solution and can be isolated in high (72%) yields by crystallisation from thf/Et$_2$O mixtures. X-ray diffraction studies confirm the formation of both **19** and **20** in this reaction.
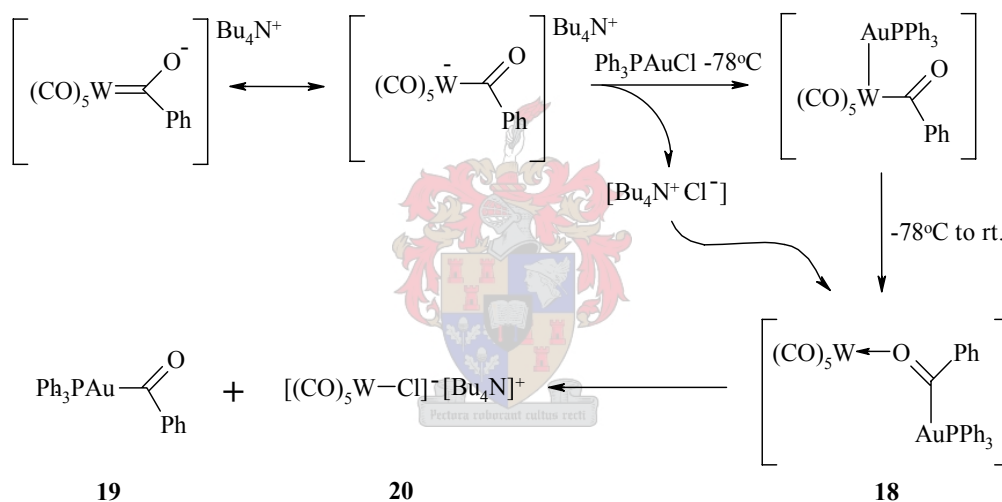
Scheme 4.12

The mechanism involved in the formation of **15-18** is not clear. In stark contrast to the formation of bimetallic metalloxy Fischer-type carbene complexes when anionic group 6 metal-acyl complexes are reacted with Cp$_2$ZrCl$_2$, Cp$_2$TiCl$_2$ and Cp$_2$HfCl$_2$,[20] acylgold(I) complexes are formed when the 'soft' electrophile, Ph$_3$PAuCl, is used. In the sole literature example where a similar conversion with Ph$_3$PAuCl is reported with anionic Re-acyl nucleophiles, Haupt suggests a concerted mechanism in which a hypothetical ion pair complex, [Re$_2${μ-PPh$_2$}$_2$(CO)$_7${C(O)R}]$^-$[AuPPh$_3$]$^+$, is converted to the acylgold(I)-coordinated rhenium complexes *via* an assumed bimetallic η^2-acyl transition state (Scheme 4.7).[13] Haupt rationalises his suggested mechanism by the

116

thermodynamically favoured change of a Re-C(acyl) bond to a Re-O(acyl) coordination and the formation of the Au-C(acyl) bond.
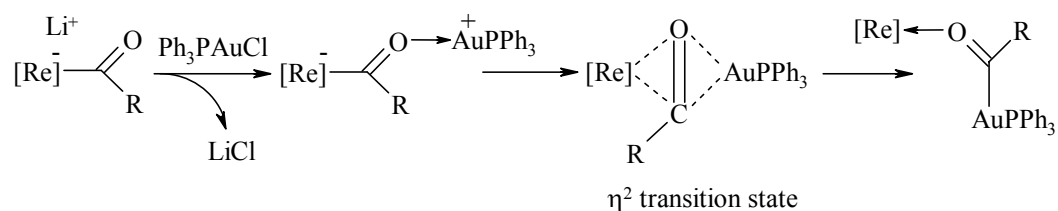
Scheme 4.7

These thermodynamic criteria are, however, not valid for the current examples. Acetyl- and benzoyl [M(CO)$_5$] (M = Cr, W) anions are very stable organometallic species,[7c, 25] whereas acyl-oxygen coordinations to 'soft' Cr(CO)$_5$ and W(CO)$_5$ fragments are known to be weak[26] - a fact that is also corroborated by the results reported in this chapter. Undoubtedly there is a thermodynamic advantage in the formation of a Au-C(acyl) bond rather than a Au-O bond. Furthermore, results presented in section 4.2.2 show that a similar conversion, then leading to imidoyl-gold(I) complexes, occurs when N-deprotonated Fischer-type aminocarbene complexes react with Ph$_3$PAuCl. This result demonstrates that not even the possible thermodynamic advantage gained by substituting the acyl oxygen atom for a nitrogen atom, so that thermodynamically more stable Au-N(amine) bonds may be formed, is able to effect electrophilic addition of AuPPh$_3^+$ onto the hetero-atom.

Fischer, Schubert and Sarkar have reported the rearrangement of Fischer-type carbene complexes to ketones or aldehydes upon thermolysis of certain carbene complexes.[27] In a recent paper Sarkar suggests a probable mechanism for such a reaction that involves electrophilic addition of a carbon electrophile onto the metal moiety, followed by a formal reductive elimination of a ketone fragment (Scheme 4.8).[28]

117
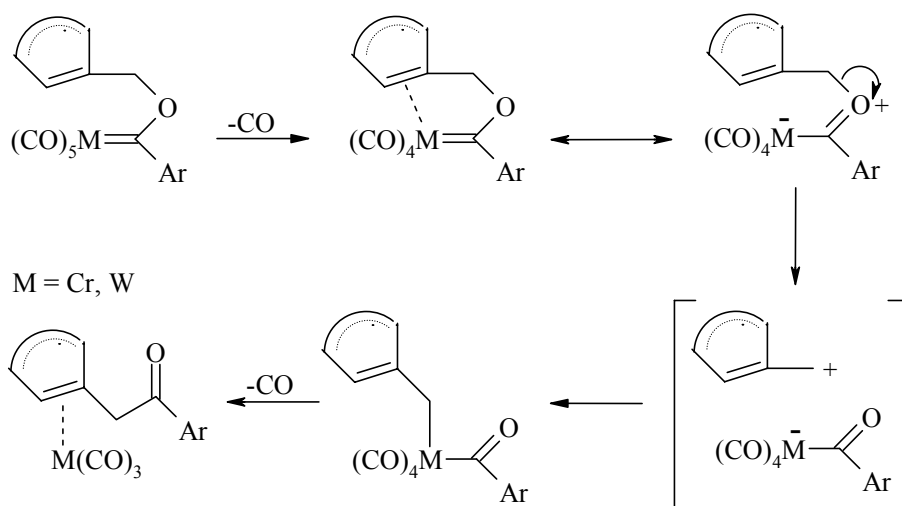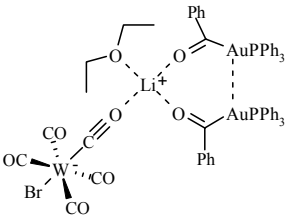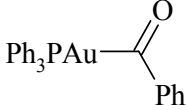
Scheme 4.8

Based on these results, we propose a mechanism for the current conversion (Scheme 4.6) that is related to Sarkar's mechanism as well as the "aurolysis" working mechanism for electrophilic addition of $AuPPh_3^+$ to β-C deprotonated Fischer-type carbene complexes (Chapters 2 & 3). After auration of the anionic metal carbonyl a formal reductive elimination of the acylgold(I) organyl occurs. This facile route to acylgold(I) complexes is believed to be enabled by the delocalisation of negative charge from the hetero-atom onto the metal carbonyl fragment, as well as the linear geometry of gold(I) bonds, which allows the $AuPPh_3^+$ electrophile, even though it is sterically large, to interact with the metal centres in the anionic acyl-$M(CO)_5$ complexes. However, our proposed mechanism still requires additional experimental support.

Physical data for the isolated new compounds are summarised in Table 4.1. Physical and spectroscopic data for **20** have been reported elsewhere.[23]

118

Table 4.1: Analytical data for complexes **18'** and **19**

Complex		
Complex	**18'**	**19**
M.p. / $^{\circ}$C	127 (decomp.)	131 (decomp.)
Colour	orange	orange
Yield (%)	65	72
M.W. (g / mol)	1613.61	564.37
Analyses (%)[a]		
C	43.52 (43.92)	53.27 (53.21)
H	2.98 (3.12)	3.61 (3.57)
O	7.75 (7.93)	2.78 (2.83)
P	3.95 (3.84)	5.50 (5.49)

[a] Required values given in parenthesis

B.   Spectroscopic characterisation of **15-19**

1.   NMR Spectroscopy

The ^{1}H, ^{13}C$\{^1$H$\}$ and ^{31}P$\{^1$H$\}$ NMR spectroscopic data of complex mixtures **15-18** and complex **19** are summarised in Tables 4.2-4.6.

Of greatest interest in the ^{1}H NMR spectra of mixtures **15** and **17** are the resonances representing the methyl protons in the acetyl-AuPPh$_3$ fragments. For **15** this signal appears as a clear doublet ($J = 8.1$ Hz), presumably due to long-range J_{P-H} coupling, at δ 0.40 and for **17** it appears as a greatly broadened singlet, at δ 0.76. These results are quite extraordinary and hardly believable as the methyl groups in these compounds

are situated next to carbonyl groups that are also potentially coordinated to a highly electron withdrawing $M(CO)_5$ fragment, and are therefore expected to be shifted much further downfield. Nevertheless, a similar result is obtained in the $^{13}C\{^1H\}$ NMR spectrum of **15**, where the resonance for the CH_3 group appears as a clear doublet (J_{P-C} = 11.1 Hz) at δ 8.1. The $^{13}C\{^1H\}$ resonance for this group in **17** unfortunately remains unresolved, due to the instability of this mixture in CD_2Cl_2 solution. Reasons for these unexpected chemical shifts for this moiety are not clearly understood. The proton resonances stated here also do not correlate well with resonances reported for the Re-coordinated acetyl-$AuPPh_3$ complex and are thus highly suspect.[13] A possible, although unlikely, explanation for these NMR shifts could be that the protons on the CH_3 groups in **15** and **17** are involved in agostic interactions with either the gold atom (Structure **I**, Scheme 4.13) or the $M(CO)_5$ fragments (Structure **II**, Scheme 4.13).

Scheme 4.13
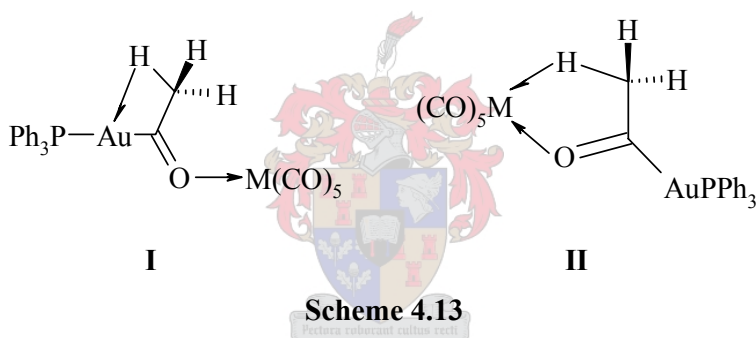
Type **I** structures for acetyl complexes involved in agostic interactions with the metallo-acyl metal centre are known for molybdenum acetyl complexes.[29] Agostic linkages of type **II** have to our knowledge not been observed for similar compounds hitherto. Both possibilities could reasonably fit the unusual NMR data obtained for **15** and **17** as agostic interactions of these types generally result in shielding of the hydrogen atoms involved and even allow for coupling interactions across the metal fragments. The dynamic behaviour often associated with such agostic interactions could also explain the broadening observed in the ^1H NMR signal observed for the acetyl protons in **17**.

At first glance the ^1H NMR spectra of **16**, **18** and **19** do not provide much structural information about these compounds since the spectra are dominated by multiplet signals representing the aromatic protons in their benzoyl and PPh_3 groups. A closer look, however, reveals some valuable information. Shifted downfield (~0.5 ppm)

from the multiplet aromatic proton resonances in the ^{1}H NMR spectra of these compounds is a clearly separated doublet resonance (Figure 4.1).
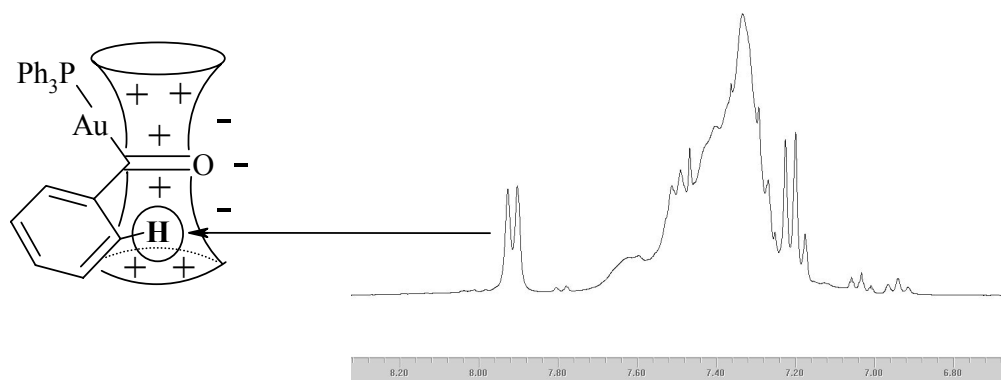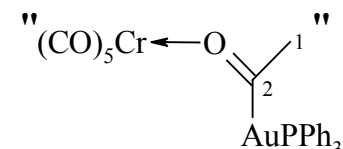
This characteristic signal is ascribed to the *ortho*-protons on the benzoyl rings in **16**, **18** and **19** which are more deshielded than the other aromatic protons as a result of interaction with the anisotropy of the acyl C=O bond. Moreover, as these signals are linked to the electronic anisotropy of the acyl C=O bond, as illustrated in Figure 4.1, any change in the electronic environment of this bond, e.g. due to metal coordination, could then be observable as a change in the chemical shift of the *ortho*-benzoyl proton resonance. The ^{1}H NMR spectra of mixtures **16**, **18** and **19** exhibit this doublet signal at δ 8.03, 8.04 and 7.91. This result suggests acyl coordination in the mixtures of **16** and **18** as the resonance for the ortho-phenyl protons in the free benzoyl-AuPPh$_3$ complex (**19**) is less affected by the anisotropy in the acyl C=O bond.

^{13}C resonances for the acylgold carbon atom were only clearly observed for **16**, **18** and **19** (δ 217.2, 203.3 and 198.1 respectively). These chemical shifts are also consistent with weak metal coordination in complexes **16** and **18** compared to a slightly more shielded acyl carbon atom in the free benzoyl-AuPPh$_3$ complex, **19**. The ^{13}C resonance for this atom in benzaldehyde appears at δ 192.0. This suggests that there is not much electron loss to the gold atom after auration in **19**. The acyl carbon atom signals for **16** and **19** are, furthermore, split into doublets (*J* = 14.3 & 6.0 Hz respectively) as a result of $^{2}J_{P-C}$ coupling across the gold atom, whereas for **18** it appears as a broadened singlet.

The $^{31}P\{^1H\}$ resonances for the PPh$_3$ groups coordinated to the gold atoms in **15-19** appear between 37.9 and 41.2 ppm, which is within the normal range for gold(I)-phosphine complexes containing an Au-C σ-bond.[30] Furthermore, the $^{31}P\{^1H\}$ resonances of **15-18** are shifted slightly downfield (~1.7 - 3.3 ppm) compared to this signal in the free benzoyl-AuPPh$_3$ complex, **19**, thus also suggesting acyl-M(CO)$_5$ coordination in the NMR samples of these compounds.

Table 4.2

Complex	"(CO)$_5$Cr←O=C^2(C^1)(AuPPh$_3$)"
	15
Solvent	CD$_2$Cl$_2$
Temperature (K)	298
^{1}H NMR H^1	0.40 (d, $^4J_{\text{P-H}}$ = 8.1 Hz, 3H)
(300 MHz) Ph	7.4-7.6 (m, 15H)
^{31}P$\{^1$H$\}$ NMR P	40.4 (s)
(121.4 MHz)	
^{13}C$\{^1$H$\}$ NMR C^1	8.1 (d, $^3J_{\text{P-C}}$ = 11.1 Hz)
(75 MHz) C^2	-^{a}
Ph-C$_{\text{ipso}}$	-^{a}
Ph-C$_{\text{ortho}}$	129.5 (d, $^2J_{\text{P-C}}$ = 10.0 Hz)
Ph-C$_{\text{meta}}$	134.8 (d, $^3J_{\text{P-C}}$ = 13.0 Hz)
Ph-C$_{\text{para}}$	131.5 (s)
CO$_{\text{cis}}$	212.6 (s)
CO$_{\text{trans}}$	221.9 (s)
υ (CO) (cm^{-1})^b	1940 (v st br)

^{a} NMR resonance not reliably detected

^{b} CH$_2$Cl$_2$ solution in NaCl
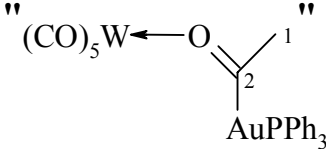
Table 4.3

Complex	"$(CO)_5Cr \leftarrow O = C^1(Ph)AuPPh_3$"
	16
Solvent	CD_2Cl_2
Temperature (K)	298
^{1}H NMR Ph	7.3-7.6 (m, 18H)
(600 MHz) Ph(benzoyl)-C_{ortho}	8.03 (d, $^3J_{H-H}$ = 7.2 Hz, 2H)
^{31}P{H^1} NMR P	39.6 (s)
(243 MHz)	
^{13}C{H^1} NMR C^1	217.2 (d, $^2J_{P-C}$ = 14.3 Hz)
(150 MHz) Ph	125.6 (s), 128.7 (s), 130.5 (s), -[a]
PPh-C_{ipso}	-[a]
PPh-C_{ortho}	129.5 (d, $^2J_{P-C}$ = 10.2 Hz)
PPh-C_{meta}	134.5 (d, $^3J_{P-C}$ = 12.7 Hz)
PPh-C_{para}	131.7 (s)
CO_{cis}	212.0 (s)
CO_{trans}	222.3 (s)
υ (CO) (cm^{-1})[b]	2063 (w $A_1^{(1)}$), 1939 (v st br)

[a] NMR resonance not reliably detected

[b] CH_2Cl_2 solution in NaCl

Table 4.4

Complex	$(CO)_5W \leftarrow O \overset{1}{\underset{2}{=}}$ AuPPh$_3$
	17
Solvent	CD$_2$Cl$_2$
Temperature (K)	298
^{1}H NMR H^1	0.76 (br s, 3H)
(300 MHz) Ph	7.3-7.6 (m, 15H)
^{31}P{H^1} NMR	
(121.4 MHz) P	41.2 (br, s)
^{13}C{H^1} NMR	
(75 MHz) C^1	- [a]
C^2	- [a]
PPh-C$_{ipso}$	130.2 (d, $^1J_{P-C}$ = 53.2 Hz)
PPh-C$_{ortho}$	129.4 (d, $^2J_{P-C}$ = 10.1 Hz)
PPh-C$_{meta}$	134.3 (d, $^3J_{P-C}$ = 12.9 Hz)
PPh-C$_{para}$	131.9 (s)
CO$_{cis}$	192.1 (s)
CO$_{trans}$	199.5 (s)
υ (CO) (cm^{-1})[b]	1935 (v st br)

[a] NMR resonance not reliably detected
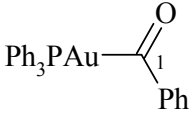
[b] CH$_2$Cl$_2$ solution in NaCl

Table 4.5

Complex		"$(CO)_5W \leftarrow O$ Ph" $\underset{AuPPh_3}{\overset{1}{\diagdown}}$
		18
Solvent		CD_2Cl_2
Temperature (K)		298
^{1}H NMR	Ph	7.2-7.6 (m, 18H)
(300 MHz)	Ph(benzoyl)-C_{ortho}	8.04 (d, $^3J_{H-H}$ = 7.2 Hz, 2H)
^{31}P{H^1} NMR	P	39.8 (s)
(121.4 MHz)		
^{13}C{H^1} NMR	C^1	203.3 (br, s)
(75 MHz)	Ph	126.1 (s), 127.9 (s), 130.7 (s) 146.9(s)
	PPh-C_{ipso}	131.2 (d, $^1J_{P-C}$ = 53.0 Hz)
	PPh-C_{ortho}	129.6 (d, $^2J_{P-C}$ = 11.1 Hz)
	PPh-C_{meta}	134.6 (d, $^3J_{P-C}$ = 13.1 Hz)
	PPh-C_{para}	131.9 (s)
	CO_{cis}	192.1 (s)
	CO_{trans}	199.5 (s)
υ (CO) (cm^{-1})[a]		1560 (m), 1870 (st, $A_1^{(2)}$), 1917 (st, 'E'), 1940 (v st, 'E'), 1972 (m, B_1), 2065 (w, $A_1^{(1)}$)

[a] KBr pellet of crystals of **18'**

Table 4.6

Complex	$Ph_3PAu-\overset{O}{\underset{Ph}{\overset{\|}{C_1}}}$	
	19	
Solvent	CD_2Cl_2	
Temperature (K)	298	
^{1}H NMR	Ph	7.2-7.6 (m, 18H)
(300 MHz)	Ph(benzoyl)-C_{ortho}	7.91 (d, $^3J_{H-H} = 7.2$ Hz, 2H)
$^{31}P\{H^1\}$ NMR	P	37.9
(121.4 MHz)		
$^{13}C\{H^1\}$ NMR	C^1	198.1 (d, $^2J_{P-C} = 6.0$ Hz)
(75 MHz)	Ph	128.8 (s), 130.1 (s), 132.2 (s), 140.1 (s)
	PPh-C_{ipso}	131.2 (d, $^1J_{P-C} = 53.0$ Hz)
	PPh-C_{ortho}	129.6 (d, $^2J_{P-C} = 11.1$ Hz)
	PPh-C_{meta}	134.6 (d, $^3J_{P-C} = 13.1$ Hz)
	PPh-C_{para}	131.9 (s)
υ (CO) $(cm^{-1})^a$	1606 (m)	

[a] KBr pellet

2.   *Infrared spectroscopy*

The infrared (IR) spectra of mixtures **15-17** were recorded as CH_2Cl_2 solutions of the complexes in a NaCl cell and are summarised in Tables 4.2 – 4.4. The IR spectra of **18'** and **19** were recorded as KBr pellets prepared from crystals of these complexes and are listed in Tables 4.5 and 4.6 respectively.

The IR spectra of **15-17** are dominated by one extremely broad and strong absorption band in the carbonyl region, appearing between 1935 and 1940 cm^{-1}. A very weak $A_1^{(1)}$ absorption mode at 2063 cm^{-1} could be observed in the IR spectrum of **16**. No clear absorption modes for the acyl C=O bonds, expected to appear between 1500 and 1700 cm^{-1}, were observed in the IR spectra of these compounds as this region of the spectrum contains many obstructing C=C$_{conj}$ stretching frequencies from the PPh$_3$ groups. It is clear from the shape and size of the vibrational modes that the IR spectra of **15-17** are poorly resolved. Reasons for this probably lie with the instability of these compounds in CH$_2$Cl$_2$ and the presence of solvent (thf) impurities in the IR samples.

In contrast to the IR spectra of **15-17**, the IR spectra of **18'** and **19** could be determined very accurately. This is ascribed to the fact that **18'** and **19** were isolated as crystalline compounds, which enabled the measurement of their IR spectra as KBr pellets.

The IR spectrum of **18'** exhibits six clearly separated absorption bands in the carbonyl region. These were assigned as indicated in Table 4.5. These values are in good agreement with reported CO vibrational modes for the BrW(CO)$_5^-$-anion in [BrW(CO)$_5$][R$_4$N] [2064 cm^{-1} (w, $A_1^{(1)}$), 1904 (st, E), 1868 ($A_1^{(2)}$)],[23] although the 'E' vibrational modes in **18'** differ somewhat. Consideration of the crystal structure of **18'**, reported below, provides possible reasons for this difference. The crystal structure of **18'** shows how the BrW(CO)$_5$-anion is coordinated through the CO ligand *trans* to the Br atom position to a Li-cation. Although the Li-coordination to O(5) (Figure 4.2) seems to have little effect on the $A_1^{(2)}$ vibrational mode, it may be responsible for substantial distortion of the W(CO)$_4$ coordination plane because it brings the anion into closer proximity to the rest of the molecule (particularly the phenyl ring of one of the benzoyl-AuPPh$_3$ fragments in the structure) in the solid state. This is also apparent in the observation of a relatively strong B$_1$ absorption mode, which is only IR active upon distortion of the C$_{4v}$ local symmetry in the BrW(CO)$_5$ moiety. Instead of the single two-fold degenerate E-vibrational mode observed for the BrW(CO)$_5^-$-anion in the [BrW(CO)$_5$][R$_4$N] complex, two non-degenerate, clearly separated vibrational modes are observed. Disorder found in the atomic positions of two CO ligands as well as the relatively long O(5)-Li separation in the crystal structure of **18'** (possibly due to steric considerations), reported below, support this interpretation of the IR data. The acyl C=O stretching frequency at 1560

cm^{-1} suggests a stronger acyl bond in **18'** than in the literature reported Re-coordinated benzoyl-AuPPh$_3$ complex [υ(C=O) 1508 cm^{-1}].

The IR spectrum of **19** exhibits a single, medium intensity, CO stretching frequency (1606 cm^{-1}) situated next to two weaker C=C$_{conj}$ IR absorption modes (1588 cm^{-1} and 1573 cm^{-1}). This result suggests, as would be expected for an uncoordinated benzoyl-AuPPh$_3$ moiety, substantially greater double bond character for the acyl C=O bond in **19** than in **18'** and the Re-coordinated benzoyl-AuPPh$_3$ complex reported in the literature.[13] The crystal structure of **19**, reported below, confirms this suggestion as it reports the shortest C=O separation of the three compounds. The isolobal hydrogen analogue of complex **19**, benzaldehyde, exhibits a C=O stretching frequency at 1702 cm^{-1}, which suggests that there is either some measure of π-electron back-donation from the gold atom to the π^*-orbital of the acyl carbon atom, or electron loss from the acyl carbon to the gold atom that weakens the C=O acyl bond in **19**.

3.   *Mass spectrometry*

The positive-ion FAB-MS of complexes **15-17**, **18'** and **19** were recorded in a *m*-nitrobenzylalcohol matrix. Similarly to the FAB mass spectra of the other organometallic products containing the AuPPh$_3$ moiety in this study, the mass spectra of these compounds are dominated by high intensity peaks for Ph$_3$PAu$^+$ (*m/z* 459) and (Ph$_3$P)$_2$Au$^+$ (*m/z* 721) fragments. Molecular ion peaks were only present for **16** and **19** [*m/z* 753(62) and *m/z* 564(10)] (intensity in parenthesis given in percentage relative to the peaks of highest intensity). Weak intensity peaks representing Cr(CO)$_5$(thf) [*m/z* 263(5)] and the acetyl-AuPPh$_3$ fragments [*m/z* 502(4)] could be detected in the mass spectrum of **15**. Peaks representing the benzoyl-AuPPh$_3$ fragments [*m/z* 564(25)], a W-Br fragment [*m/z* 263(15)], and a W(CO)-Br fragment [*m/z* 290(10)] are observed in the FAB mass spectrum of **18'**. Apart from the above-mentioned fragments, no sensible information regarding the structure of complexes **15-17**, **18'** and **19** could be gained from their mass spectra. Conventional electron ionisation mass spectrometry (EI-MS), produced mass spectra for **15-17**, **18'** and **19** that contain a single, high intensity, peak for the Ph$_3$PAu$^+$ fragment (*m/z* 459) and a large number of unassignable weak intensity peaks for a myriad of other fragmentation and decomposition products.

C.   X-ray structure determination of **18'**, **19** and **20**.

The low temperature crystal and molecular structures of **18'** (173 K), **19** (173 K) and **20** (188 K) (Figures 4.2, 4.5 and 4.9) were determined by X-ray diffraction techniques. Selected bond lengths and angles for **18'**, **19** and **20** are listed in Tables 4.7 – 4.8, according to the numbering schemes exhibited in the figures.

The molecular structure of the LiBr adduct of **18**, **18'** (Figure 4.2), revealed a novel electrostatically associated ionic structure for this compound. The structure consists of a Li-cation that is roughly tetrahedrally coordinated to an Et_2O molecule, a $BrW(CO)_5$-anion and two benzoyl-$AuPPh_3$ complexes. Coordination of the Li-cation to the $BrW(CO)_5$ anion is through the oxygen atom of the CO ligand *trans* to the Br atom, while coordination to the two benzoyl-$AuPPh_3$ complexes is through the oxygen atoms of the acyl moieties. The benzoyl-$AuPPh_3$ complexes are, furthermore, linked to each other by weak aurophilic Au-Au interactions [Au(1)-Au(2) = 3.1214(5)Å] with a torsion angle [C(6)-Au(1)-Au(2)-C(7)] of 103.0(4)° between the two pseudo linear Au(I) coordination modes. The tetrahedral coordination of the Li-cation is somewhat distorted from the ideal with the largest angle between two of the coordinating oxygen atoms being 124.2(10)° [O(6)-Li-O(7)] between the oxygen atoms of the two coordinating benzoyl-$AuPPh_3$ complexes. As the benzoyl-$AuPPh_3$ complexes are linked by aurophilic interaction this distortion is probably due to some ring strain of the resulting 7-membered Li-O(6)-C(6)-Au(1)-Au(2)-C(7)-O(7) ring, causing the coordinating metallo-acyl groups to have a wider bite angle on the Li-cation (Figure 4.2). Bond lengths and angles in the $BrW(CO)_5$-anion are normal. This fragment, however, exhibits disorder (not shown in Figure 4.2) in the positions of two of its CO ligands [C(3)-O(3) and C(4)-O(4)]. Two averaged positions, sharing the site occupancy of a single CO ligand in the ratios of 0.53:0.47 and 0.57:0.43, could be identified from the difference Fourier map for the CO ligands represented by C(3)-O(3) and C(4)-O(4) respectively. Coordination of the Et_2O molecule through its oxygen atom to the Li-cation is normal. A small degree of dynamic disorder (not shown in Figure 4.1) in the ethyl groups of the Et_2O molecule, as indicated by enlarged anisotropic displacement parameters for the atoms involved, is also observed.
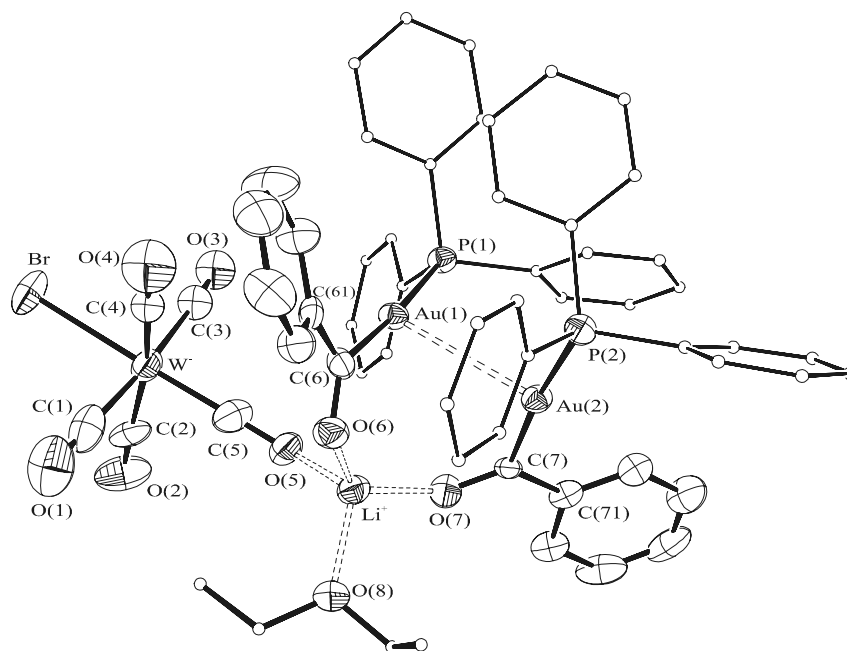
Figure 4.2: ORTEP view of **18'**, showing numbering scheme (disordered CO and Et₂O atom positions and hydrogen atoms omitted for clarity)

Table 4.7: Selected bond lengths (Å) and angles (°) with e.s.d.s in parenthesis for **18'**

Bond lengths		Bond angles	
Au(1)-Au(2)	3.1214(5)	C(6)-Au(1)-P(1)	175.6(3)
Au(1)-C(6)	2.048(10)	C(7)-Au(2)-P(2)	172.5(3)
C(6)-O(6)	1.237(11)	Au(1)-C(6)-O(6)	122.2(8)
Au(2)-C(7)	2.078(9)	Au(2)-C(7)-O(7)	121.1(7)
C(7)-O(7)	1.235(11)	C(6)-O(6)-Li	118.3(8)
O(6)-Li	1.911(19)	C(7)-O(7)-Li	138.4(8)
O(7)-Li	1.892(18)	O(6)-C(6)-C(61)	117.7(9)
O(8)-Li	1.972(17)	O(7)-C(7)-C(71)	120.0(8)
O(5)-Li	2.020(18)	O(6)-Li-O(7)	124.2(10)
O(5)-C(5)	1.186(12)	O(7)-Li-O(8)	103.1(8)
C(5)-W	1.906(12)	O(8)-Li-O(5)	109.8(9)
W-Br	2.6913(12)	O(5)-Li-O(6)	103.9(8)
Au(1)-P(1)	2.312(3)	C(5)-O(5)-Li	144.3(10)
Au(2)-P(2)	2.317(3)	W-C(5)-O(5)	178.2(10)
C(6)-C(61)	1.511(14)	Br-W-C(5)	178.6(4)
C(7)-C(71)	1.473(13)	C(6)-Au(1)-Au(2)-C(7)	103.0(4)

130

The Au-C bond lengths in the two crystallographically independent Li-coordinated benzoyl-AuPPh$_3$ complexes in **18'** are in good agreement with each other [C(6)-Au(1) = 2.048(10)Å , C(7)-Au(2) = 2.078(9)Å]. These bonds also correspond very well to typical gold(I)-carbon bond lengths, as well as to the Au-C bond length reported in the sole literature example of an acylgold(I) species [2.047(11)Å].[13] The C(6)-O(6) and C(7)-O(7) bond lengths of 1.237(11)Å and 1.235(11)Å confirm the remaining double bond character of these bonds after O-Li coordination and also compare very well to this bond distance in the known acylgold(I) complex, in which the acyl group is coordinated to a rhenium atom [1.229(11)Å].[13] Au(1)-C(6)-O(6), Au(1)-C(6)-C(61), Au(2)-C(7)-O(7) and Au(2)-C(7)-C(71) bond angles [122.2(8)°, 121.1(7)°, 117.7(9)° and 120.0(8)°] are normal for sp^2 hybridised acyl carbon atoms. C(6)-Au(1)-P(1) and C(7)-Au(2)-P(2) angles of 175.6(3)° and 172.5(3)° describe how the linear coordination mode of Au(I) is distorted towards the neighbouring gold atom due to the aforementioned aurophilic interactions in the structure. An intramolecular non-bonded face-edge phenyl-interaction, involving a phenyl ring from each PPh$_3$ group in the benzoyl-AuPPh$_3$ moieties [C(13x) and C(22x) rings] further stabilise the Au-Au linked configuration found here (Figure 4.3).
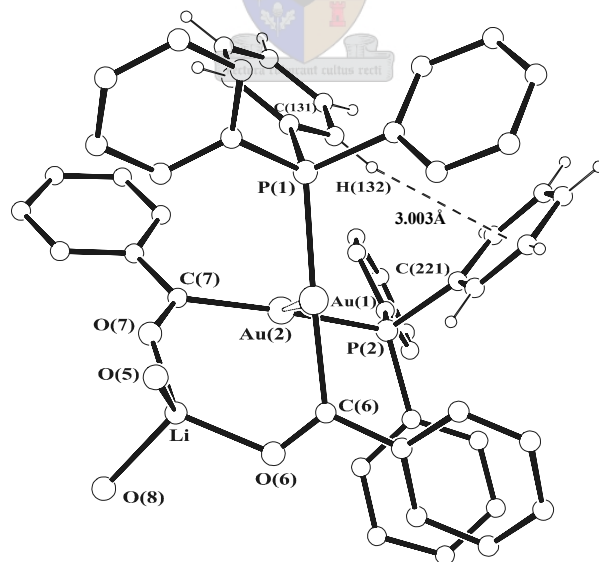

Figure 4.3: ORTEP view of **18'**, showing Li-O(6)-C(6)-Au(1)-Au(2)-C(7)-O(7) ring and face-edge phenyl-interaction [BrW(CO)$_5$, Et$_2$O fragments and hydrogen atoms not involved in the interaction are omitted for clarity]

In the unit cell, molecules of **18'** pack in the centrosymmetric spacegroup P2$_1$/n with four molecules in each unit cell. Viewed along the b-axis of the unit cell (Figure 4.4), molecules of **18'** pack in regular rows in a structure that leaves two open channels parallel to the b-axis per unit cell. Of particular interest concerning these channels is that the Li-coordinated Et$_2$O solvent molecules and the disordered CO ligands, mentioned previously, border directly on them. Rapid crystal degradation, apparently due to solvent loss, was observed upon isolation of the crystalline mass of **18'**, and is ascribed to the loss of Et$_2$O from the crystal lattice along these channels. Crystal isolation, storage and mounting procedures for **18'** had to be executed rapidly and, where possible, in an atmosphere saturated with Et$_2$O in order to prevent such crystal degradation. Furthermore, the disorder observed in the CO ligands and coordinated Et$_2$O molecules that border the channels is ascribed to freedom of movement of these groups within the crystal lattice as a result of the presence of the channels. No significant intermolecular interactions are observed in the unit cell of **18'**.
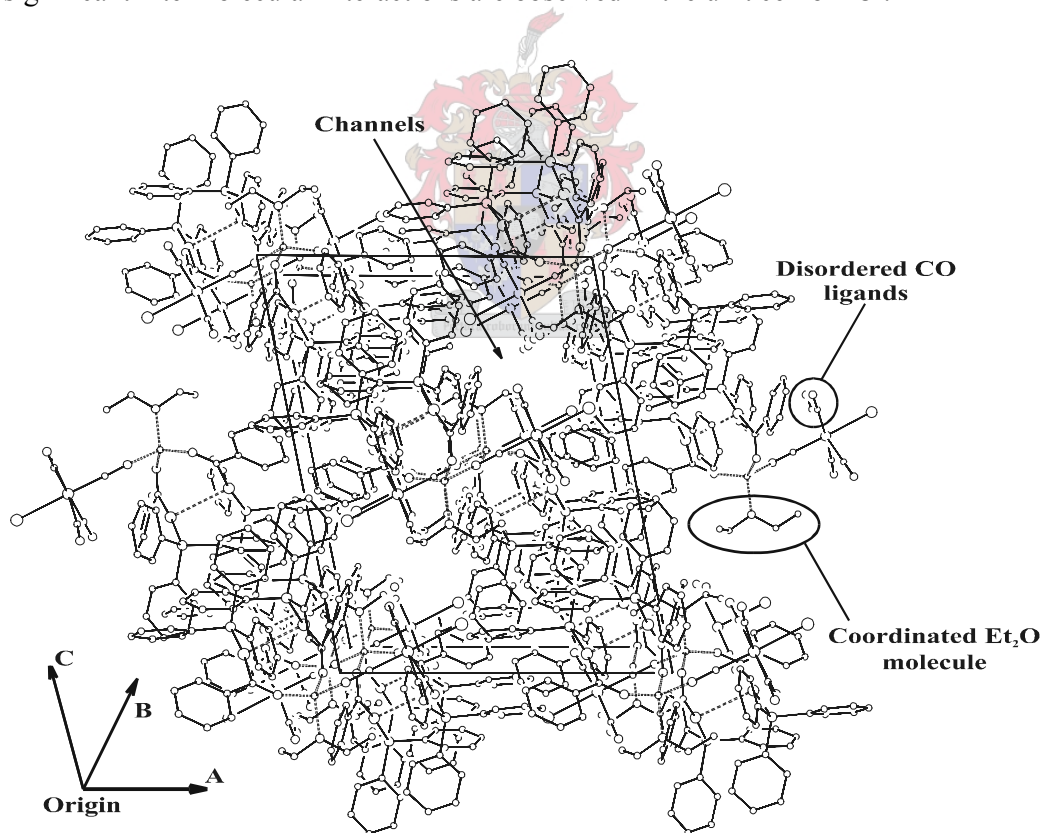

Figure 4.4: Packing diagram of **18'**, viewed along the b-axis of the unit cell showing the channels and the positions of the Et$_2$O molecules and disordered CO ligands within the unit cell.

The crystal and molecular structure of the free benzoyl-AuPPh$_3$ complex, **19**, (Figure 4.5) represents the first example of a crystal structure of this species. This uncomplicated structure clearly shows a Ph$_3$PAu fragment bonded to the sp^2 hybridised acyl carbon atom [C(1a)] of a benzoyl moiety and serves as crystallographic proof for the existence of this uncoordinated compound.

The Au(1a)-C(1a) bond [2.085(5)Å] in **19** is within the expected range for Au(I)-C(sp^2) single bonds.[31] The Au(1a)-P(1a) bond [2.313(1)Å] is also normal.[13,32] O(1a) is unmistakably double bonded to the acyl carbon atom [C(1a)-O(1a) = 1.200(7)Å]. This bond is also, as would be expected, slightly shorter than the corresponding Li-coordinated and Re-coordinated C=O bonds in the structures of **18'** and the only other structurally characterized acylgold(I) referred to above.[13] The sp^2 hybridisation of C(1a) is confirmed by its nearly perfectly flat bonding geometry [the greatest deviation from the least-squares plane defined by Au(1a), C(1a), O(1a), C(11a) is 0.012(4)Å for C(1a)]. Despite the fact that no intermolecular metal-metal interactions are observed in the crystal structure of **19**, the P(1a)-Au(1a)-C(1a) angle deviates significantly from 180° [P(1a)-Au(1a)-C(1a) = 176.4(1)°]. This is most likely due to packing effects, described below.
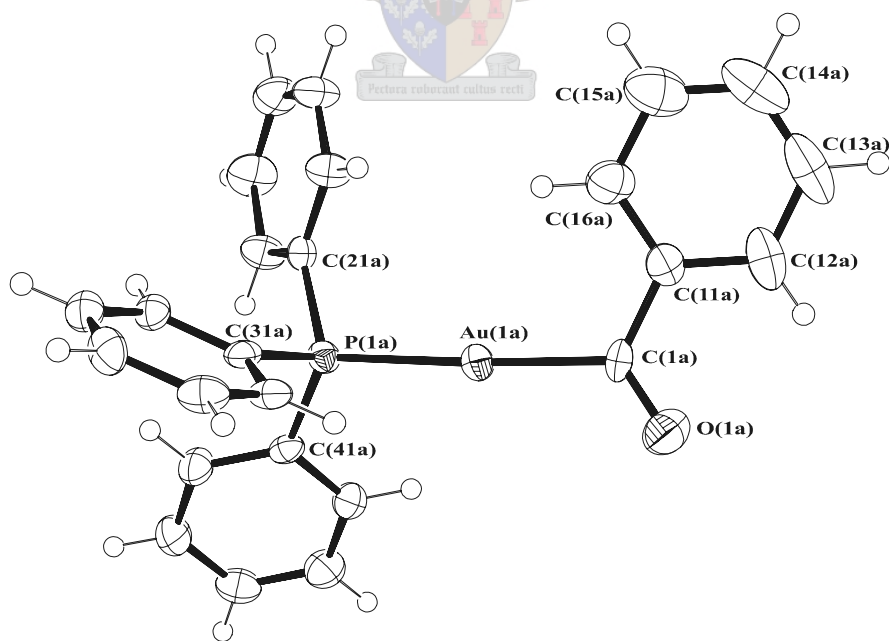

Figure 4.5: ORTEP view of **19** (a-orientation with 85.76% site occupancy), showing the numbering scheme

Table 4.8 Selected bond lengths (Å) and angles (°) with e.s.d.s in parenthesis for complex **19** (a-orientation only)

Bond lengths		Bond angles	
Au(1a)-C(1a)	2.085(5)	C(1a)-Au(1a)-P(1a)	176.4(1)
C(1a)-O(1a)	1.200(7)	Au(1a)-C(1a)-O(1a)	123.4(4)
C(1a)-C(11a)	1.501(8)	Au(1a)-C(1a)-C(11a)	117.8(5)
Au(1a)-P(1a)	2.313(1)	C(11a)-C(1a)-O(1a)	118.8(6)
P(1a)-C(21a)	1.807(7)	Au(1a)-P(1a)-C(21a)	111.1(3)
P(1a)-C(31a)	1.819(6)	Au(1a)-P(1a)-C(31a)	109.5(2)
P(1a)-C(41a)	1.819(5)	Au(1a)-P(1a)-C(41a)	116.7(2)

In the unit cell molecules of **19** pack in the centrosymmetric spacegroup $P2_1/n$ with four molecules in each unit cell. Viewed along the b-axis, the molecules of **19** pack in regular rows with the C(1a)-Au(1a)-P(1a) bond orientated roughly parallel to the b-axis (Figure 4.6). Molecules of **19** in the unit cell are, furthermore, weakly interconnected, as illustrated in Figure 4.6, by a series of face-edge phenyl-interactions involving two of the PPh_3 phenyl rings and phenyl ring of the benzoyl group of each molecule. In addition to these interactions, the acyl oxygen atom O(1a) is situated closely to the one phenyl ring of the PPh_3 group that is not involved in face-edge phenyl-interactions (Figure 4.7). These interactions most likely account for the deviation from linearity observed in the P(1)-Au(1)-C(1a) bond geometry.
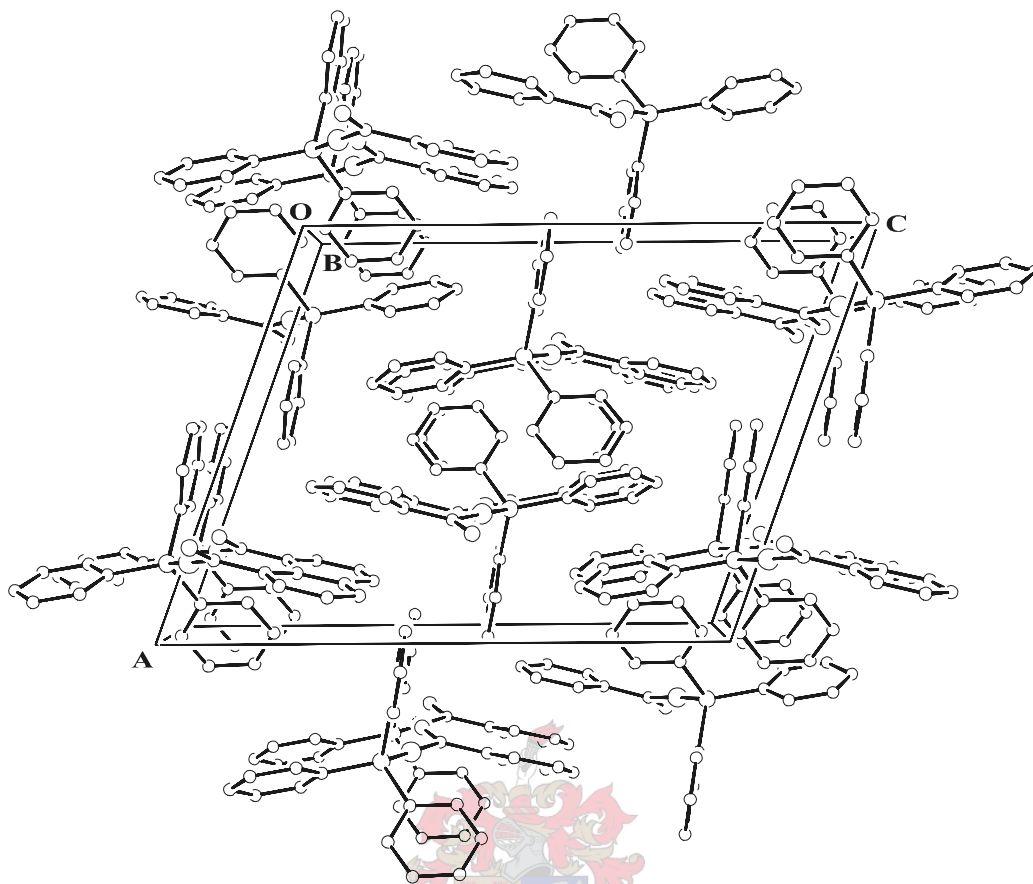
Figure 4.6: Packing diagram of **19**, viewed along the b-axis of the unit cell
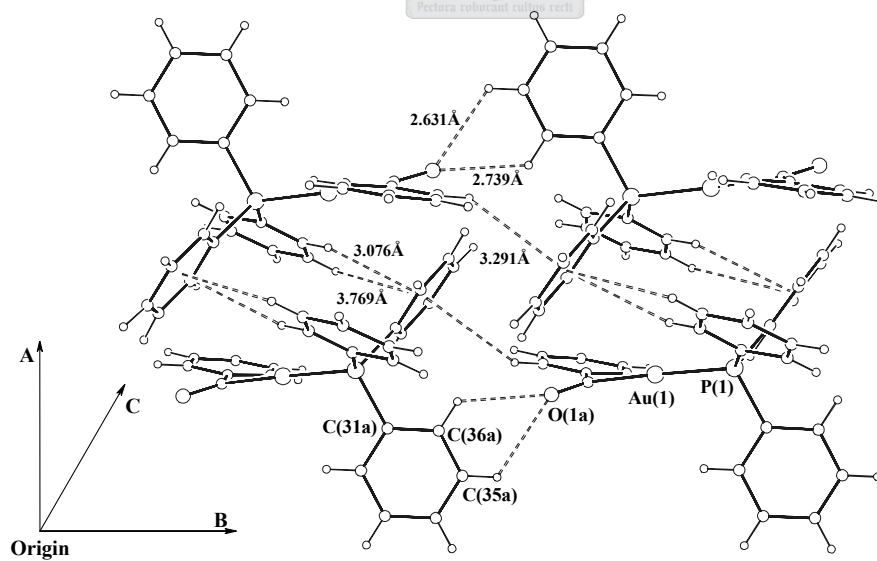

Figure 4.7: Packing diagram of **19**, showing face-edge phenyl-interactions and acyl-oxygen phenyl ring interactions between molecules

135

Finally, disorder, with respect to the direction of orientation of the benzoyl-AuPPh$_3$ molecules along the b-axis of the crystal lattice is found in the crystal structure of **19** (Figure 4.8). The final crystallographically refined ratio for the different orientations of **19**, according to the site occupancies of the (a) and (b) molecules in the crystal is, 0.8576 **:** 0.1424 (a-orientation **:** b-orientation). As a result of the low site occupancy of the b-orientation, the atom positions on the difference Fourier map corresponding to this orientation, especially the carbon atom positions, are poorly determined and could not be allowed anisotropic thermal motion during the refinement.
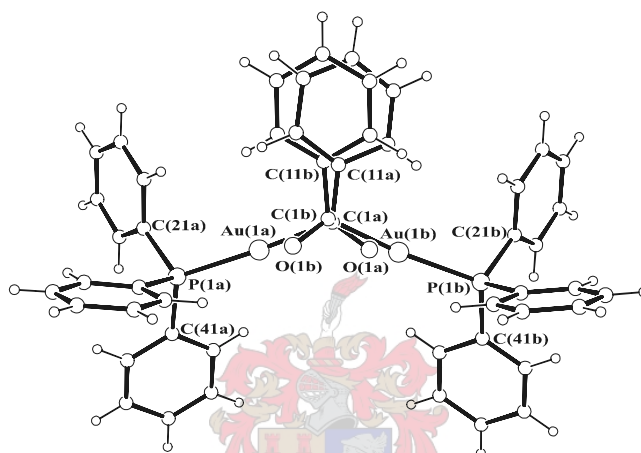

Figure 4.8: ORTEP view of **19**, showing disorder encountered in the crystal
(a-orientation **:** b-orientation = 0.8576 **:** 0.1424)

The crystal and molecular structure of [ClW(CO)$_5$][^{n}Bu$_4$N] (**20**), which precipitated from the reaction mixture of **19**, is shown in Figure 4.9. Although **20** is a well-known and stable organometallic compound and has often been applied as starting material in reaction sequences,[23] its crystal structure has not yet been reported. Bond lengths and angles within the W(CO)$_5$Cl-anionic and the ^{n}Bu$_4$N-cationic components of **20** are normal for such moieties.[33] A W-C(5) separation of 1.938(4)Å, which is ~0.1Å shorter than the other W-C separations in the structure, shows the influence of the weaker (compared to CO ligands) *trans* directing chlorine ligand. Of further interest in this structure are the carbon atoms in the n-butyl chains of the ^{n}Bu$_4$N-cation. Although these display progressively larger thermal displacement parameters the closer they are situated to the ends of the chains, they are particularly well determined. The carbon atoms in crystallographic studies of compounds containing such groups often exhibit disorder. The high degree of order observed here can be attributed to efficient packing of this complex in the unit cell, as described below.
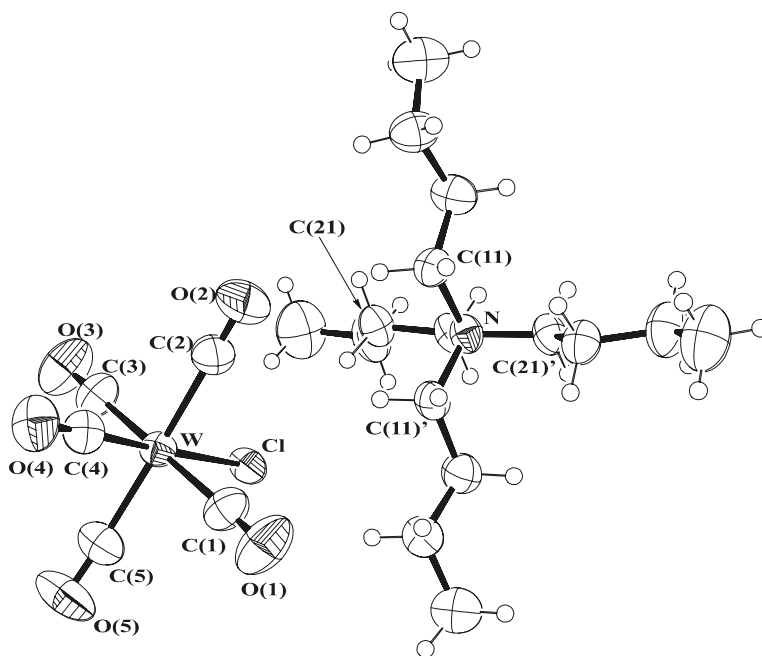
Figure 4.9: ORTEP view of **20**, showing numbering scheme

Table 4.9: Selected bond lengths (Å) and angles (°) with e.s.d.s in parenthesis for complex **20**

Bond lengths		Bond angles	
W-C(1)	2.023(4)	C(1)-W-C(3)	175.8(1)
W-C(2)	2.040(4)	C(2)-W-C(5)	172.2(1)
W-C(3)	2.049(4)	C(4)-W-Cl	177.4(1)
W-C(4)	1.938(4)	O(1)-C(1)-W	178.1(4)
W-C(5)	2.019(4)	O(2)-C(2)-W	176.2(4)
C(1)-O(1)	1.142(5)	O(3)-C(3)-W	178.8(3)
C(2)-O(2)	1.139(4)	O(4)-C(4)-W	177.9(3)
C(3)-O(3)	1.138(5)	O(5)-C(5)-W	172.9(3)
C(4)-O(4)	1.173(4)	C(11)-N-C(11)'	106.2(3)
C(5)-O(5)	1.146(4)	C(11)-N-C(21)	111.2(2)
W-Cl	2.5602(8)	C(21)-N-C(21)'	106.1(3)
N-C(11)	1.518(3)	C(31)-N-C(31)'[*]	111.3(3)
N-C(21)	1.523(4)	C(31)-N-C(41)[*]	105.9(2)
N-C(31)[*]	1.517(3)	C(41)-N-C41)'[*]	111.0(3)
N-C(41)[*]	1.518(3)		

[*]Symmetry equivalents not shown in Figure 4.9

137
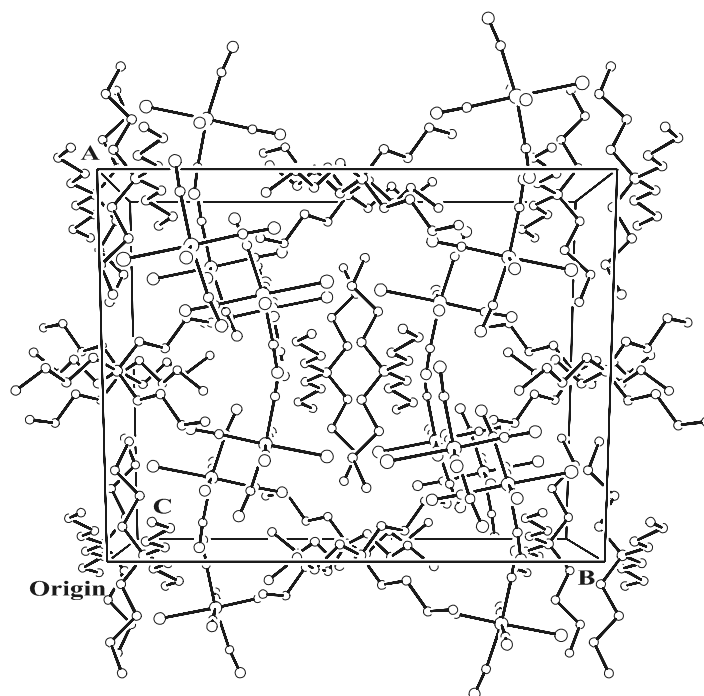
Figure 4.10: Packing diagram of **20**, viewed along the c-axis of the unit cell

A view along the c-axis of the unit cell shows how eight molecules of **20** pack in the monoclinic centrosymmetric space group C2/c (Figure 4.10). The nitrogen atoms in the $^nBu_4N$-cations are situated on special positions (a two-fold rotation axis) in this space group, showing that this moiety is remarkably symmetric. Layers of cations and anions, roughly parallel to the a-axis, form a very efficient packing arrangement in the crystal and no solvent-accessible or other significant voids or channels are present. The result is that the flexible aliphatic chains in the $^nBu_4N$-cations are not allowed any freedom of movement and thus pack with a high degree of order. This efficient packing arrangement is also likely to aid the crystallisation of **20** from the reaction mixture of **19**.

4.2.2 Imidoyl complexes of gold(I): {organoimidoyl-AuPPh₃}M(CO)₅ bimetallic complexes
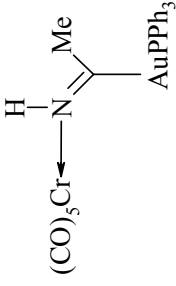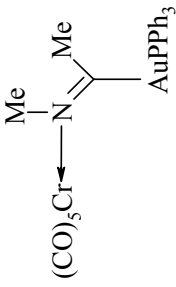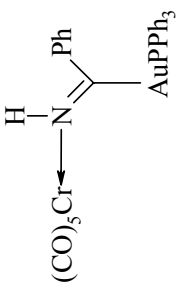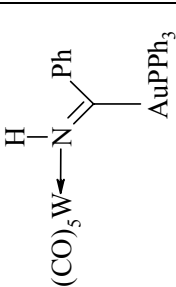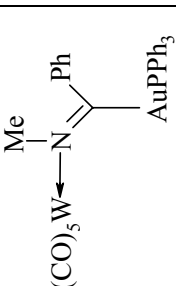
A. General preparation and discussion of (Z)-{Ph₃PAuC(N**R**)**R'**}-*N* **M**(CO)₅
M = Cr, **R** = H, **R'** = Me (**21**); **M** = Cr, **R** = Me, **R'** = Me (**22**); **M** = Cr, **R** = H, **R'** = Ph (**23**); **M** = W, **R** = H, **R'** = Ph (**24**); **M** = W, **R** = Me, **R'** = Ph (**25**).

The syntheses of complexes **21**-**25** (Scheme 4.14) were carried out by irreversible N-deprotonation of the respective group 6 metal aminocarbene complexes with 1 mole equiv. *n*-butyllithium at –78°C, followed by the addition of 1 mole equiv. Ph₃PAuCl to the reaction mixture. After addition of the Ph₃PAuCl, the reaction mixture was allowed to slowly warm up to room temperature over a period of 3 hours. Removal of the solvent *in vacuo* yielded dark yellow oily residues containing **21**-**25** (32-85% yields after separation). Separation of the complexes was carried out by low temperature (-15°C) silica gel column chromatography with hexane/diethyl ether (2:1) as eluant, followed by crystallisation from a diethyl ether solution layered with pentane at –20°C. Physical data for the isolated new compounds are summarised in Table 4.10.

21: M = Cr, R = H, R' = Me
22: M = Cr, R = Me, R = Me
23: M = Cr, R = H, R = Ph
24: M = W, R = H, R' = Ph
25: M = W, R = Me, R' = Ph
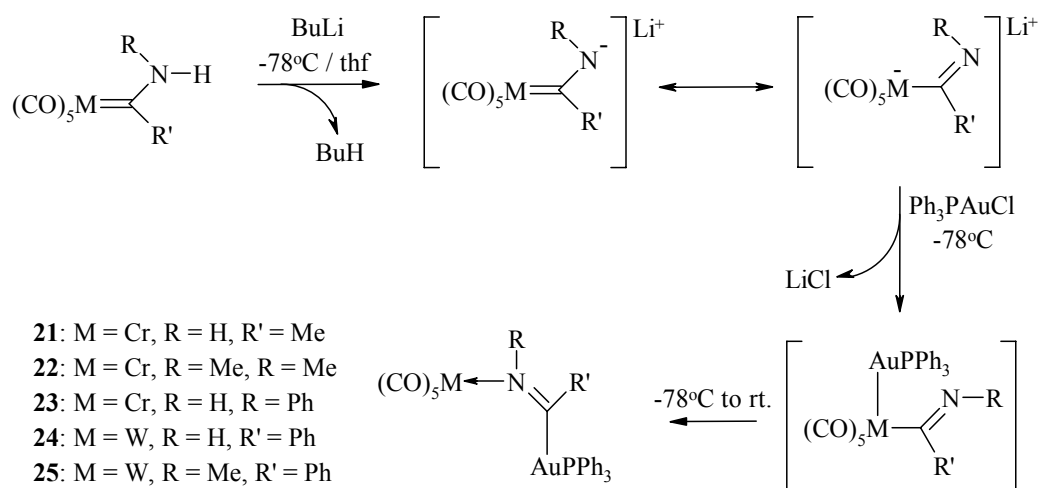
Scheme 4.14

Table 4.10

Complex	**21**	**22**	**23**	**24**	**25**
Complex	$(CO)_5Cr{\leftarrow}N(H){=}C(Me)AuPPh_3$	$(CO)_5Cr{\leftarrow}N(Me){=}C(Me)AuPPh_3$	$(CO)_5Cr{\leftarrow}N(H){=}C(Ph)AuPPh_3$	$(CO)_5W{\leftarrow}N(H){=}C(Ph)AuPPh_3$	$(CO)_5W{\leftarrow}N(Me){=}C(Ph)AuPPh_3$
M.p. / °C	112 (decomp.)	109 (decomp.)	135 (decomp.)	140 (decomp.)	121 (decomp.)
Color	yellow	yellow	dark yellow	yellow	yellow
Yield (%)	32	41	56	85	57
M.W. (g / mol)	693.36	707.39	755.43	887.29	901.31
Analyses (%)[a]					
C	43.12 (43.31)	44.01 (44.15)	47.65 (47.70)	40.54 (40.61)	41.41 (41.31)
H	2.61 (2.76)	3.05 (2.99)	2.76 (2.80)	2.46 (2.39)	2.59 (2.57)
O	11.78 (11.54)	11.39 (11.31)	10.67 (10.59)	9.08 (9.02)	8.88 (8.88)
N	2.15 (2.02)	1.96 (1.98)	2.01 (1.85)	1.65 (1.58)	1.60 (1.55)

[a] Required values given in parenthesis

The novel formation of the {acetimidoyl-AuPPh$_3$}M(CO)$_5$ and {benzimidoyl-AuPPh$_3$}M(CO)$_5$ complexes (Scheme 4.14), **21**-**25**, by the auration of N-deprotonated Fischer-type aminocarbene complexes, is accepted to proceed along a similar reaction path as the formation of complexes **15**-**19** described previously (Section 4.2.1). In fact, the analogous formation of **21**-**25**, instead of the expected N-substituted aminocarbene complexes, adds further weight to our proposed mechanism for this conversion (as described in section 4.2.1.). The concerted mechanism reported by Haupt for this type of conversion,[13] is, according the thermodynamic arguments given by him, even less likely to proceed for the analogous formation of the imidoylgold(I) complexes than for acylgold(I) complexes. Furthermore, it is interesting to note that this conversion is stereospecific and that the Z-isomers of **21**-**25** are exclusively formed. This observation must be linked to the reaction mechanism involved, but unfortunately does not favour either since compelling arguments for the exclusive formation of the Z-isomers of **21**-**25** can be constructed using both proposed mechanisms. Due to the lack of conclusive evidence our proposed reaction mechanism thus remains unproven and Haupt's suggested mechanism for this type of conversion cannot be ruled out.

An important distinction between the assumed {acyl-AuPPh$_3$}M(CO)$_5$ complexes, **15**-**18**, and their nitrogen analogues, **21**-**25**, is that coordination of the acetimidoyl-AuPPh$_3$ and benzimidoyl-AuPPh$_3$ moieties to the M(CO)$_5$ fragments through the nitrogen atoms in **21**-**25** is much stronger than the proposed {acyl-AuPPh$_3$}M(CO)$_5$ oxygen coordination. This is reflected by the fact that **21**-**25** are, unlike **15**-**18**, stable in all common laboratory solvents (under inert conditions), are not involved in any ligand substitution reactions with solvent molecules or halide salts, and can even be successfully isolated by column chromatography (SiO$_2$). A single crystal X-ray structure of **23** confirms the unique molecular structure of these compounds.

Furthermore, the formation of the bimetallic {acetylimidoyl-AuPPh$_3$}M(CO)$_5$ and {benzimidoyl-AuPPh$_3$}M(CO)$_5$ complexes (**21**-**25**) along the reaction path outlined in Scheme 4.14, is, to our knowledge, the first example in which electrophilic additions to N-deprotonated Fischer-type aminocarbene complexes have resulted in the formation of {organoimidoyl-metal}M(CO)$_5$ complexes. There are many examples in the literature of electrophilic addition reactions to N-deprotonated Fischer-type

aminocarbene complexes, which all yield useful N-substituted aminocarbene complexes.[34] The exact reasons for the formation of the {organoimidoyl-metal}M(CO)$_5$ complexes, when the Ph$_3$PAu$^+$ electrophile is employed in this conversion, are unknown.

Factors that could play important roles in directing this conversion are: The delocalisation of the negative charge onto the M(CO)$_5$ fragment upon N-deprotonation; the 'soft' nature of the Ph$_3$PAu$^+$ electrophile, which would, unlike conventional carbon electrophiles, rather interact with the anionic M(CO)$_5$ fragments than the imine nitrogen atoms in the N-deprotonated aminocarbene complexes; and the linear geometry of gold(I) bonds, which allow the Ph$_3$PAu$^+$ electrophile, although it is sterically large, to interact with the M(CO)$_5$-anions.

The closest example of a similar conversion in the literature is the thermolysis reaction of Fischer-type aminocarbene complexes in the presence of CO, which also yields imines.[35] Perhaps the term, aurolysis, used to described the reaction of the Ph$_3$PAu$^+$ electrophile with C-deprotonated methyl alkoxy/dialkylamino/alkylthio-carbene complexes in chapters 2 & 3, can therefore also be applied to describe the current reaction.

Spectroscopic data measured for **21-25**, and the crystal structure of **23**, suggest that these compounds have a highly polarised imine-M(CO)$_5$ coordination mode. Evidence presented below proposes that **21-25** are best represented by resonance structure **S** (Scheme 4.15), with a partial positive charge on the imine nitrogen atom and the corresponding negative charge located on the metal carbonyl moiety.
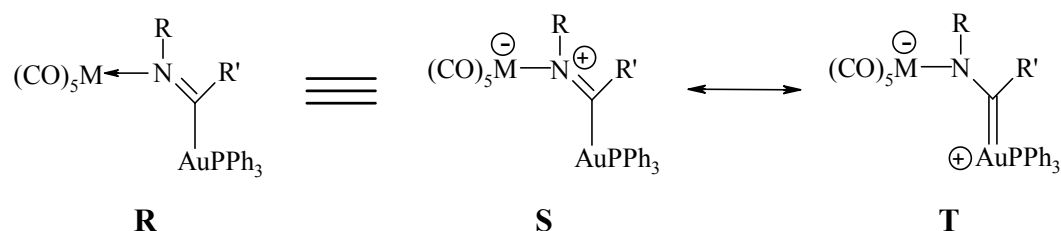
Scheme 4.15

B.   Preparation of *cis*-{η²-(Ph₃PAu)₂}PPh₃Cr(CO)₄ (**26**)

In a second consecutive N-deprotonation-auration reaction sequence (Scheme 4.16) involving complexes **21** and **23** the only chromatographically isolable product of the reaction, albeit in a low yield (10% based on Cr), is a novel triangular Au_2Cr cluster compound (**26**).

21: M = Cr, R = Me
23: M = Cr, R = Ph

26
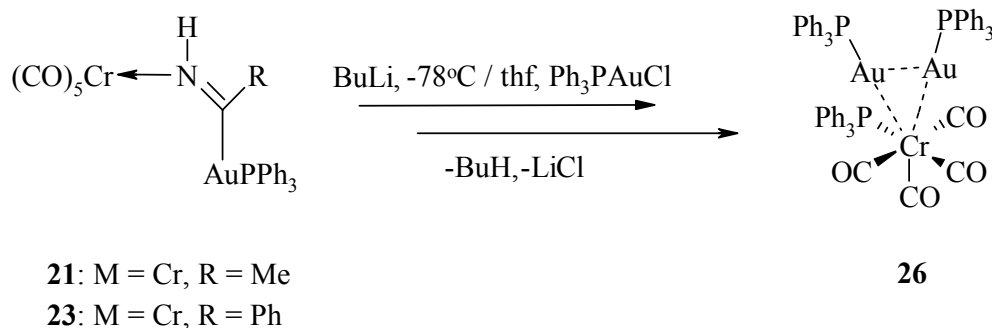
Scheme 4.16

The mechanism by which **26** is formed is unknown. Reactions for the preparation of η²-digold complexes of transition metals, typically group 8 metals, are well studied.[36] These preparations are generally carried out by reacting hydrides or anions of the metal carbonyls with Ph₃PAuCl. In this manner many examples of mixed metal di-, tri- and multinuclear gold cluster compounds have been prepared and structurally characterised.[36] Several examples, too many to mention, of cluster compounds containing other stable ratios of Ph₃PAu **:** metal-carbonyl combinations have also been prepared.[37] During the above reaction sequence it is not unthinkable that an anionic Cr-carbonyl fragment could have formed to enable the formation of **26**.

Stone *et al* demonstrated as early as 1982 how transition metal hydrides can be employed in the synthesis of bimetallic chromium-gold compounds when they prepared [(Ph₃PAu)(μ-H)Cr(CO)₅].[38] This complex provided both a rare example of a hydrido-complex of gold and an isolobal model for the unstable molecular hydrogen complex (η²-H₂)Cr(CO)₅. For unknown reasons the analogous η²-digold Cr(CO)₅ complex has never been reported. Complex **26**, inadvertently prepared here, is thus the first example of a η²-digold complex of chromium. For these reasons the physical,

analytical (Table 4.11), spectroscopic and structural data of **26** are included in this work. The closest analogue to **26** is the cationic η^2-digold $(Ph_3PAu)_2MoCp(CO)_2PMe_3$ complex recently reported by Poli *et al.*[39]

Table 4.11: Analytical data for complex **26**

Complex	
Complex	**26**
M.p. / ^{o}C	136 (decomp.)
Color	red
Yield (%)	10%
M.W. (g / mol)	1344.84
Analyses (%)[a]	
C	52.05 (51.80)
H	3.43 (3.37)
O	4.82 (4.76)
P	6.82 (6.91)

[a] Required values given in parenthesis

C. Spectroscopic characterisation of complexes **21-26**

1. NMR Spectroscopy
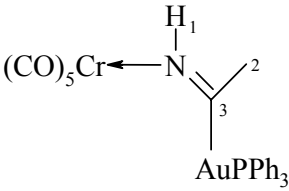
The ^{1}H, ^{13}C{^{1}H} and ^{31}P{^{1}H} NMR spectroscopic data for **21-25** are summarised in Tables 4.12-4.17. The ^{1}H NMR spectra of **21**, **23** and **24** are characterised, in particular, by broad imine proton resonances situated between 8.89 and 10.05 ppm. These chemical shifts suggest a great deal of electron donation from the imine nitrogen atom to the $M(CO)_5$ fragments, polarising the imine coordination mode as suggested by resonance structure **U** (Scheme 4.15). The fact that the imine protons are

more deshielded in the W(CO)$_5$ than in the Cr(CO)$_5$ complex (**21** vs. **23**) can be attributed to the ability of the W(CO)$_5$ fragment, due to its greater polarisability or 'softness', to better accommodate the partial negative charge. This allows even greater polarisation of the metal-nitrogen coordination mode and shifts the imine proton resonance in **23** further downfield. ^{1}H and ^{13}C{^{1}H} resonances for the methyl groups on the imine nitrogen atoms in **22** and **25** are found, also shifted downfield from the positions of these resonances in uncoordinated imines, at δ 3.24 and 32.0 (complex **22**), and δ 3.34 and 32.4 (complex **25**).[40]

A good indicator for the amount of electron donation from the imine groups to the M(CO)$_5$ fragments in **21-25** is the chemical shift of the C=N imine ^{13}C resonances. These appear as doublets ($^2J_{C-P}$ = 122.1 - 131.9 Hz) between δ 232.4 and 239.6 for **21-23** and **25**. Curiously this resonance in **24** appears in a similar region of the ^{13}C NMR spectrum (δ 238.4), but as a greatly broadened singlet. These resonances show that the imine carbon atoms are greatly deshielded and do not exclude the possibility that they could have a partial carbene-type character, as proposed by resonance structure **T** (Scheme 4.15).
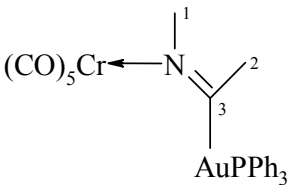
The chemical shifts of the ^{1}H, ^{13}C and ^{31}P resonances of the atoms in the PPh$_3$ residue are normal and compare well to the other compounds containing this moiety coordinated to gold reported in this work. ^{13}C resonances of the Ph groups bonded to the C=N imine carbon atom in **23-25** are characterised by a downfield shifted signal (compared to the starting material) representing the *ipso* carbon atom of this ring (δ 149.1, 149.4 and 148.8). This signal is, furthermore, broadened as a result of weak $^3J_{C-P}$ coupling. The ^{13}C resonances for the methyl carbon atoms in this position in **21** and **22** are found at δ 42.1 and 49.4, as a broadened singlet and a doublet ($^3J_{P-C}$ = 9.3 Hz) respectively.

Table 4.12

Complex		(CO)$_5$Cr←N with H$_1$, =2, 3, AuPPh$_3$
		21
Solvent		CDCl$_3$
Temperature (K)		298
^{1}H NMR	H^1	8.89 (br s, 1H)
(300 MHz)	H^2	2.28 (s, 3H)
	Ph	7.4-7.7 (m, 15H)
^{31}P{H^1}NMR:	P	41.9 (s)
(121.4MHz)		
^{13}C{H^1} NMR	C^2	42.1 (br s)
(75 MHz)	C^3	239.6 (d, $^2J_{P-C}$ = 122.1 Hz)
	Ph-C$_{ipso}$	130.3 (d, $^1J_{P-C}$ = 51.4 Hz)
	Ph-C$_{ortho}$	129.6 (d, $^2J_{P-C}$ = 11.0 Hz)
	Ph-C$_{meta}$	134.6 (d, $^3J_{P-C}$ = 13.2 Hz)
	Ph-C$_{para}$	132.0 (br s)
	CO$_{cis}$	216.6 (s)
	CO$_{trans}$	221.8 (s)
υ (CO) (cm^{-1})^a		1902 (st, A$_1$$^{(2)}$), 1929 (v st, E), 1950 (w, B$_1$), 2060 (w, A$_1$$^{(1)}$)
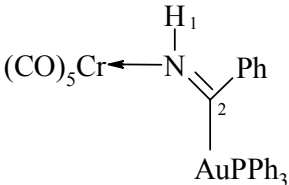
^{a} Pentane solution in NaCl

Table 4.13

Complex	$(CO)_5Cr \leftarrow N$ ... $AuPPh_3$ structure
	22
Solvent	CD_2Cl_2
Temperature (K)	298
^1H NMR H^1	3.24 (s, 3H)
(300 MHz) H^2	2.25 (s, 3H)
Ph	7.4-7.7 (m, 15H)
$^{31}P\{^1H\}$ NMR P	39.8 (s)
(121.4 MHz)	
$^{13}C\{^1H\}$ NMR C^1	32.0 (s)
(75 MHz) C^2	49.4 (d, $^3J_{P-C}$ = 9.3 Hz)
C^3	236.8 (d, $^2J_{P-C}$ = 129.8 Hz)
Ph-C_{ipso}	130.6 (d, $^1J_{P-C}$ = 52.8 Hz)
Ph-C_{ortho}	129.5 (d, $^2J_{P-C}$ = 11.0 Hz)
Ph-C_{meta}	134.6 (d, $^3J_{P-C}$ = 13.4 Hz)
Ph-C_{para}	131.9 (s)
CO_{cis}	216.0 (s)
CO_{trans}	221.8 (s)
υ (CO) (cm^{-1})[a]	1904 (st, $A_1^{(2)}$), 1931 (v st br, E), 1953 (w, B_1), 2058 (w, $A_1^{(1)}$)
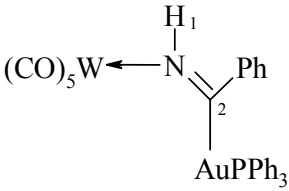
[a] Pentane solution in NaCl

Table 4.14

Complex	
	23
Solvent	CD_2Cl_2
Temperature (K)	298
^{1}H NMR	H^1	9.59 (br s, 1H)
(600 MHz)	Ph	7.3-7.7 (m, 20H)
^{31}P{^{1}H} NMR	P	42.3 (s)
(121.4 MHz)		
^{13}C{^{1}H} NMR	C^2	232.4 (d, $^2J_{P-C}$ = 131.9 Hz)
(150 MHz)	Ph$_{o/m/p}$	126.2 (s), 129.0 (s), 130.9 (s)
	Ph$_{ipso}$	149.1 (br, s)
	PPh-C$_{ipso}$	130.2 (d, $^1J_{P-C}$ = 51.2 Hz)
	PPh-C$_{ortho}$	129.5 (d, $^2J_{P-C}$ = 9.3 Hz)
	PPh-C$_{meta}$	134.5 (d, $^3J_{P-C}$ = 11.2 Hz)
	PPh-C$_{para}$	131.9 (s)
	CO$_{cis}$	216.1 (s)
	CO$_{trans}$	221.6 (s)
υ (CO) (cm^{-1})^a		1904 (st, A$_1^{(2)}$), 1930 (v st, E), 1951 (w sh, B$_1$), 2058 (w, A$_1^{(1)}$)
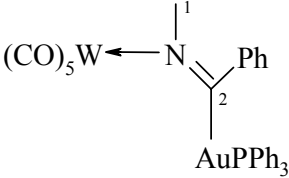
^{a} Pentane solution in NaCl

Table 4.15

Complex	
	24
Solvent	CD_2Cl_2
Temperature (K)	298
^{1}H NMR — H^1	10.05 (br s, 1H)
(600 MHz) — Ph	7.4-7.7 (m, 20H)
^{31}P{^{1}H} NMR — P	41.2 (s)
(121.4 MHz)	
^{13}C{^{1}H} NMR — C^2	238.4 (br s)
(150 MHz) — Ph$_{o/m/p}$	126.5 (s), 129.3 (s), 131.3 (s)
Ph$_{ipso}$	149.4 (br, s)
PPh-C$_{ipso}$	130.1 (d, $^1J_{P-C}$ = 54.3 Hz)
PPh-C$_{ortho}$	129.4 (d, $^2J_{P-C}$ = 9.1 Hz)
PPh-C$_{meta}$	134.3 (d, $^3J_{P-C}$ = 10.3 Hz)
PPh-C$_{para}$	132.0 (s)
CO$_{cis}$	199.6 (s)
CO$_{trans}$	203.3 (s)
υ (CO) (cm^{-1})^a	1904 (st, A$_1^{(2)}$), 1924 (v st, E), 1962 (w, B$_1$), 2062 (w, A$_1^{(1)}$)

^{a} Pentane solution in NaCl

Table 4.16

Complex	$(CO)_5W \leftarrow \overset{|^1}{N} \diagdown ^{Ph} \underset{2}{\diagup} $ AuPPh$_3$
	25
Solvent	CDCl$_3$
Temperature (K)	298
^{1}H NMR　　　　　H^1	3.34 (s, 3H)
(600 MHz)　　　　Ph	7.4-7.7 (m, 20H)
^{31}P{H^1} NMR　　P	39.3 (s)
(243 MHz)	
^{13}C{H^1} NMR　　C^1	32.4 (s)
(150 MHz)　　　　C^2	235.9 (d, $^2J_{P-C}$ = 124.6 Hz)
Ph$_{o/m/p}$	125.8 (s), 129.1 (s), 132.0 (s)
Ph$_{ipso}$	148.8 (br, s)
PPh-C$_{ipso}$	130.0 (d, $^1J_{P-C}$ = 53.2 Hz)
PPh-C$_{ortho}$	129.2 (d, $^2J_{P-C}$ = 9.0 Hz)
PPh-C$_{meta}$	134.1 (d, $^3J_{P-C}$ = 10.5 Hz)
PPh-C$_{para}$	131.8 (s)
CO$_{cis}$	199.8 (s)
CO$_{trans}$	203.6 (s)
υ (CO) (cm^{-1})^a	1905 (st, A$_1^{(2)}$), 1926 (v st, E), 1964 (w, B$_1$), 2064 (w, A$_1^{(1)}$)

^{a} Pentane solution in NaCl

The ^{1}H, ^{13}C{^{1}H} and ^{31}P NMR data for complex **26** are summarised in Table 4.17. The NMR data of **26** agree very well to those expected from its structure, as determined by X-ray diffraction techniques, reported below. Of particular interest is the greatly deshielded ^{31}P resonance (δ 71.5) ascribed to the PPh$_3$ group coordinated to the Cr(CO)$_4$ moiety, which suggests a large amount of electron donation from this group to the rest of the molecule. This efficient electron donation could be indirectly responsible for the extremely short Au-Au separation observed in the crystal structure of **26**, as explained in the discussion of the crystal structure.

Table 4.17

Complex		Ph$_3$P^1 · · · · PPh$_3$^{1} Au- - -Au Ph$_3$P^2 ⋯ / CO OC—Cr—CO CO
		26
Solvent		CD$_2$Cl$_2$
Temperature (K)		298
^{1}H NMR	Ph	6.9-7.7 (m, 45H)
(600 MHz)		
^{31}P{^{1}H} NMR	P^1	50.9 (d, $^3J_{\text{P-P}}$ = 5.4 Hz, 2P)
(243 MHz)	P^2	71.5 (d, $^3J_{\text{P-P}}$ = 5.3 Hz, 1P)
^{13}C{^{1}H} NMR	PPh-C$_{\text{ipso}}$	132.4 (t, J = 22.9 Hz)
(150 MHz)	PPh-C$_{\text{ortho}}$	129.0 (t, J = 3.3 Hz)
	PPh-C$_{\text{meta}}$	134.4 (t, J = 4.8 Hz)
	PPh-C$_{\text{para}}$	130.8 (s)
	CO	231.5 (d, $^2J_{\text{P-C}}$ = 9.9 Hz)
	CO	233.9 (d, $^2J_{\text{P-C}}$ = 18.3 Hz)
υ (CO) (cm^{-1})[a]		1839, 1864, 1942 (st, A$_1^{(2)}$, B$_1$, B$_2$)
		2004 (w, A$_1^{(1)}$)

[a] KBr Pellet

2.   Infrared spectroscopy

The infrared (IR) spectra of **21**-**25** were recorded as pentane solutions of the complexes in a NaCl cell and are summarised in Tables 4.12 – 4.16. The IR spectra measured for these complexes each exhibit four clearly separated absorption bands in the carbonyl region which could be assigned to, the now already familiar, $A_1^{(1)}$, $A_1^{(2)}$, B_1 and E vibrational modes for molecules of the type $M(CO)_5L$ [described in section 2.2.1(B)], as noted in the tables. The C=N stretching frequency, expected to appear between 1500 and 1700 cm^{-1}, could, due to the presence of many C=C_{conj} vibrational modes in the same region, unfortunately not be unambiguously identified in the IR spectra of these compounds.

Nevertheless, the energy at which the $\upsilon(CO)$ vibrational modes occur are sensitive probes for the electronic environment around the $M(CO)_5$ moiety. In general these absorption frequencies in **21**-**25**, especially the E vibrational mode, occur at lower energies than in complexes **11**-**13** [Section 3.2.2(C)], at similar energies as in complexes **1**-**5** [Section 2.2.1(C)], but at higher energies than in complexes **7**-**10** [Section 3.2.1(C)]. From this is concluded that **21**-**25** have a similar component of negative charge localised on the $M(CO)_5$ fragment as was determined in complexes **1**-**5**, and that resonance structures **S** or **T** (Scheme 4.15) play a meaningful role in the description of the polarised imine bonding modes to the $M(CO)_5$ fragments in **21**-**25**.

Furthermore, the observation of relatively low frequency (compared to other molecules of this type in the current study) $A_1^{(2)}$ vibrations (1902 to 1905 cm^{-1}), assigned to the stretching of the CO ligand situated *trans* to the acetimidoyl-AuPPh$_3$ and benzimidoyl-AuPPh$_3$ N-donor 'ligand' in **21**-**25**, is symptomatic of good σ-donating, but poor π-accepting, abilities of these moieties. This is also reflected in the crystal structure of **23**, which exhibits good retention of the double bond character of the imine bond after interaction with the $Cr(CO)_5$ fragment. Most of the metal-to-ligand back-donation to the empty π^*-orbitals of the ligands thus involve the CO ligand.

152

The IR spectrum of **26** was recorded as a KBr pellet and is summarised in Table 4.17. The C_{2v} local metal symmetry in complexes of the type *cis*-$L_2M(CO)_4$ allows for four IR active vibrational modes in the carbonyl region [2 x A_1, B_1, B_2]. All four of these were clearly visible in the IR spectrum of **26**, where they appeared at relatively low frequency in comparison to the $\upsilon(CO)$ values of other metal carbonyl compounds in this study. This shift to lower energy is ascribed to efficient electron donation from the PPh_3 ligand coordinated to the chromium atom in **26**, which increases the electron density on this atom and thus also increases the back-donation of electrons to the CO and pseudo bidentate η^2-($Ph_3PAu\cdots AuPPh_3$) ligands in this compound. In this ligand these back-donating electrons are believed to play a role in cancelling out the $Au^{\delta+}$-$Au^{\delta+}$ repulsive effects between the Ph_3PAu^+ fragments, thus allowing the gold atoms to interact more effectively. This interpretation of the IR data of **26** explains the extremely short Au-Au separation found in the crystal structure of this complex.

3.   *Mass spectrometry*

The positive-ion FAB-MS of complexes **21-26** were recorded in a *m*-nitrobenzylalcohol matrix. Similar to the FAB mass spectra of complexes containing the $AuPPh_3$ moiety throughout this study, the FAB mass spectra of **21-26** are characterised by high intensity peaks for Ph_3PAu^+ (*m/z* 459) and $(Ph_3P)_2Au^+$ (*m/z* 721) fragments. Unless stated otherwise, either of these peaks, or the peaks corresponding to the *m*-nitrobenzylalcohol matrix (*m/z* 154, *m/z* 136), were generally the peaks of greatest intensity. Molecular ion peaks were only unambiguously present in the mass spectra of **21** [*m/z* 694(55)] and **23** [*m/z* 754(100)] (intensity in parenthesis given in percentage relative to the peaks of highest intensity), whereas a signal representing a fragment that corresponds to a molecular ion that has lost two CO ligands could be identified in the mass spectrum of **24** [*m/z* 830(35)]. Furthermore, the FAB mass spectrum of **23** yielded, along with a strong molecular ion peak, a clear peak for the free benzimidoyl-$AuPPh_3$ fragment [*m/z* 564(15)] and a peak corresponding to a molecular ion that has lost four CO ligands [*m/z* 644(7)].

The FAB mass spectra of **22**, **25** and **26** yielded no information regarding the structure of these compounds.

C.   X-ray structure determination of complexes **23** and **26**.

The low temperature crystal and molecular structures of **23** (173 K) and **26** (173 K) (Figures 4.11 and 4.14) were determined by X-ray diffraction techniques. Selected bond lengths and angles for **23** and **26** are listed in Tables 4.18 – 4.19, according to the numbering schemes shown in the figures.

The structure of **23** (Figure 4.11) clearly exhibits a benzimidoyl-AuPPh$_3$ moiety coordinated through its imine nitrogen atom to a Cr(CO)$_5$ group and shows that it is the Z-isomer of this compound that forms in this conversion. The structure of **23** represents the first crystal structure of an organoimidoyl complex of gold(I). This complex, furthermore, acts as a neutral N-donor ligand to a Cr(CO)$_5$ fragment, thereby also forming the first example of a bimetallic imidoylgold(I) complex that is coordinated through the imine nitrogen atom to a metal other than gold.

The Au-C(1) bond length in **23** [2.034(7)Å] is typical for an Au(I)-C(sp^2) σ-bond.[31] The C(1)-N bond length [1.281(9)Å] confirms the double bond character of this bond and thus nominates resonance structure **S** (Scheme 4.15) as the main contributor to the polarized imine coordination mode in compounds of this kind. A near planar bonding geometry around C(1) [deviations from the least squares plane calculated through C(1), Au, C(41) and N are 0.024(5), 0.006(1), 0.008(2) and 0.010(2)Å respectively] verifies the sp^2 hybridisation of this atom. A C(1)-C(41) bond length of 1.528(10)Å is normal[41] while a Au-C(1)-C(41)-C(42) torsion angle of 20.4(7)º describes how the C(4x) phenyl ring is slightly rotated with respect to the Au-C(1) bond. An Au-P separation of 2.301(2)Å is usual.[32] Quite remarkable with regards to the P-Au-C(1) angle is that the usually linear, or pseudo-linear, Au(I) coordination mode is distorted by 8.8(2)º [P-Au-C(1) = 171.2(2)º]. Usually this degree of distortion of the Au(I) coordination mode is related to Au-Au relativistic interactions, but these are absent in the structure of **23**. The only realistic explanation for this distortion is that it could be the result of inefficient packing of molecules of **23** in the unit cell or intramolecular steric interactions between the gold atom and the C(2)-O(2) ligand, as described below.

A N-Cr separation of 2.113(6)Å compares well to the sole literature reported crystal structure containing η^1-imine coordination to zero valent chromium.[42] Deviation from planarity of the least squares plane through Cr, C(2), C(3), C(4) and C(5) of 0.044(3), -0.077(4), 0.055(4), -0.075(4) and 0.053(4) describe its distortion due to the coordination of the sterically large benzimidoyl-AuPPh$_3$ moiety. A calculated Au-C(1)-Cr-C(2) torsion angle of 13.3(5)º shows that the Au-C(1) bond is surprisingly close to parallel to the Cr-C(2) bond. This is also reflected in a Cr-C(2)-O(2) bond angle of 170.3(6)º and the P-Au-C(1) angle [171.2(2)º], mentioned above, that show how these bonds are distorted from linearity to accommodate the small Au-C(1)-Cr-C(2) torsion angle. The Au-C(2) and Au-O(2) separations are 3.199(7)Å and 3.409(5)Å, well outside Au-C and Au-O distances for bonding interactions. Furthermore, none of the other CO ligands in the pseudo planar Cr(CO)$_4$ coordination plane are involved in any significant intermolecular interactions, thus theoretically allowing the Cr(CO)$_5$ group free rotation around the C(6)-Cr-N axis to assume an energy conformation minimum in the crystal. The reason for the occurrence of this seemingly high-energy eclipsed conformation is, therefore, not understood. A C(1)-N-Cr angle of 136.6(5)º also shows how this angle is distorted from the sp^2 ideal (120º) due to the steric interactions of the Au atom with C(2) and O(2).

The position of the imine hydrogen atom (H) could be determined from the difference Fourier map and refined isotropically. Curiously, this hydrogen atom position is distorted toward the Cr(CO)$_5$ fragment, as can be seen in the C(1)-N-H and Cr-N-H angles [127(6)º and 96(6)º] and the short Cr-H separation [2.35(8)Å]. Although the distortion of the C(1)-N-Cr bond angle, described above, would certainly affect this hydrogen atom position, it does not account for the large C(1)-N-H angle. The exact reasons for this distortion are therefore unknown. The position of this hydrogen atom, as determined by X-ray diffraction techniques, is, however, relatively poorly determined and should be regarded with some caution.
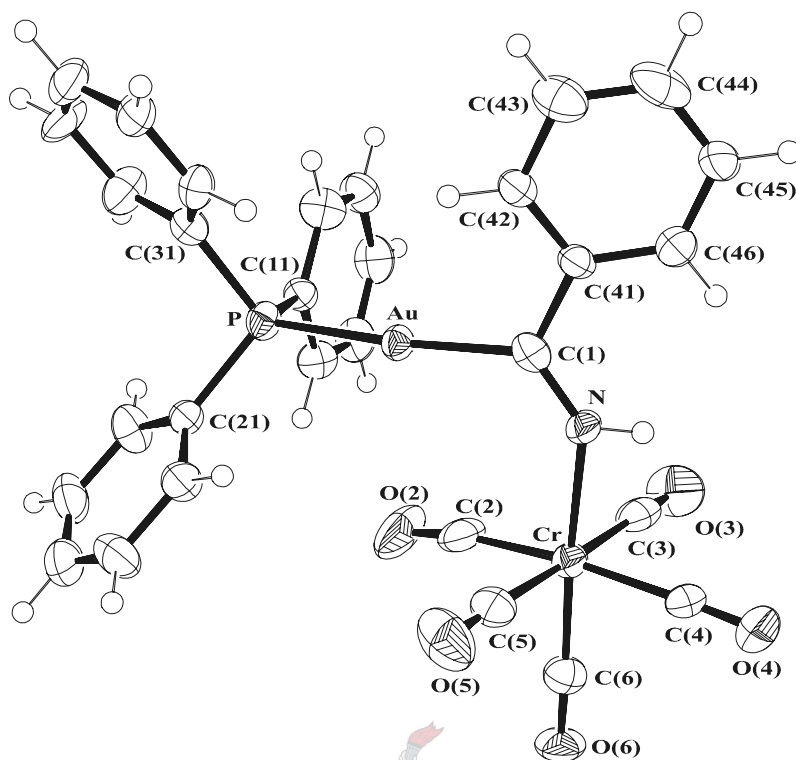
Figure 4.11: ORTEP view **23**, showing the numbering scheme

Table 4.18: Selected bond lengths (Å) and angles (°) with e.s.d.s in parenthesis for complex **23**

Bond lengths		Bond angles	
Au-C(1)	2.034(7)	C(1)-Au-P	171.2(2)
C(1)-N	1.281(9)	Au-C(1)-N	124.2(6)
N-Cr	2.113(6)	Au-C(1)-C(41)	117.9(5)
C(1)-C(41)	1.528(10)	C(41)-C(1)-N	117.8(6)
Au-P	2.301(2)	C(1)-N-Cr	136.6(5)
Cr-C(2)	1.887(11)	N-Cr-C(6)	176.5(3)
Cr-C(3)	1.913(9)	C(2)-Cr-C(4)	172.3(3)
Cr-C(4)	1.893(8)	C(3)-Cr-C(5)	178.3(3)
Cr-C(5)	1.901(8)	O(2)-C(2)-Cr	170.3(6)
Cr-C(6)	1.853(8)	O(3)-C(3)-Cr	177.1(7)
P-C(11)	1.814(7)	O(4)-C(4)-Cr	176.8(7)
P-C(21)	1.823(8)	O(5)-C(5)-Cr	177.5(8)
P-C(31)	1.814(8)	O(6)-C(6)-Cr	178.4(7)

In the unit cell molecules of **23** pack in the non-centrosymmetric orthorhombic unit cell Pc2₁b with four molecules in each unit cell. A view along the a-axis (Figure 4.12) shows how molecules of **23** stack in regular rows along the a-axis with the P-Au-C(1) bonds orientated in an offset herringbone structure along the c-axis
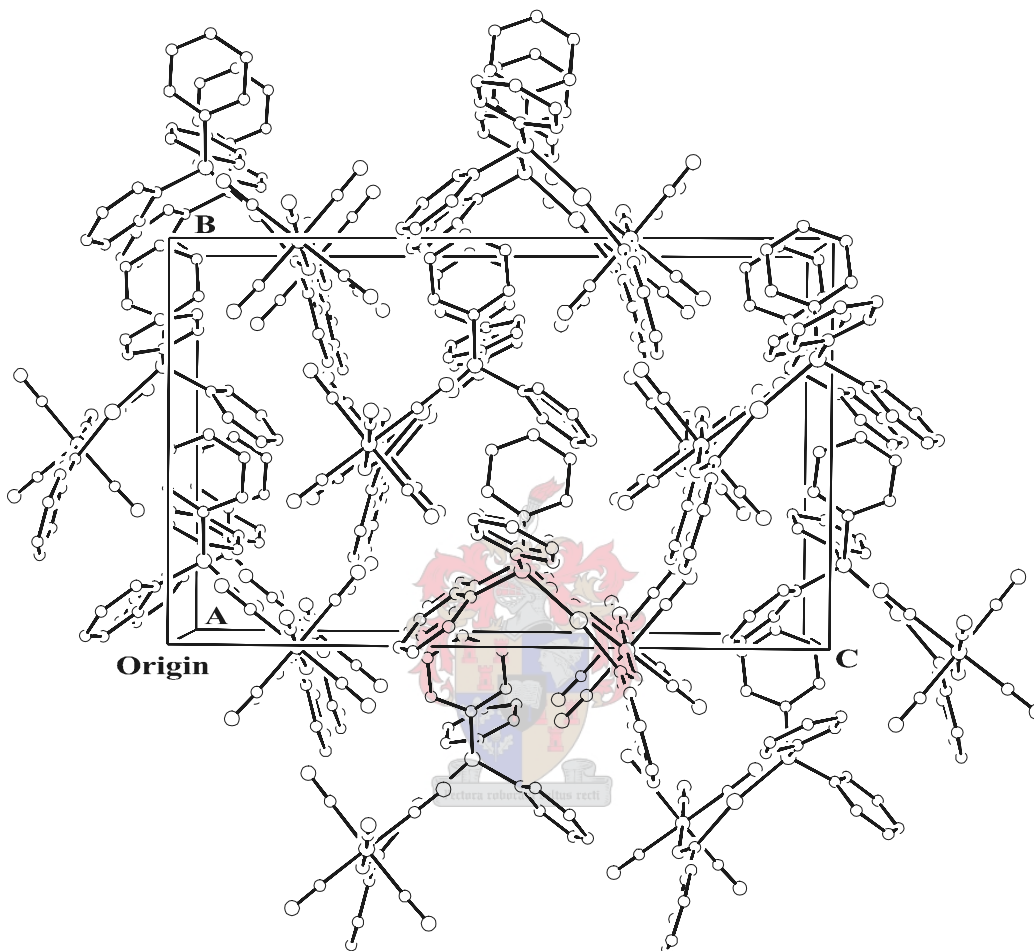
Figure 4.12: Packing diagram of **23**, viewed along the a-axis of the unit cell

Furthermore, there are short non-bonded intermolecular interactions between molecules of **23** along the a-axis of the unit cell, involving the oxygen atom [O(6)] of the CO ligand *trans* to the imine coordination, a hydrogen atom from the benzimidoyl ring [H(43)] and a hydrogen atom from a phenyl ring in the PPh₃ group [H(33)] (Figure 4.13). It is likely that this interaction, and the offset herringbone packing configuration of the P-Au-C(1) bonds, are also partly responsible for the high degree of distortion of the usually linear P-Au-C(1) coordination mode.

Figure 4.13: Simplified packing diagram of **23**, illustrating the non-bonded
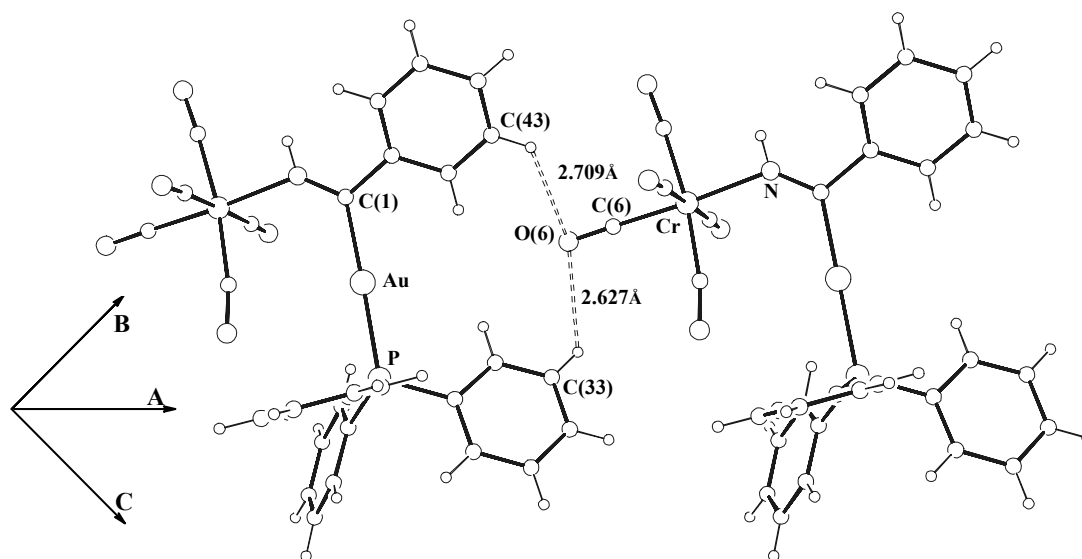
interaction between two molecules along the a-axis of the unit cell

The crystal structure of **26** (Figure 4.14) clearly exhibits a $Cr(CO)_4PPh_3$ fragment with two $AuPPh_3$ fragments interacting with the chromium atom and each other to form a trinuclear triangular $CrAu_2$ metal cluster compound. This bonding mode of two $AuPPh_3$ fragments to a neutral metal centre is also described as a 3-centre, 2-electron system in which the PPh_3Au-$AuPPh_3$ grouping is regarded as a η^2-$(AuPPh_3)_2$ 'ligand'.[36] This description of the metal-metal bonding situation in **26** is related to the hypothetical isolobal η^2-H_2 complex.[36,38]

The metal-metal separations and bond angles within the trimetallo cyclopropane ring in **26** show that it is a nearly perfect equilateral triangle [Au(1)-Cr = 2.6932(6)Å, Au(2)-Cr = 2.7038(7)Å, Au(1)-Au(2) = 2.6937(2)Å, Au(1)-Cr-Au(2) = 59.88(2)°, Cr-Au(1)-Au(2) = 60.25(2)°, Cr-Au(2)-Au(1) = 59.87(2)°]. Of greatest interest in this structure is that the Au(1)-Au(2) distance reported here is the shortest known crystallographically determined separation between two gold(I) atoms(!). Slightly shorter Au-Au separations have been reported within gold cluster compounds in which three or more gold atoms are linked to each other, but the bonding situation is difficult to describe in such compounds.[43] The Au(1)-Au(2) distance in **26** is 0.1903(2)Å shorter than in metallic gold (2.884Å)[44(a)] and thus clearly within bonding distance (Au-Au van der Waals separation is 3.32Å).[44(b)] This result supports the description of this complex as having a η^2-$(AuPPh_3)_2Cr(CO)_4PPh_3$ configuration.

Shortening of Au-Au distances in triangular MAu_2 cluster compounds has been linked to the electron density on the metal centre (M).[39] Greater electron density on M corresponds to better interaction with $AuPPh_3^+$ fragments and also decreases the $Au^{\delta+}$-$Au^{\delta+}$ repulsion. This in turn effectively increases the electron density on the gold atoms and strengthens the Au-Au aurophilic interaction to a point where the Au_2 configuration in the MAu_2 cluster can be formally regarded as a σ-Au-Au bond coordinated to a neutral metal centre (M). The presence of an excellent σ-donating PPh_3 ligand in **26** is consistent with an increase in the electron density on the chromium atom, thus explaining the extraordinarily short Au-Au separation observed in this compound. An unusually long P-Cr bond [Cr-P(3) = 2.399(1)Å], as well as the downfield shifted ^{31}P NMR resonance for this phosphorus atom and the relatively low frequency (compared to other chromium carbonyl compounds in this study) at which the CO stretching frequencies in **26** appear also support this interpretation of the structure of **26**. A C(4)-C(3)-Au(1)-Au(2) torsion angle of 29.19(8)° describes how the η^2-$(AuPPh_3)_2$ 'ligand' is orientated relative to the $Cr(CO)_3PPh_3$ coordination plane. Distortion of the Cr-C(2)-C(3)-C(4)-P(3) coordination plane is described by respective deviations of –0.0243, -0.0238, 0.0324, 0.0330 and –0.0172Å from the least squares plane through these atoms.
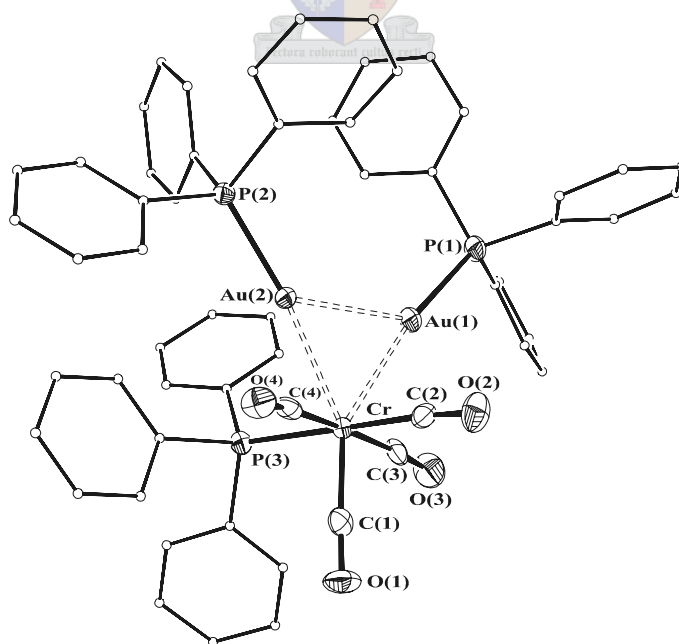

Figure 4.14: ORTEP view of **26**, showing numbering scheme (hydrogen atoms and disordered thf molecule are omitted for clarity)

159

Table 4.19: Selected bond lengths (Å) and angles (°) with e.s.d.s in parenthesis for complex **26**

Bond lengths		Bond angles	
Au(1)-Au(2)	2.6937(2)	Au(1)-Cr-Au(2)	59.88(2)
Au(1)-Cr	2.6932(6)	Cr-Au(1)-Au(2)	60.25(2)
Au(2)-Cr	2.7038(7)	Cr-Au(2)-Au(1)	59.87(2)
Cr-P(3)	2.399(1)	Cr-Au(1)-P(1)	168.12(4)
Au(1)-P(1)	2.285(1)	Cr-Au(2)-P(2)	169.74(3)
Au(2)-P(2)	2.302(1)	C(1)-Cr-Au(1)	150.3(1)
Cr-C(1)	1.830(5)	C(1)-Cr-Au(2)	148.9(2)
Cr-C(2)	1.853(4)	C(2)-Cr-P(3)	178.9(1)
Cr-C(3)	1.899(5)	C(3)-Cr-C(4)	175.6(2)
Cr-C(4)	1.887(5)	O(1)-C(1)-Cr	175.6(4)
C(1)-O(1)	1.171(5)	O(2)-C(2)-Cr	175.5(4)
C(2)-O(2)	1.166(4)	O(3)-C(3)-Cr	174.5(4)
C(3)-O(3)	1.147(5)	O(4)-C(4)-Cr	171.3(4)
C(4)-O(4)	1.162(5)	C(4)-C(3)-Au(1)-Au(2)	29.19(8)

In the crystal molecules of **26** pack together with a non-coordinated, and somewhat disordered, thf solvent molecule (not shown in Figure 4.14) in the centrosymmetric spacegroup P$\bar{1}$. There are no significant intermolecular interactions present in the unit cell of **26**.

4.2.3 Acyl and hydroxycarbene complexes of zero valent tungsten: Two interesting crystal structures of benzoyl pentacarbonyl-tungstate containing Li^+ and H^+ counterions

A. General preparation and discussion of [μ_3{diglyme}-O μ_2{W(CO)$_5$C(O)Ph}-O,O' Li] (**27**) and [μ_6{diglyme}$_2$-O Li][μ_2{H}-O {W(CO)$_5$C(O)Ph}$_2$] (**28**)

The synthesis of the ionic benzoyl pentacarbonyltungstate complexes, **27** and **28**, was carried out in much the same manner as the synthesis of the Fischer-type carbene complexes, (CO)$_5$W=C(OR)Ph, by the addition of 1.2 mole equiv. PhLi to a suspension of W(CO)$_6$ in Et$_2$O at room temperature.[5] However, instead of alkylating the lithium benzoyl pentacarbonyltungstate, to produce the carbene complex, two closely related compounds, **27** and **28**, were isolated using slightly different procedures (Scheme 4.17).
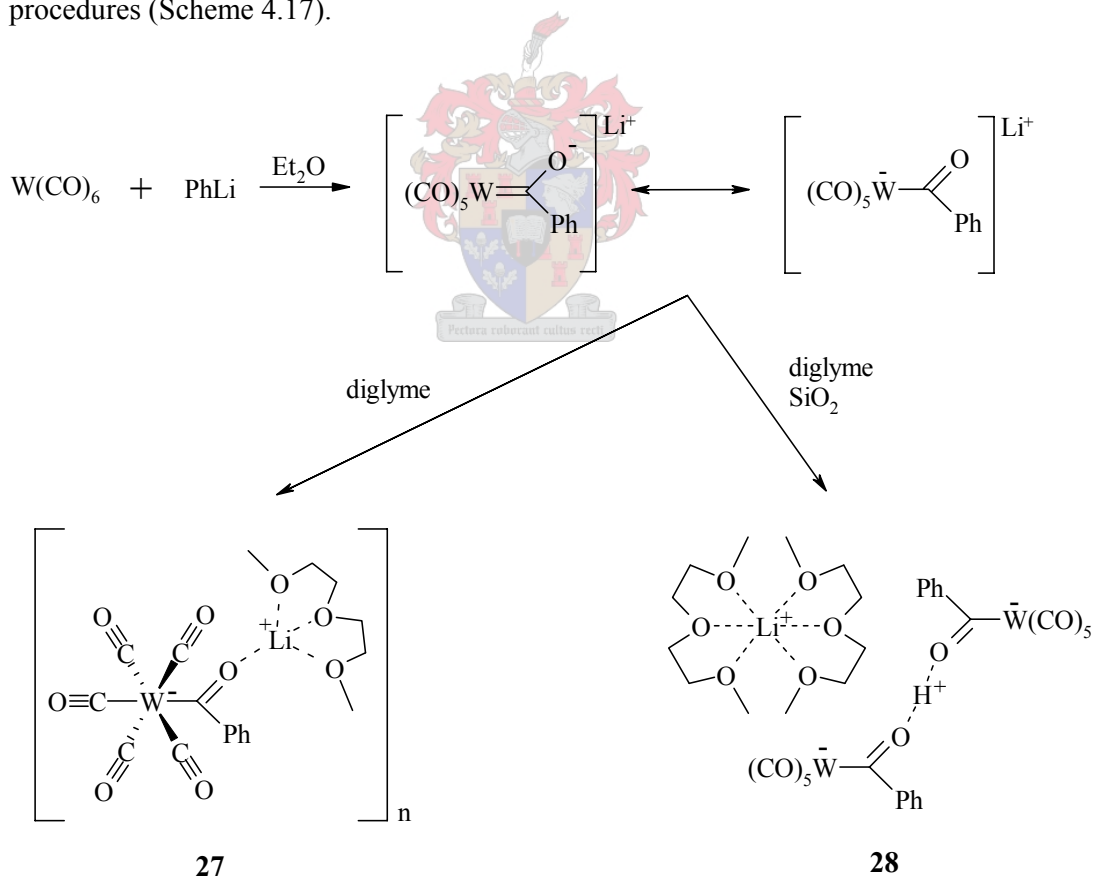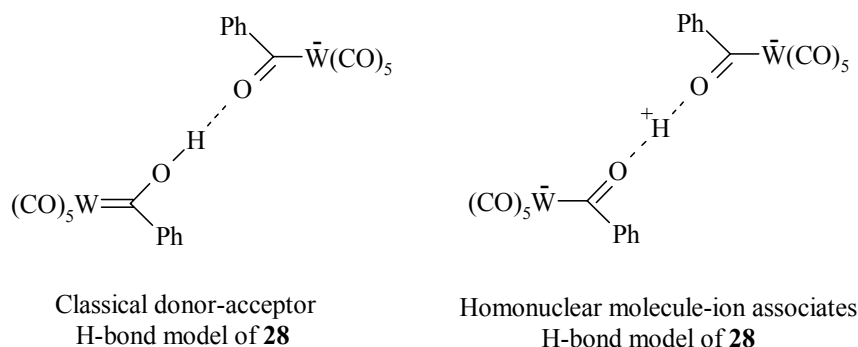

Scheme 4.17

The only difference between **27** and **28** is that the latter structure contains half the amount of Li-cations than the previous one. The balance of cations in **28** are protons, that are stabilised in a bridged hydrogen bonded structure between two benzoyl pentacarbonyltungstate anions. This arrangement allows the 1 mole equivalent of diglyme (diethylene glycol dimethyl ether), also present in the structure, to solvate the Li$^+$ cations octahedrally. Upon dissolution **28** reverts to a 50/50 mixture of lithium benzoyl pentacarbonyltungstate and phenyl(hydroxy) pentacarbonyltungsten carbene. The structure of **27**, on the other hand, crystallised from the original lithium benzoyl pentacarbonyltungstate reaction mixture in which the full mole equivalent of Li$^+$-cations are still present. These require more stabilisation than the protons in **28**, which is more than what the 1 mole equivalent diglyme also present in this structure can provide. The oxygen atoms of the benzoyl group and one CO ligand are thus employed by the Li$^+$-cation for this task, forming the polymeric configuration found in the structure of **27**. The different ion-dipole interactions required to stabilise the cations in these structures thus cause the formation of strikingly different crystal structures for these closely related ionic complexes.

The isolation of **27** and **28** was achieved as follows: The addition of 1 mole equiv. diglyme to the lithium benzoyl pentacarbonyltungstate, prepared as described above, followed by crystallisation from Et$_2$O layered with pentane (-20ºC) produced red crystals of **27** in a high yield [78%, based on W]. To prepare **28** essentially the same procedure was followed, except that the orange-red reaction mixture was carefully chromatographed through cooled (0ºC) silica gel (10-15cm, Ø 4cm) with Et$_2$O as eluant before crystallisation (concentrated Et$_2$O solution layered with pentane at -20ºC) produced red crystals of **28** in a good yield [69%, based on W].

The mechanism by which roughly half of the Li$^+$-cations are removed from the solution upon silica gel chromatography, so that **28** may crystallise, is closely linked to the amount of diglyme added to the reaction mixture before chromatography. Li$^+$-cations in the reaction mixture have to be strongly solvated in order to pass through the silica gel during the chromatographic procedure. From the fact that only one mole equivalent of diglyme is added to the reaction mixture, and two diglyme molecules are required to solvate each Li$^+$-cation (as in the crystal structure of **28**), follows that

only roughly half the Li^+-cations remain in the solution after chromatography. The other half are immobilised on the silica gel and, to balance the charge, are replaced by mobile protons from the acidic silica gel. Et_2O solvent molecules do not solvate Li^+-cations strongly enough to facilitate such efficient mobilisation through the silica gel. If, however, too much Et_2O is used to wash the brightly coloured benzoyl pentacarbonyltungstate anions through the column, it is possible that some additional Li^+-cations, weakly solvated by Et_2O molecules, are eluted through the column. It is therefore imperative that this chromatographic process be halted after the brightly coloured benzoyl pentacarbonyltungstate is removed from the column. Another route to prepare **28**, although untested, could be to prepare the hydroxycarbene complex seperately by filtering half the lithium benzoyl pentacarbonyltungstate reaction mixture though acidic silica before adding one equivalent diglyme to the recombined reaction mixture. This route, however, is probably less favourable because of the relative instability of the hydroxy(phenyl)pentacarbonyl tungsten carbene complex in in Et_2O solution.

A characteristic feature of all the crystal structures of hydroxycarbene complexes is that they, without exception, exhibit classical hydrogen bonding interactions involving the hydroxy hydrogen atom. Currently there are 15 reported structures of what can formally be regarded as hydroxycarbene complexes.[45,46] No less than 12 of these exhibit intramolecular hydrogen bonds[45] whereas the remaining three exhibit intermolecular hydrogen bonds (two with $CF_3SO_3^-$ anions and one with an acetonitrile solvent molecule).[46] From this follows that the OH protons in hydroxycarbene complexes, without consideration of their spectroscopic or thermodynamic properties, are weakly linked to what is actually a pseudo metallo-acyl oxygen atom, and require stabilisation through hydrogen bonding. This interpretation is supported by the observation that the C_{carb}-O bond in hydroxycarbene complexes displays a large component of double bond character (average C-O separation = 1.282Å). Hydroxycarbene complexes would thus perhaps be better described as ion-paired [metallo-acyl][H] complexes, exhibiting hydrogen bonding interactions between the acyl-oxygen atoms and the protons, rather than complexes with a formal oxygen-hydrogen bond (Scheme 4.18).

Classical donor-acceptor
H-bond model of **28**

Homonuclear molecule-ion associates
H-bond model of **28**

Scheme 4.18

This approach enables a better description of the hydrogen bonding interactions in structure of **28** as no classical donor-acceptor definitions are apparent in these interactions. Based on this, the hydrogen bridged structure in **28** is described as an anionic homonuclear molecule-ion associate of two benzoyl pentacarbonyltungstate anions interacting with a proton, AHA⁻. The second positive charge required to balance the charge in **28** is provided by a remaining Li⁺ cation coordinated to two diglyme molecules. For organometallic compounds similar hydrogen bridged structures have been reported for anionic $[(CO)_5Cr\{C≡N···H···N≡C\}Cr(CO)_5]$ and $[(CO)_5Cr\{C≡N···H···N≡C\}FeCp(dppe)]$ complexes, but none containing O···H···O interactions.[47]

Furthermore, of the 12 crystal structures of hydroxycarbene complexes that exhibit intramolecular hydrogen bonds, all except one[45(i)] contain two metallo-acyl moieties on one metal atom involved in the hydrogen bonding interaction. This shows that this arrangement, forming six-membered metallocyclic rings (Scheme 4.19) is particularly favoured.
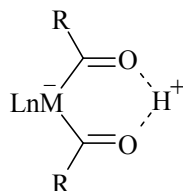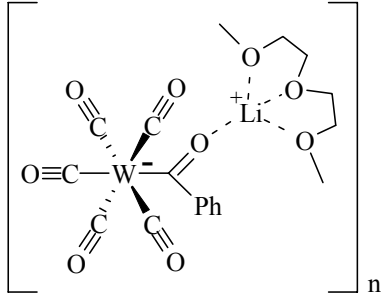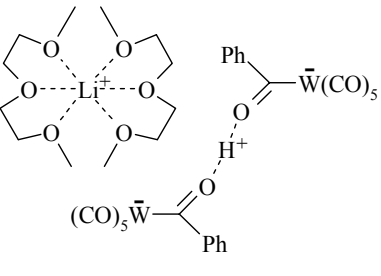
Scheme 4.19

The hydrogen bonding arrangement found in the crystal structure of **28** is similar to the ones described above (between two metallo-acyl groups), except that the metallo-acyl moieties involved in the hydrogen bonding interaction are situated on separate

metal centres and therefore do not form a six-membered ring structure. The structure of **28**, although novel, is thus not completely unexpected. Physical data for **27** and **28** are listed in Table 4.20.

Table 4.20: Analytical data for **27** and **28**

Compound		
Complex	**27**	**28**
M.p. / °C	76	68 (decomp.)
Color	orange-red	orange-red
Yield (%)	78	69
M.W. (g / mol)	570.13	1134.33
Analyses (%)[a]		
C	37.85 (37.92)	38.02 (38.12)
H	3.40 (3.36)	3.40 (3.47)
O	25.35 (25.26)	25.49 (25.39)

[a] Required values given in parentheses

B.   Spectroscopic characterisation of complexes **27** and **28**

1.   NMR Spectroscopy

The ^{1}H and ^{13}C NMR spectra of **27** contain identical resonances to those of lithium benzoylpentacarbonyltungstate, reported elsewhere,[48] whereas the ^{1}H and ^{13}C NMR spectra of **28** contain resonances for both lithium benzoylpentacarbonyltungstate and phenyl(hydroxy)pentacarbonyltungsten carbene complexes. For both compounds additional NMR resonances, representing the 1 mole equiv. diglyme in these complexes, were also present. In the ^{1}H NMR spectra of **27** and **28** these resonances appear as a singlet at δ 3.42 (6H), representing the methoxy groups, and two triplet

signals at δ 3.77 and 3.66 ($^3J_{H-H}$ ~5 Hz, 4H each), representing two sets of unique CH_2 groups in the diglyme molecule. The $^2J_{H-H}$ geminal coupling, sometimes observed within these resonances, were not resolved in the ^{1}H NMR spectra of **27** and **28**. In the $^{13}C\{^1H\}$ NMR spectra the resonances corresponding to diglyme appear at δ 59.0, 70.7 and 72.2.

2. *Infrared spectroscopy*

The infrared (IR) spectra of **27** and **28** were recorded as KBr pellets containing crystals of these complexes. The υ(CO) absorption peaks for the CO ligands in both complexes exhibit the typical pattern of $A_1^{(1)}$, $A_1^{(2)}$, B_1 and E vibrational modes for molecules of the type $M(CO)_5L$ [See section 2.2.1(B)] and are practically identical. The $A_1^{(1)}$ stretching vibration appears at 2049 cm^{-1} in both compounds. A B_1 mode (~1968 cm^{-1} in both complexes) is identified as a shoulder on the very intense and broad absorption peak of the E vibrational mode [1895cm^{-1} (**27**), 1904cm^{-1}(**28**)]. The stretching frequency of the $A_1^{(2)}$ vibrational mode also appears as a shoulder, shifted to a lower wave number (~1885 cm^{-1}), on the intense and broad E vibrational mode. The only clear deduction from the CO ligand stretching frequencies of **27** and **28** is that the metal atoms in these compounds are relatively electron rich in comparison to other complexes of the form $M(CO)_5L$ in this study. Comparison of the acyl C=O stretching frequencies [1517cm^{-1} (**27**) and 1510 cm^{-1} (**28**)] is more fruitful. The 7 cm^{-1} lower stretching frequency of this moiety in **28** indicates that this bond is slightly more reduced in this compound. This result suggests better interaction of the metallo-acyl anions with the proton in **28** than with the Li^+-cation in **27** and corresponds to the results described by the crystal structures of these complexes, reported below.

An interesting exercise was to also measure the IR spectra of **27** in solution (CH_2Cl_2). Dissolution of **27** results in a large change in the stretching frequency of the acyl vibrational mode (89 cm^{-1} 'blue shift'). The $A_1^{(2)}$ vibration, assigned to the stretching frequency of the CO ligand trans to the metallo-acyl moiety, is not clearly observed in the solution IR spectrum of **27**. It is barely observable as a narrow shoulder on the intense E absorption peak, but is nevertheless shifted to higher energy (~10-15 cm^{-1}). These shifts are rationalised by consideration of the solid-state structure of **27**, reported below. In the solid state there is a clear interaction of the Li^+-cations with the

metallo acyl group, as well as with the CO ligand *trans* to the metallo acyl bond on a neighbouring anion. The shifts in the IR absorption frequencies observed here strongly suggest that these interactions do not persist in methylene chloride solution. No interaction with Li^+-cations means that there is no loss of electrons from the oxygen atoms in the groups that interact with the cation in the solid state. This translates to stronger $C \equiv O$ and $C = O$ bonds in these groups, which correspondingly vibrate at higher energy in the dissolved compound. The fact that the $\upsilon(CO)$ for the acyl group is much more affected upon dissolution than the $A_1^{(2)} \upsilon(CO)$ frequency can also be explained by the X-ray structure of **27**. The metallo-acyl oxygen-lithium separation [O(1)-Li = 1.875(4)Å] is 0.196(4)Å shorter than the CO-lithium separation [O(3)-Li = 2.071(4)Å]. This indicates that the Li^+ interaction with the metallo-acyl group is much stronger than the interaction with the coordinated CO ligand and is thus expected to have a much greater effect on the acyl $C = O$ bond order in the solid state. The 7 cm^{-1} and 10cm^{-1} blue shifts in the B_1 and E vibrational modes upon dissolution are ascribed to solvent interactions. The $A_1^{(1)}$ stretching frequencies are identical.

The solution IR spectrum of **28** (CH_2Cl_2) is dominated by an extremely broad and intense absorption band at ~1900 cm^{-1} and is not resolved. Reasons for this probably lie with the fact that, upon dissolution, **28** reverts to a 50/50 mixture of lithium benzoyl pentacarbonyltungstate and phenyl(hydroxy)pentacarbonyltungsten carbene from whence it crystallised, and thus gives an IR spectrum for both compounds with overlapping and broad absorption bands.

C.   X-ray structure determination of complexes **27** and **28**.

The low temperature crystal and molecular structures of **27** (173 K) and **28** (173 K) (Figures 4.15 and 4.17) were determined by X-ray diffraction techniques. Selected bond lengths and angles for **27** and **28** are listed in Tables 4.21 and 4.22, according to the numbering schemes shown in the figures.

The structure of **27** (Figure 4.15) clearly shows a benzoyl pentacarbonyltungstate anion interacting with a Li^+-cation through its acyl moiety. Li^+-coordination to the CO ligand *trans* to the benzoyl group in neighbouring anions results in infinite zig-zag chains of alternating benzoyl pentacarbonyltungstate anions and Li^+-cations along the

a-axis of the unit cell of **27** (Figure 4.16). The remaining coordination positions on the Li⁺-cation are occupied by a diglyme molecule, coordinating to the cation through all three of its ether oxygen atoms. The coordination of the 5-coordinate Li⁺-cation is best described as distorted square pyramidal, with O(3) at the apex, rather than distorted trigonal bipyramidal. O(5) lies on the underside of the square pyramid, beyond bonding distance [Li-O(5) = 3.506(4)Å], but sterically preventing the diglyme molecule from assuming a coordination mode that is closer to trigonal bipyramidal.
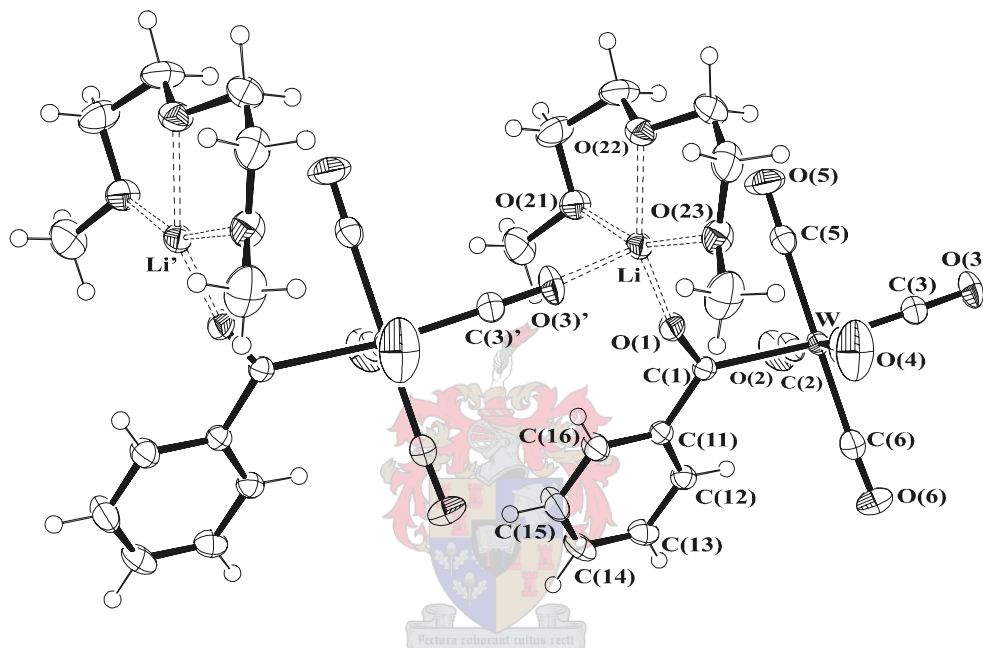
Figure 4.15: ORTEP view of **27** (two asymmetric units) showing numbering scheme and the polymeric structure observed in the crystal

Table 4.21: Selected bond lengths (Å) and angles (°) with e.s.d.s in parenthesis for complex **27**

Bond lengths		Bond angles	
W-C(1)	2.284(2)	C(1)-W-C(3)	171.82(8)
C(1)-O(1)	1.239(2)	C(2)-W-C(4)	175.00(9)
C(1)-C(11)	1.522(3)	C(5)-W-C(6)	179.45(9)
O(1)-Li	1.875(4)	W-C(1)-O(1)	119.8(2)
Li-O(3)	2.071(4)	W-C(1)-C(11)	126.6(1)
Li-O(21)	2.095(4)	C(11)-C(1)-O(1)	113.6(2)
Li-O(22)	2.083(4)	O(1)-Li-O(3)'	105.2(2)

168

Table 4.21(continued):

Bond lengths		Bond angles	
Li-O(23)	2.070(4)	O(1)-Li-O(21)	95.8(2)
W-C(2)	2.025(2)	O(1)-Li-O(22)	150.5(2)
W-C(3)	1.980(2)	O(1)-Li-O(23)	102.4(2)
W-C(4)	2.047(3)	O(21)-Li-O(23)	154.0(2)
W-C(5)	2.047(2)	O(3)'-Li-O(21)	95.6(2)
W-C(6)	2.022(3)	O(3)'-Li-O(22)	104.1(2)
C(2)-O(2)	1.151(3)	O(3)'-Li-O(23)	97.3(2)
C(3)-O(3)	1.165(3)	O(2)-C(2)-W	178.8(2)
C(4)-O(4)	1.137(3)	O(3)-C(3)-W	178.3(2)
C(5)-O(5)	1.140(3)	O(4)-C(4)-W	177.9(3)
C(6)-O(6)	1.146(3)	O(5)-C(5)-W	179.2(2)
		O(6)-C(6)-W	177.5(2)
		O(1)-C(1)-C(11)-C(16)	8.9(3)
		C(5)-W-C(1)-O(1)	34.7(2)

An interesting feature in the structure of **27** is the variation in the Li-O separations. The Li distances to the diglyme molecule oxygen atoms and to the CO ligand, O(3), are normal [average of these four Li-O separations = 2.080(4)Å], but the Li-acyl oxygen separation is 0.205(4)Å shorter than this [Li-O(1) = 1.875(4)Å]. In the absence of any obvious steric reasons for this difference in the Li-O separations, this result indicates that there is a much greater electronic interaction of the lithium cation with O(1) than with any of the other oxygen atoms.

The W-C(1) and C(1)-O(1) bond lengths [2.284(2) and 1.239(2)Å] in **27** are consistent with a bonding situation in which a small amount of charge delocalisation from the acyl C=O double bond to the W-C bond has occurred due to Li^{+}-acyl coordination. Pure zero valent tungsten $W-C_{sp2}$ single bonds are usually slightly longer [~2.31Å][49] whereas uncoordinated acyl C=O double bonds are usually slightly shorter [~1.21Å].[50] An O(1)-C(1)-C(11)-C(16) torsion angle of 8.9(3)° describes the orientation of the phenyl ring toward the acyl moiety. The sp[2] hybridisation of C(1) is confirmed by its nearly perfectly flat bonding geometry [the greatest deviation from the least-squares plane through W, C(1), O(1) and C(11) is 0.004(2)Å for C(1)]. A

C(5)-W-C(1)-O(1) torsion angle of 34.7(2)° describes how the benzoyl ligand is rotated on the W(CO)$_4$ coordination plane. Distortion of the W(CO)$_4$ coordination plane from planarity, due to bonding of the benzoyl ligand, is described by deviations from planarity from the least squares plane through W, C(2), C(4), C(5) and C(6) of -0.0253(9), 0.0477(11), -0.0472(11), -0.0334(11) and -0.0362(12)Å respectively, and, furthermore, supports the observation of a relatively intense and infra red active B$_1$ absorption mode in the carbonyl region of the infra red spectrum of **27**.
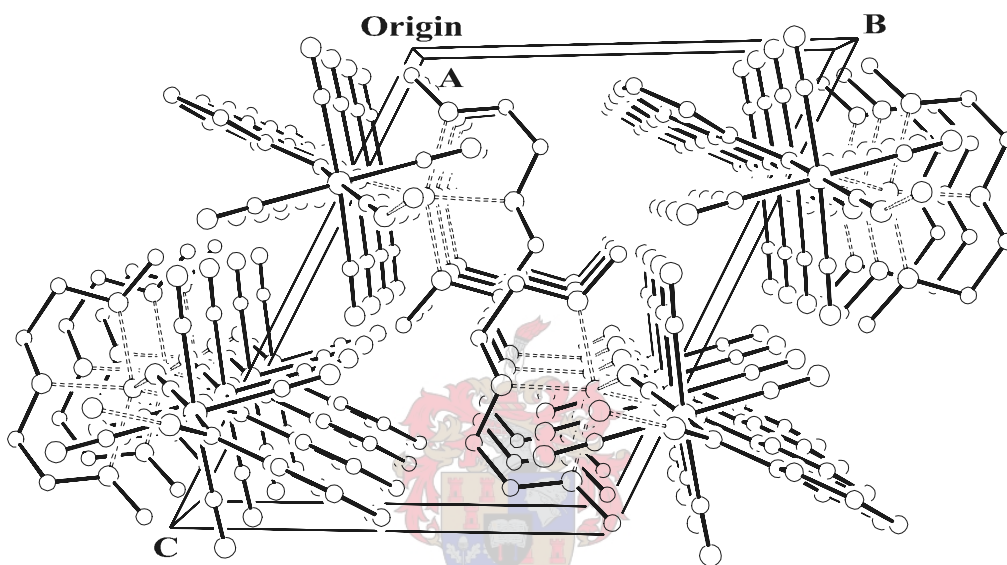
Figure 4.16: Packing diagram of **27**, viewed along the a-axis, showing infinite chains of linked molecules

In the crystal, asymmetric units of **27** pack in infinite polymeric chains, as described above, along the a-axis of the unit cell in the triclinic centrosymmetric spacegroup, P$\bar{1}$ (Figure 4.16). No significant intermolecular interactions, other than the intramolecular Li-O(3) ion-dipole interactions, are observed in the crystal structure of **27**. It is also believed that the highly ordered polymeric chain structure observed for **27** is partly responsible for the very low crystal mosaicity [0.464(1)°] in the crystal selected for the X-ray diffraction study. It is noteworthy that this crystal yielded excellent diffraction data and that hence a very well determined crystal structure could be obtained for **27** [R$_1$($F_o > 2\sigma F_o$) = 1.31% (!) - see Table 4.25].

Finally, although lithium alkyl/aryl pentacarbonyl chromates/molybdates/tungstates are common organometallic intermediates in the synthesis of many alkyl/aryl alkoxy Fischer-type carbene complexes, the structure of **27** is, to our knowledge, the first example of a crystal structure of this commonly employed organometallic Li-salt. The structure of a complicated lithium-(μ^2-benzoyl)-1,10-bis(diphenylphosphino)-(1,4,7,10-tetraoxadecane)Mo(CO)$_3$ complex, specifically designed to crystallise this Li$^+$ metallo-acyl species, has, however, been reported.[51]

The crystal and molecular structure of **28** (Figure 4.17), although possessing a very similar empirical formula to **27** (Table 4.25) and containing the same moieties, exhibits a completely different molecule arrangement. The structure of **28**, which is formally also a rare example of a Fischer-type hydroxycarbene complex, clearly shows a Li$^+$-cation coordinated to two diglyme molecules, and two benzoyl pentacarbonyltungstate anions that are linked *via* a hydrogen bond between their acyl oxygen atoms. The reason for the vast difference in structure between **27** and **28** lies with the change in potential ion-dipole and hydrogen bonding interactions that are introduced by replacing half the Li$^+$-cations in **27** with protons. Protons, unlike Li$^+$-cations, are sufficiently stabilised in a neutral two- coordinate hydrogen bonded system. Li$^+$-cations, on the other hand, can easily accommodate up to eight oxygen donor species and are rarely stabilised by less than three neutral oxygen donor atoms in the solid state.[52] Replacing half the Li$^+$-cations in solution thus allows the Li$^+$-cation to very efficiently coordinate to two diglyme molecules, whereas the strongly hydrogen bonded proton in **28** is situated between two acyl groups of separate benzoyl pentacarbonyltungstate anions.

Compared to **27**, the W-C(1) bond in **28** exhibits significantly more double bond character [W-C(1) = 2.238(5)Å]. The C(1)-O(1) double bond in **28** is also significantly reduced [C(1)-O(1) = 1.276(6)Å]. These changes indicate that there is a stronger bonding interaction between the proton and the acyl oxygen atoms in **28** than between the Li$^+$ cation and the acyl oxygen atom in **27**. There, however, still remains a large negative charge component residing on the tungsten atom. The O···H$^+$···O oxygen separation [2.442(6)Å] is relatively short, indicating that the hydrogen bond is indeed a strong one.[47] The position of the proton could be reliably determined from the difference Fourier map and is, as would be expected for a homonuclear molecule-

ion association of the type AHA⁻, evenly spaced between the metallo-acyl oxygen atoms [O(1)-H = 1.233(12)Å]. The bridging proton, furthermore, is situated on a crystallographic two-fold rotation axis that lies parallel to the b-axis of the unit cell and relates the anions in the formula unit to one another. The Li^+-cation also resides on this two-fold rotation axis, indicating that the $Li(diglyme)_2$ coordination possesses two-fold symmetry. The asymmetric unit of **28** thus contains a single benzoyl pentacarbonyltungstate anion hydrogen bonded to a shared proton, and one diglyme molecule coordinated to a shared Li^+-cation. An interesting observation regarding the position of the hydrogen-bonded proton in this structure is that it does not lie linearly between the metallo-acyl oxygen atoms [O(1)-H-O(1)' = 164(2)°]. This measurement is also not biased by the fact that the proton lies on a special position. The deviation from linearity in the O(1)-H-O(1)' angle is dependent on the unique coordinate of the proton along the b-axis of the unit cell, which is free to refine during the structure refinement. The reason for this kink in the hydrogen bridge is not entirely clear. It is most likely linked to the location of the lone-pair electron clouds, interacting with the proton in this strong hydrogen bond, on the metallo-acyl oxygen atoms. Similar kinks in hydrogen bonding interactions have been reported between anionic organometallic fragments.[47]

An O(1)-C(1)-C(11)-C(12) torsion angle of 29.1(6)° describes the orientation of the phenyl ring toward the acyl moiety. Curiously, the sp^2 hybridisation of C(1) is somewhat more distorted from trigonal planar geometry than in **27**, possibly due to steric considerations [the respective deviations from the least-squares plane through W, C(1), O(1) and C(11) are 0.012(1), -0.044(4), 0.018(2) and 0.015(1)Å]. A C(5)-W-C(1)-O(1) torsion angle of 36.0(5)° is similar to that in **27**, and describes how the benzoyl ligand is rotated on the $W(CO)_4$ coordination plane. Distortion of the $W(CO)_4$ coordination plane from planarity, due to bonding of the benzoyl ligand, is also more than in **27**, and is described by deviations from planarity from the least squares plane through W, C(2), C(4), C(5) and C(6) of -0.013(2), -0.057(3), -0.054(3), -0.063(3) and -0.061(3)Å respectively. Coordination of the Li^+-cation to the six ether oxygen atoms of the two diglyme molecules is best described as a flattened and distorted, yet symmetrical, octahedron with O(22) and its symmetry equivalent, O(22)' occupying the axial positions. Li-O separations in this arrangement are usual.[52(c)]
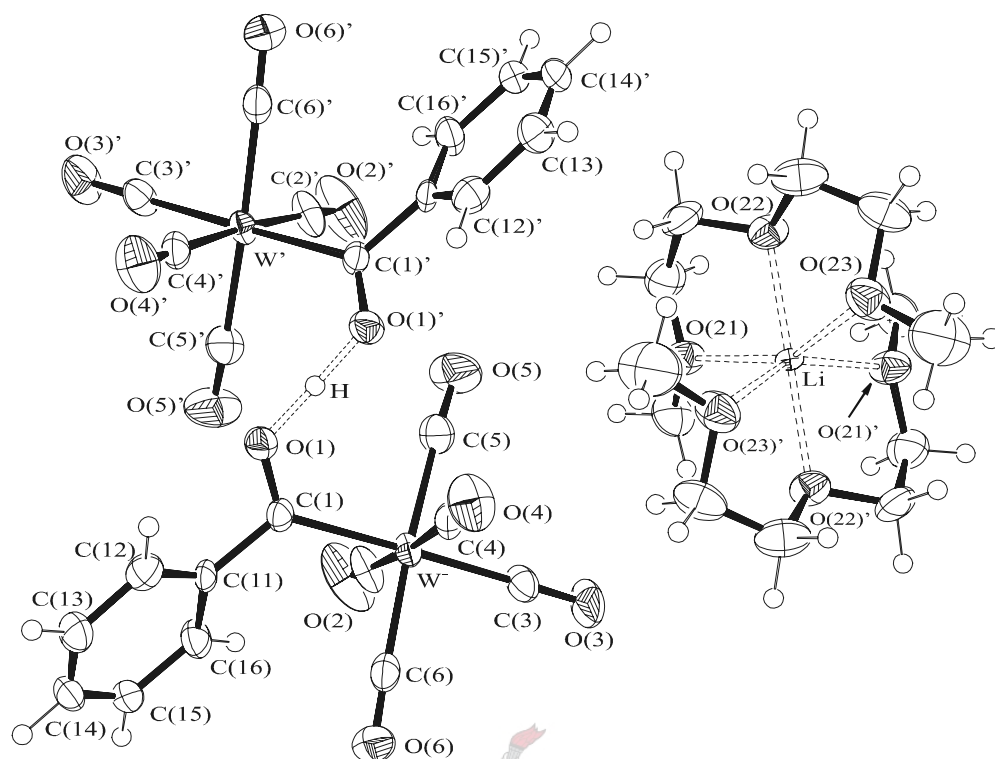
Figure 4.17: ORTEP view of **28** (two asymmetric units) showing numbering scheme and interactions observed in the crystal

Table 4.22: Selected bond lengths (Å) and angles (°) with e.s.d.s in parenthesis for complex **28**

Bond lengths		Bond angles	
W-C(1)	2.238(5)	O(1)-H-O(1)'	164.1(3)
O(1)-H	1.233(12)	C(1)-W-C(3)	174.0(2)
C(1)-O(1)	1.276(6)	C(2)-W-C(4)	176.1(3)
C(1)-C(11)	1.505(7)	C(5)-W-C(6)	174.7(2)
O(1)-O(1)'	2.442(6)	W-C(1)-O(1)	125.1(3)
W-C(2)	2.017(7)	W-C(1)-C(11)	123.9(3)
W-C(3)	1.996(6)	C(11)-C(1)-O(1)	110.6(4)
W-C(4)	2.027(6)	O(2)-C(2)-W	176.3(5)
W-C(5)	2.045(6)	O(3)-C(3)-W	178.4(6)
W-C(6)	2.029(6)	O(4)-C(4)-W	178.5(5)
Li-O(21)	2.168(7)	O(5)-C(5)-W	175.2(5)
Li-O(22)	2.075(3)	O(6)-C(6)-W	177.4(5)

173

Table 4.22 (continued):

Li-O(23)	2.170(9)	O(21)-Li-O(23)	150.7(2)
C(2)-O(2)	1.151(8)	O(22)-Li-O(22)'	167.9(6)
C(3)-O(3)	1.146(6)	C(5)-W-C(1)-O(1)	36.0(5)
C(4)-O(4)	1.135(7)	O(1)-C(1)-C(11)-C(12)	34.1(6)
C(5)-O(5)	1.148(6)		
C(6)-O(6)	1.154(6)		

In the crystal, molecules of **28** pack in the unusual orthorhombic and non-centrosymmetric face-centered space group, Fd2d. A view along the b-axis of the unit cell (Figure 4.18) shows how 8 molecules (16 asymmetric units) pack in the unit cell with the proton and lithium ions situated on the eight two-fold rotation axes parallel to the b-axis in this spacegroup. No significant intermolecular interactions are observed in the crystal structure of **28**.

Figure 4.18: Packing diagram of **28**, viewed along the b-axis of the unit cell, showing packing arrangement of the dimeric units in the crystal

174

4.3   Conclusions and future work

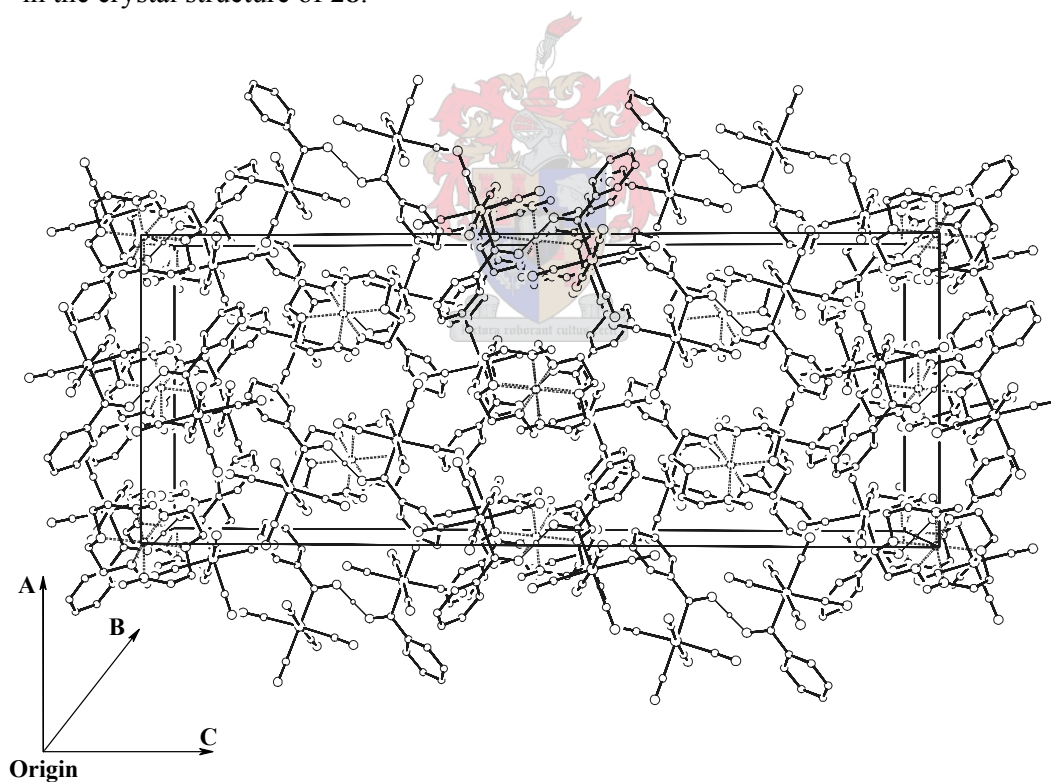The reaction of Ph₃PAuCl with anionic group 6 M(CO)₅-acyl complexes leads, as in the analogous reaction with anionic Re-acyl complexes reported previously, to the formation of bimetallic acylgold(I)-M(CO)₅ complexes. Evidence presented here suggests that the acylgold(I)-M(CO)₅ coordination through the acyl oxygen atom is very weak. The result is that the acylgold(I) organyl 'ligands' in these complexes are readily replaced by halide anions (Cl⁻ or Br⁻), which form ionic adducts with the M(CO)₅ moiety. This characteristic of these unstable bimetallic complexes ultimately led to the development of a preparative route to gain, and structurally characterise, the first example of a free acylgold(I) complex, benzoyl-AuPPh₃. This reaction path to acylgold(I) complexes, furthermore, illustrates how anionic metal acyl complexes may be effectively employed as sources of the acyl anion in preparative organometallic chemistry. Also, a unique crystal structure of an ionic electrostatically associated LiBr adduct of an unstable product from this conversion was obtained.

The acylgold(I) complexes produced in this conversion are proposed to form along a reaction mechanism that is closely related to the aurolysis reaction of β-metallo CH-deprotonated Fischer-type carbene complexes with Ph₃PAuCl. We propose electrophilic addition of the Ph₃PAu⁺ fragment at the anionic group 6 metal centre, followed by formal reductive elimination of the acylgold(I) organyl in this conversion. A closer examination of the reaction mechanism involved in this conversion should, however, be a topic of further research in this field.

The analogous reaction of Ph₃PAuCl with anionic N-deprotonated group 6 Fischer-type aminocarbene complexes, which are best represented as anionic group 6 metal imidoyl complexes after deprotonation, leads to the regioselective formation of novel bimetallic (Z)-{imidoylgold(I)PPh₃}-*N* M(CO)₅ complexes, and not the expected N-aurated Fischer-type aminocarbene complexes. The novel structure of these complexes was confirmed by an X-ray diffraction study. In contrast to the weak acyl-M(CO)₅ coordination described above, the imidoylgold(I) fragments in these bimetallic complexes coordinate remarkably strongly to the M(CO)₅ fragments through their imine nitrogen atoms. This is evident by the fact that these bimetallic complexes could be successfully purified by means of low temperature

chromatographic procedures (SiO₂). This conversion is the first example in which N-deprotonated Fischer-type aminocarbene complexes have reacted in this manner. It illustrates how these aminocarbene complexes can be employed as useful and efficient sources of the imidoyl anion in the preparation of imidoyl-gold(I) complexes. A similar reaction mechanism to the one described for the formation of acylgold(I) complexes above is proposed for this conversion. Lastly, the regioselectivity of this conversion may have significance in future applications of the products obtained here.

A second N-deprotonation, auration reaction sequence performed on suitable bimetallic (Z)-{imidoylgold(I)}-*N* M(CO)$_5$ complexes yielded the novel triangular Au$_2$Cr cluster compound, *cis*-{η^2-(Ph$_3$PAu)$_2$}PPh$_3$Cr(CO)$_4$, as the only isolable product. A single crystal X-ray diffraction study performed on this compound revealed that it contains the shortest known crystallographically determined separation between two gold atoms in cluster compounds of the type Au$_2$M. Possible links between this observation and the spectroscopic characteristics of this compound are discussed.

X-ray diffraction studies performed on lithium benzoylpentacarbonyl tungstate stabilised by 1 mole equiv. of diglyme and a closely related crystal obtained from a solution of lithium benzoylpentacarbonyl tungstate, in roughly half the Li$^+$-cations have been replaced by protons, illustrate how such a small difference in composition can translate into completely different crystal structures for these compounds. Different ion-dipole and hydrogen bonding interactions are mainly responsible for the vastly different structures observed in the crystals. This result highlights the important role these interactions play in directing the solid-state structure of compounds.

Potential future work sprouting from the results presented here, to name but a few interesting possibilities, include: Acidification/alkylation reactions at the acyl oxygen atom of the acylgold(I) complexes prepared in this work in order to synthesise the first examples of cationic Fischer-type hydroxy- and alkoxycarbene complexes of gold(I). Isolation and structural characterisation of acetyl-AuPPh$_3$ in order to determine whether CH-Au agostic interactions are possible for gold(I)complexes. Oxidative addition reactions of halides (X$_2$) to the isolated acylgold(I) complexes to prepare *trans*-dihalo-PPh$_3$-acyl-gold(III) complexes followed by

acidification/alkylation reactions on the acyl moieties of these compounds to produce the first examples of cationic gold(III) Fischer-type hydroxy- and alkoxycarbene complexes. Expansion of this conversion to include other 'soft' transition metal electrophiles (e.g. AgCl, HgCl etc.) with the aim of gaining new synthetic pathways to their acyl and carbene complexes. Isolation of the $M(CO)_5$ coordinated imidoylgold(I) complexes and the study of the same possible reactions as described above for the acylgold(I) complexes with these complexes.

4.4   Experimental

4.4.1 Materials

All solvents were dried and purified by conventional methods and freshly distilled under nitrogen shortly before use. Unless otherwise stated, all common reagents were used as obtained from commercial suppliers without further purification. PhLi was freshly prepared by the reaction of $Li_{(s)}$ with bromobenzene in Et_2O. MeLi, PhLi and ^{n}BuLi were standardised before use according to the procedure reported by Winkle.[53] Ph_3PAuCl,[54] the tetrabutylammonium acetyl/benzoylpentacarbonyl chromates and tungstates,[55] and the group 6 metal pentacarbonyl Fischer-type aminocarbene starting complexes[56] were prepared according to procedures described in the literature.

4.4.2 Physical methods

All reactions and manipulations involving organometallic reagents were carried out under a dry nitrogen atmosphere using standard Schlenk and vacuum-line techniques. NMR spectra were recorded on Varian INOVA 600 (600 MHz for ^1H, 151 MHz for $^{13}C\{^1H\}$ and 243 MHz for $^{31}P\{^1H\}$) or Varian VXR 300 (300 MHz for ^1H, 75.4 MHz for $^{13}C\{^1H\}$ and 121.5 MHz for $^{31}P\{^1H\}$) NMR spectrometers. ^1H and ^{13}C chemical shifts are reported in ppm relative to the ^1H and ^{13}C residue of the deuterated solvents. ^{31}P chemical shifts are reported in ppm relative to an 85% H_3PO_4 external standard solution. IR spectra (4000 to 400 cm^{-1}, resolution 4 cm^{-1}) were recorded on a Perkin-Elmer 1600 series FTIR spectrometer. FAB-MS were recorded on a Micromass DG

70/70E mass spectrometer at the University of Potchefstroom, South Africa, using xenon gas as bombardment atoms and *m*-nitrobenzylalcohol as matrix. Flash column chromatography was performed with "flash grade" silica (SDS 230-400 mesh). Melting points were determined on a standardised Büchi 535 melting point apparatus. Crystal structure data collection and correction procedures were carried out on a Nonius KappaCCD diffractometer by Dr. J. Bacsa and Ms. Hong Su of the University of Cape Town structural chemistry research group. All structure solutions, refinements, analyses and descriptions were carried out by the author.

4.4.3 Preparations and procedures

4.4.3.1 Experimental procedures for the preparation of mixtures **15-18**.

1.2 mole equiv. of standardised MeLi (**15** and **17**) or PhLi (**16** and **18**) were added dropwise to 0.8 mmol of the corresponding $M(CO)_6$ compound (M = Cr: 176mg; M = W: 282mg) suspended in 20ml Et_2O at room temperature over a period of 10-15 min. After addition of the MeLi/PhLi the mixture was stirred at room temperature for 30 minutes, after which it was cooled to –78 ^{o}C. $AuPPh_3Cl$ (0.8mmol; 395 mg) was then added to the cooled reaction mixture. After stirring at –78 ^{o}C for 30-45 minutes the reaction mixture is allowed to warm to room temperature over a period of 2½ hours, during which the $AuPPh_3Cl$ dissolves and a white LiCl precipitate forms. The mother liquor of the product mixtures, was carefully removed with a syringe upon settling of the LiCl precipitate. Carefully cooling the mother liquor of **18** upon removal of the solvent *in vacuo* resulted in the formation of crystals of **18'**. The complex mixtures **15**-**17** were isolated by careful filtration through Celite and partial removal of the solvent *in vacuo*. Yields of **15**-**17** are not meaningful as large amounts of solvent were still present. **18'** was isolated in moderate yield [65%]. Yields were not optimized.

4.4.3.2 Experimental procedures for the preparation of **19** and **20**.

Complexes **19** and **20** were prepared in much the same way as mixtures **15-18**, except that 0.8 mmol $^nBu_4N$ benzoylpentacarbonyl tungstate, prepared and isolated

seperately, was employed in this reaction instead of the freshly prepared lithium acetyl-/benzoyl-pentacarbonyl chromates and tungstates used previously. Instead of a LiCl precipitate forming in the reaction mixture upon completion of the conversion, a precipitate of **20** forms which is isolated in near quantitative yield (96%) by careful removal of the cooled (-20 ^{o}C) mother liquor, now containing only **19**, with a syringe. The isolated precipitate of **20** can be washed with cooled 10 ml portions of Et$_2$O to remove any remaining traces of **19** if so required. **19** was isolated in high yield (75%) by prolonged crystallisation (~10 weeks) at –20°C from concentrated Et$_2$O solutions, prepared directly from the mother liquor. Yields were not optimized.

4.4.3.3 Representative experimental procedures for the preparation of **21-25**.

0.4 ml 1.6M ^{n}BuLi (1 mole equiv.) was added to a solution of the Fischer-type aminocarbene complex (0.8 mmol) in 15 ml thf cooled to –78 ^{o}C. The mixture was stirred at that temperature for 10 minutes, after which 1 mole equiv. Ph$_3$PAuCl (395 mg) was added to the solution. After stirring this mixture at –78 ^{o}C for 30 minutes the mixture was allowed to warm to room temperature over a period of 2½ hours. Removal of the solvent *in vacuo* resulted in dark yellow to brown oily residues containing a mixture of products (TLC). The products were isolated in moderately low to high yields [32% (**21**), 41% (**22**), 56% (**23**), 85% (**24**) and 57% (**25**)] as broad yellow bands by means of low temperature (-15 ^{o}C) silica gel column chromatography (hexane/diethyl ether, 2:1). Yields were not optimized.

4.4.3.4 Experimental procedures for the preparation of **26**.

Complex **26** was inadvertently prepared in a second deprotonation-auration reaction sequence after the initial synthesis of **21** or **23**. The reaction was carried out directly after the initial synthesis of **21** or **23** in thf, without isolation of these complexes. After completion of the preparation of **21** or **23**, as described above, the reaction mixture was once again cooled to -78 ^{o}C followed by the addition of 0.4 ml 1.6M ^{n}BuLi. The mixture was stirred at that temperature for 10-15 minutes after which a second molar equivalent Ph$_3$PAuCl (395 mg) was added. The mixture was stirred at –78 ^{o}C for 30 minutes after which it was allowed to warm to room temperature over a period of 2½ hours. Removal of the solvent *in vacuo* produced a dark brown oily

residue containing low yields of a range of gold containing products (TLC). **26** was the only product which could be isolated in a significant yield (10%) by means of low temperature (-15 °C) silica gel column chromatography of the reaction mixture. It was washed from the column as a fast moving red band with thf after elution with other solvent mixtures failed to separate any other products of this reaction in significant yields.

4.4.3.3 Crystal structure determination of complexes **18'**, **19**, **20**, **23**, **26**, **27** and **28**

The crystal data collection and refinement details for complexes **18'**, **19**, **20**, **23**, **26**, **27** and **28** are summarised in Tables 4.23 - 4.25. X-ray quality orange prismatic single crystals of **18'** were obtained by crystallisation of the cooled reaction mixture of **18**. Orange platelet crystals of **19**, suitable for X-ray diffraction, were obtained by prolonged crystallisation (~10 weeks) from a concentrated thf solution layered with Et₂O and cooled to -20 °C. Good quality crystals of **20** (yellow platelets), **26** (red prisms), **27** (red prisms) and **28** (red prisms) were obtained overnight by re-crystallisation of the isolated compounds from a thf solution layered with pentane and cooled to -20 °C. Sizable X-ray quality crystals (yellow needles) of **23** were only obtained after very long periods (2-3 months) of crystallisation from a concentrated Et₂O solution layered with pentane at –20°C.

Low temperature (-100 °C for **18'**, **20**, **23**, **26**, **27** and **28**, and -85 °C for **19**) diffraction data for all the crystals were collected on an Enraf-Nonius KappaCCD diffractometer[57] using graphite monochromated Mo-K$_\alpha$ radiation (λ = 0.71073 Å). All the data sets were scaled, reduced and corrected for Lorenz and polarisation effects using DENZO-SMN[58]. The structures of **18'**, **23** and **26** were solved with direct methods (SHELXS)[59] and refined anisotropically for all the non-hydrogen atoms, except those mentioned below, by full-matrix least squares calculations (SHELXL-97)[59] on F^2. Disorder found in the positions of the C(3)-O(3) and C(4)-O(4) CO ligands in the structure of **18'** prevented the anisotropic refinement of these atom positions. Similarly, the disorder found in the oxygen and carbon atom positions of the non-coordinated thf molecule in the structure of **26** prevented their anisotropic refinement.

The structures of **19**, **20**, **27** and **28** were solved by the interpretation of Patterson syntheses (SHELXS),[59] which produced the positions of the metal atoms in these crystal structures. The structures were completed by full-matrix least squares calculations (SHELXL-97)[59] on F^2 and, unless stated otherwise, anisotropic thermal motion was allowed for all the non-hydrogen atoms during the final cycles of refinement.

Extensive disorder, in the form of a complete molecule of **19** orientated in roughly the opposite direction of the P-Au-C bond was found in the crystal structure of **19**. The final refined ratio of different orientations of molecules in the structure of **19** is, according to the different site occupancies of the two crystallographically independent molecules of **19** found in the structure, 0.8576 (a) **:** 0.1424 (b). Furthermore, the phenyl ring carbon atom positions in the low site occupancy orientation of **19** were restrained to idealized 6-membered rings with the C-C distance restrained to 1.39Å using the AFIX 65 and AFIX 66 commands in SHELXL.[59] The C(1b) atom in this orientation of **19** was also restrained to a sensible position by fixing the Au-C(1b) and C(1b)-C(11b) bond length to sensible values. As a result of the low site occupancy and poor accuracy of the atom positions in the b-orientation of this structure the carbon atoms corresponding to this component in the crystal could not be allowed anisotropic thermal motion.
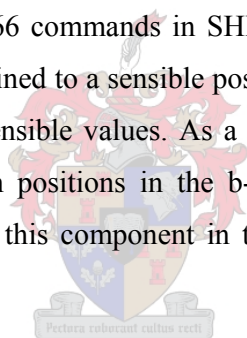
Many hydrogen atom positions in the structures of **18'**, **19**, **20**, **23**, **26**, **27** and **28** could be located from the difference Fourier map, with the obvious exclusion of those situated on disordered atoms, described above. Despite this they were all, with the exception of the imine hydrogen atom in the structure of **23** and the bis(metallo-acyl) coordinated proton in **28**, placed in idealised positions with their thermal parameters fixed at 1.5 times (for aliphatic hydrogen atoms) or 1.2 times (for aromatic hydrogen atoms) the equivalent isotropic displacement parameters of their parent atoms. Both the aforementioned hydrogen atoms in **23** and **28** could be located on the difference Fourier map and refined isotropically. The hydrogen (H) in **28**, furthermore, lies on a special position (a two-fold rotation axis). ORTEP-III for Windows was used to generate the various figures of **18'**, **19**, **20**, **23**, **26**, **27** and **28** at the 50% probability level.[60]

All other crystallographic information, including the hkl data and structure factors, is included on the CD of supplementary material provided in the back cover of this work, or is available from the author upon request.

Table 4.23: Crystallographic Data for **18'** and **19**

	18'	19
Chemical Formula	$C_{59}H_{50}O_8BrLiP_2Au_2W$	$C_{25}H_{20}OPAu$
MW (g/mol)	1613.61	564.37
Crystal system	Monoclinic	Monoclinic
Space group	$P2_1/n$	$P2_1/n$
a (Å)	15.4626(3)	12.8710(3)
b (Å)	19.2859(5)	10.3025(3)
c (Å)	19.7262(4)	16.6403(5)
α (°)	90	90
β (°)	101.147(2)	109.771(1)
γ (°)	90	90
Volume ($Å^3$)	5771.6(2)	2076.5(1)
Z	4	4
d_{calcd} (g/cm^3)	1.857	1.805
Temp (K)	173(2)	188(2)
$\mu_{Mo\,K\alpha}$ (cm^{-1})	7.859	7.174
$2\theta_{max}$ (°)	24.71	29.13
Radiation	Mo Kα, graphite monochromated	Mo Kα, graphite monochromated
Crystal size (mm)	$0.05 \times 0.09 \times 0.13$	$0.06 \times 0.08 \times 0.15$
Index range	$-18 \leq h \leq 18$	$-17 \leq h \leq 17$
	$-22 \leq k \leq 21$	$-14 \leq k \leq 12$
	$-23 \leq l \leq 22$	$-22 \leq l \leq 22$
No. of reflections collected	17356	9883
No of independent reflections	9760 (R_{int} = 0.0512)	5507 (R_{int} = 0.0451)
No. of observed reflections	6855	4031
Refinement	Full matrix on F^2 (SHELXL)	Full matrix on F^2 (SHELXL)
Parameters	669	325
R_1 ($F_o > 2\sigma F_o$)	0.0479	0.0395
wR_2 (all data)	0.0964	0.0867

Table 4.24: Crystallographic Data for **20**, **23** and **26**

	20	23	26
Chemical Formula	$C_{21}H_{36}O_5NClW$	$C_{30}H_{21}O_5NPAuCr$	$C_{58}H_{45}O_4P_3Au_2Cr \cdot C_4H_8O$
MW (g/mol)	601.81	755.43	1416.85
Crystal system	Monoclinic	Orthorhombic	Triclinic
Space group	C2/c	Pc2_1b	$P\bar{1}$
a (Å)	15.7654(2)	11.0724(2)	11.4841(2)
b (Å)	19.5093(2)	12.6013(2)	13.5642(3)
c (Å)	18.0605(2)	20.4100(3)	17.5171(4)
α (°)	90	90	87.147(1)
β (°)	107.932(1)	90	88.062(1)
γ (°)	90	90	81.073(1)
Volume (Å^3)	5285.1(1)	2847.74(8)	2691.4(1)
Z	8	4	2
d_{calcd} (g/cm^3)	1.513	1.762	1.738
Temp (K)	173(2)	173(2)	173(2)
$\mu_{Mo\ K\alpha}$ (cm^{-1})	4.499	5.623	5.775
$2\theta_{max}$ (°)	27.00	26.99	27.00
Radiation	Mo Kα, graphite monochromated	Mo Kα, graphite monochromated	Mo Kα, graphite monochromated
Crystal size (mm)	$0.17 \times 0.21 \times 0.25$	$0.05 \times 0.10 \times 0.13$	$0.17 \times 0.27 \times 0.35$
Index range	$-19 \leq h \leq 20$	$-14 \leq h \leq 13$	$-14 \leq h \leq 14$
	$-23 \leq k \leq 24$	$-15 \leq k \leq 16$	$-13 \leq k \leq 17$
	$-23 \leq l \leq 23$	$-26 \leq l \leq 23$	$-22 \leq l \leq 22$
No. of reflections collected	18275	15131	15589
No of independent reflections	5762 (R_{int} = 0.0314)	6056 (R_{int} = 0.0674)	11417 (R_{int} = 0.0261)
No. of observed reflections	4547	4414	8532
Refinement	Full matrix on F^2 (SHELXL)	Full matrix on F^2 (SHELXL)	Full matrix on F^2 (SHELXL)
Parameters	267	356	658
R_1 ($F_o > 2\sigma F_o$)	0.0245	0.0374	0.0330
wR_2 (all data)	0.0569	0.0710	0.0629

Table 4.25: Crystallographic Data for **27** and **28**

	27	28
Chemical Formula	$C_{18}H_{19}O_9LiW$	$C_{18}H_{19.5}O_9Li_{0.5}W$
MW (g/mol)	570.12	567.16
Crystal system	Triclinic	Orthorhombic
Space group	$P\bar{1}$	Fd2d
a (Å)	8.8289(1)	14.8039(2)
b (Å)	11.1285(1)	15.1227(3)
c (Å)	12.9991(2)	37.8020(7)
α (°)	113.709(1)	90
β (°)	95.826(1)	90
γ (°)	108.179(1)	90
Volume ($Å^3$)	1072.55(2)	8462.9(3)
Z	2	8
d_{calcd} (g/cm^3)	1.765	1.781
Temp (K)	173(2)	173(2)
$\mu_{Mo\ K\alpha}$ (cm^{-1})	5.429	5.504
$2\theta_{max}$ (°)	25.00	27.48
Radiation	Mo Kα, graphite monochromated	Mo Kα, graphite monochromated
Crystal size (mm)	$0.17 \times 0.20 \times 0.25$	$0.20 \times 0.30 \times 0.40$
Index range	$-10 \leq h \leq 10$	$-19 \leq h \leq 13$
	$-13 \leq k \leq 13$	$-18 \leq k \leq 19$
	$-15 \leq l \leq 15$	$-48 \leq l \leq 37$
No. of reflections collected	7414	10455
No of independent reflections	3787 (R_{int} = 0.0144)	4599 (R_{int} = 0.0350)
No. of observed reflections	3651	4094
Refinement	Full matrix on F^2 (SHELXL)	Full matrix on F^2 (SHELXL)
Parameters	264	261
R_1 ($F_o > 2\sigma\ F_o$)	0.0131	0.0277
wR_2 (all data)	0.0309	0.0502

4.5   References

1.   (a) Coates, G.E., Green M.L.H., Wade K. "*Organometallic compounds*", Methuen, London, **1968**, *2*, 257-63. (b) Wojcicki, A. *Adv. Organomet. Chem*. **1973**, *11*, 87. (c) Calderazzo, F. *Angew. Chem., Int. Ed. Engl.*, **1977**, *16*, 299. (d) Kuhlman, E.J., Alexander J.J. *Coord. Chem. Rev.*, **1980**, *33*, 195. (e) Collman, J.P., Hegedus, L.S., Norton, J.R., Finke, R.G. "*Principles and Applications of Organotransition Metal Chemistry*", 2nd ed. University Science Books, Mill Valley, CA, **1980**, 619.

2.   (a) Durfee, L.D., Rithwell, I.P. *Chem.Rev.*, **1988**, *88*, 1059. (b) Cutler, A.R., Hanna, P.K., Vites, J.C *Chem.Rev.*, **1988**, *88*, 1363. (c) Kinnunen, T., Laason, K. *J. Organomet. Chem.*, **2001**, *628*, 222.

3.   Moss, J.R. *J. Mol. Catal. A: Chem.*, **1996**, *107*, 169.

4.   Dry M.E. *Catal. Today*, **1990**, *6*, 183.

5.   (a) Fischer, E.O., Maasböl, A. *Angew. Chem., Int. Ed. Engl.*, **1964**, *3*, 580. (b) Fischer, E.O., Maasböl, A. *Chem. Ber.*, **1967**, *100*, 2445.

6.   Semmelhack, M.F., Lee, G.R. *Organometallics*, **1987**, *6*, 1839.

7.   See for example: (a) Van Doorn, J.A., Masters, C., Volger, H.C. *J. Organomet. Chem.*, **1976**, *105*, 245. (b) Gladysz, J.A., Selover, J.C., Strouse, C.E., *J. Am. Chem. Soc.*, **1978**, *100*, 6766. (c) Fischer, E.O. *Adv. Organomet. Chem.*, **1976**, *14*, 1.

8.   Shambayati, S., Crowe, W.E., Schreiber, S.L. *Angew. Chem., Int. Ed. Engl.*, **1990**, *29*, 256 and references therein.

9.   (a) Carmona, E., Sánchez, L.J., Poveda, M.L., Marín, J.M., Atwood, J. L. Rogers, R.D., *J. Chem. Soc., Chem. Commun.*, **1983**, 161. (b) Carmona, E., Sánchez, L.J., Marín, J.M., Poveda, M.L., Atwood, J. L., Riester, R.D., Rogers, R.D. *J. Am. Chem. Soc.*, **1984**, *106*, 3214. (c) Carmona, E., Contreras, L., Sánchez, L.J., Poveda, M.L. *J. Am. Chem. Soc.*, **1991**, *113*, 4322. (d) Contreras, L., Monge, A., Pizzano, A., Ruíz, C., Sánchez, L.J., Carmona, E. *Organometallics*, **1992**, *11*, 3971.

10. Theopold, K.H., Becker, P.N., Bergman, R.G. *J. Am. Chem. Soc.*, **1982**, *104*, 5250.

11. (a) Morrison, J.D. *Asymmetric Synthesis, Vol. 3*, Academic Press, Orlando, FL. **1984**. (b) Siegel, C., Thornton, E.R. *J. Am. Chem. Soc.*, **1989**, *111*, 5722.

(c) Wulff, W.D., Anderson, B.A., Toole, A.J., Xu, Y.Ch. *Inorg. Chim. Acta*, **1994**, *220*, 215.

12. (a) Ellis, J.E. *J. Organomet. Chem.* **1975**, *86*, 1. (b) King, R.B. *Acc. Chem Res.*, **1970**, *3*, 417.

13. Haupt, H.–J., Petters, D., Flörke, U. *J. Organomet. Chem.*, **1998**, *553*, 497.

14. Willner, H., Schäbs, J., Hwang, G., Mistry, F., Jones, R., Trotter, J., Aubke, F. *J. Am. Chem. Soc.*, **1992**, *114*, 8972.

15. Herzberg, G. "*Molecular Spectra and Molecular Structure, Vol. 1: Spectra of Diatomic Molecules*", 2nd ed. Van Nostrand, New York, **1950.**

16. Raubenheimer, H.G., Cronje, S. in "*Gold, Progress in Chemistry, Biochemistry and Technology*", Schmidbaur, H. Ed., J. Wiley & Sons, Chichester, **1999**. 557-632.

17. Kharash, M.S., Isbell, H.S. *J. Am. Chem. Soc.*, **1931**, *52*, 2919.

18. Nesmeyanov, A.N., Perevalova, K.I., Grandberg, K.I., Lemenovskii, D.A. *Izv. Akad. Nauk. SSSR, Ser. Khim.*, **1974**, 1124.

19. Komiya, S., Sone, T., Ozaki, S., Ishikawa, M., Kasuga, N. *J. Organomet. Chem.*, **1992**, *428*, 303.

20. Brüll, R., Kgosane, D., Neveling, A., Pasch, H., Raubenheimer, H.G., Sanderson, R., Wahner, U.M. *Macromol. Symp.*, **2001**, *165*, 11.

21. (a) Burini, A., Bravi, R., Fackler Jr., J.P., Galassi, R., Grant, T.A., Omary, M.A., Pietroni, B.R., Staples, R.J. *Inorg. Chem.*, **2000**, *39*, 3158. (b) Fehlhammer, W.P., Dahl, L.F. *J. Am. Chem. Soc.*, **1972**, *94*, 3370. (c) Raubenheimer, H.G., Scott, F., Kruger, G.J., Toerien, J.G., Otte, R., van Zyl, W., Taljaard, T., Olivier, P., Linford, L. *J. Chem. Soc., Dalton Trans.*, **1994**, 2091. (d) Raubenheimer, H.G., Olivier, P.J., Lindeque, L., Desmet, M., Hrusak, J., Kruger, G.J. *J. Organomet. Chem.*, **1997**, *544*, 91. (e) Kwang Ming Lee, Ching Kuan Lee, Lin, I.J.B. *Angew. Chem., Int. Ed. Engl.*, **1997**, *36*, 1850.

22. (a) Balch, A.L., Olmstead, M.M., Vickery, J.C. *Inorg. Chem.*, **1999**, *38*, 3494. (b) Lanfranchi, M., Pellinghelli, M.A., Tiripicchio, A., Bonati, F. *Acta Crystallogr., Sect.C (Cr. Str. Comm.)*, **1985**, *41*, 52. (c) Tiripicchio, A., Camelini, M., Minghetti, G. *J. Organomet. Chem.*, **1979**, *171*, 399. (d) Vickery, J.C., Balch, A.L. *Inorg. Chem.*, **1997**, *36*, 5978.

23. Atwood, J.L., Bott, S.G., Junk, J.C., May, M.T. *J. Organomet. Chem.*, **1995**, *487*, 7 and references therein.

24. Schubert, U., Friedrich, P., Orama, O. *J. Organomet. Chem.*, **1978**, *144*, 175.

25. Cardin, D.J., Cetinkaya, B., Lappert, M.F. *Chem. Rev.*, **1972**, *72*, 545.

26. Song, J.-S., Szalda, D.J., Bullock, R.M. *Inorg. Chim. Acta.*, **1997**, *259*, 161.

27. (a) Fischer, E.O., Schubert, U. *J. Organomet. Chem.*, **1979**, *170*, C13. (b) Schubert, U., Hörnig, H., *J. Organomet. Chem.*, **1984**, *273*, C11. (c) Nandi, M., Sathe, K.M., Sarkar, A. *J. Chem. Soc., Chem. Commun*, **1992**, 793.

28. Sathe, K.M., Nandi, M., Amin, Sk.R., Puranik, V.G., Sarkar, A. *Organometallics*, **1996**, *15*, 2881.

29. Contreras, L., Pizzano, A., Sánchez, L., Carmona, E. *J. Organomet. Chem.*, **1995**, *500*, 61.

30. Shaw III, C.F. in *"The Chemistry of the Organic Derivatives of Gold and Silver"*, Patai, S., Rappoport, Z., Eds. 1999, John Wiley & Sons, Chichester, p. 67.

31. (a) Raubenheimer, H.G., Kruger, G.J., Marais, C.F., Hattingh, J.T.Z., Linford, L., van Rooyen, P.H. *J. Organomet. Chem.*, **1988**, *355*, 337. (b) Raubenheimer, H.G., Desmet, M., Kruger, G.J. *J. Chem. Soc., Dalton Trans.*, **1995**, 2067.

32. (a) Jones, P.G., *Gold Bull.*, **1981**, *14*, 102 and 159. (b) *ibid*., **1983**, *16*, 114. (c) *ibid*., **1986**, *19*, 46.

33. Burschka, C., Schenk, W.A. *Z. Anorg. Allg. Chem.*, **1981**, *477*, 149.

34. (a) Powers, T.S., Wulff, W.D., Quinn, J., Shi, Y., Jiang, W., Hsung, R., Parisi, M., Rahm, A., Jiang, X. W., Yap, G.P.A., Rheingold, A.L. *J. Organomet. Chem.*, **2001**, *617-618*, 182. (b) Lafolleé-Bezzenine, S., Parlier, A., Rudler, H., Vaissermann, J., Daran, J.-C. *J. Organomet. Chem.*, **1998**, *567*, 83.

35. Connor, J.A., Rose, P.D. *J. Organomet. Chem.*, **1972**, *46*, 329.

36. (a) Coffey, C.E., Lewis, J., Nyholm, R.S. *J. Chem. Soc.*, **1964**, 1741.(b) Arndt, L.W., Ash, C.E., Darensourg, M.Y., Hsiao, Y.M., Kim, C.M., Reibenspies, J., Youngdahl, K.A. *J. Organomet. Chem.*, **1990**, *394*, 733. (c) Hall, K.P., Mingos, D.M.P. *Prog. Inorg. Chem.*, **1984**, *32*, 237 and references therein.

37. (a) Lewis, J., Johnson, B.F.G. *Pure Appl. Chem.*, **1982**, *54*, 97 and references therein. (b) Johnson, B.F.G., Kaner, D.A., Lewis, J., Raithby, P.R., Taylor, M.J. *J. Chem. Soc., Chem., Commun.*, **1982**, 314. (c) Mays, M.J., Raithby,

P.R., Taylor, P.L., Henrick, K. *J. Organomet. Chem.*, **1982**, *224*, C45. (d) Lauher, J.W., Wald, K. *J. Am. Chem. Soc.*, **1981**, *103*, 7648. (e) Ellis, J.E. *J. Am. Chem. Soc.*, **1981**, *103*, 6106 and references therein. (f) Pignolet, L.H., Krogstad, D.A. in "*Gold, Progress in Chemistry, Biochemistry and Technology*", Schmidbaur, H., Ed., 1999, John Wiley & Sons, Chichester, p. 429.

38.   Green, M., Orpen, G.A., Salter, I.D., Stone, F.G.A. *J. Chem. Soc., Chem. Commun.*, **1982**, 813.

39.   Galassi, R., Poli, R., Quadrelli, A.E., Fettinger, J.C. *Inorg. Chem.*, **1997**, *36*, 3001.

40.   Brunet, J.-J, Capperrucci, Chauvin, R. *Organometallics*, **1996**, *15*, 5254.

41.   Schubert, U., Ackermann, K., Aumann, R. *Cryst. Struct. Commun.*, **1982**, *11*, 591.

42.   Deutsch, M., Stein, F., Funke, F., Pohl, E., Herbst-Irmer, R., de Meijere, A. Chem. Ber., **1993**, *126*, 2535.

43.   (a) Cheetham, G.M.T., Harding, M.M., Haggit, J.L., Mingos, D.M.P, Powell, H.R *Chem. Commun.*, **1993**, 1000. (b) F.P., Gabbai, Schier, A., Riede, J., Schmidbaur, H. *Inorg. Chem.*, **1995**, *34*, 3855.

44.   (a) Jones, P.G. *Gold Bull.*, **1983**, *16*, 114. (b) Jones, P.G. *Gold Bull.*, **1981**, *14*, 159.

45.   (a) Schultz, A.J., Srinivasan, K., Teller, R.G., Williams, J.M., Lukehardt, C.M. *J. Am. Chem. Soc.*, **1984**, *106*, 999. (b) Gerisch, M., Heinemann, F.W., Bruhn, C., Scholz, J., Steinborn, D. *Organometallics*, **1999**, *18*, 564. (c) Heinemann, F.W., Gerisch, M., Steinborn, D. *Z. Kristallogr. –New Crystal Structures*, **1997**, *212*, 181. (d) Jones, C., Steed, J.W., Thomas, R.C. *J. Chem. Soc., Dalton Trans.*, **1999**, 1541. (e) Steinborn, D., Gerisch, M., Bruhn, C., Davies, J.A. *Inorg. Chem.*, **1999**, *38*, 680. (f) Steinborn, D., Gerisch, M., Hoffmann, T., Bruhn, C., Israel, G., Muller, F.W., *J. Organomet. Chem.*, **2000**, *598,* 286. (g) Steinborn, D., Gerisch, M., Heinemann, F.W., Bruhn, C. *Chem. Commun.*, **1997**, 843. (h) Gerisch, M., Bruhn, C., Porzel, A., Steinborn, D. *Eur. J. Inorg. Chem.*,**1998**, 1655. (i) Knox, J.R., Prout, C.K. *Acta Crystallogr., Sect. B*, **1969**, *25*, 1952.

46.   (a) Klingler, R.J., Huffman, J.C., Kochi, J.K. *Inorg. Chem.*, **1981**, *20*, 34. (b) Motz, P.L., Ho, D.M., Orchin, M. *J. Organomet. Chem.*, **1991**, *407*, 259. (c)

Ishii, Y., Ogio, K.-i., Nishio, M., Retboll, M., Kuwata, S., Matsuzaka, H., Hidai, M. *J. Organomet. Chem.*, **2000**, *599*, 221.

47.   Bär, E., Fuchs, J., Rieger, D., Aguilar-Parrilla, F., Limbach, H.-H., Fehlhammer, W.P. *Angew. Chem., Int. Ed. Engl.*, **1991**, *30*, 88.

48.   Butts, S.B., Strauss, S.H., Holt, E.M., Stimson, R.E., Alkock, N.W., Shriver, D.F. *J. Am. Chem. Soc.*, **1980**, *102*, 5093 and references therein.

49.   For example see: Casey, C.P., Polichnowski, S.W., Tuinstra, H.E., Albin, L.D., Calabrese, J.C. *Inorg. Chem.*, **1978**, *17*, 3045.

50.   (a) Petillon, F.Y., Quere, J.-L., Le Floch-Perennou, F., Guerchias, J.-E., Gomes De Lima, M.-B., Manojlovic-Muir, L., Muir, K.W., Sharp, D.W.A. *J. Organomet. Chem.*, **1984**, *255*, 231. (b) McGuiggan, M.F., Doughty, D.H., Pignolet, L.H., *J. Organomet. Chem.*, **1980**, *185*, 241.

51.   Powell, J., Kuksis, A., May, C.J., Nyburg, S.C., Smith, S.J. *J. Am. Chem. Soc.*, **1981**, *103*, 5941.

52.   (a) Purath, A., Koppe, R., Schnöckel, H. *Chem. Commun.*, **1999**, 1933. (b) Emmerich, C., Huttner, G. *J. Organomet. Chem.*, **1993**, *447,* 81. (c) Palitzsch, W., Bohme, U., Roewer, G. *Chem. Commun.*, **1997**, 803.

53.   Winkle, M.R., Lansinger, J.M., Roland, R.C. *J. Chem. Soc., Chem. Commun.*, **1980**, 87.

54.   Fackler Jr., J.P. *Inorg. Synth.*, **1982**, *21*, 325.

55.   (a) Hegedus, L.S., McGuire, M.A., Schultz, L.M. *Org. Synth.*, **1987**, *65*, 140. (b) Fischer, E.O., Maasböl, A. *Chem. Ber.*, **1967**, *100,* 2445.

56.   Fischer, E.O., Leupold, M. *Chem. Ber.*, **1972**, *105*, 599.

57.   Nonius, B.V. "*COLLECT, Data collection software*", **1999**, Delft, The Netherlands.

58.   Otwinowski, Z.; Minor, W. *Methods Enzymol.* **1997**, *276*, 307.

59.   Sheldrick, G. M.   *SHELX-97*. Program for crystal structure analysis, University of Göttingen, Germany, **1997**.

60.   Farrugia, L.J. *J. Appl. Cryst.*, **1997**, *30*, 565.